HELMHOLTZ GEMEINSCHAFT

GKSS FORSCHUNGSZENTRUM in der HELMHOLTZ-GEMEINSCHAFT

AWI

OBSERVING THE COASTAL SEA

An Atlas of Advanced Monitoring Techniques

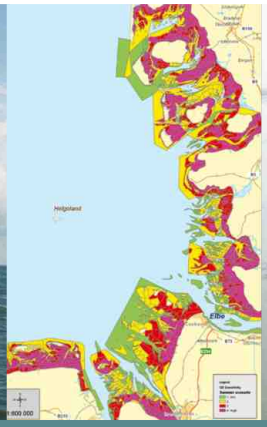

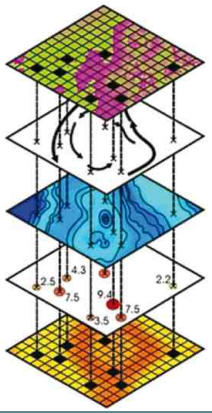

New Developments within the MARCOPOLI Research Programme of the Helmholtz Research Centres GKSS, AWI and Partners

LOICZ

LOICZ Reports and Studies No. 33

OBSERVING THE COASTAL SEA

An Atlas of Advanced Monitoring Techniques

Contributers

GKSS Research Centre Geesthacht

Alfred Wegener Institute for Polar and Marine Research

Research and Technology Centre Westcoast
of the University of Kiel

Centre for Marine and Atmospheric Sciences
of the University of Hamburg

Brockmann Consult

Regional Office of the Schleswig-Holstein
Wadden Sea National Park

LOICZ Reports and Studies No. 33

Impressum

Publisher

LOICZ International Project Office at the GKSS-Research Center Geestacht GmbH
Institute for Coastal Research
Max-Planck-Straße 1
D-21502 Geesthacht
www.loicz.org

The Land-Ocean Interactions in the Coastal Zone Project is a Core Project of the “International Geosphere-Biosphere Programme and the International Human Dimensions Programme on global environmental change, of the International Council of Scientific Unions.

The LOICZ IPO is financially supported by the Institute for Coastal Research at GKSS in Geesthacht, Germany. GKSS is part of the Helmholtz Association of National Research Centres.

Concept of the Atlas

Roland Doerffer (GKSS)

Design & Production

Julika Doerffer (GKSS)
This atlas was realised with the open source desktop publishing programme ecribus (www.scribus.net)

Editorial board

Franciscus Colijn (GKSS), Roland Doerffer (GKSS) and Justus van Beusekom (AWI)

Citation

Doerffer, R., Colijn, F., van Beusekom, J. (Eds.) (2008). Observing the Coastal Sea - an Atlas of Advanced Monitoring Techniques. LOICZ Reports & Studies No. 33. Geesthacht, Germany: GKSS Research Centre.

ISSN

1383 4304

Cover

The cover photos show from left to right the research vessel "Prandtl", parts of an oil sensitivity map by Ulrike Kleeberg, GKSS scientists in the Sylt tidal flats, information layers in a GIS (AWI).

Disclaimer

The designations employed and the presentation of the material contained in this report do not imply the expression of any opinion whatsoever on the part of LOICZ or the IGBP and the IHDP concerning the legal status of any state, territory, city or area, or concerning the delimitations of their frontiers or boundaries. This report contains the views expressed by the authors and may not necessarily reflect the views of the IGBP and the IHDP.

The LOICZ Reports and Studies Series is published and distributed free of charge to scientists involved in global change research in coastal areas.

Observing the Coastal Sea

An Atlas of Advanced Monitoring Techniques

Why this atlas

In a period where global change becomes obvious, regarding climate, habitats, biodiversity and hazards, monitoring of changes is an important issue for science and management. The state and the development of the environment need to be observed and analysed and have to be reported to agencies and policy to trigger measures in case of unwanted trends. Public awareness is needed for acceptance of changing lifestyles and adaptation to new conditions.

Data are needed to understand the complex interactions between compartments of the environment on different spatial and temporal scales. They are needed to feed and validate models, which are necessary to quantify the manifold interaction of processes and to describe possible future developments in form of scenarios. New advanced observation and information processing technologies allow a much deeper and quicker insight into the environment, but they have to be integrated into monitoring services.

Within the framework of the HGF MARCOPOLI research programme of GKSS and AWI, one of the themes is the development of new observational techniques and information processing and assessment procedures for coastal waters. With this atlas we present results of this programme and demonstrate how the new techniques are applied.

The coastal zone is estimated to provide far more than half of all global ecosystem goods and services to nature and humanity. This implies multiple and interdisciplinary research, which is addressed globally by the Land-Ocean Interactions in the Coastal Zone, LOICZ, project. Today it operates under the auspice of the International Geosphere Biosphere Programme (IGBP, Stockholm) and the International Human Dimensions Programme on Global Environmental Change (IHDP, Bonn). Its office is hosted by the GKSS Research Centre. Since 1993 LOICZ has been challenged to address issues of biogeochemical cycles and fluxes, the river catchment-coast water continuum and, collectively with other projects, the shelves and continental margins. Integrating human dimensions is a new key agenda item in LOICZ. Identifying the right indicators and to employ the latest state of the art of monitoring techniques are pivotal to LOICZ. We are therefore glad to publish this volume as part of its globally distributed Reports and Studies series. The MARCOPOLI outcomes reflect an important milestone in contribution to the world wide growing and complex challenges for a meaningful continued observation of our coastal seas.

Franciscus Colijn (Director Institute for Coastal Research GKSS)

Roland Doerffer (Coordinator MARCOPOLI Monitoring Research Programme)

Hartwig Kremer (CEO IPO LOICZ, GKSS)

Content

What is Monitoring Research

The mission of environmental monitoring agencies is to provide all the information which is necessary to understand the state and development of a section of the environment, such as the coast, with a minimum of effort and costs. Monitoring research has to develop and provide the necessary tools, including instruments, procedures and strategies, to fulfill these requirements.

One part of monitoring research is to study advanced observation methods and to develop corresponding sensors. This is a wide field with very different requirements: Common to all monitoring techniques is the requirement for reliability, robustness, high sensitivity, minimal maintenance, automation and standardisation. The methods should be easy to use, they should cover a large range of the variable to be measured and should be, if possible, non-destructive and insensitive to other variables.

The second important area of hardware development is the instrument infrastructure, including fixed and moving platforms, remote control, data storage and transmission systems, quick look analysis and failure resistance. A strong need exists for automatic or even autonomous systems.

For all new instruments, procedures have to be developed to qualify, test, calibrate and validate the instruments and data. Algorithms have to be developed to derive the variables of interest from the primary physical variables, such as a concentration measurement from a specific light absorption spectrum. The scope of an instrument and a procedure has to be determined as well as the errors involved.

In national and international programmes all instruments and procedures have to be standardised, intercalibration, round robin calibration and validation procedures have to be developed and all accepted procedures have to be documented in form of protocols.

Another wide field is the research for optimum monitoring strategies. This includes investigations to find an optimum sampling strategy with respect to sample locations and temporal resolution. This, in turn, necessitates information about spatial and temporal distribution patterns of the variables of interest. The impact of an (extreme) event can easily be missed and then lead to a misinterpretation of an observed state or development. Furthermore, the selection of variables is an important issue. Proxy variables which are relatively easy to measure as well as indicators may be used to reduce the effort significantly. However, this requires knowledge about possible relationships between different variables, the stability of these relationships, their scope and errors and uncertainties. It has to be known how frequent proxy relationships have to be validated and corrected. Strategic research includes questions of representativity of sample stations and selection of diagnostic sites and transects.

Procedures have to be developed to establish long time series and include historical data sets and which allow merging of different data with different quality into a homogeneous data set.

Of particular interest are procedures to use the synergy of different monitoring systems, such as remote sensing, in situ sampling, transects with ferryboxes and time series at fixed stations. Since different sensors and platforms provide information about different variables on different temporal and spatial scales, these procedures require process models to integrate the different data and to reveal the cause and effect interrelationships between the variables on different temporal and spatial scales. Furthermore, data assimilation procedures are necessary to continuously update and correct models.

Finally, the required information has to be retrieved and visualised from the vast amount of data. This requires sophisticated information management tools, including geographic information systems (GIS) but also assessment models. This, in turn, depends on the question to be addressed. Modern approaches use hierarchical monitoring portfolio strategies, which, depending on the task, allow to combine different monitoring methods from a “tool-box” in a flexible way. In the following chapters we will present methods and their applications on all levels of monitoring research which have been developed within the context of the MARCOPOLI programme, ranging from advanced analysis of biochemical health indicators of marine mammals to remote sensing techniques and finally the highly integrated product of an oil sensitivity map for intertidal flats.

New sensors and techniques

Fundamental basis for monitoring are the methods and techniques to determine the variables of interest. They have to be sufficiently specific, sensitive, reliable and cost effective. To cover large areas and observe long term developments and also short term events, automatic systems are required for the continuous recording of data. New developments in detecting principles, sensors, computerization, miniaturisation and information processing enable us to design a new generation of equipment.

However, new instruments and methods have to be tested, qualified and documented to prove their maturity for being implemented in routine monitoring operations. In the case they should replace precursor equipment and principles it is necessary to have a sufficient overlap in time with both the previous and the new method to ensure continuity in long term records.

In this chapter we present some recent developments which were achieved in the research program and which are in the test and qualification phase before they can be used routinely.

Content

Remote sensing of zooplankton

Methods & Techniques

Introduction

A global task in marine ecology is the determination of zooplankton distributions. Zooplankton is a basic element of food chains, and due to the enormous number of species and individuals it is one of the most important trophic resources in the oceans. Knowledge about the impact of physical parameters like temperature, salinity and oxygen on the community of zooplankton species is important, but limited. Physical gradients in the water may separate communities and thus cause heterogeneous vertical distribution patterns. Recent investigations have shown the importance of such patterns for trophodynamic relationships and the understanding of climate change scenarios (Schulz et al., 2007). However, sampling performed with traditional gears, such as nets, is not capable of resolving fine-scale distributions along gradients. Unequal catch efficiencies of different net types and retention pressures due to various mesh sizes also bias results. Therefore, a new and promising concept for fast optical in-situ detection of zooplankton was developed that allows the investigation of fine scale distributions. Developments were carried out in a joint project between the Alfred Wegener Institute for Polar and Marine Research and the small and medium enterprise iSiTEC.

Methodology

Since the 1950s several approaches tried to visualise zooplankton species in-situ (reviewed by Wiebe & Benfield, 2003). The combination of digital imaging techniques combined with environmental sensors helps to achieve the goal of small-scale investigations over large ranges. However, in-situ imaging of zooplankton species presents investigators with some specific problems.

Imaging and light

With increasing magnification the amount of light from the area that has to be imaged decreases. Additionally, the distance in water between the camera and the imaged volume needs to be short, as floating particles detract image quality. High magnifications at short distances also result in a small depth-of-field (DOF). Only points in the object plane are correctly imaged on the chip area of the camera sensor. Thus, taxonomic features, important for the identification of species, can only be obtained within a narrow DOF at high magnifications. High f-values (small aperture opening) enlarge the DOF by mini- mising the circles of confusion, but reduce utilised light. Consequently, the development of illumination devices with a high light flux and precise targeting is a pivotal precondition for in-situ imaging of small planktonic species.

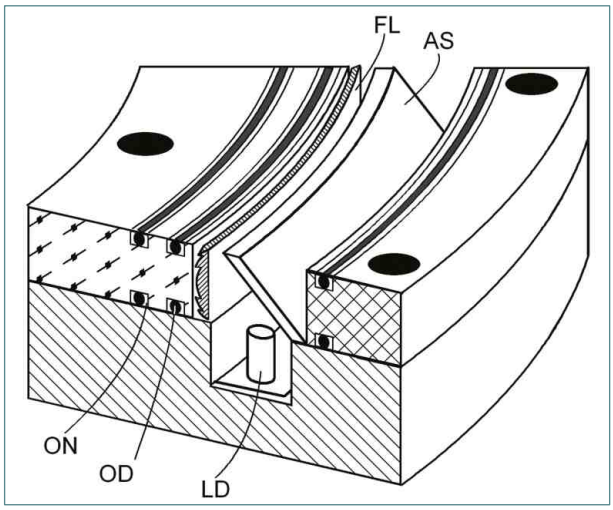

▲ Figure 1
Schematic section of the circular illumination device. AS: Circular mirror, FL: Fresnel-lens, LD: LED, OD: Seal ring, ON: Seal ring notch. Pending patent application (Schulz, 2007).

The estimation of abundances requires to quantify the volume scanned per image frame. This requires the knowledge of width, height and depth of the observed volume. While the first two are physically presented by the size of the photosensitive sensor, the principal axis is infinite and needs to be constrained. As the DOF is narrow, illumination is only necessary within this range. To avoid casting shadows a circular device was designed to illuminate scenes from all sides simultaneously. With high efficiency LED's and cylindrical Fresnel-lenses a homogeneous and constrained light field was obtained (Fig. 1). The system projects a light frame of high luminous flux into the water. The camera aims with an angle of 90° at this light frame (Fig. 2), whose depth is in the range of the DOF. Particles within this frame are illuminated, while those outside are nearly invisible. Thus, the required clipping along the principal axis is obtained for the depth axis. Image quality allows to determine major taxonomic groups and often species identification (Fig. 3). As the observed volume is rather small, species of low abundance more often remain undetected. Therefore, the developed system was named Light-frame On-sight Key-species Investigation (LOKI).

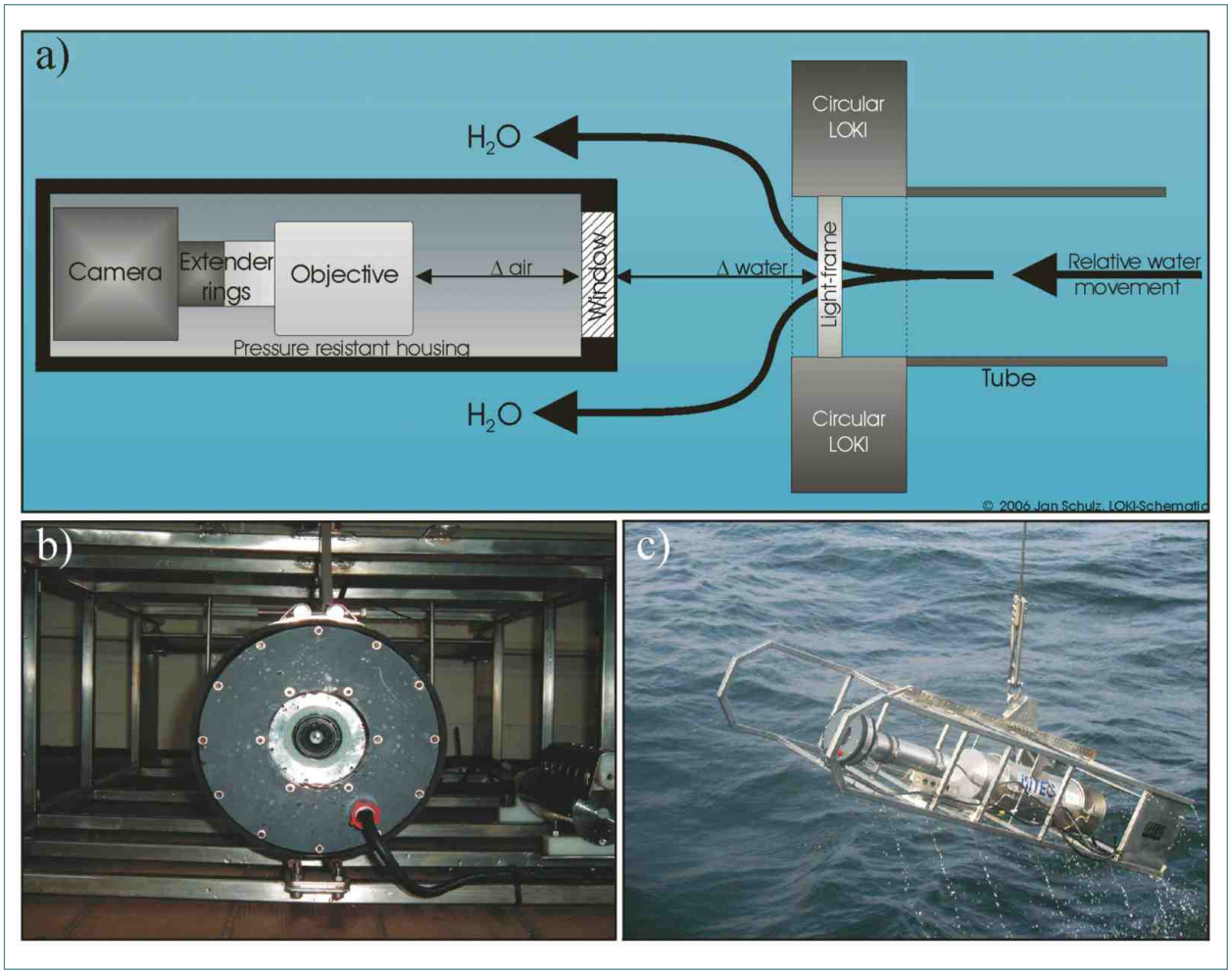

▲ Figure 2
a) Schematic overview of the LOKI application. b) View from the front through the circular LOKI illumination and into the lens of the camera. c) The prototype during an initial test in the North Sea, showing the different components. From left to right the circular illumination device, the camera housing and the main housing can be seen, bearing the PC and micro controller units. The CTD is located between the two housings.

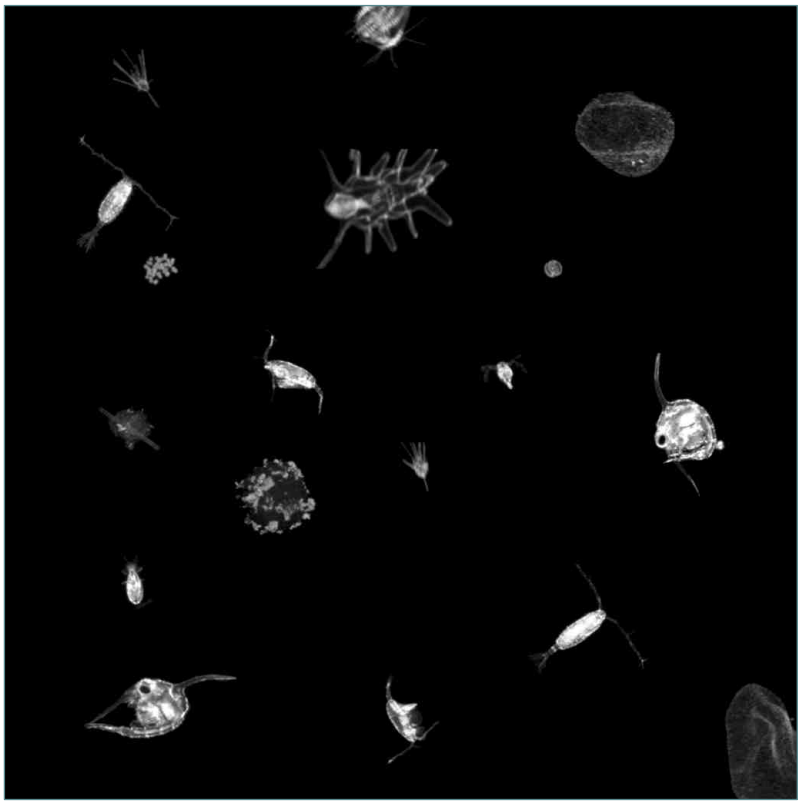

◀ Figure 3
Plankton compilation of a North Sea LOKI deployment aboard R/V Heincke (Expedition HE 266).

Remote sensing of zooplankton

Instruments & Processing

System specifications

The camera operates with a frequency of 15 frames per second and triggers the flash frequency of the illumination device. Shutter times can be adjusted down to 100 µs. In towed operation mode the movement replaces water and entrained objects between two frames. The camera is connected via GigE to a Dual Xeon® board that processes ~60 MB s^{-1} image data. Frames are preprocessed in real time in the underwater unit and only parts that contain objects of a certain size are stored as Area-Of-Interest (AOI). The computer unit communicates with several microcontroller subunits by an internal ethernet network. These subunits gather environmental information from various sensors, perform preliminary calculations and assist in the communication with the surface. Thus, every AOI can be assigned to sensor readings of the ambient environmental parameters within a time frame of one second. The communication between surface and the underwater unit is achieved by an internet protocol signal (TCP/IP) modulated onto the power supply.

A new multi frequency modem enables the use on ships with cables bearing just two-conductors for connection and operates over more than 8 km of copper coax cable. Thus, the gear can even be operated on unmanned platforms, while configuration and data access is accomplished by a remote operator via internet.

Several modules have been devised to facilitate bulk classification. The challenge is the identification of common discriminating parameters for objects imaged in any spatial orientation. Therefore, higher statistical moments, as well as texture information on the images are extracted. A competitive approach of a mixed model environment (including Linear Discriminant Analysis, Support Vector Machines, Self Organising Maps and others) in the open source R software (www.r-project.org) allows automated classification. Results can be reimported into the LOKI-Browser and aligned with the manual classification to find the best discriminating setups for different classes of species and particles.

Benchtop LOKI

Based on the experience with the field device a benchtop system was developed. It scans live zooplankton net samples aboard or preserved samples in the laboratory. The sampling volume is imaged in a flow cell, giving the system the name Flow-cell-LOKI (FLOKI). A fluid circulation system, controlled by hydrostatic pressure and pumps, allows to process samples and to filter objects from the rinsing solvent into a sampling reservoir (Fig. 4). The system has been successfully tested under field conditions during an expedition with the research vessel Polarstern in 2007.

Conditions can be adjusted prior to analysis and modified if necessary to obtain brighter and better illuminated images than with LOKI (Fig. 5). Thus, they are more appropriate for taxonomic identification, but in return lack information about the original ordination among two objects in their natural environment.

Processing and outlook

To handle the enormous number of images and environmental data an upgradable SQL database was designed. An interface is provided by the interactive LOKI-Browser that allows accessing the data backend and enables investigators to make specific enquiries. It allows exploring the distribution of species and other objects considering the assigned readings.

A drag and drop function allows an easy manual classification of images on the monitor. The underlaying classification tree can be retroactively enhanced or modified without losing existing allocations.

Further information

Additional project information, concept and ideas:
http://www.awi.de/en/research/research_programme/topic_co/co4_observation_and_information_for_coastal_management/

Remote sensing of zooplankton and background information:
www.code10.info

Hard and software development:
iSiTEC GmbH, Stresemannstraße 46, 27570 Bremerhaven, Germany: www.isitec.de

Image recording and processing:
Medea AV, Am Weichselgarten 23, 91058 Erlangen, Germany: http://www.medea-av.de

Funding

This joint project was funded by the Bremerhavener Gesellschaft für Investitionsförderung und Stadtentwicklung mbH (BIS 56008/2-Z and BIS 68036/2-Z), cofinanced by the European Community.

Authors

Jan Schulz, Dirk Mengedoht, Kristina Barz, Adrian Basilico, Milan Henrich and Hans-Jürgen Hirche (AWI)

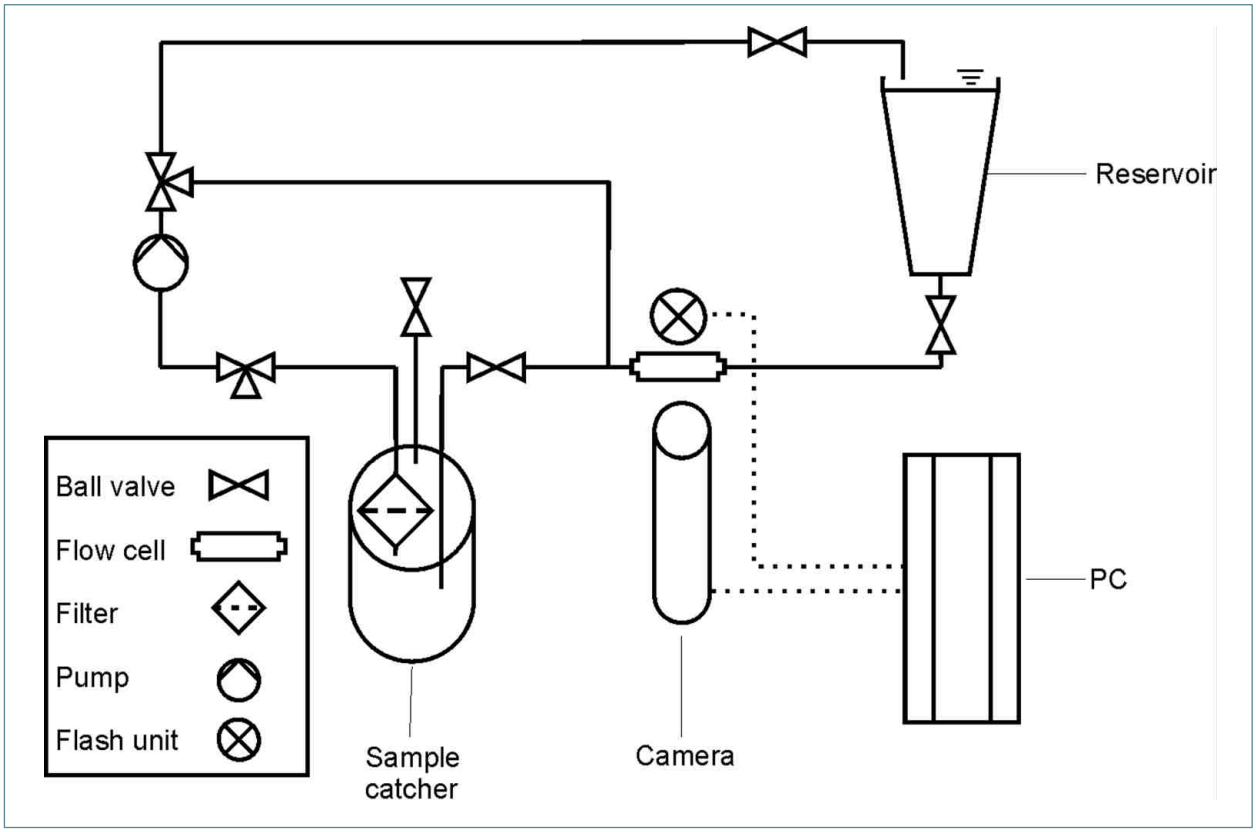

▲ **Figure 4**
Schematic of the FLOKI imaging system. A suction pump creates a flow from the reservoir through the flow cell. In a recovery tank species and objects are removed from the rinsing solvent, before entering the pump. Thus, samples can be scanned without loss, while the rinsing solvent is recycled. For cleaning purposes or in case of plugging at high densities pumping direction is reversible. Additionally the system can be easily disassembled for servicing.

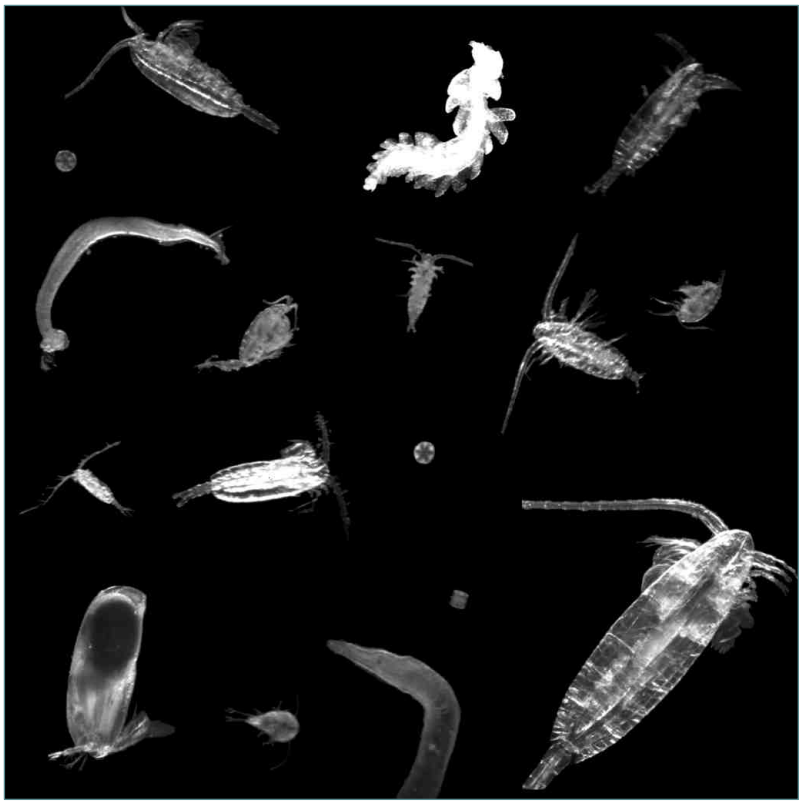

◄ **Figure 5**
Plankton compilation of pictures from the arctic ocean and North Sea samples with the FLOKI benchtop system.

Differentiation of major algal groups by optical absorption signatures

Methods & Implementation

Introduction

Phytoplanktonic microalgae form the basis of most marine ecosystems. Knowledge of the taxonomic composition of phytoplankton is important for many ecological and biogeochemical aspects. Identification of the major taxonomic groups can help to identify algal bloom organisms, to estimate the role of functional groups in the food chain and to tag or forecast harmful algal blooms (HABs) (Millie et al., 2002).

Optical characteristics of algae are specific for each algal group. To discriminate algal groups in a monitoring system, techniques are needed to measure these specific optical properties. One possibility is to use the chlorophyll fluorescence excitation spectra (AOA, bbe Moldaenke, Germany). Fluorescence techniques are simple, relatively sensitive, and thus can be applied in natural waters. However, only the chlorophyll pigments can be detected. By using the absorption spectrum of a water sample also other pigments (photo-protective and photosynthetic) can be identified. Most major groups can be discriminated by a group-specific pigment combination, e.g. chlorophyll-b occurs only in chlorophytes, prochlorophytes and euglenophytes etc., and phycobiliproteines only in rhodophytes, cryptophytes and cyanobacteria. Groups with the same pigment composition can, however, be discriminated due to group-specific pigment ratios. As these pigments have specific absorption maxima which are visible in a total absorption spectrum of a water sample, they can be measured with the newly developed PSICAM technique. It allows to measure a sample of water in real time and to use this data to differentiate algal groups online.

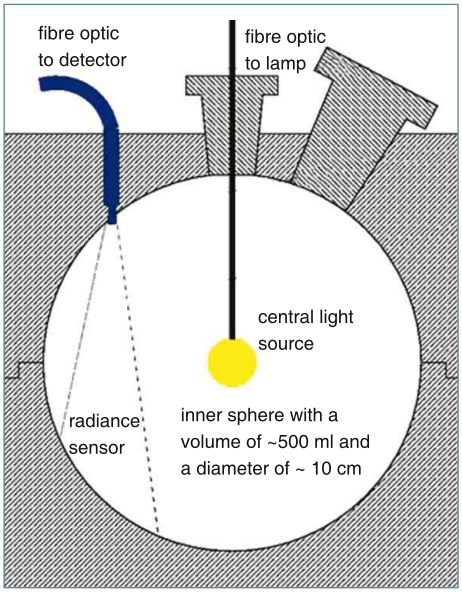

► **Figure 1**
Schematic interior view of the PSICAM block
The block consists of a white material with a reflectivity of ~99.9 %. The inner sphere is filled with the water sample.The photons from the central light source get reflected at the wall multiple times and travel for optical path lengths between 1-3 m until they reach the radiance sensor. Due to the diffuse light field, additional scattering by particles has a negligible effect on the absorption determination so that failures due to adverse scattering effects and self shadowing are minimised.

Methods and Techniques

The absorption meter (point-source integrating-cavity absorption meter, PSICAM) (Fig.1 and 2) was developed to measure the low absorption by phytoplankton in natural waters (Kirk, 1995, Röttgers et al., 2007). It can 1) measure pure absorption without the error caused by particle scattering, 2) it is sufficiantly sensitive even for very clear water, and 3) it can be used unattended in a flow-trough mode. With a PSICAM the total absorption by all water constituents can be determined, namely phytoplankton, gelbstoff and detritus.

In seawater samples only phytoplankton pigments show narrow absorption peaks in the range between 350 and 700 nm. The position and the relative amount of these absorption maxima can be extracted using common spectral analysis techniques like the calculation of the fourth derivatives (Fig. 3). A database of absorption and fourth derivative spectra from different cultured algal species of all major taxonomic groups was established. It includes information of species- , class- and group-specific characteristics. The data also includes taxon-specific variations as the individual pigment composition partly depends on the genetic, photo-acclimative and photophysiological status of the algae. This database and a robust mathematical correlation technique are used to determine the abundance of each algal group in a sample.

Implementation

Tests were performed to assess the reliability of the algal group identification. The absorption spectra of individual cultured species from various groups were combined mathematically. In the combined absorption spectrum the abundance of each group was determined. These tests were performed for each group and for some thousand group combinations. One example of the outcome is shown in Fig. 4.

The implementation of a PSICAM instrument in a FerryBox system will allow to identify the absolute phytoplankton biomass and its major taxonomic groups online and in real time. In case of an algal bloom, this technique can identify the major group or even some individual species that are known to build HABs.

Authors

Rüdiger Röttgers and Steffen Gehnke (GKSS)

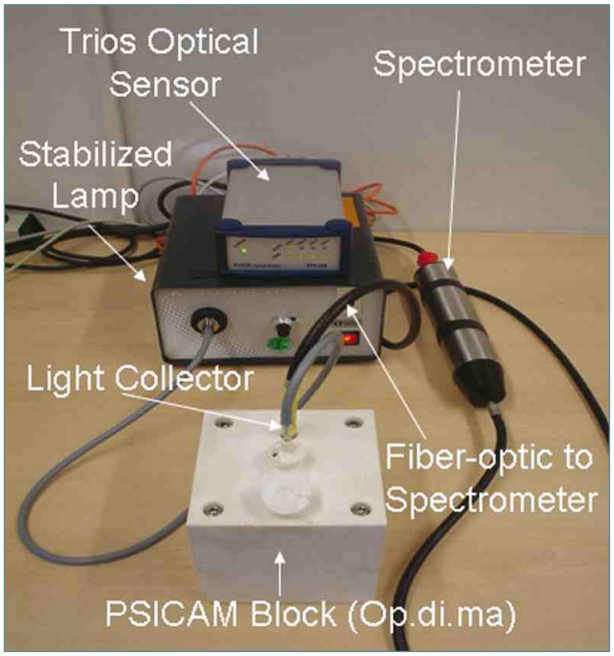

▲ Figure 2
The laboratory unit of the Point-Source: Integrating-Cavity Absorption Meter (PSICAM).

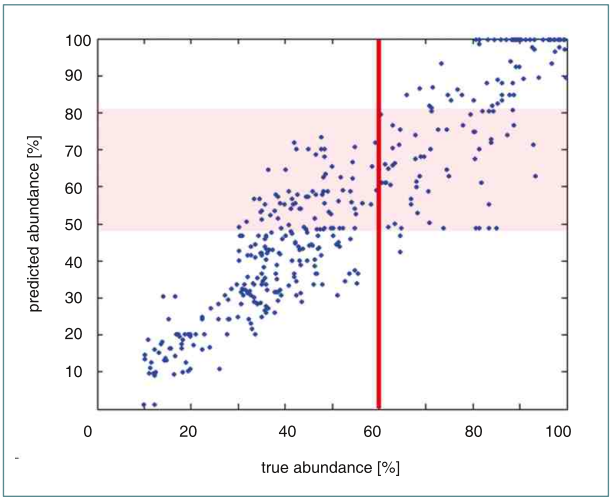

▲ Figure 4
Example for a simulation of a mixture of green algae and diatoms. The x-axis gives the retrieved percentage of diatoms in the composed sample (e.g. 60%, red line). The y-axis shows the percentage of diatoms identified by the program (e.g. 50-80 %, pink bar).

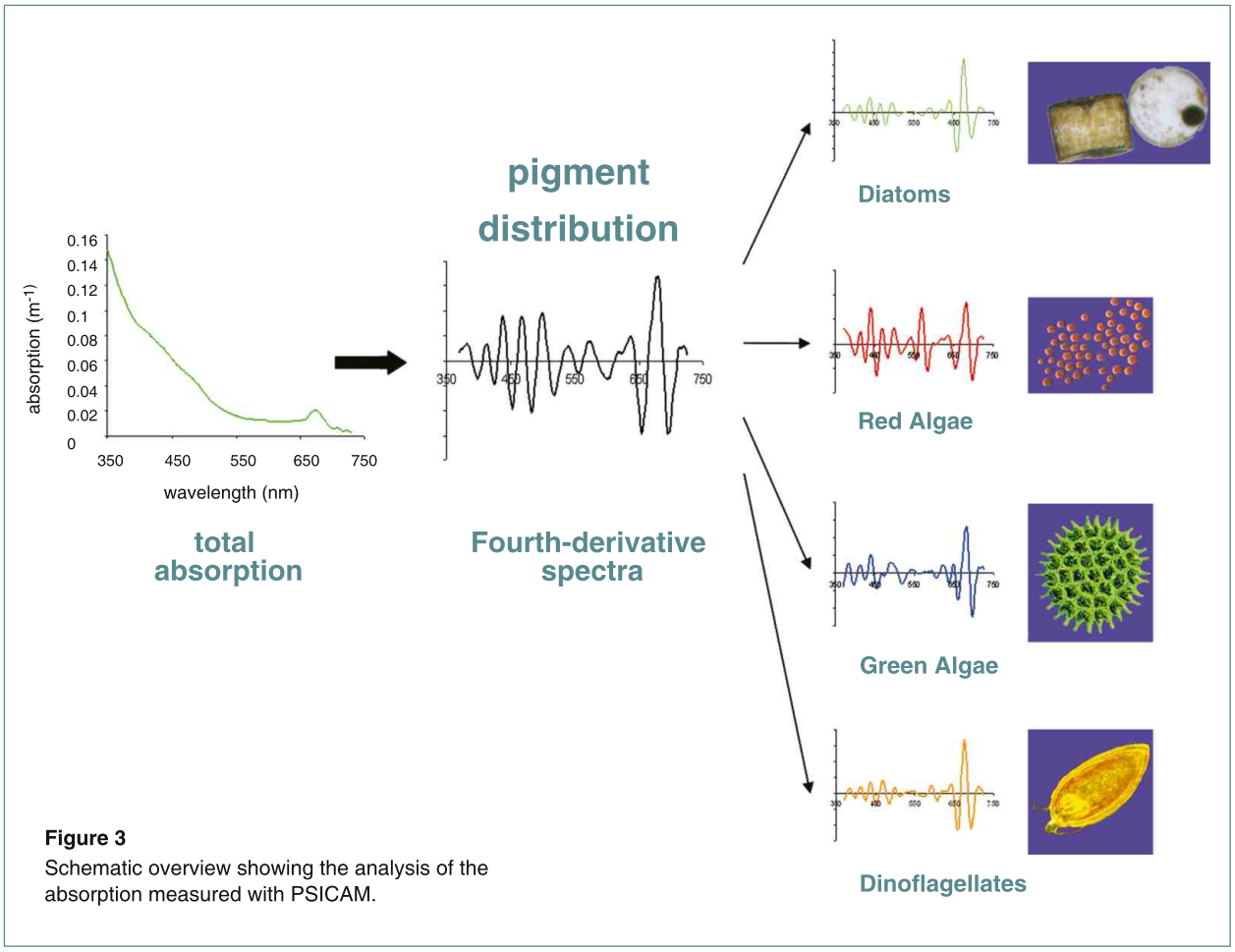

Figure 3
Schematic overview showing the analysis of the absorption measured with PSICAM.

Submarine groundwater discharge in coastal regions: development of a new sampling technique

Methods & Techniques

Introduction

At least since the days of the Romans the discharge of freshwater from submarine springs has been known. Long overlooked and considered as a “local phenomenon”, several studies underlined the relevance of submarine groundwater discharge (SGD) during recent years. Associated with submarine groundwater discharge is the release of nutrients, xenobiotics, as well as trace gases. Furthermore, SGD affects hydrological budgets as well as landside studies on groundwater renewal. Recent data compilations revealed the worldwide occurrence of SGD in coastal areas. For example, in the Mediterranean Sea a freshwater volume of more than 300 m^3/s is discharged from the seafloor at a single site. For comparison, this amount is three times larger than the discharge by the river Ems.

Methods & Techniques

In porous, sandy sediments of the North Sea and the Baltic Sea it is difficult to exactly locate the position of discharge sites. One way is to analyse the composition of porewater, the water filling the spaces between the sediment grains. But sampling of porewater in porous or sandy sediments is often a complex task, which requires new geochemical and geophysical techniques.

For investigations of seawater and freshwater flow at freshwater discharge sites we developed the Rhizon In Situ Sampler (RISS, Fig. 1). This device can be deployed in shallow coastal zones but also in deeper waters near the continental margins.

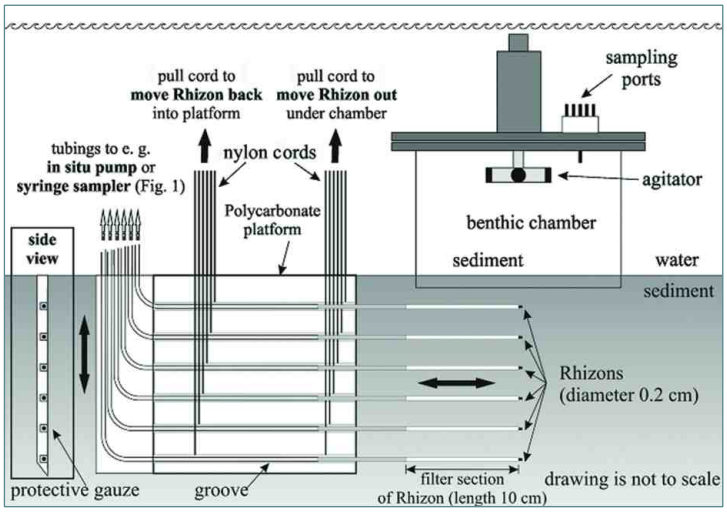

▲ **Figure 1**
Schematic diagram of a RISS (Seeberg et al., 2005) combined with a benthic flux chamber. Porewater profiles can be determined underneath a benthic chamber or a flow chamber.

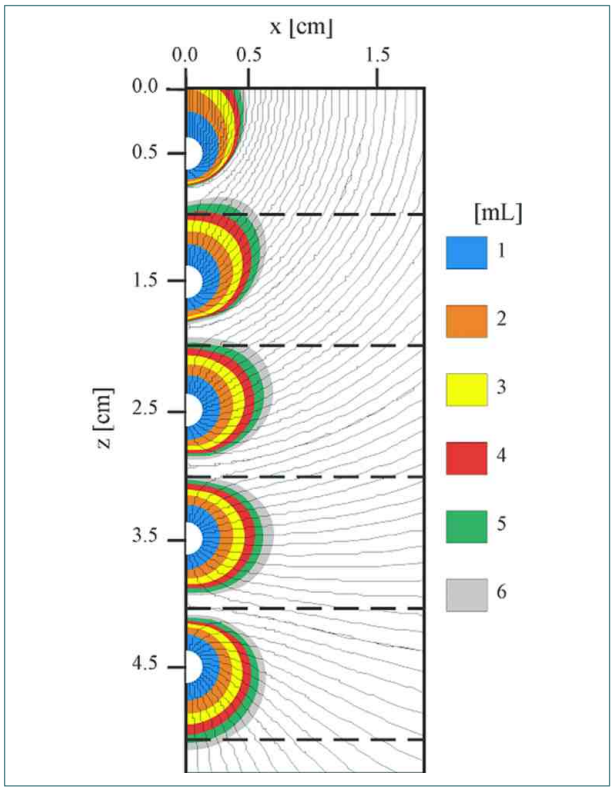

▲ **Figure 2**
Results of numerical modeling, applying the COMSOL software package, of the flow field and the catchment areas around Rhizons.

The key parts of our sampling device are Rhizons, which are used in soil research for sampling water in soils from the unsaturated zone. Rhizons are made of hydrophilic porous polymer tubes with a typical pore diameter of 0.1 µm. The outer diameter of a Rhizon is 2.4 mm and the filter section has a length of 5 or 10 cm. For the porewater sampling, in situ peristaltic pumps are applied. The entire sampling procedure is computer controlled.

With laboratory experiments and by numerical modelling we investigated the minimal spacing of the sampling ports (Fig. 2). The in situ porewater sampling provides, due to its neglibile impact on the sediment structure, data for the modelling of freshwater flow at discharge sites. By these means the freshwater discharge was studied in the Wadden Sea at Cuxhaven (Fig. 3 and 4). In this region SGD occurs at distinct spots (“sand boils”) and diffuse flow over larger areas (Fig. 5). Associated with the discharge is the release of nutrients and of trace gases like radon and methane.

Authors

Michael Schlüter, Stefan Bartsch and Torben Gentz (AWI)

◄ **Figure 3**
Examples for a “sand boil”, where freshwater is flowing out of the sediment.

▲ **Figure 4**
Sediments at low tide of the Wadden Sea area at Cuxhaven (Germany). This area is affected by the discharge of freshwater. The discharge occurs at distinct spots (“sand boils”) and as diffuse flow through sediments.

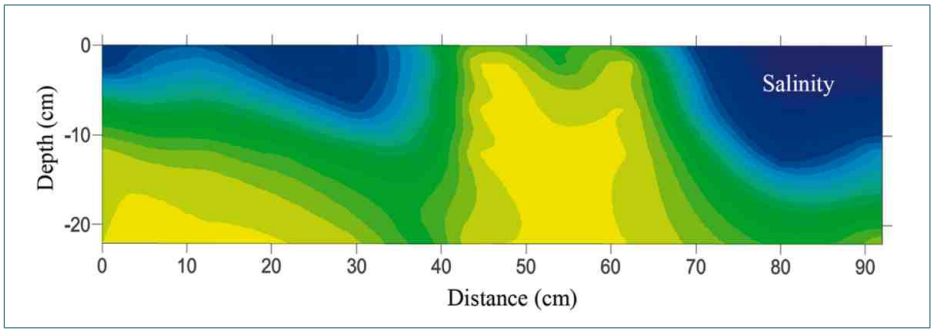

▲ **Figure 5**
Since the small Rhizon sampler has a negligible effect on the flow field around a sand boil, it is possible to derive the 2D flow field of freshwater at these freshwater discharge sites. The picture shows that freshwater (yellow) dominates in the deeper parts of the sediment and that saline water (blue) dominates in the surface layer. Only at distinct areas of the sediment, does the freshwater protrude through the surface layer.

ALGADEC - Detection of toxic algae with a semi-automated nucleic acid biosensor

Methods & Techniques

Introduction

Microalgae are the major producers of biomass and organic compounds in the aquatic environment. Among the marine microalgae there are 97 toxic species (mainly dinoflagellates) known to have the potential to form "Harmful Algal Blooms", the so called HABs (Fig. 1). In recent decades, the public health and economic impacts of toxic algae species appear to have increased in frequency, intensity and geographic distribution (Zingone and Enevoldsen, 2000; Daranas et al., 2001; Hallegraeff, 2003; Moestrup, 2004). In order to minimise the damage to human health or living resources, such as shellfish and fish, as well as economic losses to fisherman, aquaculture and the tourist industry, efficient monitoring methods are required for monitoring potentially toxic algal species (identification and quantification) (Andersen et al., 2003). The identification of unicelluar algae with conventional methods like light microscopy requires a thorough taxonomic expertise and is time-consuming. It is also costly if larger numbers of samples need to be processed. In some cases toxic and non-toxic varieties (strains) belong to the same species. They are morphologically identical, and cannot be distinguished by conventional methods. Consequently, improved monitoring methods that allow rapid detection and counting of toxic algae are needed. In the past decade, a variety of molecular methods have been adapted for the detection of harmful algae. Most of these techniques focus on the genetic information in the DNA or RNA (both nucleic acids) of the organisms. However, most of these new techniques are lab-based and not suited to be carried out in the field.

Methods and techniques

In order to detect toxic algae in the field, a portable semi-automated nucleic acid biosensor was developed in the ALGADEC project (www.algadec.net). This device enables the electrochemical detection of microalgae from water samples in less than two hours, without the need of expensive equipment. The detection of the toxic algae is carried out on a sensor chip and is based on the so-called sandwich hybridisation technique (Fig. 3).

Sandwich hybridisation

A sandwich hybridisation is a molecular probe-based method for rapid target identification that uses two molecular probes targeting ribosomal RNA (rRNA). A capture probe bound to a solid surface immobilises the target ribosomal RNA and forms a hybrid complex with a second signal probe. An antibody-enzyme complex binds to the signal moiety of the signal probe and reacts with a substrate forming an electrochemical current on the biosensor (Metfies et al., 2005).

Molecular Probes

Molecular probes are short oligonucleotides (18-25 bases) that are complementary to specific sequences in the genomes of the target organism. Ribosomal RNA genes are widely used targets for the development of molecular probes. They appear in high numbers in target cells and have both conservative and highly variable regions, which make it possible to develop probes that are specific at different taxonomic levels (Groben et al., 2004).

▲ Figure 1
Bloom of *Noctiluca scintillas* in October 2002, Leigh, New Zealand.

The ALGADEC detection device is semi-automatic. The main steps are executed automatically but filtering and a lysis procedure (digestion of the filtered material) has to be done by hand. The core of the biosensor is a multi-probe chip (Fig. 4) that can be used for the simultaneous detection of 14 different toxic algae plus two controls. Thus, it can be used to detect the species composition in harmful algal blooms.

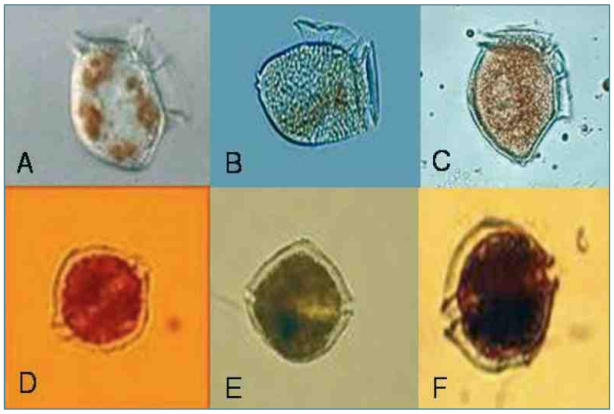

▲ **Figure 2**

Pictures of the toxic dinoflagellates **(A)** *Dinophysis acuta* **(B)** *Dinophysis accuminata* **(C)** *Dinophysis norvegica* **(D)** *Alexandrium minutum* (**E)** *Alexandrium ostenfeldii* **(F)** *Alexandrium tamarense*.

The photos illustrate the high morphological similiarity and the challenge for the identification of the species by conventional methods.

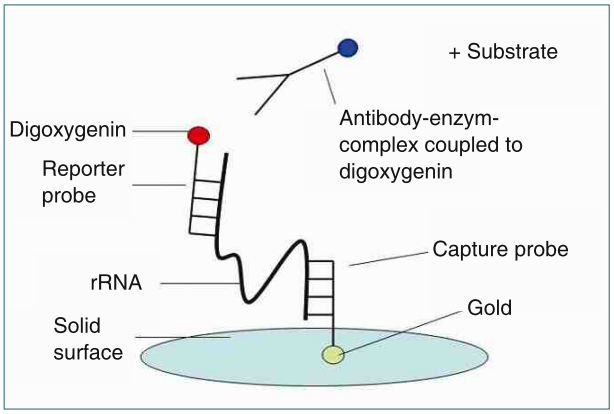

▲ **Figure 3**

Schematic drawing of a sandwich hybridisation. The target organism is identified by binding of two species specific molecular probes to the ribosomal RNA (rRNA). One of the probes is immobilised on the surface of the sensorchip and the other is coupled to digoxigenin, which binds to an antibody enzyme-complex. The enzyme catalyses a redox-reaction that can be measured as an electrochemical signal.

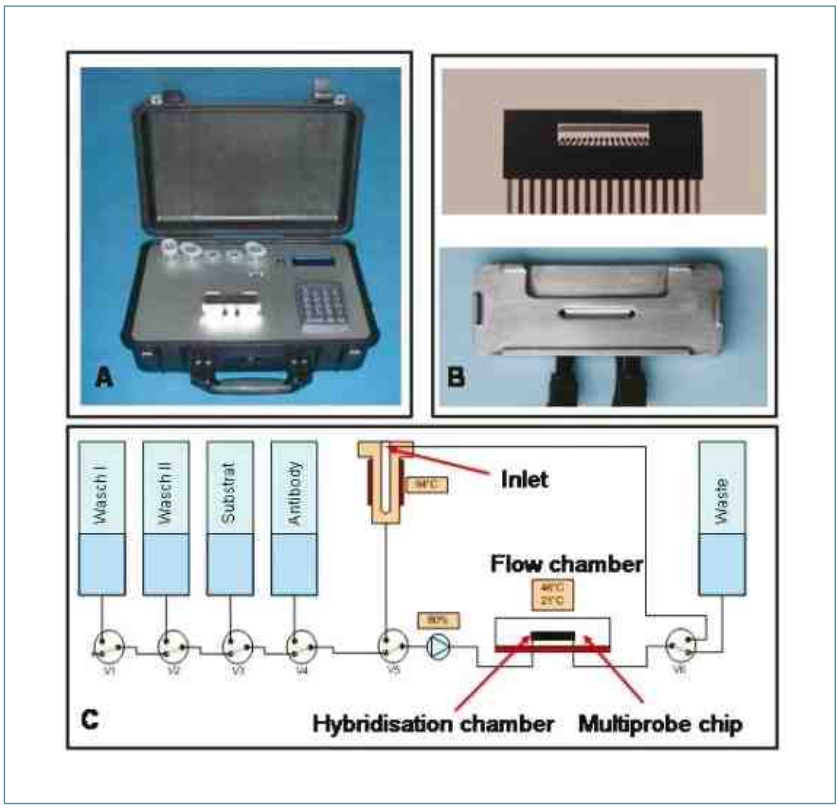

◄ **Figure 4**

(A) The biosensor in briefcase format. Subsequent to a manual filtration of a water sample and addition of the lysis-buffer, all steps involved in the detection of toxic algae are carried out automatically in the device.

(B) The top part shows a disposable multiprobe sensor chip with 16 electrodes. The multiprobe chip allows the detection of 14 analytes and a positive, as well as a negative control in parallel. The lower part shows the hybridisation-chamber that hosts the detection reaction. Prior to the detection reaction, the multiprobe sensorchip has to be inlayed into the block with the hybridisation chamber.

(C) Process chart of the nucleic acid biosensor. After addition of lysis buffer, the filtered sample is inserted to the inlet and pumped into the hybridisation chamber. The different steps of the diction reaction like hybridisation, washing, addition of redox-substrate are executed automatically. Temperature regulation in the hybridisation chamber is carried out by a pellitier element.

ALGADEC - Detection of toxic algae with a semi-automated nucleic acid biosensor

Implementation & Results

Implementation

The goal of ALGADEC was the automatic detection of the different toxic algae species in three different areas in Europe: Skagerrak in Norway, the Galician coast in Spain and the area of the Orkney Islands in Scotland. Thus, chip sets for different toxic algae have been developed and tested in the lab for specificity with cultures of known toxic and non-toxic varieties of the same species (Diercks et al., 2008). The applicability of the ALGADEC biosensor for the detection of toxic algae in the hands of lay persons was evalutated in a workshop with end users of the device. After an introduction of the end users to the handling manual, contaminated field samples from the Orkney Islands (UK) were successfully screened by the end users for the presence of cells from the genus Pseudonitzschia. Chip sets for the following toxic algae are currently available:

- *Dinophysis sp.*
- *Pseudonitzschia sp.*
- *Lingolodinium polyedrum*
- *Chrysochromulina polylepis*

Prospects

In the course of the ALGADEC-project it was possible to develop a semi-automatic nucleic acid biosensor for the detection of toxic algae. The functionality of the device, even in the hands of lay persons, was shown with laboratory algae cultures, field samples spiked with algae cultures and field samples with naturally occurring toxic algae. However, in the future, the system has to be calibrated and optimised in respect to sensitivity for the detection of the target organisms. The sensitivity of the device is a crucial issue and has to be adapted, to the reference values for toxic algae e.g. toxic *Alexandrium sp.* in sea water of around ~100 – 250 cells/liter.

The original idea of the ALGADEC project was to develop a nucleic acid biosensor for the detection of toxic algae. But the technology suggests an adaptation e.g. to the monitoring of microalgae in general. Therefore, molecular probes will be developed for key species of the phytoplankton of the North Sea. Furthermore, we are currently working on the automation of all steps involved in the analysis of water samples. In the long term a fully automated nucleic acid biosensor will be available that could work on its own or be implemented to the FerryBox-System in order to monitor microalgae autonomously at species level.

Authors

Katja Metfies, Sonja Diercks (GKSS) and Linda Medlin (AWI)

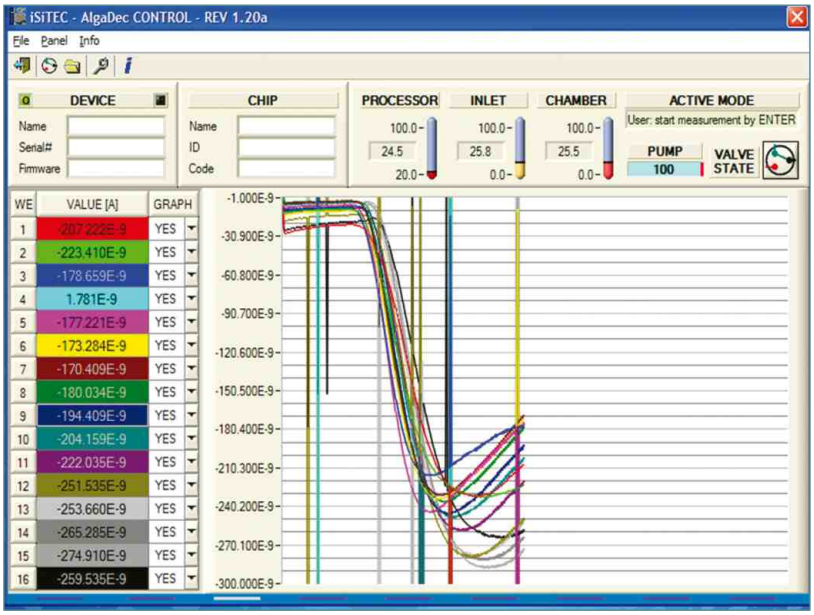

► **Figure 5**
Screenshot of the evaluation software. The different colours on the left side represent the different electrodes. The more negative a signal is, the more target nucleic acid is bound to the surface of the biosensor.

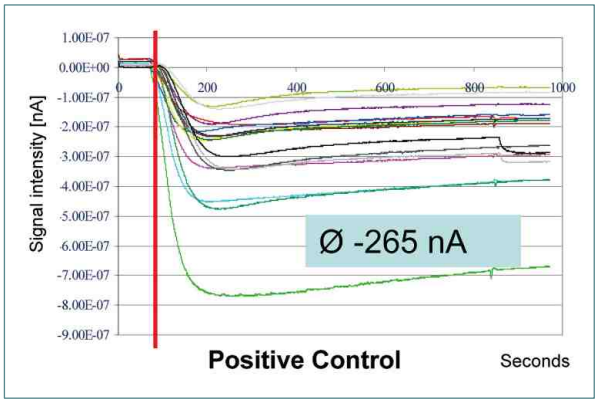

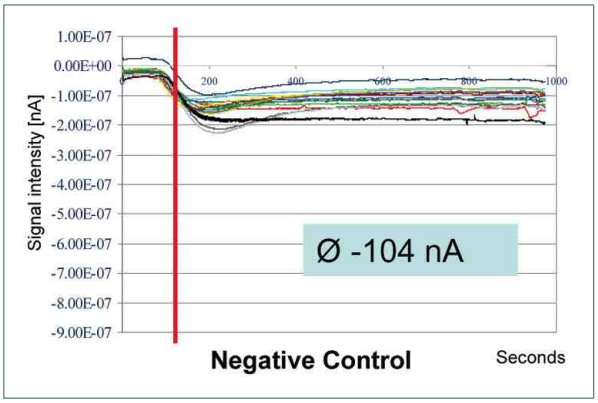

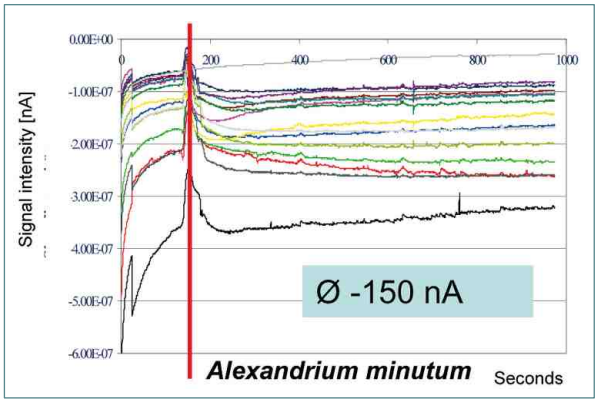

Figure 6
Identification of the toxic dinoflagellate *Alexandrium minutum* with the ALGADEC biosensor. Ribosomal RNA isolated from a laboratory culture was hybridised to a multiprobe sensor chip with 16 electrodes covered with a molecular probe that binds to the rRNA of *Alexandrium minutum*. In addition, a positive and a negative control were hybridised to similar chips. As the positive control a 60-mer oligonucleotide was used for the hybridisation. For the negative control, no target nucleic acid was added to the hybridisation solution.

▼ Figure 7
Filtration unit that was used for manual filtration. The pump can be operated manually and makes the user independent of expensive laboratory pumps.

▼ Figure 8
End user workshop of the ALGADEC project Dec. 2006 at the University of Westminster. The group of the end users was composed of biologists but also staff from a fish farm.

Remote sensing of the coastal sea

The requirement for covering large areas paired with a high temporal resolution has led to remote sensing techniques. Earth observing satellites provide a global coverage often in one day with a spatial resolution of 1 km.

Since most local processes in the coastal sea are linked to regional or even global developments it is necessary to monitor not only the area of immediate interest but also the far field in order to be able to understand the local development. Furthermore, remote sensing is the only possibility to continuously cover large areas with a high spatial and temporal resolution.

In this chapter we show optical and microwave methods, which have been developed and are in use for research in coastal waters. For a high temporal resolution, which is necessary to resolve the tidal cycle, aircraft and ground based remote sensing systems have been proven as most useful, such as special Radar equipment for monitoring changes in bathymetry due to coastal erosion processes during storm event.

Content

Current fields in the German Bight

Methods & Implementation

The background

In 2006 and 2007, partly funded by the Ministry of Science, Economic Affairs and Transportation of the state of Schleswig-Holstein and coordinated by Rathyeon Anschütz GmbH, a consortium of ten marine technology companies and the three research institutes, FTZ Westcoast, IfM Geomar and GKSS developed an environmental monitoring and warning system for oceans and, especially, for coastal waters. "Classical" sensors for environmental monitoring are combined with components for maritime safety techniques and traffic surveillance, remote sensing, model simulations and operational forecasts as well as information, alarm and warning functions. At present the OMS (Ocean Monitoring System) comprises remote sensing components like two X-band radars with wave detection software and two over the horizon radars for surface current measurement. It also includes oceanographic data acquisition units (three multi-sensor buoys and one measuring pile) as well as a data base, web-based visualisation and information structures, real time numerical modelling capacities (high resolution regional forecast models with data assimilation) and broadcast solutions for public warning.

The data centre of the OMS is located at the FTZ Westcoast in Büsum. This institute of Kiel University also operates the three buoys and the pile for ocean data acquisition. Each of the buoys is equipped with an Acoustic Doppler Current Profiler (ADCP). Among other purposes, ADCP data are used to validate measurements from the over the horizon radars (Fig. 1). Antenna arrays of these systems are deployed on the island of Sylt as well as on the jetty of Büsum harbour (Fig. 2 and 3, HF radar on Helgoland is intended).

Over the horizon radar for surface current fields measurements

A ground wave HF radar for coastal applications called WEllen RAdar (WERA) was developed at the University of Hamburg (Gurgel et al., 1999). The system is obtainable from Helzel GmbH. HF radars are operated in the 3-30 MHz frequency range (50 m to 10 m wavelength), where the electromagnetic waves can travel far beyond the horizon by ground wave propagation along a good conducting layer (salty ocean water). The signals are scattered back from ocean waves of half the electromagnetic wavelength (Bragg scattering).

The system measures the Doppler spectrum caused by moving ocean waves, which can be processed to give the speed of the ocean surface current. The second-order modulation of the sea echoes can be used to detect the ocean wave height and the wave directional spectrum. Ground wave radar systems can be installed at the coast close to the water to ensure a good coupling to the ocean and achieve working ranges up to 200 nautical miles. Because one HF radar measures the radial component of the current, a second HF radar some 10 km away is required to calculate the 2-dimensional surface current from the two radial components.

The system is running successfully. The next step is to validate the results between the different systems shown in Fig. 2 for the observed area.

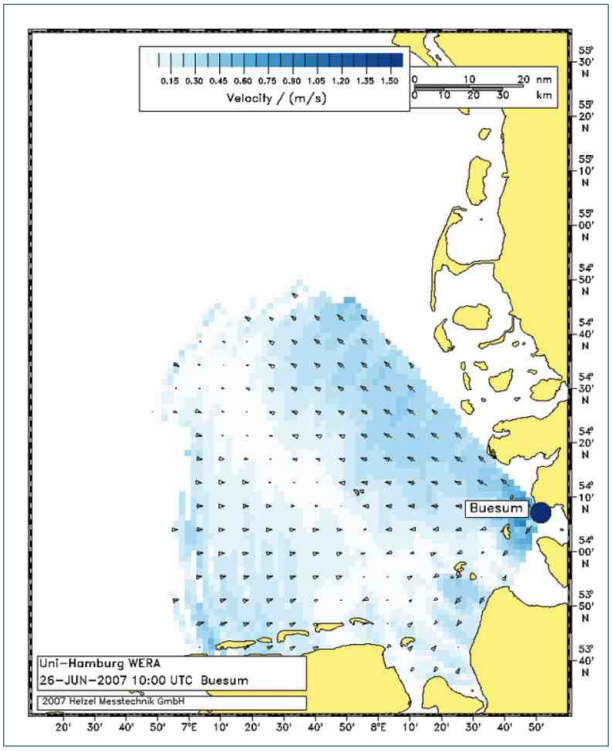

▲ Figure 1
Radial component of the ocean surface current measured from Büsum.

Authors

Klaus Heinrich Vanselow, Klaus Ricklefs (Research and Technology Centre Westcoast of the University of Kiel) and Klaus-Werner Gurgel (ZMAW, University of Hamburg)

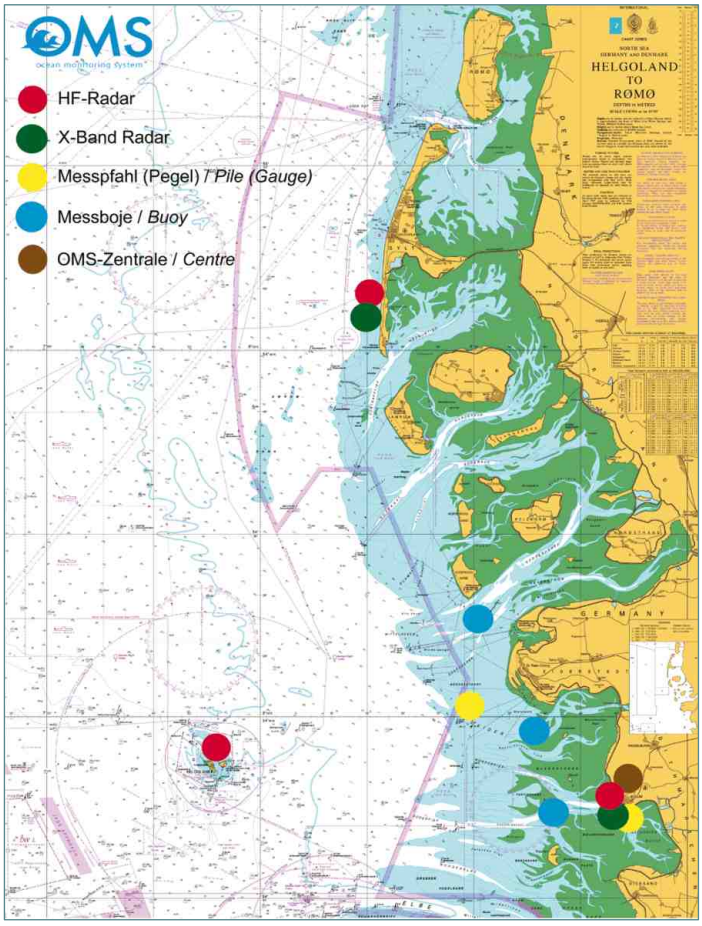

◄ Figure 2

Map of the installed systems within the OMS project. Crown Copyright and/or database rights. Reproduced by the permission of the Controller of Her Majesty's Stationery Office and the UK Hydrographic Office.

▼ Figure 3

Over the horizon radar installation at the west jetty of Büsum harbour. The system measures current maps in the range between Cuxhaven and St. Peter Ording (see Fig. 1).

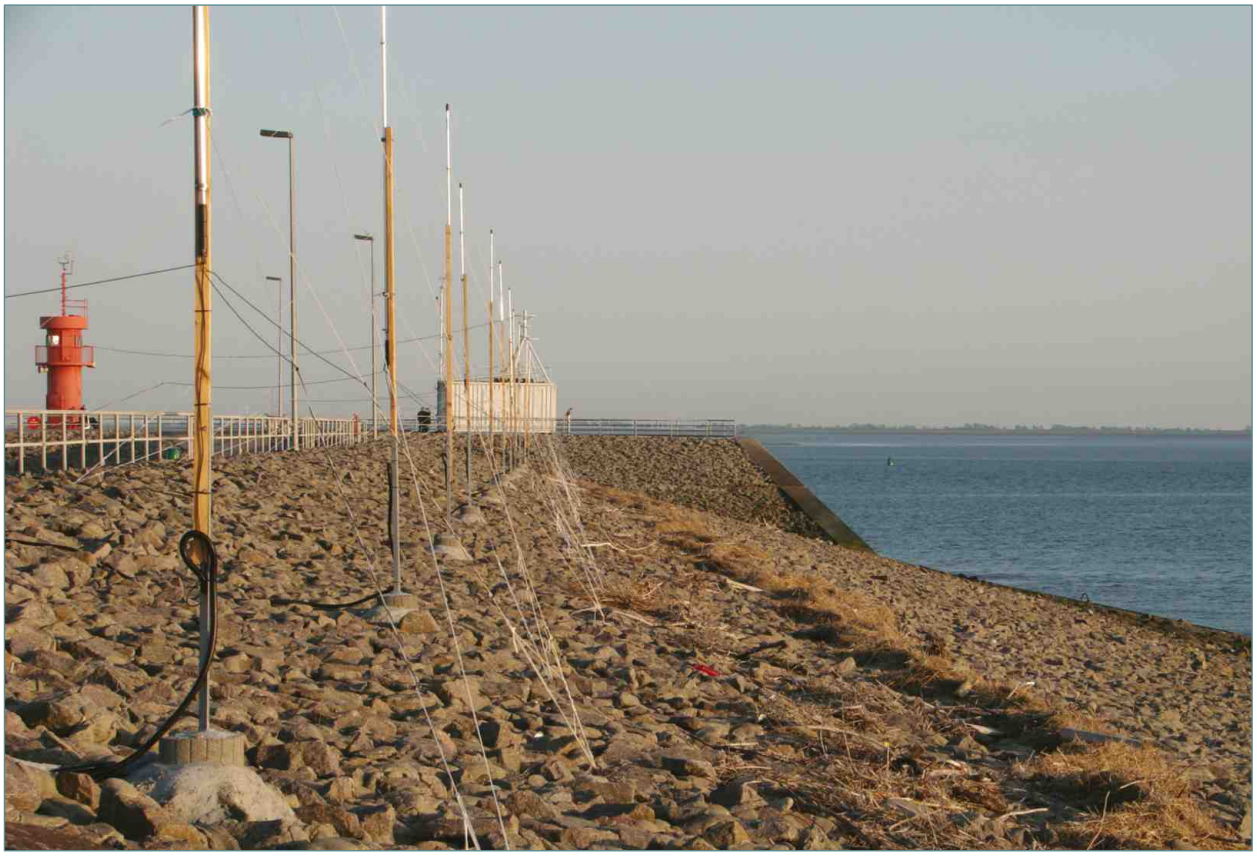

WiRAR - A marine radar wind sensor

Methods & Techniques

Introduction

A marine radar has the capability of measuring the backscatter from the ocean surface in space and time independently of light and under most weather conditions (Fig. 1). The backscatter at the X-band frequency is strongly dependent on the surface roughness, which is induced by the local wind field and therefore enables us to measure the ocean wind with microwave radars. In contrast to most wind sensors radar retrieved winds are not affected by biases due to motion and height of the sensor. Since the wind is determined from the roughness of the ocean surface far beside the platform, the structure does not interfere with the measurement.

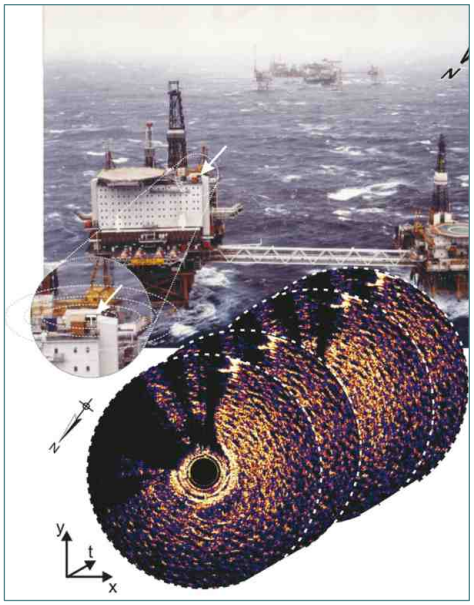

► **Figure 1**
Ekofisk 2/4 k platform of the Ekofisk oil field in the North Sea. The WaMoS system is installed at the north-west corner of the platform. In the radar images several shadows are visible, which are due to the equipment of the platform. The large backscatter in the south originates from the oil field which is visible in the background of the photo.

Methodology

WiRAR is a tool, which enables us to retrieve ocean surface winds from standard marine radars in real time (Dankert and Horstmann, 2007). The wind direction retrieval in WiRAR is based on linear features, which are visible in radar data (Fig. 2). Most of these features are associated with wind streaks or streaks from foam or material floating on the surface at scales between 50 and 500 m. Orientation of these linear features are extracted by using the Local Gradient Method (Horstmann et al., 2002; Koch, 2004). In principle the gradient of the backscatter intensity of an image (grey-level) is computed from pixel to pixel. The direction of the strongest local gradient is perpendicular to the local wind direction. WiRARs wind speed retrieval utilizes the strong dependency of the normalized radar cross section (NRCS) on the local wind vector and the imaging geometry (Fig. 3). It is described by a Geophysical Model Function (GMF), which is developed by the training of a Neural Network (NN). The only requirement for application of an NN to radar wind speed retrieval is the relative radiometric stability of the radar system. Unfortunately, marine radars are not calibrated, so that a NN has to be trained for each individual radar system.

Wind direction retrieval

In a first step a radar-image sequence is integrated over time, typically 32 images which represents 60 s of data (Fig. 1). By this integration the wind signatures are separated from other signatures. In particular patterns are removed, which are highly variable such as ocean surface waves. In the next step, the integrated radar image is sequentially smoothed and reduced to resolutions of 20, 40, and 80 m. From each of these images, local orientations are computed from the local intensity (i.e. grey level) gradients, which are normal to the local wind directions. Only the most frequent orientations in a predefined area are selected. However, it remains a 180° ambiguity. This can be removed either by determining the motion of wind patterns in radar-image sequences or by computing the cross-correlation function (CCF), which is used to estimate the shift of moving image patterns between two images.

Wind speed retrieval

To describe the dependence of the wind speed on wind direction (determined from NRCS) and imaging geometry, a NN is utilized. Therefore, the mean NRCS image (image sequence integrated over time) is subdivided into subareas, with five intervals of 300 m in range, which start at a distance of 600 m and with sectors of 5° in azimuth. Reason for this subdivision is the radial gradient in radar backscatter: the intensity decreases from the centre to the border of the radar image, as visible in Fig. 4. For every subarea the mean NRCS is determined. A NN is trained which has the following parameters as input: (1) in situ measured wind speeds , (2) radar-measured wind direction, (3) the mean radar intensities in both crosswind directions, and (4) the antenna look direction. To improve the wind speed determination, the dependencies of the NRCS on additional parameters such as sea state and atmospheric stability can be considered in the training of the NN (Dankert and Horstmann 2007). Information on the sea state can be extracted from the radar datasets (Borge et al., 1999), while atmospheric stratification conditions, such as the air-sea temperature difference and the relative air humidity, need to be measured by external sensors.

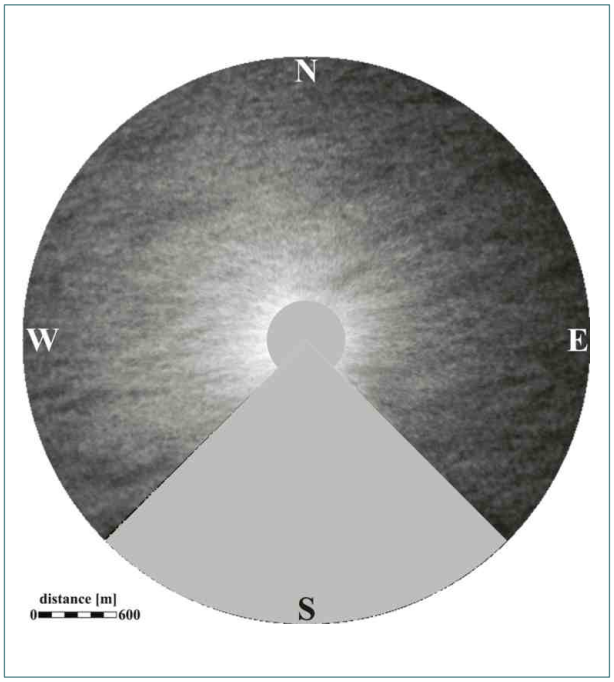

▲ Figure 2
High-resolution RAR image of the ocean surface, acquired at grazing incidence with the X-band at horizontal (HH) polarization in transmission and reception. The image is the result of an average of 32 RAR images, which were sampled with a period of 60 s. Wind-induced streaks are clearly visible at scales below 500 m.

▼ Figure 4
The image is the mean of a radar sequence. Each radar image was subdivided into bins, each of which has an azimuth of 5° and a range of 300 m as indicated by the superimposed grid. The masked areas were not considered in the investigation.

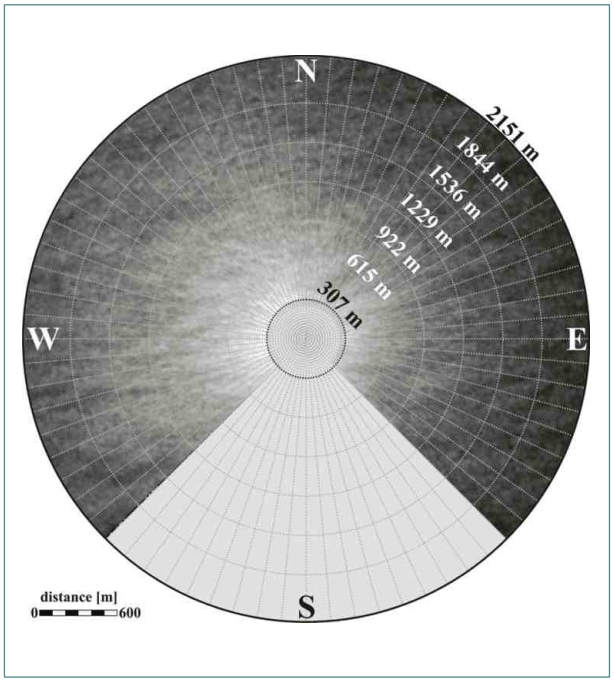

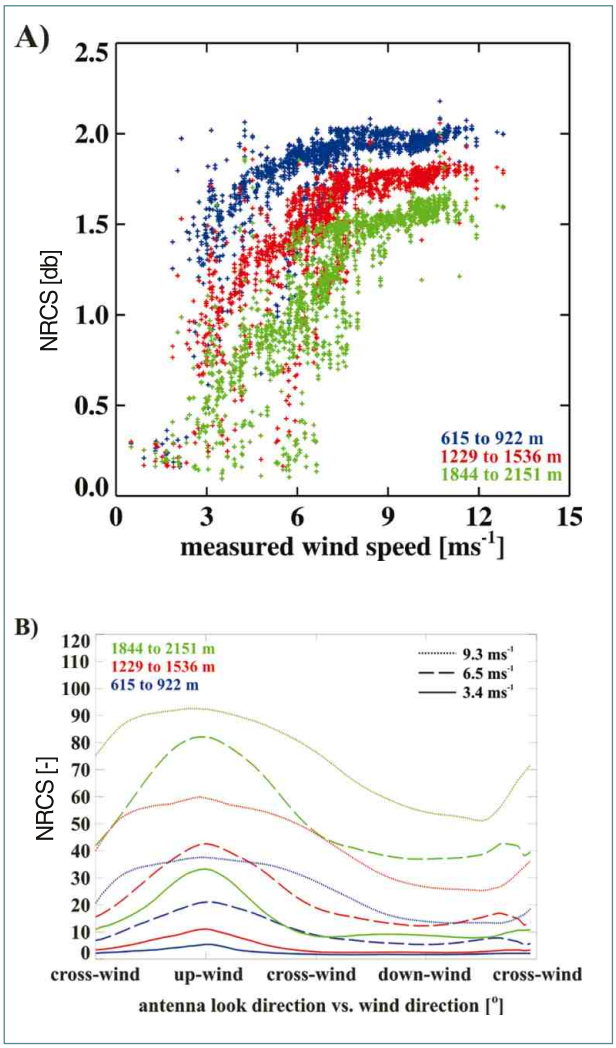

▲ Figure 3
Dependence of the NRCS on **a)** wind speed and **b)** on wind direction with respect to the radar viewing direction.

WiRAR - A marine radar wind sensor

Implementation & Results

Implementation

WiRAR was applied to the marine radar installed at the research platform FINO-I, which is located in the German Bight, North Sea, 45 km north of the island Borkum (Fig. 5). The radar aboard FINO-I is a commercial marine radar- which operates at 9.5 GHz (X band) and observes the surface under a shallow grazing angle (Fig. 6). The 2.4 m antenna rotates with a period of 2.5 s and has a spatial resolution of approximately 10 m at a distance of ~750 m. All data, used here, were acquired in the near-range mode, where the radar covers an area within a radius of ~ 2000 m. Each sequence consists of 32 images representing 80 s. The validation was performed on a data set collected over a period from August 2003 until November 2004, representing 4786 acquisitions. Fig. 5 shows the research platform FINO-I with its 100 m long mast. The radar antenna is mounted just below the helicopter deck at the northern part of the platform. The radar-image sequence depicts a wave field propagating in a southwesterly direction (Fig. 7). The southern quadrant of the images contains radar shadows originating from the platform equipment, which have been masked (black sector) and which were excluded from the investigations. At FINO-I meteorological and oceanographic parameters are measured at various heights and depths.

Validation of wind directions

One example is given in Fig. 8. The resulting local mean directions are plotted as blue arrows. It can be seen that they agree well with the wind direction measured at the radar platform at a height of about 30 m (red arrows). For validation of the wind direction retrieval method of WIRAR, the radar-retrieved mean wind directions of 4786 image sequences are compared to the in situ measurements recorded at FINO-I at a height of 30 m. The result is given in Fig. 9: the correlation coefficient of 0.99, the bias of 0.3°, and the standard deviation of 12.8°. Investigation of the dependence of the standard deviation on wind speed shows a significant decrease of the standard deviation with increasing wind speed, as the wind streaks become more pronounced.

► **Figure 5**
Research platform FINO-I with its ~101 m tall measurement mast. The marine radar is located below the helicopter deck. The radar-image sequences depicts a wave field propagating in easterly direction.

Validation of wind speeds

A scatter plot of in situ wind speeds versus radar-retrieved wind speeds, which considers the NRCS as well as the radar retrieved wind direction, is given in Fig. 10. Varying crosswind directions within ±15° of the true crosswind direction were used with the NN retrieved GMF. The result was a correlation coefficient of 0.96 with a bias of 0.01 ms^{-1} and a standard deviation of 0.90 ms^{-1}. The standard deviation was slightly decreased to 0.89 ms^{-1}, when only the true crosswind direction was considered. Therefore, an accuracy of ±15° for wind direction measurements is sufficient for accurate wind speed retrieval. To improve the given GMF for wind speed determination, the dependencies of the NRCS on additional parameters, such as sea state and atmospheric conditions, have to be considered. Information on the sea state can be extracted from the radar datasets, while atmospheric stratification conditions, such as the air-sea temperature difference and the relative air humidity, need to be measured by external sensors. In Fig. 11, in situ wind speeds are plotted together with the wind speeds, which come from the marine radar image for which the above listed parameters were used in addition. The correlation coefficient is 0.99, with a bias of 0.01 ms^{-1} and a standard deviation of 0.41 ms^{-1}.

Conclusion

The validation has shown that WiRAR is an ideal instrument tmeasure wind vectors with an accuracy of ~0.5 ms^{-1} in speed and ~13° in direction. In contrast to traditional offshore wind sensors, the retrieval of the wind vector from the NRCS of the ocean surface makes the system independent of the sensor's motion and installation height as well as of the effects due to platform-induced turbulence. With the preexisting installations of radar systems on marine structures, harbours, platforms, and ships, the measurements can be acquired in a very cost-efficient way.

Authors

Jochen Horstmann (GKSS) and Heiko Dankert (GKSS, present position: California Institute of Technology)

▲ **Figure 6**
Typical installation of an antenna of a X-band marine radar system.

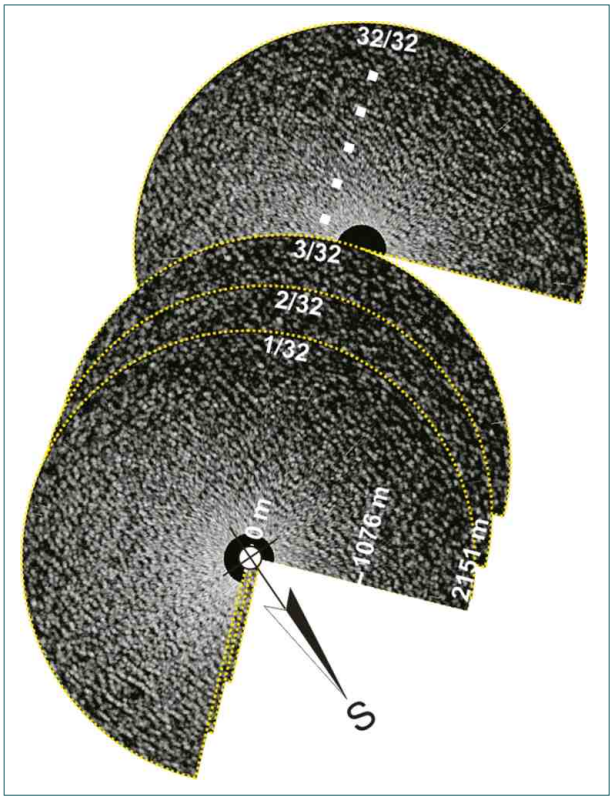

► **Figure 7**
Radar image sequence as acquired by the radar. Obvious is a wave system, which travels from west to east.

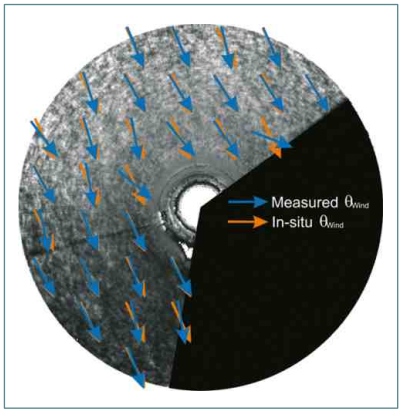

▲ **Figure 8**
Mean RCS of an acquired radar-image sequence. The wind measured at the platform was 8 ms^{-1} with a wind direction of 335° (red arrows). Superimposed are the local wind vectors as retrieved from the radar (blue arrows).

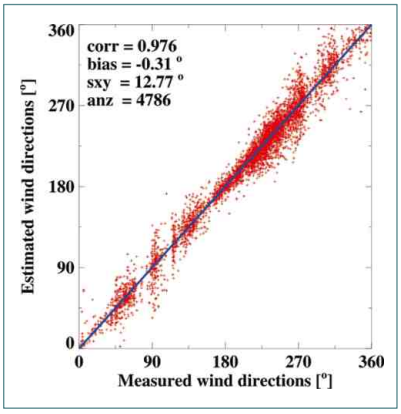

▲ **Figure 9**
Scatter plot of in-situ wind directions versus radar estimated wind directions.

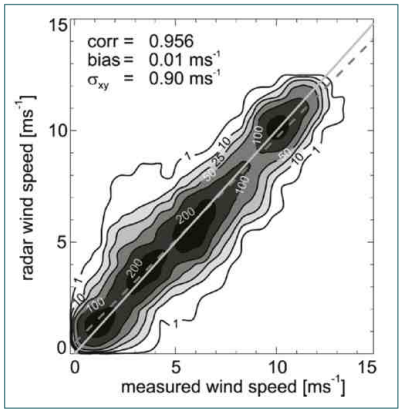

▲ **Figure 10**
Comparison of in situ wind speeds versus wind speeds retrieved via WiRAR. The radar wind speeds were retrieved using the intensity of the mean radar image and the radar retrieved wind direction.

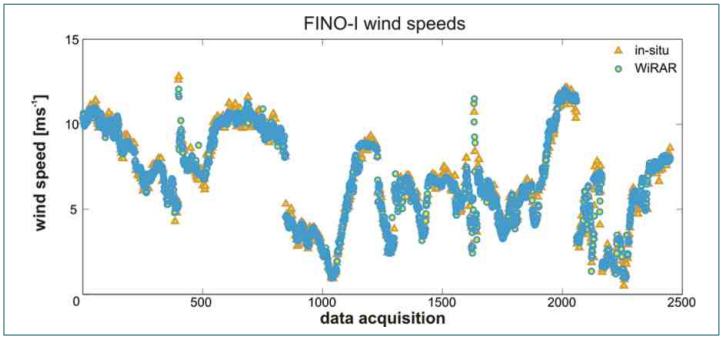

◄ **Figure 11**
Times series of WiRAR and in situ wind speed measurements at FINO-I. WiRAR retrieved wind speeds consider the air-sea temperature differences as well as radar retrieved wave parameters.

WiSAR - Wind retrieval from synthetic aperture radar

Methods & Results

Introduction

Today, several scatterometers (SCATs) are available that measure ocean surface wind fields with a resolution of up to 25 km on a global and operational basis. Originally they were not designed to observe also samll-scale wind features, which are especially important in coastal areas. However, satellite-borne synthetic aperture radars (SARs) offer this unique opportunity, as they image the ocean surface with a much higher resolution than SCATs, typically below 100 m (Fig. 1). Several SARs have been launched in the last 12 years and are valuable tools for measuring geophysical parameters such as ocean surface winds, waves, and sea ice.

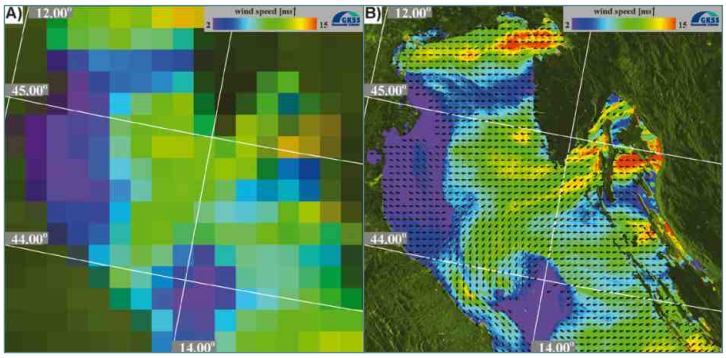

▲ **Figure 1**

Wind fields of the Adriatic Sea resulting from scatterometer data **a)** resolution of 25 km and from SAR data **b)** resolution of 300 m. The small scale coastal wind jets, which are visible in the WiSAR retrieved wind field cannot be detected in the simulated scatterometer wind field.

Most satellite borne SAR systems operate at the C-band at moderate incidence angles between 15° and 50°. For the electromagnetic wavelength of ~ 5 cm and of the incidence angles of 15-50°, the backscatter of the ocean surface is primarily caused by the small-scale ocean surface roughness with a horizontal scale of 5–10 cm. The small-scale surface roughness is strongly influenced by the local wind field, and therefore allows it to relate the radar backscatter to the wind parameters.

SAR wind retrieval

The retrieval of ocean surface wind from SAR is a two-step process; in the first step, wind directions are retrieved, which are a necessary input in the second step. Wind directions are extracted from wind-induced streaks, which are aligned with wind direction and which are visible in the SAR image (Fig. 2). Orientations of these streaks are extracted by using the Local Gradient (LG) Method (Horstmann et al., 2002, Koch, 2004). In the second step wind speeds are retrieved from the backscattered normalized radar cross section (NRCS) of the ocean surface by utilizing a geophysical model function (GMF). The GMF describes the dependence of the NRCS on the wind and radar imaging geometry (Horstmann and Koch, 2005).

For the retrieval of wind direction, the SAR image is smoothed and reduced to resolutions of 100, 200, and 400 m, so that three SAR images are generated. From each of these images, local directions are computed, which are defined by the normal to the LG, which have a 180 degree ambiguity in wind direction. In the next step, all pixels that are affected by non wind- induced features are masked and excluded from further analysis (Fig 3.). Therefore, high resolution land masks and SAR image filters are applied (Koch 2004). From all of the resulting directions, only the most frequent directions in a predefined grid cell are selected. The 180 directional ambiguities are removed by considering weather prediction models.

For wind-speed retrieval a GMF is applied. It relates the NRCS of the ocean surface to the local near-surface wind speed, wind direction and incidence angle. In case of the SARs, which operates at C-band with vertical polarization (VV), a well tested empirical GMF exists. For wind-speed retrieval from C-band, SAR images acquired with horizontal (HH) polarization, no similar well-developed models exist, so that the horizontal polarized NRCS is converted to the vertical polarized NRCS via the polarization ratio (PR). So far, the PR is not well known and several different PRs have been suggested in literature. However, it has been shown that an incidence dependent PR shows sufficient good results for SAR wind speed retrieval (Horstmann et al., 2000).

Validation

Several comparisons of SAR retrieved wind fields with results from numerical weather prediction models at wind speeds below 25 ms^{-1} have shown that WiSAR is capable of retrieving winds with a typical error of ~20° in wind direction and ~2 ms^{-1} in wind speed (Horstmann et al., 2003; Horstmann and Koch, 2005; Koch and Feser, 2006). It has also been shown that it is possible to retrieve wind fields under extreme high wind situations (Horstmann et al. 2005). Fig. 4 shows an example of a WiSAR retrieved wind field of hurricane Ivan (10. September 2004). However, recent studies of SAR retrieved wind fields from tropical cyclones have shown that the error in wind speed is significantly larger at wind speeds above 25 ms^{-1}.

Authors

Jochen Horstmann and Wolfgang Koch (GKSS)

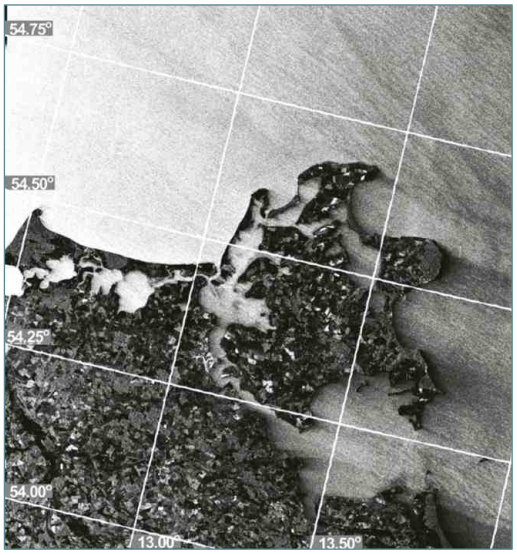

▲ **Figure 2**
SAR image of the island Rügen, Germany, acquired by the European satellite ERS-1 on August 12th 1991.

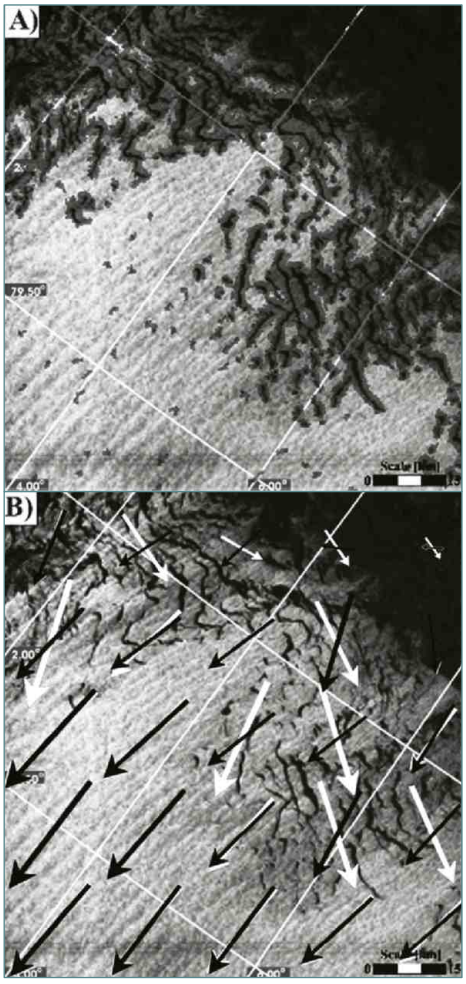

► **Figure 3**
SAR image acquired by the European satellite ERS-1 in the marginal ice zone off the coast of Spitzbergen. **a)** The mask that results from filtering and **b)** wind directions resulting from the LG method with (black arrows) and without (white arrows) consideration of the filter.

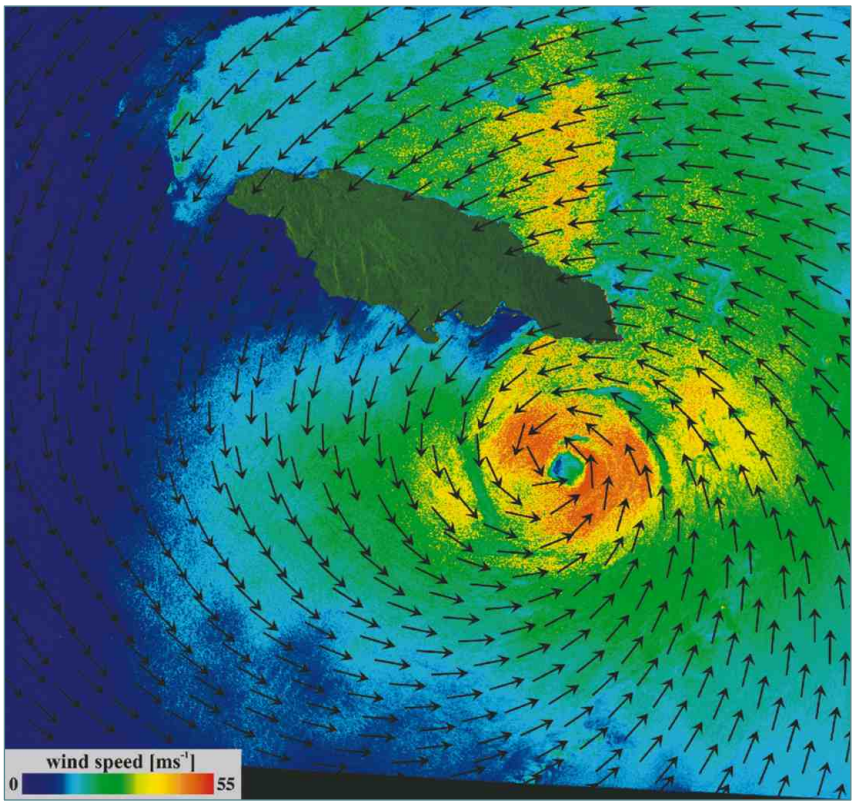

◄ **Figure 4**
WiSAR retrieved wind field of hurricane Ivan. The SAR data were acquired by the Canadian satellite Radarsat-1 on September 10th 2004 at 2307 UTC. The eye of hurricane Ivan is situated about 80 km south of Kingston, Jamaica

Observing small scale morphodynamic processes during storm events

Methods & Results

Introduction

A particular challenge for management of sandy coasts is erosion during storm events. Wind waves and swell transport a high amount of energy towards the coastline, which has to be dissipated within a short distance when arriving at the beach. This energy leads to a short but heavy increase in erosion, transport and re-deposition of sand. To protect the coast, measures such as “beach nourishment” have been established for the stabilization and conservation of the shoreline sediment. To observe the processes during a storm event and to monitor the success of any measures requires knowledge of the local interactions of waves and currents within the near shore area. Furthermore, longterm observations are necessary to study the change of the coast and the transfer of sediment.

Here we present the use of an area covering observation method which is based on RADAR technology that allows a continuous survey of the morphodynamical forcing by currents and waves as well as the response of the bathymetry even during storm events. The area of investigation (covering about 5 km²) lies at the north end of the Island of Sylt in the German Bight (Fig. 1).

Methodology

The local water depths and the local current vectors (velocity and direction) are deduced from the Radar backscatter signal by an inverse modelling technique. During 10 minutes of radar observation the radar detects and tracks wave crests in space and time, from which the local change of the dispersive wave propagation is computed (for the physical background see next section). The dispersion describes the propagation speed of the different wave components. For this procedure a national and international patent was awarded in 2003. The method was developed at the Department of Radar Hydrography of the Institute for Coastal Research/GKSS and is licensed as a commercial product (DiSC) by Vision 2 Technology GmbH (www.v2t.de), partner of the Geesthachter Innovations- und Technologie-Zentrum (GITZ).

The dispersion relation for sea surface gravity waves is derived from the Eulerian equations of motion, the continuity equation and from the dynamic kinematic boundary conditions at the sea surface and the sea floor. A detailed description is given in Senet et al. (2008). As the wave height does not influence the dispersion, the positions of the wave crests as they are tracked by the radar can be used for the inversion of the local water depths directly from the radar. The three dimensional Fourier decomposition of the radar images gives the actual effective dispersion of the waves, which is controlled by the local water depth and current. Deviations from the undisturbed dispersion are used to determine the spatial distribution of these two hydrographic parameters, which then are composed into a grid, and used to construct a map of water depth (bathymetry) and current.

Bathymetry

The examples in Fig. 2 and 3 show the water depth map as derived from Radar observations and the current fields observed during flood and ebb phases.

Furthermore, the depth measurements have been averaged over a full tidal cycle before and after a storm (wind speed 8-9 Bft.) to estimate the change in sediment mass of the observed area. First, by using gauge measurements, the two maps have been set to a common reference. The difference of the sediment volume between the beginning and the end of the storm is estimated to be + 50.000 m³. It is considered to be the sediment net increase of the area under investigation. Following Flampouris et al. (2008), the accuracy for each grid cell lies within ±10%. However, the uncertainty of the assumption that the mean sea level remains constant during the two observations decreases the accuracy of the calculation.

Current

While the main impact of waves on the shore is erosion, currents mainly determine sediment transport and deposition. Fig. 3 illustrates an example of a current field observation acquired on February 25th 2002. Although the radar coverage is the same as for the cases shown in Fig. 2 the current field was computed for an area which was slightly shifted north - eastward (Fig. 1). The wind speed during acquisition was about 5 Bft. In addition to the current field a time series of current vectors is given in the upper part of Fig. 3. The position where the time series has been captured is marked with a magenta dot in the vector field. From the two dimensional vector field and the time series special features of the flood phase become evident. At the beginning of the flood phase the northward directed current is blocked by the pressure of the current, which flows along the main gully in the North, where the water depth increases to 20 m and more. Due to the rise of the water level during flood this effect diminishes and the water transport rotates toward the north, following more and more the morphology of the side gully.

Authors

Friedwart Ziemer and Stylianos Flampouris (GKSS)

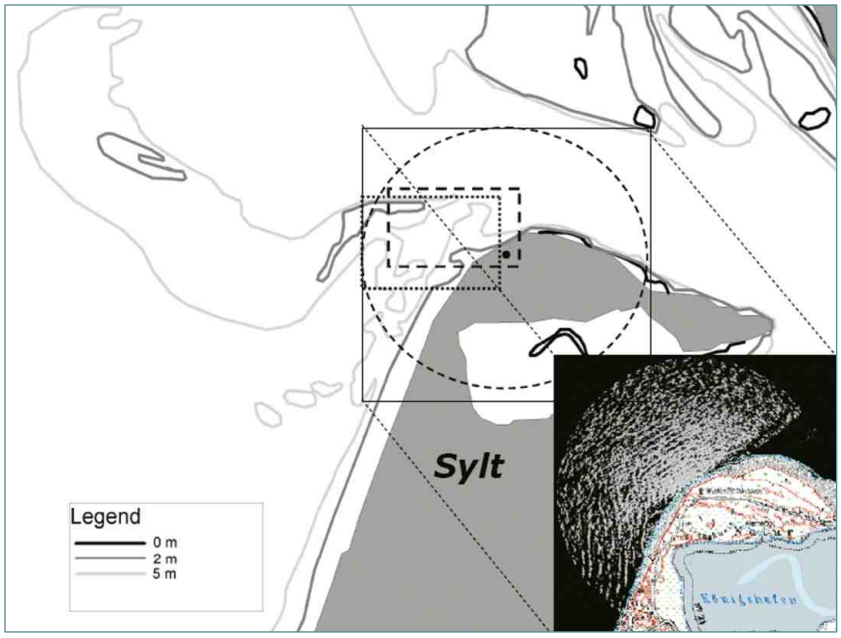

◄ **Figure 1**
Area of investigation at the north end of the island of Sylt. The area is characterised by a sand hook pointing westward into the direction of the ebb transport of the tidal currents. The near shore part of the hook (see circle indicating the radar coverage) has a highly variable bathymetry with a long shore sand transport. The dashed and dotted frames indicate the areas for which the current field has been computed (Fig. 2-3). **Dotted line:** change of the bathymetry during the storm in February 2002, **dashed line:** the current example

► **Figure 2 (left)**
Bathymetries deduced from radar wave observations before and after a storm (8 to 9 Bft.) The upper figure shows the situation on February 22nd and the lower on February 28th 2002. Isolines are referenced to NN. Evident during the storm is an increase of sand along the ship way, 500 m west of the shore. Loss of sand is observed close to the shore and in the northwest corner.

► **Figure 3 (right)**
Current fields observed on 25th of February 2002 (**upper part**)**.** The time series of the current vector is given for the position marked by the purple dot (**lower part**). The vector field was acquired at the beginning of flood tide, which corresponds to the first time step of the series.

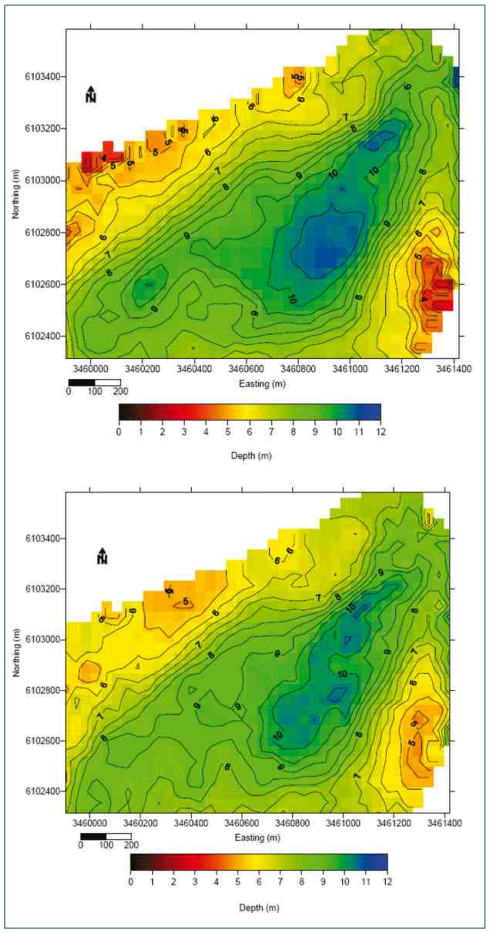

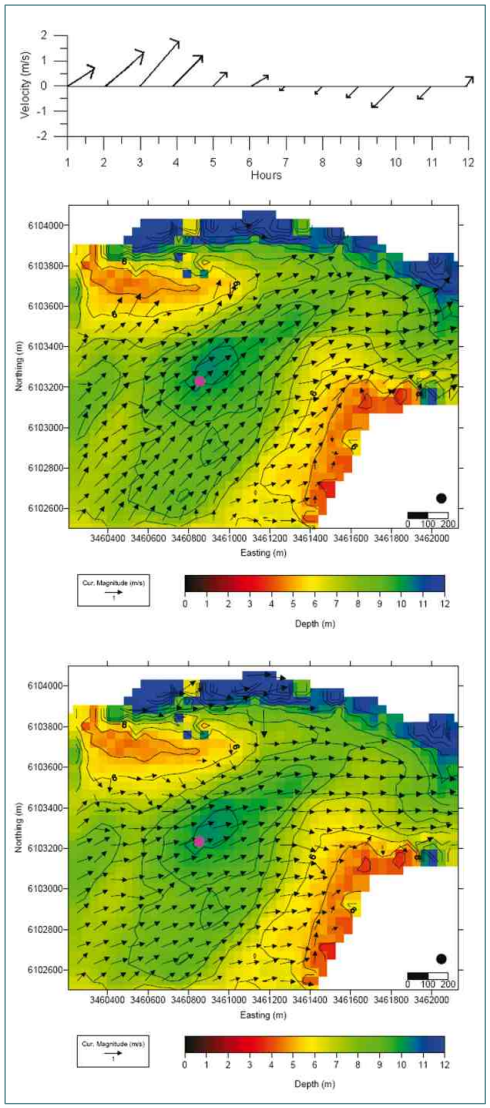

Determining coastal water constituents from space

Methods & Techniques

Introduction

Coastal seas are highly dynamical areas. In particular, the water of the shallow soft-bottom coast of the North Sea, with its strong tidal currents, continuously changes its properties. Monitoring these properties, such as suspended particulate matter with all its components and phytoplankton, is a very demanding challenge. Ocean colour remote sensing is one possibility to determine some of the key variables and to provide weekly or monthly maps of their distribution with a high spatial resolution (Fig. 1). In contrast to the open ocean, the optically complex coastal waters, with different classes of substances, pose a number of problems for optical remote sensing. With the launch of the Medium Resolution Imaging Spectrometer MERIS on the European earth observing satellite ENVISAT in 2002, a new generation of instruments became available, which allows also remote sensing of turbid coastal water. The sensor has a spatial resolution of 300 m, a revisit period of 1-2 days at mid latitudes and 15 spectral bands. For using this instrument for coastal water remote sensing, special procedures are necessary to derive the in-water optical properties and concentrations from the reflectance spectra. At the Institute for Coastal Research of GKSS, the required algorithms have been developed, which are based on artificial neural networks, and which are implemented in the ground segment for the routine processing of MERIS data at the European Space Agency ESA (Schiller & Doerffer, 2005; Doerffer & Schiller, 2007).

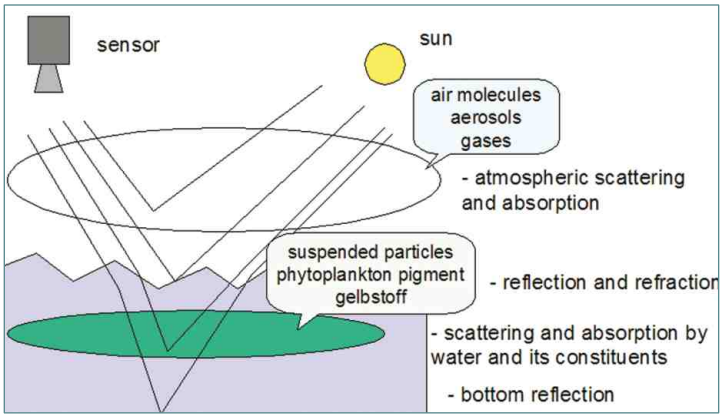

▲ Figure 1

The basic principle of ocean colour remote sensing: The radiance, which arrives at the satellite consists of 4 components: (1) radiance which is scattered in the atmosphere, (2) radiance which is specularly reflected at the sea surface, (3) radiance which is backscattered by water and its constituents and (4) in shallow water, radiance, which is reflected from the sea bottom. All 3, or in case of shallow water 4, components have to be determined to retrieve the radiance leaving the water, i.e. component 2.

In this chapter we provide an overview of the steps which are necessary to compute a concentration map from the level 1 data of MERIS, i.e. the spectral radiances at the top of the atmosphere (TOA) .

Methods and techniques

Ocean colour remote sensing requires two major steps (Fig. 2). First, the influence of the atmosphere and the reflectance at the water surface have to be computed to get the radiance reflectance leaving the water, i.e. the sunlight, which is backscattered by the water molecules and all water constituents, including phytoplankton (Fig. 3). This atmospheric correction step is extremely critical, because the atmosphere, in most cases, causes more than 90 percent of the radiance at the top of the atmosphere. As the second step, the inherent optical properties, which are the absorption and scattering coefficients, as well as the concentrations of the substances in water have to be derived from the radiance reflectance spectrum leaving the water. For this purpose, different kinds of procedures have been developed, which are partly empirical, but for coastal waters they are based on radiative transfer models in most cases.

For the correction of the atmosphere, an aerosol optical model has to be defined, because scattering by different aerosols, including thin cirrus clouds, is the most variable optical component in the atmosphere within the visible spectrum. The properties are selected according to measurements of the sun photometer network AERONET. GKSS operates one of these instruments on the island of Helgoland. A Monte Carlo photon tracing model is then used to simulate TOA radiance reflectances, which are the basis to train a neural network. Finally, this neural network is included into the processor to determine the radiances leaving the water from the TOA radiances as measured by MERIS.

For the second step, a bio-optical model of the water constituents is necessary. This model is derived from various optical measurements in coastal waters, which have been performed by GKSS and partner institutes during the past years. Based on this model, radiance spectra leaving the water are simulated which cover the range of concentrations found in most coastal waters. This set of spectra again is used to train a neural network, which determines the optical properties and the concentrations from the radiance spectra leaving the water. The result are maps of absorption and scattering coefficients, of the concentrations of suspended matter and phytoplankton and of the water transparency (Fig. 4).

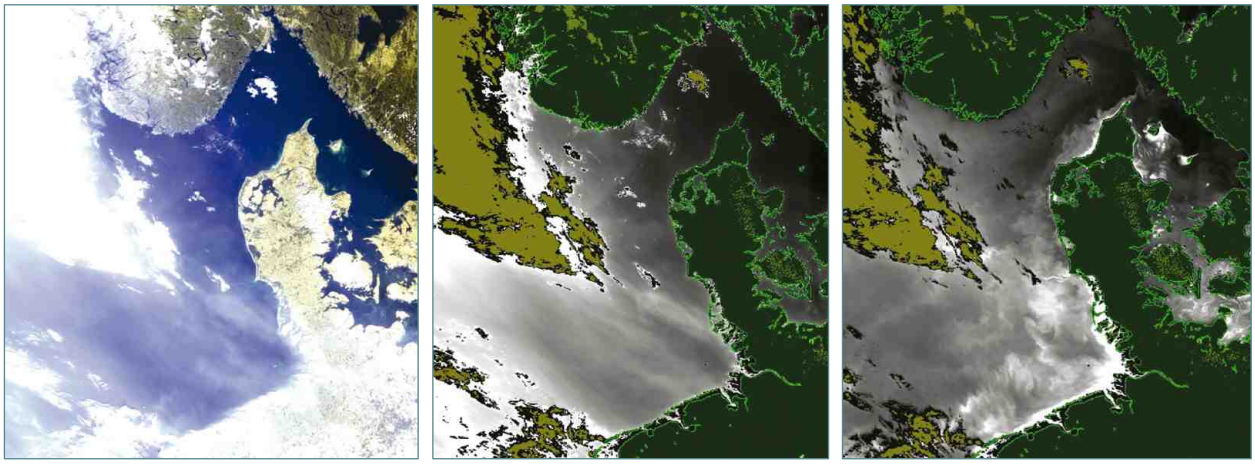

▲ **Figure 2**
MERIS scene of the North Sea: the radiance at the top of the atmosphere (RGB image**)**, **(a)** is split into two major components by using the atmospheric correction procedure: the path radiance, which consists of the radiance scattered in the atmosphere and specularly reflected at the sea surface **(b)**, and the radiance leaving the water **(c)**, which is used in the next processing step to determine the water constituents.

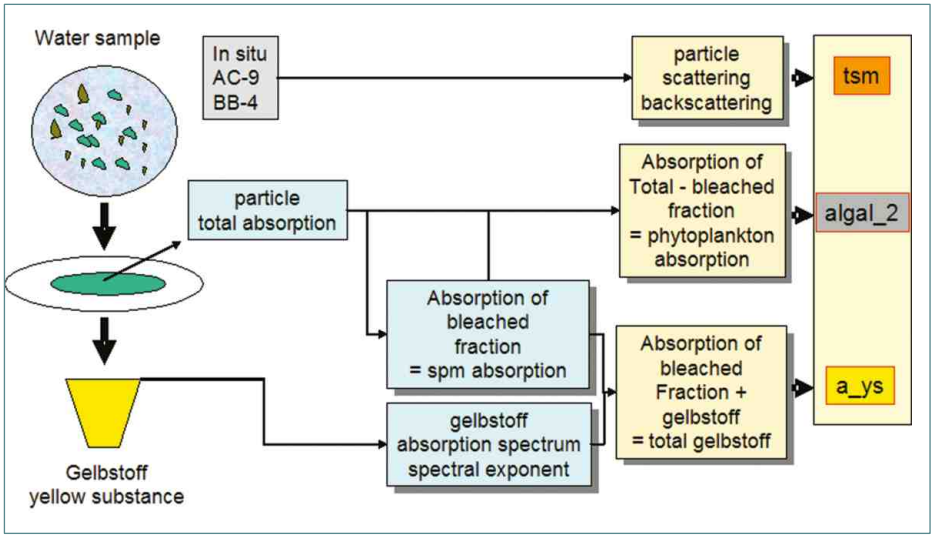

◄ **Figure 3**
All constituents of a water sample are grouped into 4 optical components: the absorption coefficient of the water, which passes a filter with a pore size of 0.47 µm is defined as yellow substance (Gelbstoff). The absorption coefficient of the particles which remain on the filter is split by a bleaching process into 2 components, i.e. the absorption of phytoplankton pigments (difference before and after bleaching) and the absorption of the material after bleaching.

A further component is the scattering coefficient of all particles in water, including phytoplankton. The absorption coefficient of phytoplankton pigment is converted into chlorophyll concentration and the scattering of all particles into suspended matter dry weight per litre.

▼ **Figure 4**
The three products which are derived from the radiance leaving the water: **(a)** the absorption coefficient at 443 nm of Gelbstoff and bleached particles, **(b)** the chlorophyll concentration and **(c)** the SPM dry weight concentration.

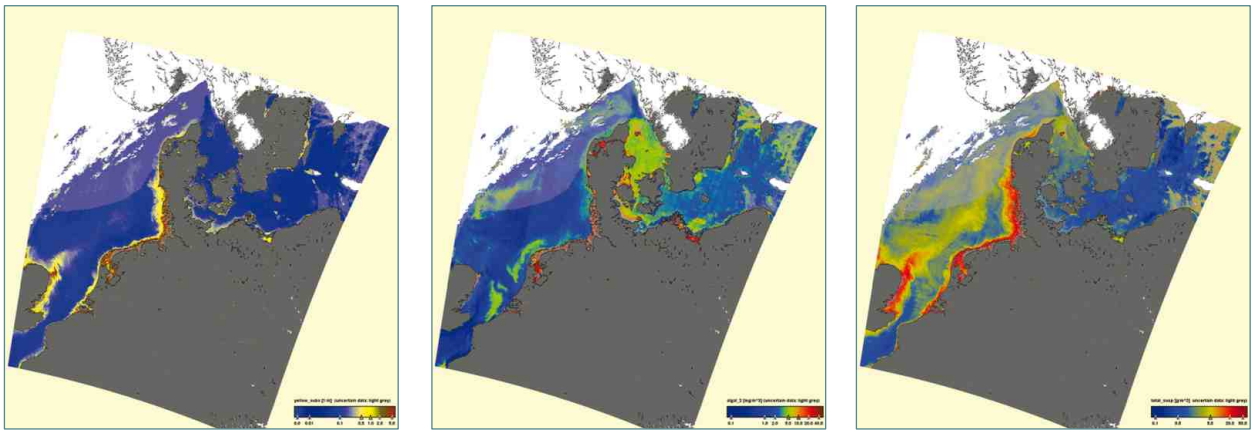

Determining coastal water constituents from space

Implementation & Results

Seasonal patterns of phytoplankton in the North Sea

One application of ocean colour remote sensing is investigation of the horizontal distribution patterns of phytoplankton in the North Sea at different seasons. It might change in the future due to climate change, with possibly significant consequences for the North Sea ecosystem including its fish stocks.

In springtime, when the water is rich in nutrients, light is the most important factor which controls the development of phytoplankton growth (Fig. 5). During winter conditions, the days are too short combined with a low sun elevation and the water column is well mixed in most parts of the North Sea. Since a phytoplankton cell can be everywhere in the water column, including the dark depths, it will not get sufficient light during 24 hours to grow. When the days become longer, phytoplankton growth starts in the shallow water, where the light per day is sufficient even when the water column is well mixed. In the surface layers of deep waters growth can start only when calm and sunny weather with sufficient heating produces a stratification of the water column. Under these conditions the phytoplankton can stay in the upper mixed layer without sinking into the dark deeper layers. It gets enough light and starts to grow rapidly. In the deep northern North Sea water the growing season normally begins around mid April. The growing phase is interrupted or stops when strong winds destroy the stratification or when the nutrients are depleted. Also, grazing by zooplankton, which follows the phytoplankton development, reduces the phytoplankton biomass.

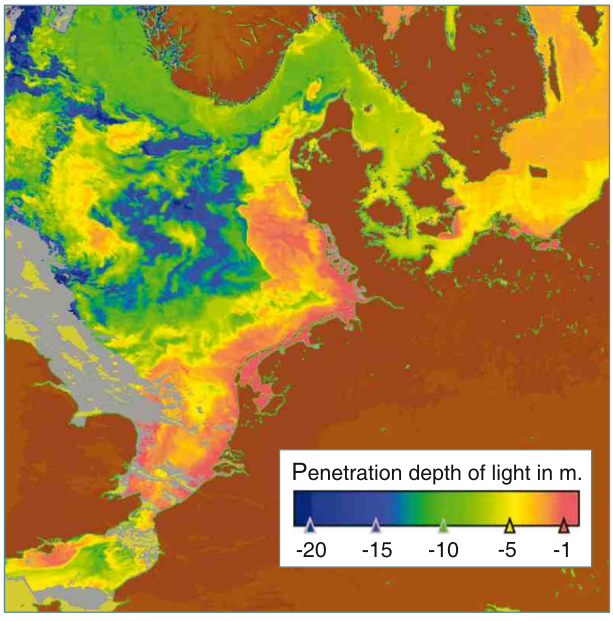

▲ Figure 5
The penetration depth of light [m] is important fpr primary production of phytoplankton, MERIS on April 22nd 2008.

A special case exists in the Skagerrak and the Norwegian Trench. Here, stratification can be caused by less saline light water from the Balitc Sea, which flows into the North Sea as an upper layer and follows the Norwegian coast due to the normally anticlockwise circulation in the North Sea. Thus, the phytoplankton growing season starts much earlier due to the better light conditions in this upper layer.

Later in the year, a bloom of Coccolithophores is observed quite frequently in the Skagerrak and along the southern Norwegian coast (Fig. 7). These algae make the water extremely bright because of the high scattering coefficient of their coccoliths. These are plates which form quasi a shield of calcium carbonate around the cell.

During the summer period, other phytoplankton blooms occur in the southern North Sea, which are summarised under "red tides", because - due to their pigments - they discolour the water from green to red (Fig. 8). Some of these blooms are harmful to other marine organisms, e.g. to mussels or fish, and can severely damage maricultures. Along the coast of the Netherlands and in the German Bight, high phytoplankton concentrations can be observed throughout the summer, due to the high nutrient concentrations, which are collected by the coastal current from all the rivers which discharge into the North Sea and which are transported to the north. In contrast in the central and northern North Sea, the chlorophyll concentration decreases during the summer period due to nutrient depletion and grazing by zooplankton. In autumn stronger winds and less insolation causes a breakdown of the stratification so that fresh nutrients are mixed up from deeper layers to the surface. A second phytoplankton bloom can briefly develop until the decreasing light ends the growing season.

Another factor which limits the growth of phytoplankton and thus controls the distribution pattern is turbidity, i.e. the attenuation of light by suspended matter. This factor can also be estimated from the spectral reflectance data of MERIS.

Authors

Roland Doerffer, Helmut Schiller, Kerstin Heymann, Rüdiger Röttgers, Wolfgang Schönfeld and Hansjörg Krasemann (GKSS)

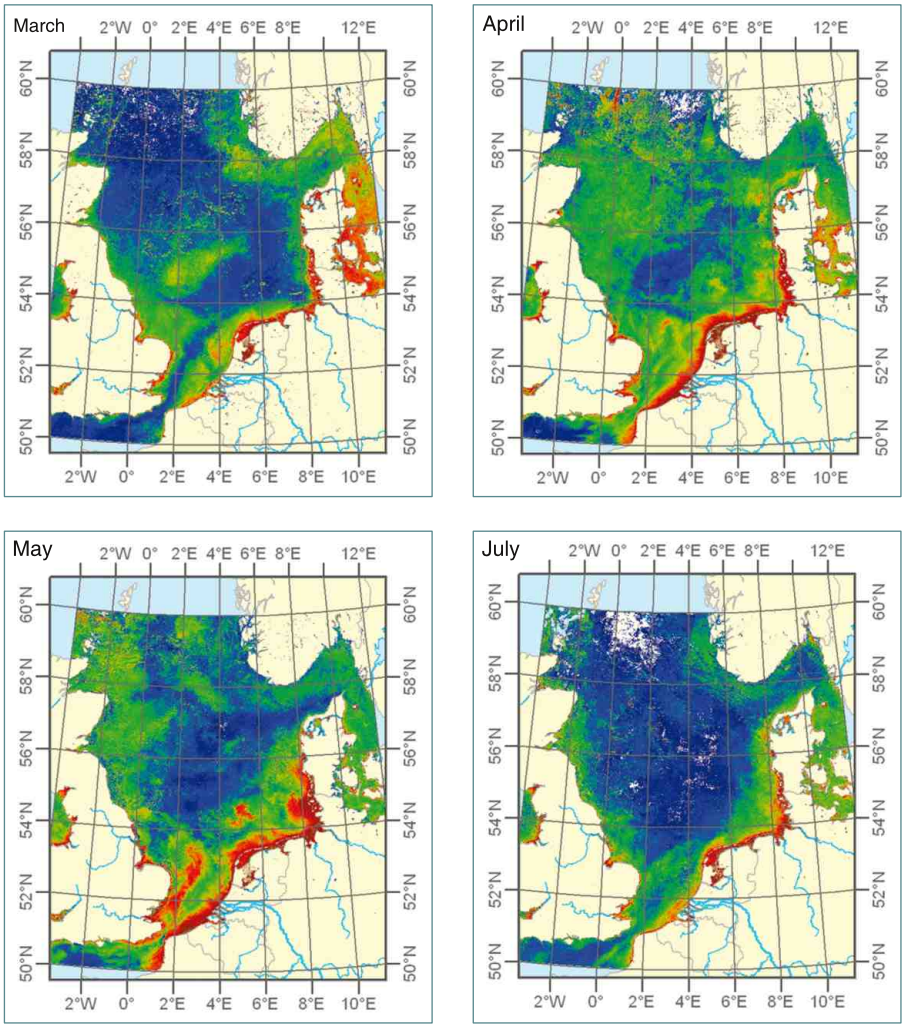

◄ Figure 6

The maximum chlorophyll concentration in the North Sea per month for spring/summer 2007 derived from MERIS.

In **March** maximum values are found along the coasts of the southern North Sea. Also, the shallow Dogger Bank shows higher values due to the better light conditions. In the deeper northern part of the North Sea values are low. Obvious are the high concentrations in the Skagerrak and around the southern part of Norway.

In **April** we see the whole North Sea with chlorophyll concentration around 5 mg/m^3 except for the Dogger Bank where the nutrients ar now depleted.

In **May** we see maximum concentrations also in the northern North Sea, while they have dropped in the southern central part.

In **July** the chlorophyll concentrations are low in the central part, but high along the coasts including the Skagerrak.

Legend

The chlorophyll concentration in mg/m^3.

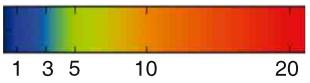

▼ Figure 7

MERIS view of a bloom of *Emilia huxleyii* (*Coccolithophore*) in the Skagerrak in June 2003.

▼ Figure 8

MERIS view of a red tide of *Myrionecta rubra* in the German Bight on August 3rd 2008.

Estimation of spatial distribution of phytoplankton in the North Sea

Methods & Implementation

Introduction

Satellite images can reveal spatial patterns of e.g. the distribution of phytoplankton. Its abundance is represented by the chlorophyll concentration, which is one of the standard products of MERIS (Medium Resolution Imaging Spectrometer). The images have a temporal resolution of approximately one per day, the spatial resolution is 1.2 km, which corresponds to unprojected "Reduced Resolution" scenes (compared to 300 m Full Resolution mode).

The concentrations of three colour-defining substances in the water are derived from the monitored bands in the visual spectral range. The pigments of the phytoplankton - for the most abundant species that is chlorophyll - change the spectral characteristics of the backscattered light mainly by absorption; the total amount of anorganic particles (total suspended matter) accounts mainly for scattering and organic matter for absorbtion (yellow substance). Because of the dependence on the visual spectral range clouds are responsible for missing data.

To study the spatial and temporal variability of phytoplankton in the North Sea by satellite images, geostatistical methods are applied to cope with the missing data, e.g. the Kriging technique (for an overview consult Wackenagel, 2003 or Olea, 1999). For further investigations the ESA standard product algal_2 is used which represents algal concentrations in case2 waters.

Estimation of missing data values

The most commonly used method to avoid the correction for missing data and to gathering information about the whole area of interest is the calculation of the monthly mean (or median). By sacrificing temporal resolution, gaps can be filled by accumulating successive satellite images.

To illustrate the kriging technique, an exceptionally cloud-free satellite image of the North Sea (Fig. 2) is chosen (May 10th 2006) and overlaid with a cloud mask (February 2nd 2008) (Fig. 4). To estimate the missing data values several steps in data processing are arranged (Fig. 1).

For the applicability of Kriging technique the trend - i.e. the pattern of the expected value over the area - has to be negligible. The North Sea cannot be regarded as an area without spatial trend, because it exhibits almost all-the-year high chlorophyll concentrations in the coastal areas and shows recurring patterns of algal blooms in the spring season.

To correct for the time-dependent, dominant spatial trend a weighted monthly mean (Fig. 3) is calculated from any data which has been collected two weeks before and after the day of interest. Data close to the day of interest receive the higher weights. After removal of the trend the residuals, which are less spatially patterned than the original chlorophyll data, are used for geostatistical prediction. The estimates can be considered as corrections to the weighted monthly mean. These results will cover the area where the trend has been calculated, and therefore this process might not be sufficient to fill all missing data points. In a second step, the remaining missing values can be calculated relying on the original data and the newly estimated values.

The variogram, which measures the variance of pairs of points within certain distance classes, is calculated from the residuals and used in the ordinary Kriging procedure. This estimates the residuals at locations that are covered by the cloud mask and where a data point is available for comparison. In combination with the weighted monthly mean the (estimated) residuals function as corrections to the spatial trend. Remaining gaps persist at locations where no trend data is available (Fig. 4).

The difference between estimates and original data is small (Fig. 6 and 7). Major differences occur at locations where the trend has been calculated from a single sample which is distant in time to the original image and lies in a region of high temporal variability.

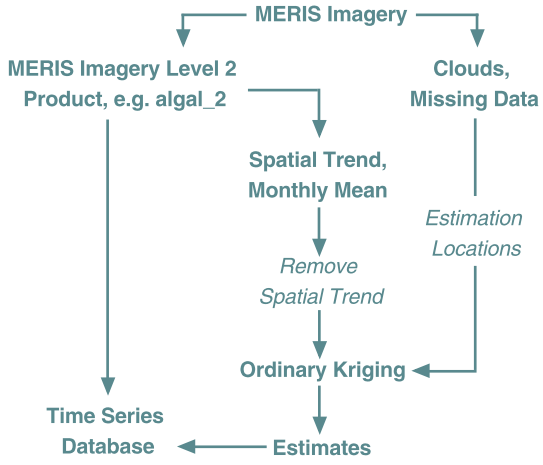

▲ **Figure 1**

To apply the ordinary Kriging technique to satellite data, the following steps have to be taken: the data and the missing data positions are onto the same grid, the spatial trend – estimated by a weighted monthly mean – is removed from the data. To save computation time the variogram is calculated from a subset of data and the Kriging technique takes only a fixed number of nearest-neighbours to the estimation location into account.

Authors

Dagmar Müller (GKSS)

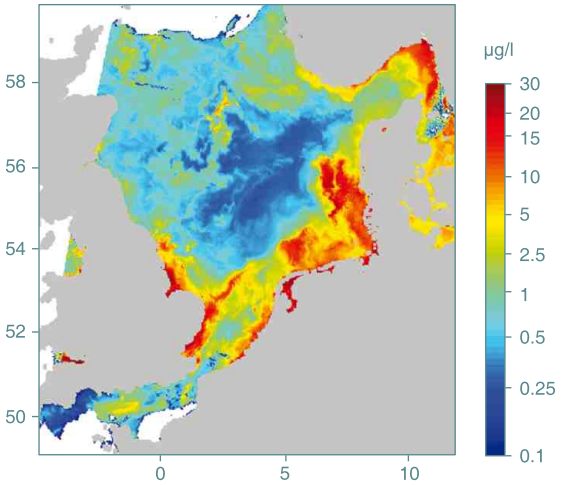

▲ **Figure 2**

MERIS chlorophyll product 'algal_2' for May 10th 2006. High chlorophyll concentrations (in µg/l) and strong patterns are found in the Danish North Sea. The data has been smoothed by a 3-by-3-pixel median filter.

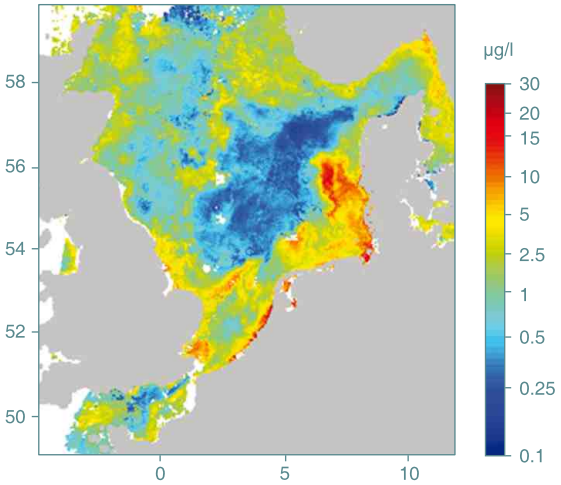

▲ **Figure 3**

Weighted monthly mean of chlorophyll concentration. 13 images of data two weeks before and after May 10th 2006..

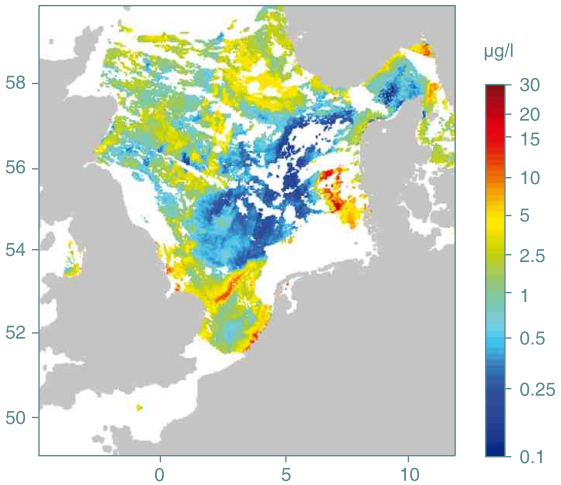

▲ **Figure 4**

Chlorophyll concentration (May 10th 2006) and cloud mask (February 2nd 2008). For 80230 data points estimations can be compared to original data..

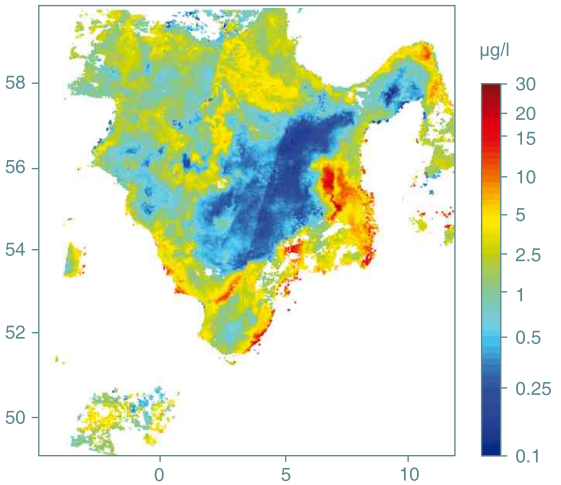

▲ **Figure 5**

Estimates and original data combined. Remaining gaps persist at locations, where no trend data is available.

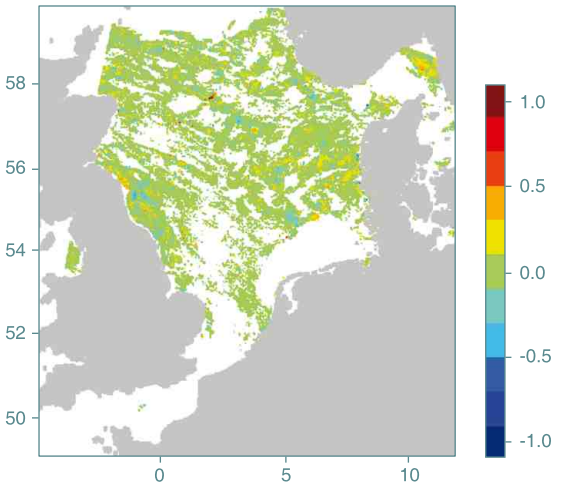

▲ **Figure 6**

Difference between original data and estimates.

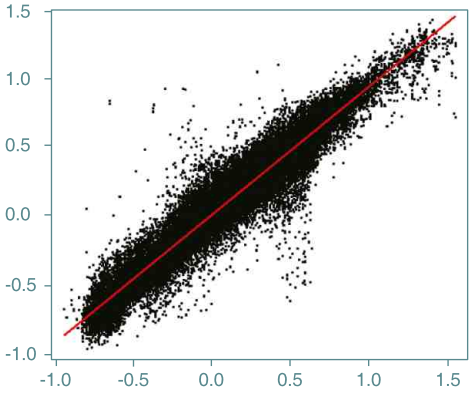

▲ **Figure 7**

To measure the reliability of estimates under a cloud cover, a cloud cover was simulated. The distribution shows the correlation of the original values versus the estimates under the simulated cloud cover of the same satellite image.

Detecting the unknown - novelty detection of exceptional water reflectance spectra

Methods & Results

Introduction

Synoptic monitoring of large areas in coastal waters can be performed by remote sensing using multispectral sensors on-board satellites. Many methods are in use which enable the detection and quantification of 'standard algae' or specific algae blooms using their known spectral response. The 'novelty detection' aims to find spectra outside the known range which are referred to as exceptional spectra.

Поди туда – не знаю куда,
принеси то – не знаю что.

Go I know not where
bring back I know not what

This order given to the hero of a Russian fairy tale could be used to summarise the request received to detect exceptional water reflectance spectra.

A recent review of the novelty detection techniques available is presented by (Markon and Singh, 2003).

The present study aimed to develop a novelty detection scheme for water reflectance data which could be used operationally. The basic idea behind this approach is to use a large number of reflectance spectra from one complete year for a defined region, here the North Sea, so as to include the annual cycle of plankton species (including their blooms etc.) to teach a learning system 'what is normal.' Only distinctive deviations from these known spectra should be classified as novel. Thus, the algorithm should accept all reflectance spectra from the training period as being normal but should still be sensitive enough to detect novel situations.

The Algorithm

The selection of the appropriate algorithm is one central issue of novelty detection. It is intimately connected with the type and structure of the data to be tackled. The water reflectances are measured at nine different wavelengths, all of which will be used in the present algorithms. Bio-optical models often exclude several wavebands or give other wavelengths more weight. Examples of water reflectance spectra are shown in Fig. 1.

Since our aim is to detect novel situations with unknown spectral signature we use all the information available. However, due to the resulting high dimensionality of the data set, nine dimensions of a point correspond to the nine wavelengths, the performance of different algorithms was carefully analysed. Different approaches of novelty detection, namely: a) a simple statistical scheme, b) an auto-associative Neural Net, c) a Neural Net classifier, and d) a tessellation scheme were analysed. Fig. 2 shows the enclosement of the different methods for a 2-dimensional case. The tessellation showed to be the optimal novelty detection scheme.

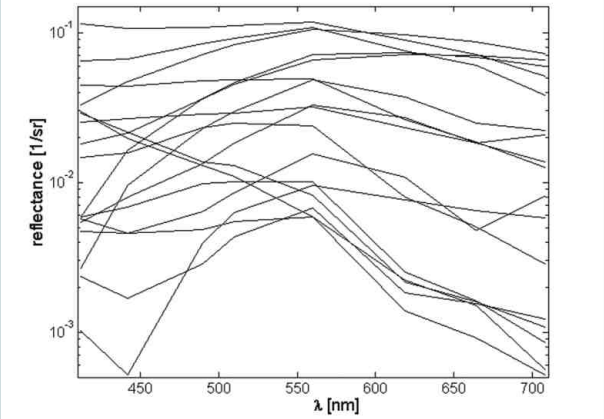

▲ **Figure 1**
Examples of water reflectance spectra measured by MERIS.

Scheme

The tessellation starts by choosing a radius R in the 9-dimensional space (dimensions for 9 wavelengths).

- The first point (spectrum) becomes the first centre.
- For each of the remaining points the smallest of the distances to all centres is compared with *R*. If the distance is larger than *R* the point is included in the set of centres.
- In the second step each point is assigned to that centre to which it is closest (*Voronoi tessellation*).

For each of the patches obtained by the tessellation the mean (centre of gravity) and the covariance matrix is calculated and finally for a given point (spectrum) the minimal Mahalanobis distance to all centres of the tessellation is determined.

This minimal Mahalanobis distance to all centres of the tessellation is the main parameter to find new, unknown points i.e. spectra. A flowchart of the tessellation scheme is shown in Fig. 3.

To minimize 'false alarms' and to optimise the discrimination power two additional conditions have to be fulfilled. The pixel must have a minimal distance to clouds of 3 pixels and only pixels within larger patches are considered.

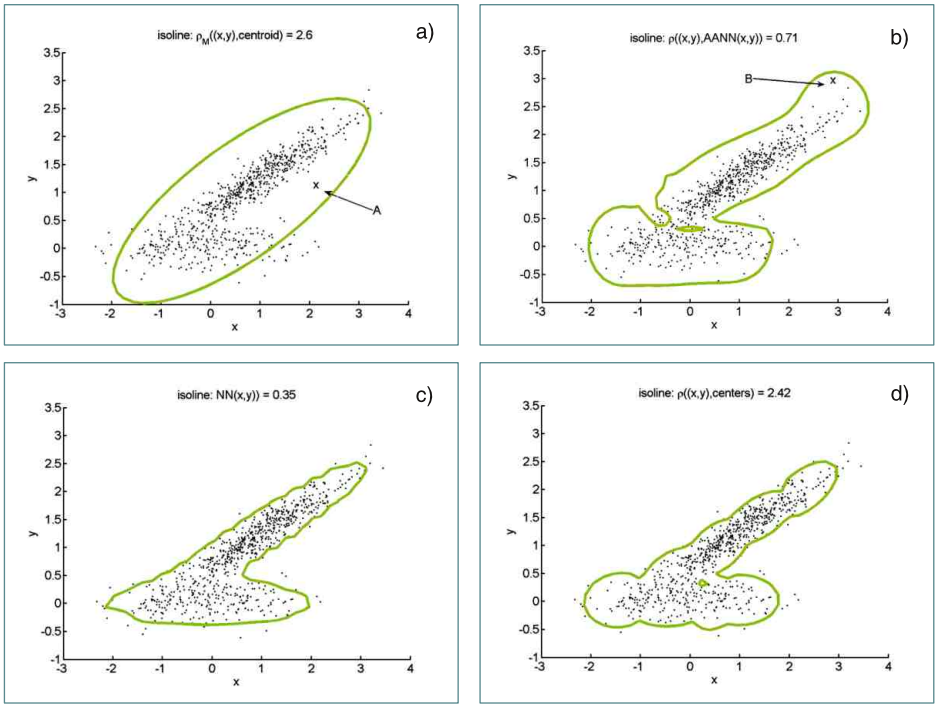

◄ Figure 2
The figures show a subset of a 2 dimensional dataset together with isolines of the measure ρ(x) which enclose 95% of the data for the four different approaches.
a) refers to the statistical model,
b) to the auto-associative Neural Net,
c) to the Neural Net classifier and
d) to the tessellation.

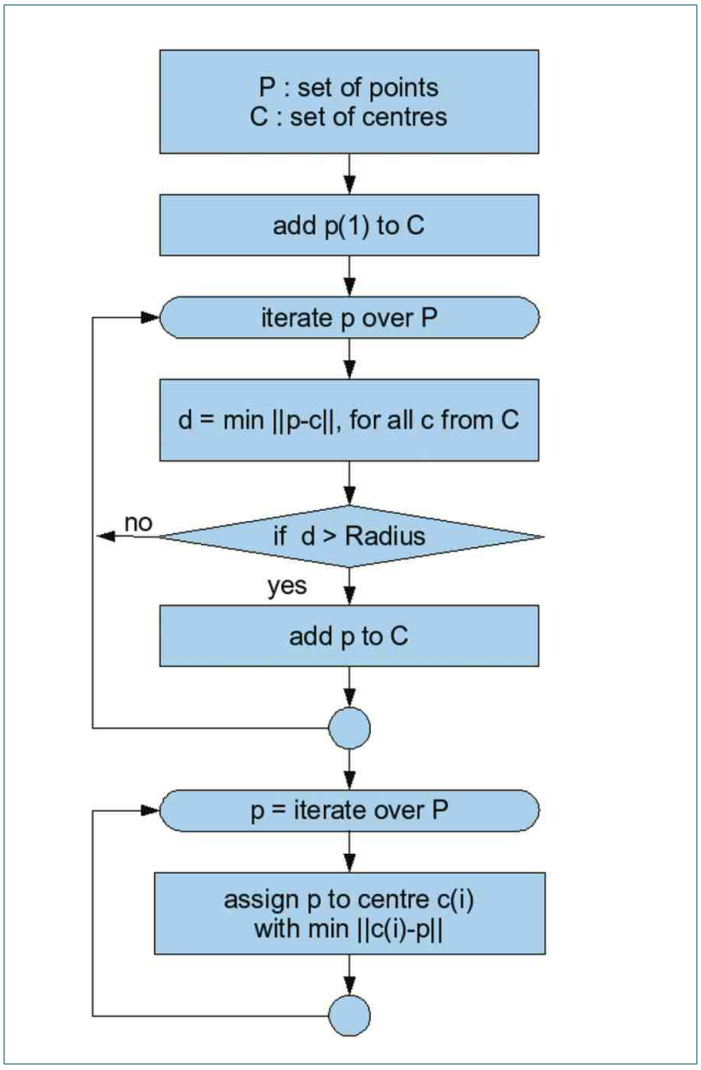

◄ Figure 3
Flowchart of the tessellation scheme

Detecting the unknown - novelty detection of exceptional water reflectance spectra

Implementation & Results

North Sea MERIS Data

As an application for the tessellation novelty detection scheme we used MERIS data of the North Sea. The logarithms of the remote sensing reflectances in the first nine MERIS channels (centred at wavelengths λ = 413, 443, 490, 510, 560, 620, 665, 681, 708 nm) were used to span the space.

For the dataset defining the 'normal' situation we used all MERIS scenes from June 26th 2003 to June 29th 2004 from a region of the North Sea (Fig. 4). We excluded pixels from the sun glint part as well as those which had one or more negative reflectances (bad atmospheric correction). Then ~ 1,000 pixels from each scene were randomly sampled thus ending up with 115,331 pixels for the 'training'.

▲ Figure 4
North Sea novelty training region

We decided to declare points as representing novelty if their distance to the tessellation was above 7.5. The distance cut-off of 7.5 left only 38 pixels remaining from the training points. However, if we applied the cut to the 288 complete scenes, with 16,575,000 pixels of the time range from which the training data set was selected, we found 110,718 pixels. After applying a cloud distance cut (3 pixels) and a minimal patch size cut (19 out of 5 x 5) we reduced this number to 2,670 in 26 scenes.

To remove remaining 'false alarms' in the training period we identified four groups of spectra for which we calculated the centre of gravity and the covariance matrix and appended them to the existing tessellation information. After this addition only one false alarm remained in the training set.

Finding Novelties

The test application data set comprised 223 scenes from June 30th 2004 to October 13th 2005. 10 scenes were initially marked as novelty.

In the scene from November 19th 2004 novelty was signaled in the Skagerrak area, however, after further inspection this was shown to be simply a processing failure in that a significant number of water reflectances were just unity.

Several scenes show 'novelties' (June 19th, 23rd, 26th, 28th and July 2nd, 18th 2005) and are located in the central and northwestern North Sea. These findings look like distinctive blooms of coccolithophores, which are in general quite frequent every year, but these spectra were classified as novelties due to their more pronounced blue reflectance as compared to those events within the training period.

For further practical novelty detection, and for those not immediately interested in coccolithophore bloom alarms, one would append these spectra to the tessellation as outlined in the previous paragraph.

Beside one false alarm three scenes with signaled novelties show a red tide near the island Helgoland on July 30th and on August 3rd and 5th 2004 (Fig. 5). This red tide was visible from satellite image (Fig. 6) and also at sea (Fig. 7) where observed during a measuring campaign between Cuxhaven and Helgoland on August 3rd 2004 and identified as *Myrionecta rubra*. Standard algorithms also detected an increase in the chlorophyll content.

Conclusion & Outlook

A novelty detection scheme which is suitable for regular monitoring purposes using multispectral remote sensing data has been constructed. It was applied to MERIS water reflectances and has a low failure (false positive) rate. It was successful in finding exceptional algae blooms, one of which was also identified as a red tide by in situ measurements.

To reach this low failure rate it was necessary to use not only the spectral information but also to avoid pixels close to clouds and to require a minimum novelty patch size.

The novelty detection scheme developed is flexible and adaptable to various monitoring needs. It is currently operating as standard service within InterRisk, an FP6-IST project addressing interoperable GMES services for environmental risk management in marine and coastal areas of Europe.

Authors

Helmut Schiller, Wolfgang Schönfeld and Hansjörg Krasemann (GKSS)

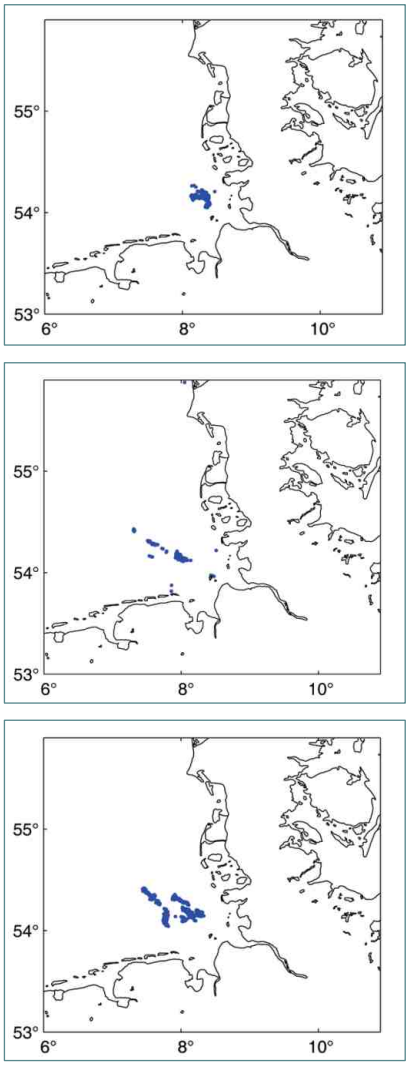

▲ Figure 5
Location of the novelty found on July 30th 2004, August 3rd 2004 and August 5th 2004 indicated in blue.

▲ Figure 6
North Sea MERIS scene from August 3rd 2004. The water-colour enhanced picture shows a reddish colour in the German Bight were the novelty was detected (Fig. 4).

◄ Figure 7
German Bight water on August 3rd 2004 with an obvious reddish colour stemming from a significant bloom of *Myrionecta rubra*.

Hydroacoustic monitoring

Knowledge about the underwater topography and the distribution of habitats with their benthic organisms, in particular about changes due to natural events and activities such as dredging or bottom trawl fishing are of high interest for managing the coastal sea.

To map this underwater world hydro-acoustic methods are the main techniques, which cover a sufficient swath also in turbid water. The interpretation of the data requires sophisticated methods similar to those of satellite data for the sea surface.

We present two techniques, one for monitoring coastal morphodynamics, the other for mapping kelp beds at the rocky coast of Helgoland.

Content

Monitoring coastal morphodynamics using high-precision multibeam technology

Methods & Techniques

Introduction

Coastal erosion, bathymetric changes of the near coast seabed or the stability and dispersal of dredged and disposed material are among the key questions of coastal management: What are the effects of coastal protection measures? How effective are they? Do they generate new burdens on the coastal system? Which processes control the movement of the seabed? What are the typical scales for the rearrangement of bed material? What types of seabed structures contribute most to the transport of the bed material? To what extent are morphological changes predictable?

Answers to these questions are still limited by a lack of observational evidence. Most of all, area-wide data are required to allow for comprehensive views of the relevant bed structures ranging over horizontal scales from decimeters to kilometers. The detection of seabed changes over these wide ranges of scales requires observational systems that combine high spatial resolution down to decimeters with high precision and accuracy in the horizontal and vertical positioning of the seabed structures in the range of centimeters.

Techniques and Methods

In the last decade multibeam echosounder systems became a widely used tool for seabed mapping and have replaced the traditional single beam surveys. Seabed mapping based on single beam transects relies substantially on spatial interpolation methods, often guided by manual expert interference. In contrast, multibeam systems provide dense observational two-dimensional networks of depth soundings, from which a continuous digital terrain model of the seabed can be constructed.

The high spatial resolution of the multibeam method is achieved by high frequency transmission of an echosounder swath that is received in highly directional resolution by means of phase discrimination technique. The characteristic numbers of the system used by GKSS are listed in Table 1 and the system's components depicted in Fig. 1. Beam arrival times are transformed into distances by sampled vertical sound profiles combined with modelling of ray propagation. Any ship movement is compensated for by rapidly sampling motion sensors. Dynamical vertical and horizontal positioning of the multibeam-transducer with cm-precision is achieved using real-time kinematic global positioning (GPS-RTK) and a high quality gyro compass.

Limitations and Problems

The multibeam system requires a water depth of at least 3 m, a value that is also needed for shipping safety. The quality of the observations depends strongly on the effective compensation of the ship motion and a high quality of the GPS signals. This constrains the range for high-quality mappings to distances of 10 to 20 km away from the land-based GPS- reference stations and survey periods to moderate wave conditions. Repeated sampling of stable immobile seabed structures (fishing drag-board traces, ship wrecks) indicates that the reconstructed overall vertical position with respect to a fixed chart datum may vary by more than 10 cm from survey to survey. The causes of this variation have not been resolved yet. Hence, with- out a vertical reference present within the surveyed area overall variations in the seabed of less than 20 cm cannot be derived unambiguously over periods longer than several months. In contrast, using a fixed seabed structure as vertical reference the precision of multibeam data can be less then half a meter in the horizon- tal and one centimeter in the vertical, as demonstrated at the German Baltic coast (Fig. 2).

Provider	Kongsberg Maritime AS
Sound frequency	300 kHz
Soundings per ping	max. 254
Maximum Ping Rate	40 Hz
Maximum angular coverage	130°; swath 3.5 times the water depth
Beam width (transmission and reception)	1.5°

◀ **Table 1**
Characteristics of the EM 3002 multibeam system.

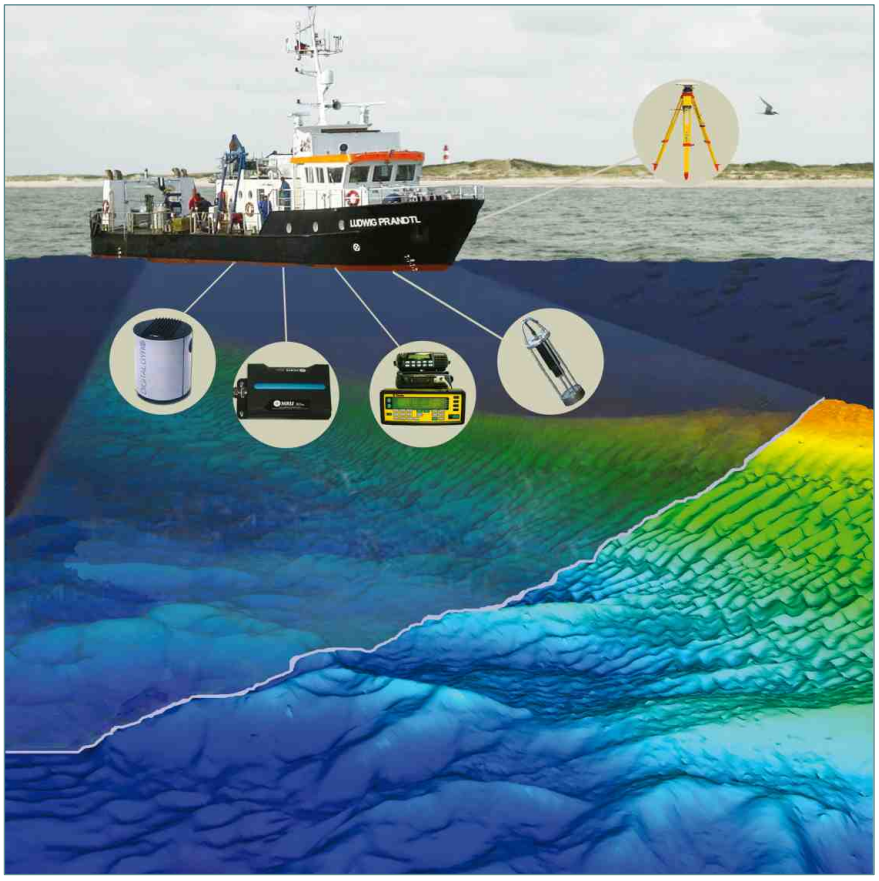

◄ Figure 1
The multibeam system as implemented onboard RV "Ludwig Prandtl". The light underwater cone symbols the beam swath, devices inside the circles show (from left to right) gyro compass, motion senor, ship-borne GPS-RTK, sound profiler, and RTK land base.

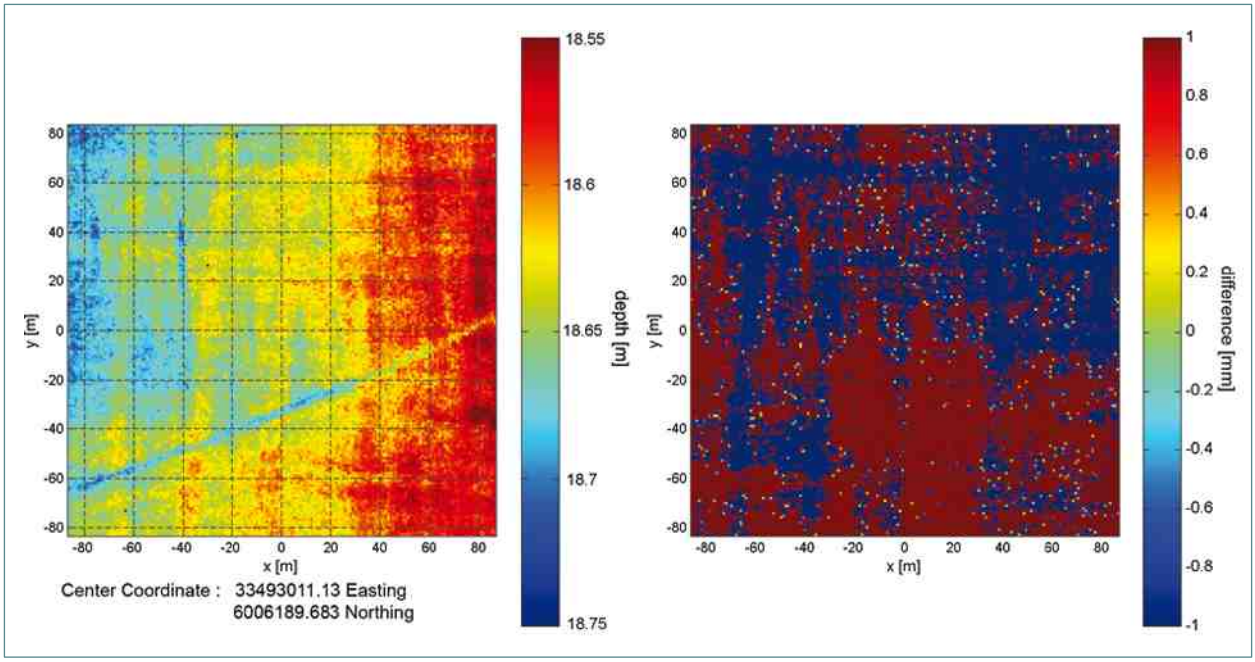

▲ Figure 2
Left: Digital terrain model (DTM) around a fishing drag board trace as obtained at the Baltic Coast in August 2001 during the DYNAS project. This drag board trace stayed nearly unchanged over more than three years. The centre coordinate is given in UTM32 projection. "y"-axis is in the north direction. Depth is with respect to the normal chart datum.
Right: Difference DTM plot October 2003 - August 2001. The high precision (i. e. reproducibility) of the observations can be derived from the complete disappearance of the trace in the difference plot. Note the expanded vertical scale at the right hand side of the panels, which for the right panel ranges from -1 to +1 mm.

Monitoring coastal morphodynamics using high-precision multibeam technology

Implementation & Results

Example: The fate of dumped material at the German Baltic Coast

Problem

Harbours, rivers and estuaries all over the world have to be dredged to remain navigable for modern sea traffic. Dredged material is often highly polluted and there is much concern about the dispersal of the material during and after dumping. For the German Baltic coast, this was studied in more detail close to Rostock-Warnemünde harbour (Fig. 3) within the framework of the DYNAS-project (Dynamics of natural and anthropogenic sedimentation, Harff et al., 2003, 2005). The fate of dredged material dumped into a site closed for shipping activity was followed over more than three years from June 2001 to August 2004 by means of multibeam technology (Stockmann et al., in print).

Results

The settled disposals consisted mainly of glacial till and formed crater-like structures reflecting the transfer of downwards into radial momentum after impact (Fig. 4). The seabed structures of the disposals showed only little change over time and their quantification by the multibeam echosounder surveys required a high measuring precision in the order of a few cm in the vertical. Volume estimations of the bed disposals revealed that material was transported away only during the dumping phase. Over the following years only reworking of the material took place: the surface smoothed out (see Fig. 4) and this process was faster at smaller horizontal scales (see Fig. 5). From the rate of the observed bathymetric changes, the material properties and model based wave and bed shear stress statistics it was estimated that these structures as a whole would persist for about a century (see Table 2).

Management implications

The observations have some consequences for the dumping management. As long as glacial till is dumped at comparably sheltered sites the loss and further dispersal of the dredged material is negligible over decades. Dumped material consisting of silt and sand may be transported away to a substantial degree in the form of plumes and be widely dispersed due to low settling velocities. As silt is the material with the lowest settling velocities in dredged sediment mixtures and also the most polluted material, coastal zone management must focus on the handling of this fraction of the dredged material. At the same time, glacial till chunks have a limited use in covering highly polluted seabed. Although they possess a high stability when deposited on the bed it will be most demanding to achieve a sufficient area-wide coverage as the radial dispersion of the settled material is very limited and further spreading very slow.

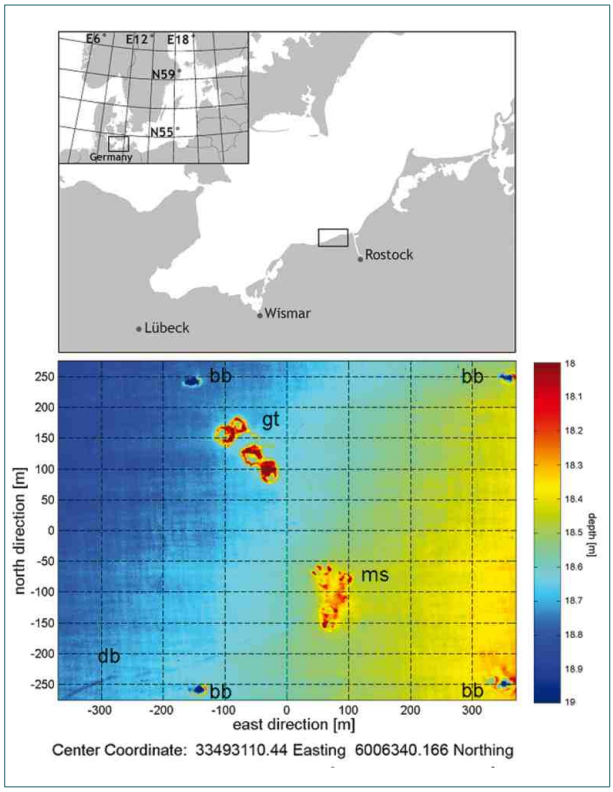

▲ Figure 3

Map of the study site located at the German Baltic coast

The lower panel represents the DTM of the August 2001 survey. The centre coordinate is given in UTM32 projection. The corresponding WGS 84 co-ordinates are N 54° 12.08', E 11° 54,14'. The depth is given with respect to the normal chart datum. The mounds of the dumped glacial till **(gt)** and the mixed soil **(ms)** are clearly visible. Other bed features are a fishing drag board trace **(db)** and the scour holes around the anchor stones of the boundary buoys **(bb)**.

Authors

Rolf Riethmüller, Karina Stockmann and Martina Heineke (GKSS)

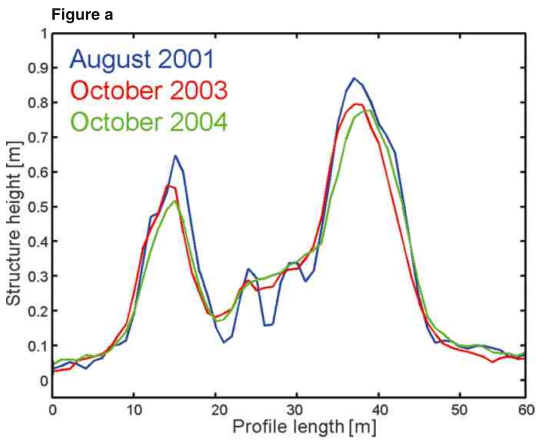

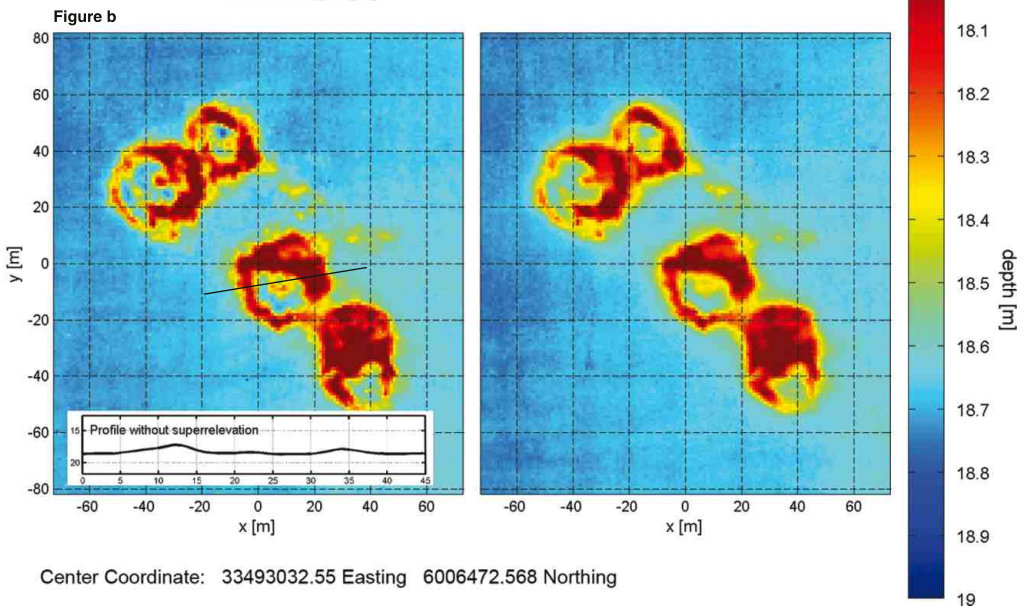

Figure 4

a) Bed elevation profiles across the glacial till transect shown in the right panel as obtained in August 2001, October 2003, and October 2004.

b) DTM of the glacial till dumping site as obtained in August 2001 and October 2004. The centre coordinate is given in UTM32 projection. "y"-axis is in North direction. Depth is with respect to the normal chart datum. The inset in the left panel shows the not exaggerated bed elevation profile along the transect across one of the ring structures as indicated by the black line.

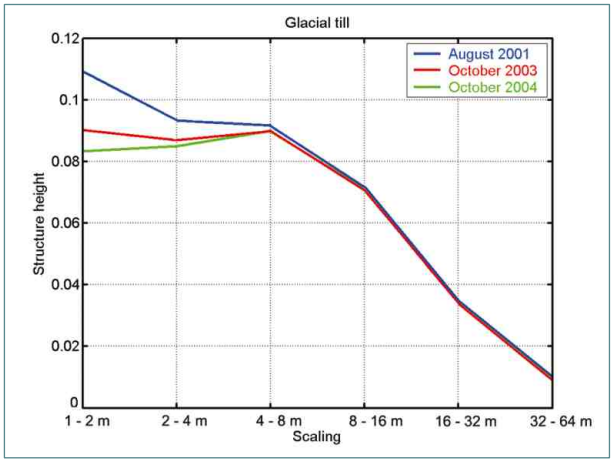

▲ Figure 5

Mean structure height of the glacial till mounds versus the horizontal scales of the mounds' surface structure elements for August 2001, October 2003 and October 2004. Flattening of the smaller structures takes place first at the smallest scales and becomes very slow at horizontal scales above eight meters.

Scaling method	Horizontal structure size [m]		
	1 - 2	2 - 4	4 - 8
	Surface flattening times [a]		
linear	6	16	70
exponential	12	35	134

▲ Table 2

Estimated surface flattening times for increasing horizontal structure size.

The temporal smoothing of the surface structures was extrapolated into the future using two different approaches: (1) a linear function, i.e. assuming a constant smoothing rate, and (2) by an exponential function, i.e. assuming a smoothing rate proportional to the surface variance.

Acoustic kelp bed mapping in shallow rocky coasts - case study Helgoland (North Sea)

Methods & Techniques

Introduction

Kelp beds are named after their habitat structuring organisms which are perennial brown macroalgae of several metres length, living submersed in the light penetrated zone of temperate and polar rocky shores (Fig. 1). Kelps provide substrate, food and protection for hundreds of different marine fishes, invertebrates, or other macroalgal species. A change or loss will have drastic consequences for coastal ecosystems.

In recent years worldwide reports of changing kelp beds have been published (e.g.: Japan: Kirihara et al., 2006; Norway: Moy et al., 2003; France: Cosson, 1999; Morizur, 2001; Australia: Australian Marine Conservation Society, www.amcs.org.au/). In Europe, including Helgoland (Gehling & Bartsch, submitted), there is evidence of a biomass decrease and/or change in depth distribution of some species. As the marine protected area off Helgoland is the only rocky area within the southern North Sea, this habitat is extremely important. Spatial information on the extent of the prevailing kelp beds is urgently needed as a baseline from which to judge future changes. This led to the current investigation.

Methods and techniques

Traditionally, diving transects have been used to investigate the sublittoral zone off Helgoland (Lüning, 1970, Gehling & Bartsch, submitted). This technique is precise with respect to species identification and abundance recording but does not provide spatial information and is very slow. To enhance monitoring speed geo-referenced underwater video transects are being evaluated. Although this technique is much faster in the field than diving, data evaluation still has to be done manually. Acoustic devices on single beam echo sounder basis such as Roxann (Sonarvision) promise rapid measurement of transects at 4 knots and offer the possibility of automated signal processing and interpretation. Furthermore, interpolation techniques may be employed to generate spatial maps from a grid of regular transects. Normally this technique is used for seabed habitat mapping in greater depths (Brown et al., 2005; Humborstad et al., 2004). Here, we applied the method to depths from -2 m mean low water spring and below, which is at the technical limits as the reflected pulses at low water depth return too fast to be correctly recorded. The Roxann signal processor includes a Furuno stereo trans-ducer system (28 and 200 kHz) mounted on board the research vessels (Fig. 2). Both echosounder signals are recorded synchronously. In order to correlate Roxann data with seafloor characteristics, selected areas and transects were chosen for intense groundtruthing with the help of under water video and diving transects.

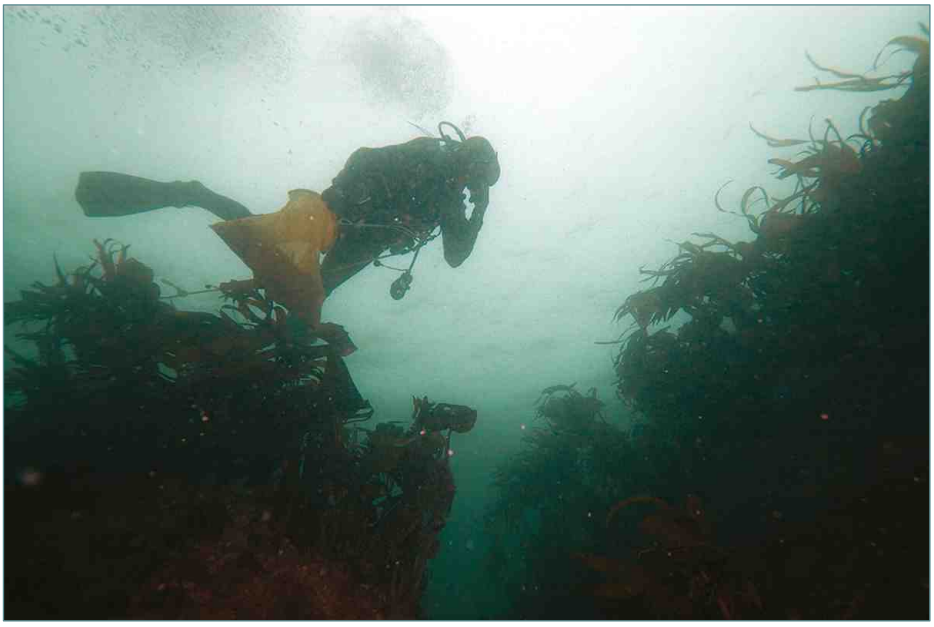

◄ Figure 1
Aspect of the kelp forest off Helgoland. The main structuring species is the brown alga *Laminaria hyperborea* which grows to a length of approx. 1-2 m and provides shelter and substrate for many other species.

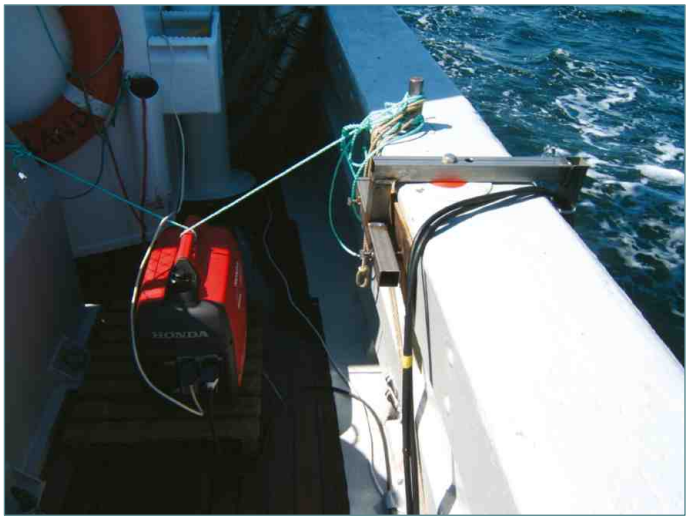

Figure 2 ▲ and ►
The stereo transducer system for RoxAnn mounted on board of the small research vessel 'MS Aade'. **Left:** The sonar is fastened by a long u-shaped stainless-steel bracket at the ship's rail. **Right:** The stainless steel duct holds the sonar just below the water surface at a defined depth.

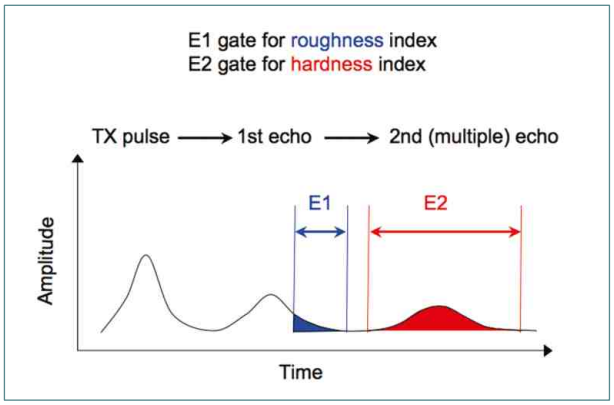

◄ Figure 3
Principle of RoxAnn data recording: Energy of the coloured regions is integrated to form two indices: E1 (roughness) and E2 (hardness). The first echo contains ambiguous sub-bottom reverberations, thus, summation begins electronically gated one pulse length from the echo start for E1 **(blue)**. For E2 the entire second echo is integrated **(red)** (after Hamilton, 2001).

Seafloor classification system RoxAnn (Sonar Vision)

This system uses the first and second echo returns to analyse seafloor properties (Fig. 3). The transceivers transmit pulses over a variety of angles. A perfectly smooth seafloor would reflect only the energy from the 0° angle. Echoes from other angles would travel away from the transceiver. The rougher the seafloor is, the more energy is received back and thus the higher is the E1 value. Thus E1 is a measure for the roughness of the seafloor. The echoes travel from the seafloor to the sea surface (including ship's hull), back to the sea floor and again up to the sea surface where they are recorded as the first multiple (E2). The harder the seafloor, the higher becomes the E2 value, which thus is a measure for the hardness of the seafloor (Chivers et al., 1990; Hamilton, 2001). Both parameters characterise the properties of the seafloor and are used for its classification (Fig. 4).

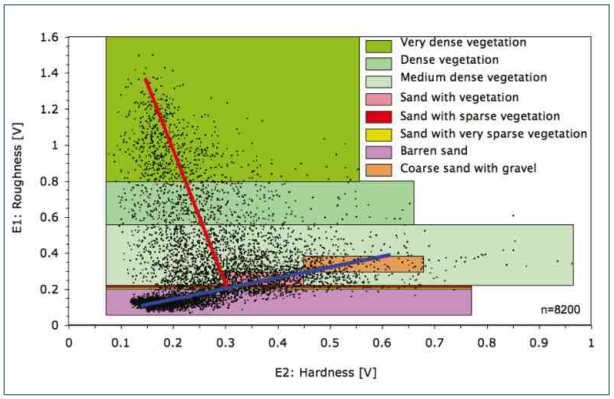

▲ Figure 4
Plot of E2 (hardness) vs. E1 (roughness) and the positions of the RoxAnn classes.The straight lines suggest the influence of the sediment (blue, hardness component dominant) and the vegetation (red, roughness component dominant) on the data.

Acoustic kelp bed mapping in shallow rocky coasts - case study Helgoland (North Sea)

Implementation & Results

Implementation

First campaigns with the RoxAnn seafloor-discrimination system took place in summer (2005 and 2006), the time of the year when kelp bed development is best. We investigated the ridges south of Dune Island and north of the main island (Fig. 5) in detail using BAH research vessel "Aade" (Fig. 6). Detailed data processing has so far only been carried out for the area south of Dune Island. This area covers 1.4 km². The total length of the transects is about 30 km. A total of 28 lines were measured perpendicular to the extension of the kelp-inhabited areas. Duration of data acquisition was approx. 4 h during one day. Recorded data included DGPS data (position, date, time) and RoxAnn data (water depth, E1 and E2 values for each frequency). Ground-truthing took place within one month. This is possible as macrophyte vegetation in summer is quite stable unless there is a severe storm.

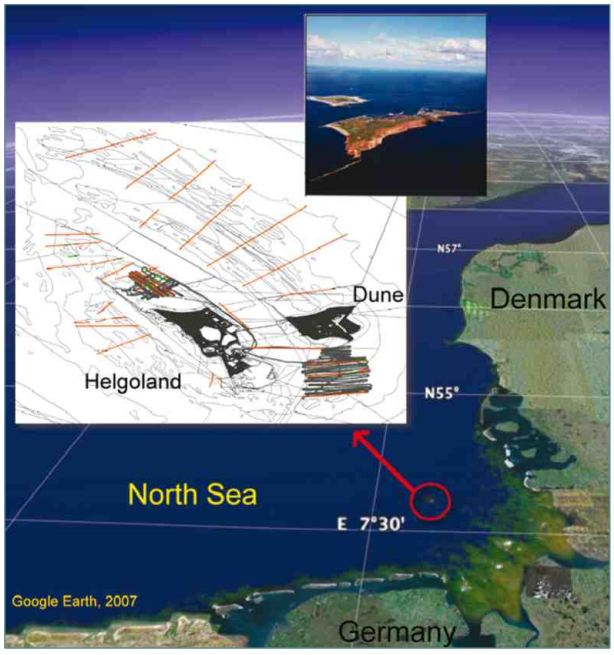

▲ Figure 5
Investigation area off Helgoland during the campaign in 2006. RoxAnn tracks are in grey. Ground-truthing was done by under-water video transects **(orange)** and diving transects **(green)**. Under-water videos were acquired in cooperation with the research vessel Aldebaran (www.aldebaran.org).

Terrain model

The RoxAnn data were used to create an underwater terrain model, which is now available for the first time (Fig. 7). Tidal effects were excluded on the basis of a DGPS working in real-time kinematic mode (RTK) that allows precision in the cm-range. The corresponding DGPS reference station has been installed on the main island. All depth values were filtered to exclude bad measurements and the remaining data were used to produce a data grid using the kriging method. South of Dune Island water depth values range between 2 and 14 m. The hard rock ridges emerge from the otherwise unstructured seafloor which is covered here by sand.

Sea floor classification

In order to generate a classified map of the seafloor, in the lab, the following classes were first established as a basis and then correlated with the E1/E2 values by comparing ground-truth information and RoxAnn data:

1. Very dense vegetation (kelp beds)
2. Dense vegetation (kelp beds)
3. Medium dense vegetation (kelps and red algae)
4. Sand with vegetation
5. Sand with sparse vegetation
6. Sand with very sparse vegetation
7. Barren sand
8. Coarse sand with gravel

The results are shown in Fig. 8. It is obvious that the elevated ridges are covered with dense kelp bed vegetation, thinning out to the margins. In some areas there is sparse vegetation on sand and the area in between the two prominent ridges is filled with sand, which is totally unvegetated. In the western part of the investigation area sand intrudes and covers the rock ridges. The classes 1-3 and 7-8 are reproducible while the discrimination of sparsely vegetated areas still delivers variable results.

Prospects

Since it can be assumed that current and wind action is responsible for the sand cover that is entering the western ridge south of Dune Island, the coverage with kelps and other seaweeds will be variable here. Thus this area is of great interest to monitor interannual changes. The main kelp-bed area, however, is located north of Dune and the main island. With these promising results as background, they will be investigated by the same method soon.

The presented data are preliminary and not yet published. Please refer to the authors for further information.

Authors

Christian Hass and Inka Bartsch (AWI)

◄ Figure 6
Research vessel "Aade" of the Biologische Anstalt Helgoland was used for the mapping campaign. The red box on the pier in the foreground contains the RoxAnn signal processor.

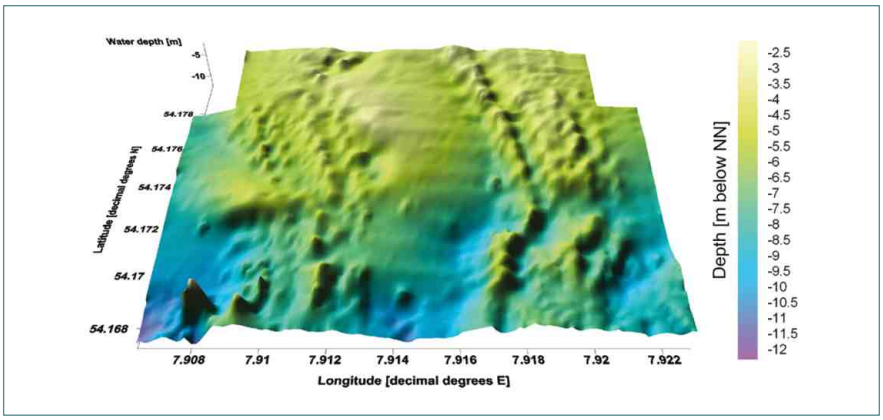

► Figure 7
Digital underwater terrain model of the area south of Dune island at Helgoland. These data allow for the first time a visualisation of the underwater morphology. The visible depth differences comprise approx. 10 m. The partial coverage of ridges and the intrusion of sand at the western ridge are clearly visible.

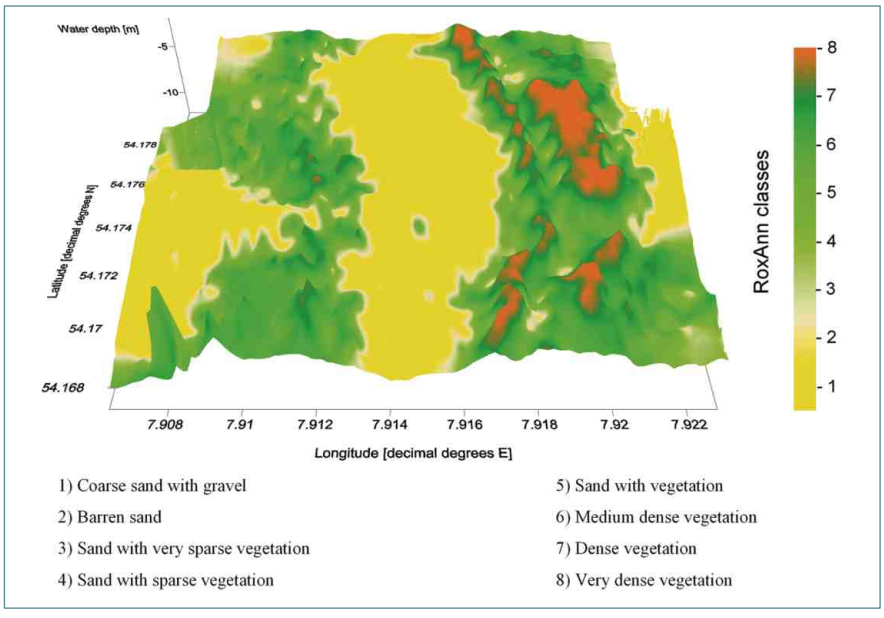

◄ Figure 8
Classification of seabed characteristics south of Dune Island evaluated by comparison of ground-truth information and relationships of E1 and E2 values. The ridges visible in Fig. 7 are covered by dense kelps (see Fig. 1) thinning out to the margins. Unvegetated sands dominate between the ridges.

Monitoring parameters of organism and ecosystem health

The health of marine organisms and their ecosystems is a central issue for monitoring the coastal environment.

Marine mammals and sea birds as top predators in the food chain require our particular attention. Their population size, distribution and health status have to be quantified for effective protection measures. On the other side trace substances have to be monitored, which are partly the cause for the stress on organisms and ecosystems and are accumulated in the top predators.

The methods presented here are procedures to record the populations of a whale species, the harbour porpoise, and of sea birds and to detect contaminants by trace compounds.

Content

How to estimate the abundance of marine mammals?

Methods & Results

Background

For basic and applied research as well as management of marine mammals, it is essential to have reliable information on the size of a population and the use of different marine ecosystems. Monitoring concepts and the estimation of effects of anthropogenic activities on marine mammals require fundamental knowledge on the biology and ecology. The standard method, internationally approved, for assessing distribution and abundance of marine mammals, is the line transect sighting survey using ships or airplanes. With this method it is possible to give estimates on the abundance, to investigate distribution patterns and to analyse spatial and seasonal differences in density and distribution.

The Research and Technology Centre Westcoast (FTZ) conducted a line transect sighting survey that covered waters in the German exclusive economic zone (EEZ) and the 12 nautical miles zone of the North and the Baltic Sea from May 2002 to June 2006.

Line transect methodology

The methodology followed the line transect distance sampling technique, where the observer travels along a transect line, recording detected objects and the distance from the line to each object (Buckland et al., 2001). The survey design comprised a grid of systemically spaced transect lines randomly superimposed on the study area. As transect direction should not parallel some physical or biological feature to avoid an unrepresentative sample, transects were placed perpendicular to water depth gradients, as recommended by Buckland et al. (2001).

Surveys were flown at 100 knots (185 km/h) at an altitude of 600 feet (183 m) above the water surface in a Partenavia P68, a high-wing aircraft equipped with two bubble windows to allow scanning directly underneath the plane. The survey team consisted of two observers and one data recorder (navigator). Sighting data were acquired by the two observers in parallel, each positioned on one side of the aircraft at a bubble window. The navigator entered all reported data online into a computer, interfaced with a global positioning system (GPS). The computer stored the aircraft's position every 2 sec.

Surveys were only conducted when Beaufort sea state was less than or equal to three and when visibilities were greater than 3 km. Environmental conditions were recorded at the beginning of each transect and were updated with any change. Data collected on environmental conditions included Beaufort sea state, water turbidity, percentage of cloud cover, and for each observation position, glare and overall viewing quality (good, moderate or poor). All data recorded in poor sighting conditions (e.g. Beaufort sea state > 3) were excluded from subsequent analysis.

Data recorded for each harbour porpoise sighting included: exact position when the group passed perpendicular to the window, angle of inclination to the group, estimated group size, number of calves, sighting cue, behaviour and swimming direction. The perpendicular distances from the transect line to the group were later calculated from aircraft altitude and declination angle.

During the census of cetaceans it is never possible to detect all objects present on the transect line. Two factors influence detectability: i) availability bias and ii) perception bias (Marsh & Sinclair, 1989; Laake et al., 1997). These two factors are usually combined in g(0), which is the probability of detecting an object on the transect line (Buckland et al., 2001). The availability bias describes the probability of an animal being available for detection (i.e., at or near the surface), whereas the perception bias incorporates the probability that an animal, when it is physically available for detection, is missed by the observer (e.g. due to fatigue, observer experience or environmental condition). For determining g(0) the Hiby racetrack data collection method was used, which involves (some) doubling-back to re-survey previously flown transect segments (Hiby & Lovell, 1998; Hiby, 1999). From the time and position of the original as well as the re-sightings the Hiby algorithm determines the probability of sightings the same group.

Distribution mapping

Data of the six study years (2002-2006) were pooled across seasons, since prior statistical tests did not detect any significant variation between data collected in different years. The winter months were excluded due to poor effort and thus insufficient coverage of the study area. For the spatial analysis in ArcGIS 8.3 (ESRI), a grid with a resolution of 10x10 km was created, dividing the study area into 550 quadrate cells. Mean density could then be estimated per grid cell ($\hat{D}$ [indiv. km^{-2}]):

$$\hat{D} = \frac{n_{indiv.}}{effort}$$

where $n_{indiv.}$ is the sum of harbour porpoises per cell and *effort* is the area searched effectively (in km^2).

Authors

Anita Gilles and Ursula Siebert (Research and Technology Centre Westcoast of the University of Kiel)

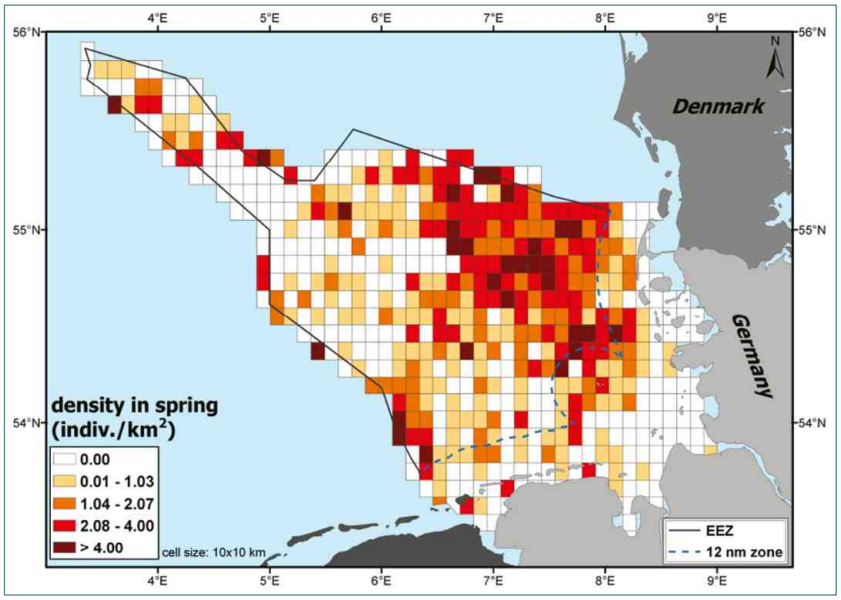

Figure 1a

The following figures give examples of the seasonal variation of harbour porpoise distribution and density in the German exclusive economic zone (EEZ) of the North Sea.

High densities of harbour porpoises were consistently found in spring and summer in the north-eastern part of the study area, on the Sylt Outer Reef.

In spring, another hotspot of high densities was detected in the area Borkum Reef Ground.

In summer, a pronounced north-south density gradient was observed.

In autumn, porpoises are more evenly dispersed and the overall density is lowest in comparison to other seasons.

Figure 1b

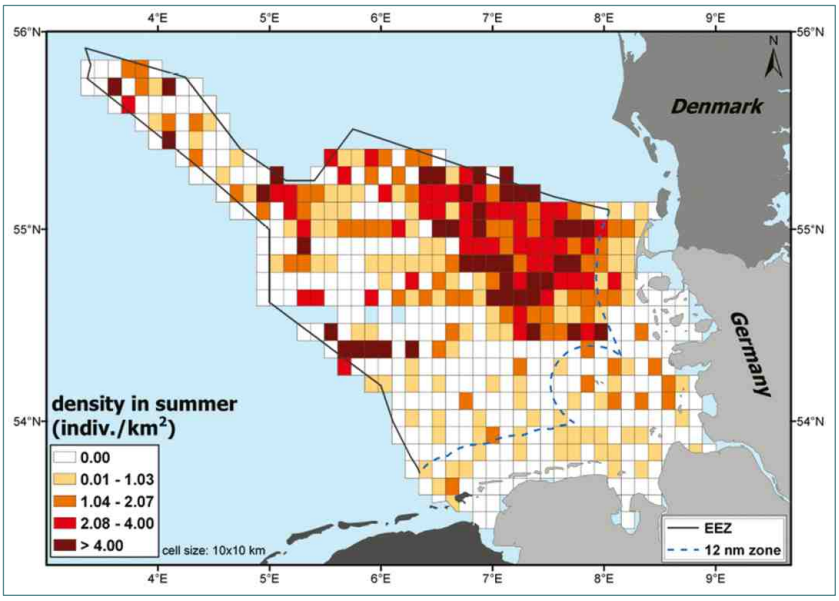

Figure 1 a-c

Mean density of harbour porpoises in the German EEZ and 12 nm zone. Data, collected during aerial surveys, from the study years 2002 to 2006 were pooled. **a)** spring (March-May), **b)** summer (June-Aug.), **c)** autumn (Sep.-Nov.).

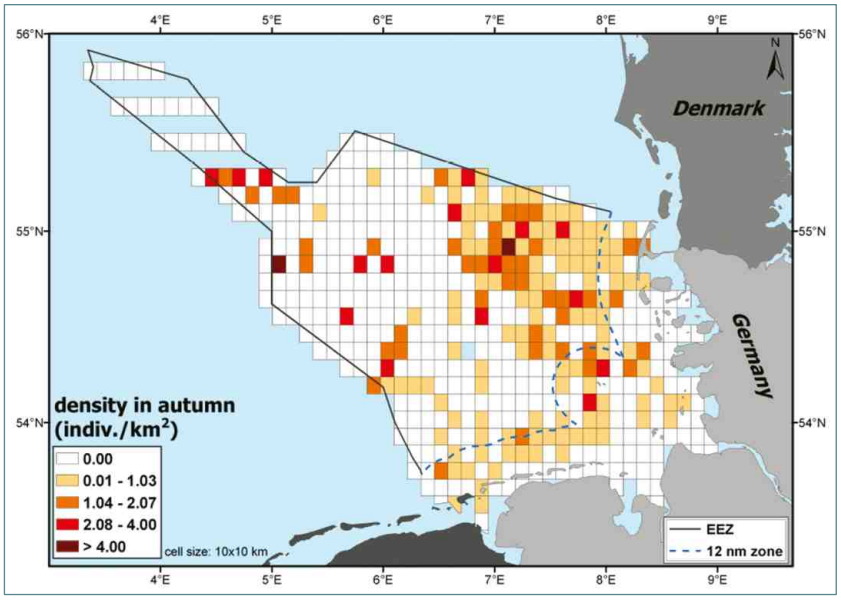

Figure 1c

Acknowledgements

The study was funded by the German Federal Ministry for the Environment, Nature Conservation and Nuclear Safety (BMU) through the MINOS and MINOSplus projects . Data of the project EMSON, funded by the Federal Agency for Nature Conservation (BfN), were used in spatial analysis of distribution patterns.

Counting seabirds from ships and aircraft

Methods & Results

Introduction

A few decades ago, knowledge about seabirds at sea was hardly available. In comparison, information on breeding ecology was more available, as brooding seabirds are easily to study. Systematic seabird surveys for the North Sea and the Baltic Sea have only been carried out during the last 2 or 3 decades. At present, studies for the German waters focus mainly on basic and applied research topics like functional relationships between the marine environment and seabird occurrence as well as their spatio-temporal dynamics. Applied approaches strongly increased with the first plans to set up offshore wind farms. The need to designate protected areas at sea, e.g. according to the EU Wild Birds Directive, as well as shipping traffic, fisheries and oil pollution, led to further data collections and analyses. In the meantime, surveying seabirds at sea became more and more part of national monitoring programmes. Here, we briefly describe the method used for counting seabirds at sea and illustrate results for one selected species, the Northern Fulmar (*Fulmarus glacialis*) (Fig. 1).

Counting methods from ships and aircraft

The common counting method for seabirds at sea from ships and aircraft is the counting along transects (Fig. 2). The transect width is 300 m for ship-based surveys and usually 397 m for aerial surveys. Since 1991 this method is the international standard for the north-east Atlantic region. For the two observation platforms, the transect strip is subdivided into bands which allow the later distance correction. The transects are set perpendicular to one or both sides of the ship/aircraft. All birds in the transect are counted and, if possible, are identified at species level. Additional information is, if possible, gathered on sex, age, and behaviour.

During ship-based surveys, swimming and flying individuals are counted in different manners. Birds flying over the area of the transect strip are only counted at certain intervals, usually every full minute, thus the birds' movements are “frozen” and an overestimation of flying birds is avoided. Individuals crossing the transect strip during other times and outside the transect area are usually also recorded, but are not included in density calculations. During all surveys, geographical positions are recorded every minute on boats and every 5 seconds on aircraft.

Both methods have their advantages and disadvantages. Aerial surveys enable large coverage in a short time, with more or less constant environmental conditions, while these conditions may change more often during long ship-based surveys. In contrast, aerial surveys can only be conducted during calm conditions (max. 3-4 Bft). At higher seastates many birds remain unobserved. For some taxa species identification during aerial surveys is only possible to a very limited extent, e.g. divers, loons, auks, gulls and terns. For some species, aerial surveys provide better counting results. On the other hand, ship-based surveys allow much more detailed protocols, especially on bird behaviour, and hydrographic measurements can be carried out. The appropriate counting method depends largely on the study goals. Ideally the two methods are combined.

Finding food is the main activity of all seabirds at sea. The foraging activities give information on the occurrence of birds in open waters and coastal areas and thus, particular attention is paid on the birds’ foraging behaviour during ship surveys. Most bird species in the German North Sea forage on, at or slightly below the water surface. Therefore, standard techniques for assessing food availability, such as hydroaccoustic surveys as they are used for fish, cannot be used for technical reasons. Instead, the foraging behaviour of seabirds gives often the only information on the marine and hydrographical processes which control the distribution of the birds at sea. They are ideally complemented by analyses of stomach contents and regurgitated food remains, obtained from other studies. Ship-based surveys are also appropriate to synoptical studies of the birds' habitats.

Results: the example of the Northern Fulmar

In Germany, the Northern Fulmar breeds only in a small colony on the island of Helgoland with about 100 breeding pairs but most individuals in German waters are non-breeders or originate from colonies in the U.K. or further north. However, the species is widespread at sea during all seasons. Total numbers in the German North Sea including the Exclusive Economic Zone (EEZ) and the territorial waters of the Federal States of Schleswig-Holstein and Niedersachsen have been estimated at 11,500 individuals in spring, 40,000 ind. in summer, 24,000 ind. in autumn and 10,500 ind. in winter (Garthe et al., 2007). These changes in total numbers become even more visible in the maps for the German Bight (Fig. 3). Northern Fulmars are clearly more abundant in summer than in winter. The distribution of this species is closely linked to the Central North Sea Water while the Continental Coast Water is usually avoided (Garthe, 1997; Markones, 2007). The shown distribution is only an average with substantial variation, which is related to the hydrographic and meteorological regime.

Authors

Stefan Garthe (Research and Technology Centre Westcoast of the University of Kiel)

▲ **Figure 1**
The Nortthern Fulmar (*Fulmarus glacialis*) is one of the most common seabirds in the Northeast Atlantic and the North Sea.

▲ **Figure 2**
Counting birds at sea on a ship survey.

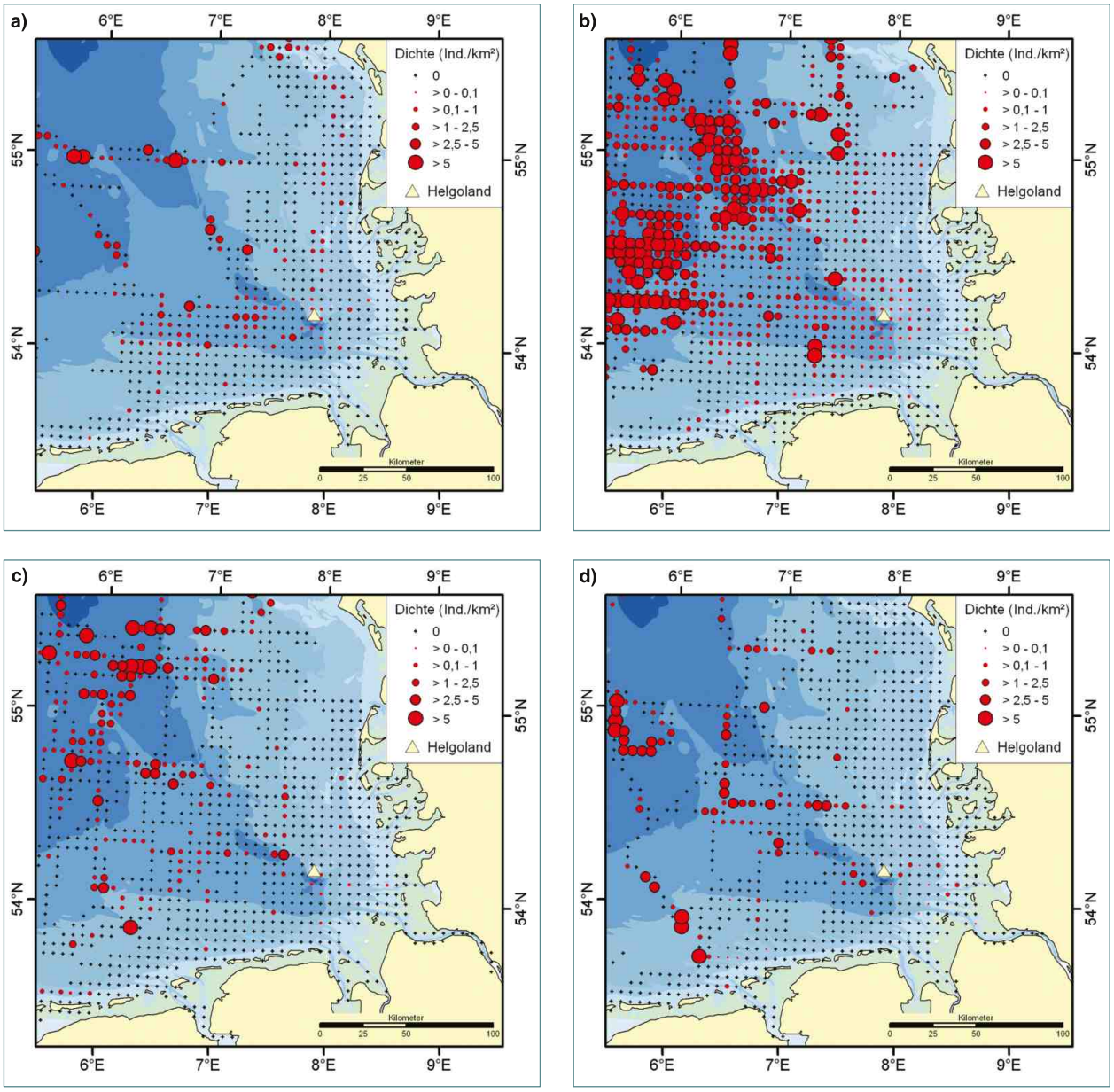

▲ **Figure 3 a-d**
Distribution of Northern Fulmars in the German Bight over the yearly cycle: a) spring, b) summer, c) autumn and d) winter. The data originate from ship-based surveys in the years 1990-2006.

Marine mammals' health as an indicator of ecosystem health - tools for monitoring

Methods & Techniques

Introduction

Marine mammals serve as indicators of ecosystem change (Trilateral Monitoring and Assessment Program, TMAP, Fig. 1). They are top predators in the marine food web. Increasing commercial use, e.g. fisheries and offshore wind parks, as well as the inputs of pollutants, influence the North and Baltic Sea ecosystems, including native marine mammals such as harbour porpoises, harbour seals and grey seals. Thus, the aim is to establish effect-monitoring tools for early diagnosis of the health status of marine mammals.

Immune system parameters are measured via biomolecular and biochemical methods. Non-destructive biomarkers will be identified and chemically characterised to serve as biochemical indicators.

Common Package of TMAP Parameters

Chemical Parameters	Biological Parameters	Human Use Parameters
• Nutrients • Metals in sediment • Contaminants in Blue Mussels, Fluonders and bird eggs • TBT in water and sediment	• Phytoplankton • Macroalgae • Eelgrass • Macrozoobenthos • Breeding birds • Migratory birds • Beached Birds Survey	• Fishery • Recreational activities • Agriculture • Coastal protection
Habitat Parameters	**• Harbor Seals**	**General Parameters**
• Blue Mussel beds • Salt marshes • Beaches and Dunes		• Geomorphology • Flooding • Land use • Weather conditions • Hydrology

▲ Figure 1

The harbour seal as top predator is an important biological parameter of the Trilateral Monitoring and Assessment Program (TMAP). This program was founded by The Netherlands, Denmark and Germany, for the protection and conservation of the Wadden Sea. It includes management, monitoring and research, as well as political matters.

Methodology

Blood samples of captive and wild living animals are the study objects (Fig. 2). Selected parameters which play a central role in controlling disease processes are determined. The following immune system parameters were selected: the lymphocyte proliferation as important immune cell function, the expression of cytokines released by immune cells, which are regulators of an immune reaction, as well as cytokine-induced acute phase proteins (APPs) for the early diagnosis of inflammation and stress. The combined investigation of these parameters allows a statement about the immune status of the animals and the impact of pollutants.

Technique for measurement of lymphocyte proliferation

Lymphocytes were isolated from the blood sample and cultured with and without stimulation using a lymphocyte transformation test (LTT, Fig. 2). After incubation transformation and proliferation were examined and a stimulation index calculated.

Technique for quantification of cytokine expression

Cytokine expression is measured quantitatively by analysing mRNA amounts with the real time reverse transcriptase-polymerase chain reaction (RT-PCR, Fig. 2). Detecting the amount of the mRNA allows us to calculate ratios between cytokines and thus establish the main focus of the immune response. Investigations of the cytokine expression pattern (Interleukin-1, -2, -4, -6, -10, -12, TNF, TGFß) allow the status of the immune reaction to be differentiated, whether the emphasis is on the cellular or humoral (body liquid) immune response.

Technique for the analysis of acute phase proteins

The acute phase proteins of harbour seals are characterised quantitatively and qualitatively to find relevant biochemical indicators for their health status. After their isolation, the structures of selected proteins are elucidated with mass spectrometric techniques. Bio-analytical procedures will be established to determine disease-related structural variations, i.e. in the pattern of glycosylation. Based on the findings, specific bio-assays will be developed for monitoring the health status of marine mammals.

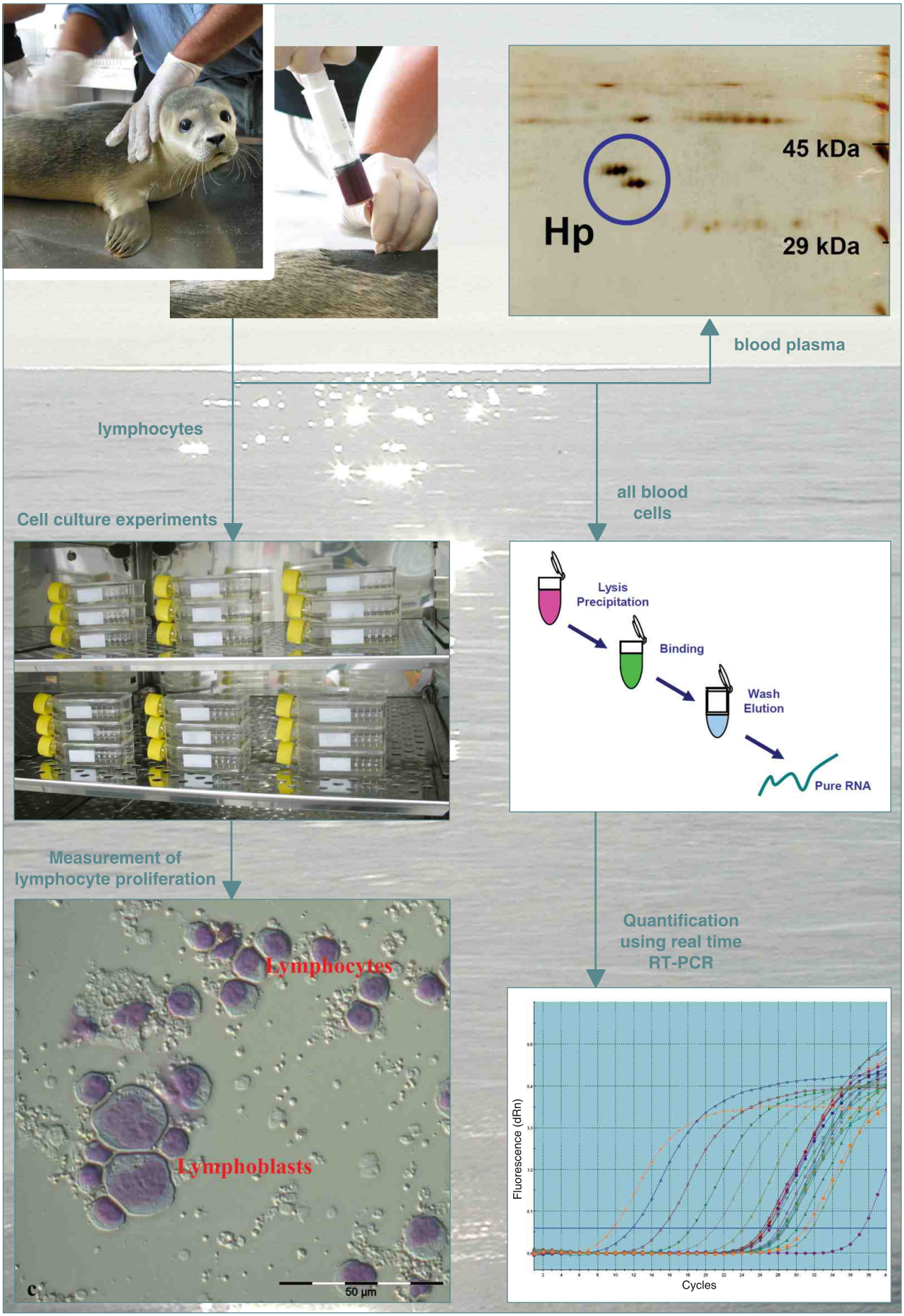

▲ Figure 2

Overview of immunological investigations using blood samples of marine mammals.

Marine mammals' health as an indicator of ecosystem health - tools for monitoring

Implementation & Results

Metal pollution – influence on immune system

Pollution with metals may affect the immuno-competence of free-ranging populations of marine mammals in many areas of the industrialised world. An imbalance of the immune system caused by pollutants has been suggested to play a role in the incidence of infectious diseases in marine mammals (Jepson et al., 1999; Siebert et al., 1999; Bennett et al., 2001). Metals influence the function of immuno-competent cells by a variety of mechanisms. Depending on the particular metal, its speciation, concentration and bioavailability, and a number of other factors, a continuous metal exposure will result in immuno-suppression or immuno-stimulating effects (Fig. 5).

• Metal hypersensitivities in seals

The chronic intake of metal pollutants makes marine mammals susceptible to developing hypersensitivity reactions (Fig. 5). Metal-specific hypersensitivity reactions were found in different pinnipeds from the North Sea (Kakuschke, 2006). The frequency of sensitising metals was in the order Mo > Ni >Ti > Cr, Al > Pb, Be, Sn. A relationship between the blood levels of metals to metalspecific hypersensitivity reactions was reported (Kakuschke et al., 2005). A relationship between lymphocyte proliferation and cytokine expression could be shown: in a study of a grey seal, a hypersensitivity reaction to Ni and Be has been correlated to alterations in the cytokine pattern (Kakuschke et al., 2006).

• High susceptibility of the immune system to the toxic effect of pollutants in pups

Pups are exposed to metals due to the transplacental transfer mother/fetus, the transfer through the milk and later by contaminated prey. In addition to immuno-enhancement, metals can induce immuno-suppression (Fig. 5). Kakuschke et al. (2007) found that lymphocytes of seal pups are particularly susceptible to the toxic effects of metals in the newborn period and that this susceptibility decreases subsequently (Fig. 3).

Stress – influence on the immune system

The cytokine expression can be modulated by numerous factors, including stress. Fonfara et al. (2007) compared cytokine mRNA expression from harbour porpoises exposed to different environments. Blood samples were taken from two healthy porpoises living in captivity at the Fjord and Belt Centre Kerteminde, Denmark, and from four wild porpoises accidentally caught in Danish waters. The results are suggestive of stress-induced modulation of the immune responses in the accidentally caught animals.

Challenges

Anthropogenic influences lead to changes of the health status of the animals. A set of reliable medical parameters enables us to investigate routinely a higher number of animals and to obtain information at population level. This information is part of the assessment of the status of the ecosystem as required by the TMAP.

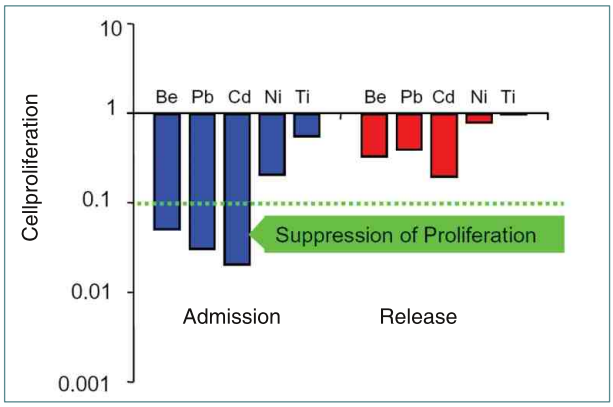

▲ Figure 3

Directly after arrival in the Seal Station the lymphocytes of newborns were particularly susceptible to the toxic effect of metals. A lot of metals tested e.g. beryllium, lead and cadmium inhibit the lymphocyte proliferation (value <0.1). This effect decreased during the time of rehabilitation.

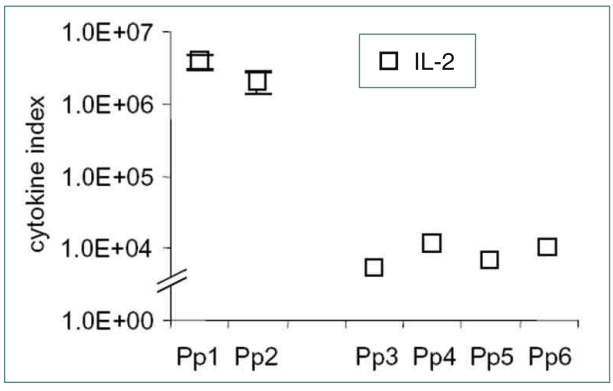

▲ Figure 4

Cytokine index of IL-2 mRNA from the blood samples of two harbour porpoises living in captivity (Pp1, Pp2) and four accidentally caught animals (Pp3–Pp6).

Authors

Antje Kakuschke, Katharina Kramer and Sonja Fonfara (GKSS)

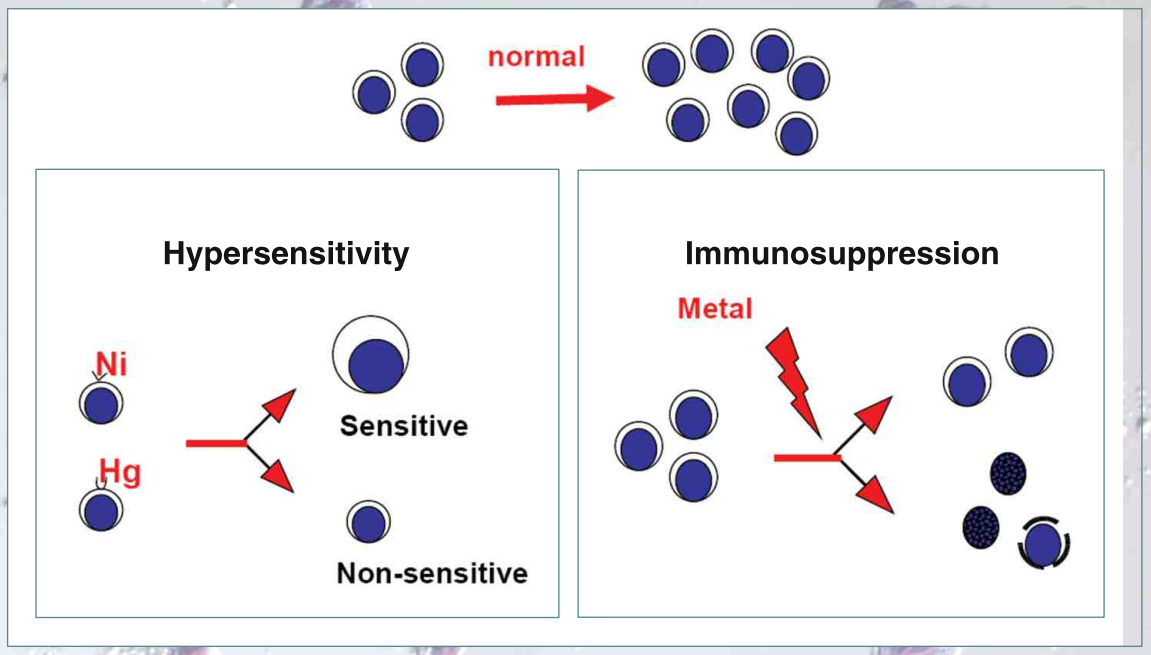

▲ **Figure 5**
Chronic metal exposure can lead to abnormal lymphocyte proliferation, and both hypersensitivity as well as immune suppression is known to be induced by chronic metal exposure. Some metals induce the formation of memory cells. By re-exposing these memory cells a rapid immune reaction is induced and transformation into blasts and proliferation take place. Other metals lead to immune suppression by unspecific inhibition of lymphocyte proliferation or show cell toxic influences.

► **Figure 6**
In cooperation with the FTZ Büsum seals were caught in the Danish and German Wadden Seas, specifically at the Islands Rømø and Helgoland and the sandbank Lorenzenplate. The seals were caught with a long net and for further investigations put in small individual nets. Several clinical parameters were collected and blood samples were taken. Additional blood samples were taken from pups during rehabilitation in the Seal Station Friedrichskoog.

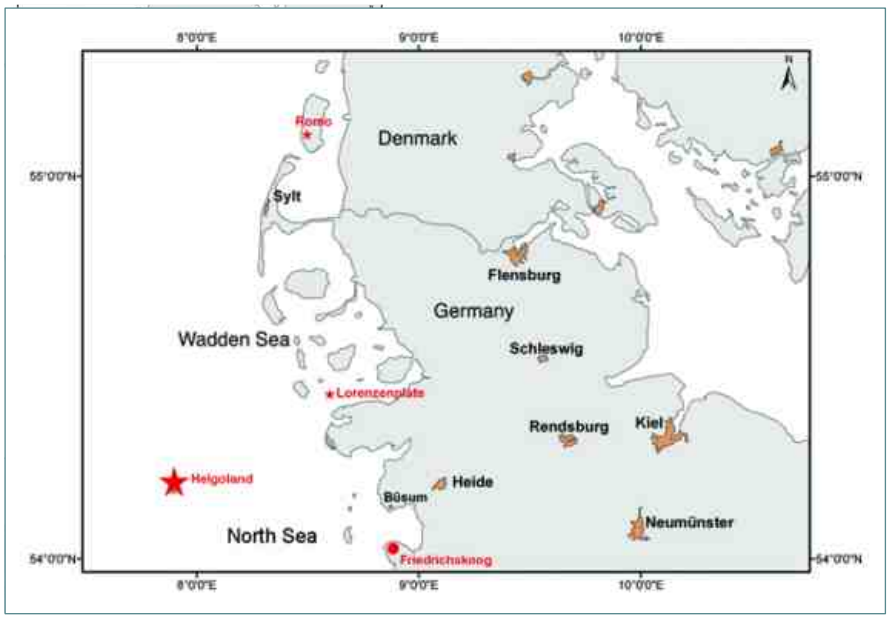

Elemental mass spectrometry - a tool for monitoring trace element contaminants in the marine environment

Methods & Techniques

Introduction

To understand the role and effects of trace elements and their species in marine ecosystems sensitive techniques are necessary to monitor their distribution between different environmental compartments. Since the beginning of industrialisation, anthrophogenic activities such as smelting, energy production, traffic, corrosion processes and landfill, and natural processes such as alteration, leaching or volcanism both influenced the specific distribution of trace elements within the marine environment.

Even though the element concentrations in the water phase are relatively low, as indicated in Fig. 1, significantly increased concentrations at higher levels of the food chain can be observed due to biomagnification effects. Especially top predators such as marine mammals are influenced, and different metal related effects on their health status have been recently investigated (Kakuschke et al., 2005). Therefore, precise information on the pattern of trace elements within the ocean as well as their concentration in selected animal species is of great importance to understand the related biological effects.

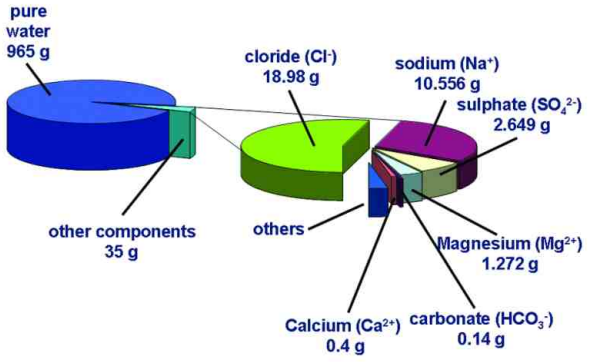

Element (ng/L)	North Pacific	North Atlantic
Mo	5000-10000	5000-10000
U	1800-2800	1800-2800
V	1630-1834	509-1172
As	1498-1798	1498-1573
Ni	117-704	117-352
Zn	7-536	7-105
Cu	32-286	64-127
Cr	156-260	14-165
Se	39-182	39-118
Mn	4-165	3-56
Cd	0,1-112	0,1-39
Fe	1-56	3-56
Pb	1-10	4-31
Co	0,8-3	1-2

▲ Figure 1
Average matrix composition of 1 kg seawater (values taken from Grasshoff et al., 1999).

Challenges

Environmental samples such as seawater, biological fluids or tissues are complex mixtures. Often, they contain a few highly abundant elements (g l^{-1} level), which interfere with the sensitive determination of the remaining less concentrated elements (ng l^{-1} level) (Fig. 3).

Established methodologies often require complex separation schemes to remove the interfering matrix components. Often, they are prone to errors and contamination, which leads to inaccurate results. Furthermore, most of them do not allow the simultaneous determination of a set of elements.

Methodology

To overcome these limitations, a method based on elemental mass spectrometry, namely the collision/reaction cell inductively coupled plasma mass spectrometry (CC-ICP-MS) has been developed (Fig. 4 and 5). It enables us to quantitatively determine a set of elements within a sample simultaneously (Leonhard et al., 2002). Here, an inductively coupled argon plasma is used to dry and to destroy the sample matrix as well as to generate mainly singly charged element ions, which makes them detectable by mass spectrometry.

Plasma
Partly ionised gas, which contains electrons and ions. For the formation of singly charged element ions temperatures have to be up to 8000 K.

As shown in Fig. 2, ICP-MS allows the determination of nearly all relevant elements present in the periodic table with outstanding sensitivity and accuracy (Fig. 6 and 7).

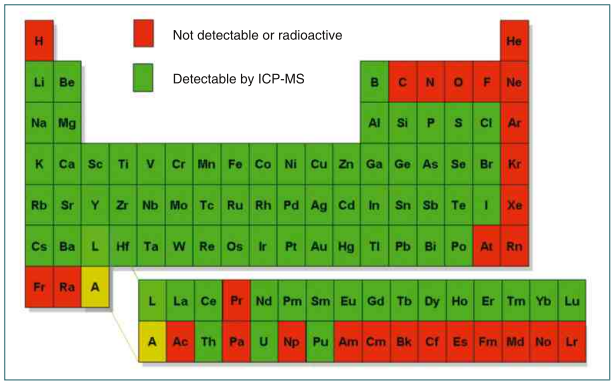

▲ Figure 2
Overview of the ICP-MS detectable elements within the periodic table.

^{51}V	$^{35}Cl^{16}O$, $^{37}Cl^{14}N$, $^{40}Ar^{11}B$
^{52}Cr	$^{36}Ar^{16}O$, $^{40}Ar^{12}C$, $^{35}Cl^{16}OH$, $^{37}Cl^{14}NH$
^{55}Mn	$^{40}Ar^{14}NH$, $^{39}K^{16}O$, $^{23}Na^{32}S$, $^{37}Cl^{18}O$
^{54}Fe	$^{40}Ar^{14}N$, $^{38}Ar^{16}O$, $^{37}Cl^{16}OH$, $^{40}Ca^{14}N$
^{56}Fe	$^{40}Ar^{16}O$, $^{40}Ca^{16}O$
^{58}Ni	$^{40}Ar^{18}O$, $^{23}Na^{35}Cl$, $^{42}Ca^{16}O$
^{59}Co	$^{36}Ar^{23}Na$, $^{24}Mg^{35}Cl$, $^{42}Ca^{16}OH$, $^{23}Ca^{35}ClH$
^{60}Ni	$^{23}Na^{37}Cl$, $^{25}Mg^{35}Cl$
^{63}Cu	$^{40}Ar^{23}Na$, $^{40}Ca^{23}Na$
^{64}Zn	$^{40}Ar^{24}Mg$, $^{40}Ar^{23}NaH$, $^{32}S^{16}O^{16}O$
^{65}Cu	$^{40}Ar^{25}Mg$, $^{40}Ar^{24}MgH$
^{66}Zn	$^{40}Ar^{26}Mg$
^{68}Zn	$^{40}Ar^{14}N^{14}N$
^{75}As	$^{40}Ar^{35}Cl$, $^{40}Ca^{35}Cl$
^{78}Se	$^{40}Ar^{38}Ar$, $^{40}Ar^{37}ClH$, $^{38}Ar^{40}Ca$
^{80}Se	$^{40}Ar^{40}Ar$, $^{40}Ar^{40}Ca$, $^{32}S^{16}O_3$, ^{79}BrH
^{98}Mo	$^{40}Ar^{23}Na^{35}Cl$
^{111}Cd	$^{79}Br^{32}S$
^{114}Cd	$^{98}Mo^{16}O$
^{123}Sb	$^{88}Sr^{35}Cl$, $^{36}Ar^{87}Sr$

◄ Figure 3

Environmental samples such as seawater, biological fluids or tissues are complex mixtures. Often they contain a few highly abundant elements, which interfere with the sensitive determination of the remaining less concentrated elements. Different isobaric polyatomic ions are formed in an argon plasma, which interfere with the determination of various elements. The red font indicates interferences due to a sea water matrix.

▼ Figure 4

Schematic view of a collision/reaction cell ICP-MS system used for trace element determination in the marine environment. The collision/reaction cell allows a significant reduction of polyatomic ions, which interfere with the sensitive determination of most elements due to gas phase reactions with hydrogen (H_2) or helium (He).

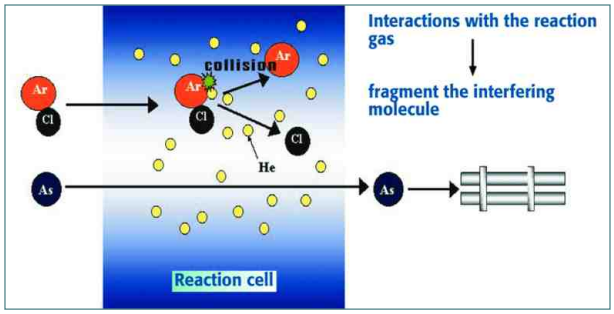

▲ Figure 5

Schematic view of the function of a collision/reaction cell. Polyatomic ions are reduced due to their dissociation caused by collisions with the cell gas, while the analyte ions are transferred to the quadrupole mass filter.

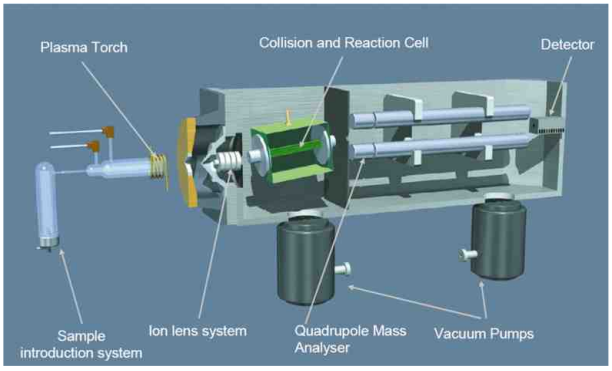

Isotope	Gas	Certified conc. / 10 [ng/L]	Measured conc. [ng/L]	Reproducebility [%] n = 6	Recovery [%]
^{51}V	He	120*	123 ± 17	14	103
^{52}Cr	He	11.0	11 ± 1.4	13	100
^{55}Mn	H_2	91.9	94 ± 7	7	102
^{56}Fe	H_2	20.7	21 ± 6	29	101
^{59}Co	He	1.1	1.2 ± 0.3	25	109
^{58}Ni	He	25.3	24 ± 4	17	95
^{63}Cu	He	29.7	26 ± 5	19	88
^{64}Zn	He	10.2	11 ± 3	27	108
^{75}As	He	127	131 ± 20	15	103
^{95}Mo	He	960	895 ± 70	11	93
^{111}Cd	H_2	2.3	2.2 ± 0.5	22	105
^{208}Pb	H_2	0.8	0.8 ± 0.2	25	100
^{238}U	H_2	260*	295 ± 27	9	113

▲ Figure 7

The results obtained from the analysis of a certified sea water reference material (NASS 5) clearly demonstrate the potential of collision/reaction cell ICP-MS for the sensitive, reproducible and accurate multi-element determination of complex samples.

Isotope	Standard mode (ng/L)	H_2 mode (ng/L)	He mode (ng/L)
^{51}V	-	-	2.7
^{52}Cr	-	5	-
^{55}Mn	-	2.1	-
^{56}Fe	-	10	-
^{59}Co	-		0.7
^{58}Ni	-	17	-
^{63}Cu	-		1.8
^{64}Zn	140	6.6	-
^{75}As	-	-	50
^{78}Se	80	8	-
^{98}Mo	2.2	15	-
^{111}Cd	1.8	1.5	-
^{208}Pb	2.5	0.5	-
^{238}U	0.5	5.7	-

▲ Figure 6

The developed methodology allows the detection of element concentrations at trace levels in environmental samples such as sea water. Instrumental detection limits down to the pg l^{-1} have been obtained in three different modes.

Elemental mass spectrometry - a tool for monitoring trace element contaminants in the marine environment

Implementation & Results

Application fields

Vertical profiles in the Baltic Sea

Within an intercalibration exercise, the collision/reaction cell ICP-MS method has been compared with an analytical method for trace element determination in seawater, which is based on a complex chemical matrix separation strategy and atomic absorption spectro- scopy (AAS). For ICP-MS measurements the samples were only acidified and diluted ten times with ultra pure water. The results of both methods were in good agreement, which indicates the potential of the developed methodology for the fast and reliable multi-element analysis of seawater samples.

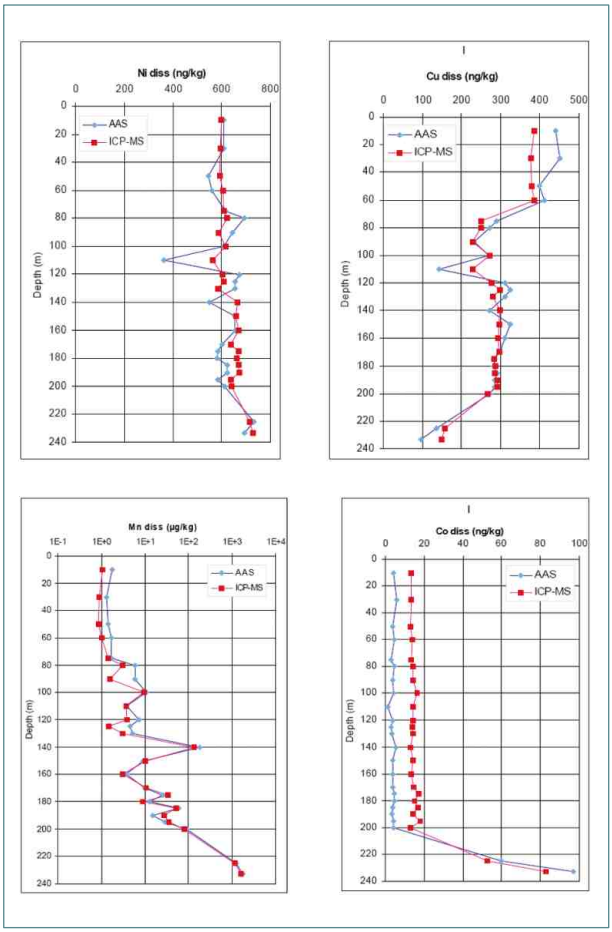

▲ Figure 8

Trace element determination in Baltic Sea water, sampled at the “Gotland Tief”. Method intercalibration between CC-ICP-MS and AAS with chemical matrix separation revealed comparable results.

Metal body burdens in seals

Even though the original collision/reaction cell ICP-MS was developed for trace element analysis of marine water samples, it is easily adapted to new tasks such as the determination of metal body burdens of marine mammals.

As part of the monitoring of the health status of marine mammals, trace element levels in blood and tissue samples are under investigation, using ICP-MS for a reliable multi-element screening.

The concentrations of selected elements were measured in fresh whole blood samples of 80 harbour seals, captured at three different locations of the German and Danish Wadden Sea.

For essential elements, such as calcium, iron or zink, low variations in the concentration level (12-25%) were observed due to their homeostatic regulation. Also no significant relation with gender, age or locality has been observed, and the levels were in the same order of magnitude as in humans.

In contrast, the level of trace elements shows a much wider variation of 30-287%. Blood levels of these elements were more directly influenced by dietary sources.

Furthermore, differences between sampling sites in the North Sea have been observed and could be explained by geographical variation of differently contaminated prey. In comparison with other trace elements, especially high arsenic concentrations have been observed (Griesel et al., 2007).

Outlook

These examples show the potential of elemental mass spectrometry for the investigation of trace elements in the marine environment. Beside the amount of an element, also its chemical form (speciation) is of great importance, especially for its toxicity and, accordingly possible effects in the marine environment. CC-ICP-MS can be readily combined with chromatographic separation techniques allowing the investigation of relevant element species such as organotin, mercury or lead compounds.

Authors

Daniel Pröfrock, Antje Kakuschke, Simone Griesel and Rudolf Pepelnik (GKSS)

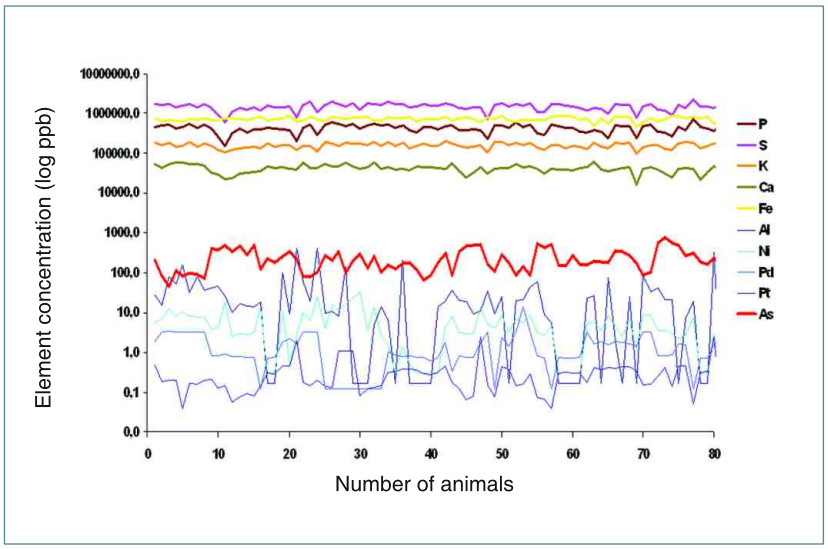

◀ Figure 9

The concentration of selected elements measured in blood samples of 80 seals reveals less variation in the concentration level of essential elements (RSD 12-25 %) due to their homeostatic regulation. Also, no significant relation with gender, age or locality has been observed. In contrast the level of trace elements show a much wider variation of 30-287%. Blood levels of these elements were more directly influenced by dietary sources.

Polyfluorinated compounds - a new class of global pollutants in the coastal environment

Introduction

Introduction

A few years ago a new class of chemical substances with toxic and persistent properties was detected in the environment - the polyfluorinated compounds (PFCs). At the Institute for Coastal Research scientific studies are performed on the PFC-contamination of coastal waters, marine mammals and the atmosphere with emphasis on the mechanisms of global transport and distribution of PFCs.

Polyfluorinated compounds have been industrially manufactured for over 50 years with global production currently reported to be in the order of thousands of tons per year. PFCs are used for surface treatment in carpets, textiles, leather and paper, in polymer production, fire-fighting foams, cosmetics and cleaning agents as well as in numerous other industrial and consumer applications.

Nowadays PFCs are detected everywhere in the marine environment. As they resist degradation, possess toxic properties and bioaccumulate in the food web they are regarded as a new and emerging class of environmental contaminants. Furthermore PFCs are considered to be “candidates” for the Stockholm convention list of the so-called POPs (persistent organic pollutants). POPs are chemical substances that persist in the environment, are transported through air and water, across international boundaries, and deposit far from the place of release, where they accumulate in terrestrial and aquatic ecosystems.

PFCs have the ability to repel both water and oil, which makes them suitable as surface-active substances. This surfactant-like character gives them the specific features desired by producers and consumers.

About 350 polyfluorinated compounds of different chemical structures are known. The most discussed representatives of the PFC-group are the acids PFOA (perfluorooctanoate) and PFOS (perfluorooctane sulfonate) (Fig.1).

Analysis of PFCs and levels of contamination

Although PFCs have already been produced for about half a century analytical detection in the environment is only possible with adequate instrumentation which has been available just for a few years. Low amounts of PFCs in soil, water, air and biota as well as their surfactant-like character require analytical methods with very low detection limits. The rapid development in the field of gas chromatography and high pressure liquid chromatography, both coupled with mass spectrometers, results in considerably lower detection limits and allows the determination of concentrations in the parts-per-billion-range and beneath.

PFCs are man-made compounds. Currently, natural sources are not known. PFCs can be detected worldwide in almost all matrices of the environment. High amounts of PFOS and PFOA are found in food, human blood and human milk. Surprisingly high concentrations were determined in fish, seals, seabirds, and, most notably, in polar bears from the Arctic. Compared to other POPs like chlorinated hydrocarbons PFCs are found in higher ambient concentrations. In Swedish studies of human blood from 1997 to 2000 the mean PFC-concentration was 20 to 50 times higher than the concentration of the polychlorinated biphenyls and about 300 to 450 times higher than that of hexachlorobenzene, two classical organic pollutants, which are known to be hazardous (Kärrman et al., 2006).

Temporal trend of PFC contamination

In the year 2005 Danish scientists published the results of their studies in seals from Greenland from 1982 to 2003. During this period PFOS concentrations in livers increased from about 30 ng/g to 100 ng/g wet weight (Bossi et al., 2005) (Fig.2).

At the GKSS Institute for Coastal Research the liver of a seal found in 2005 near the German island Amrum was analysed. It is worth remarking that PFOS concentration was about 20 times higher than the values determined in Greenland seals from 2003 although a direct comparison is problematic. Thus, the PFOS contamination of marine mammals not only increased during recent years but probably will also increase in the future. Within the framework of studies supported by the Scholarship Programme of the German Federal Environmental Foundation (Deutsche Bundesstiftung Umwelt, DBU) the livers of 80 seals from the Research and Technology Centre West Coast (FTZ) will be analysed by the GKSS Institute for Coastal Research. Analyses of PFCs will give information about changes in the contamination of seals over the last 20 years and allow for a reconstruction of the contamination of the North Sea in the past.

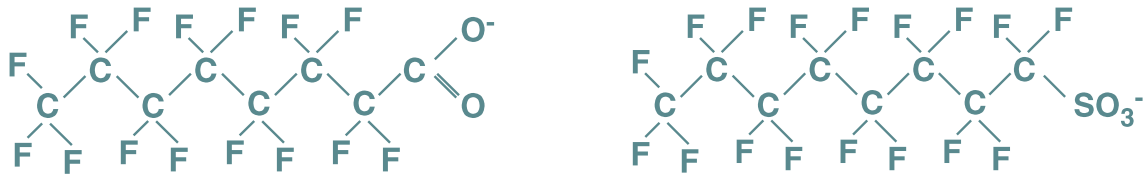

▲ **Figure 1**

Left: Perfluorooctanoate (PFOA), **right:** Perfluorooctane sulfonate (PFOS)

Chemical characteristics of PFCs

PFCs are characterised by their carbon chains of varying length with 4 to 18 carbon atoms. Most of the hydrogen atoms in the carbon chain are replaced with fluorine. This fluorinated end of the carbon chain is responsible for the water-repellent function of the molecule. At the other end of the carbon chain a carboxylic-, sulfonic- or a similar polar group is bound making the molecule hydrophilic and oil-repellent respectively.

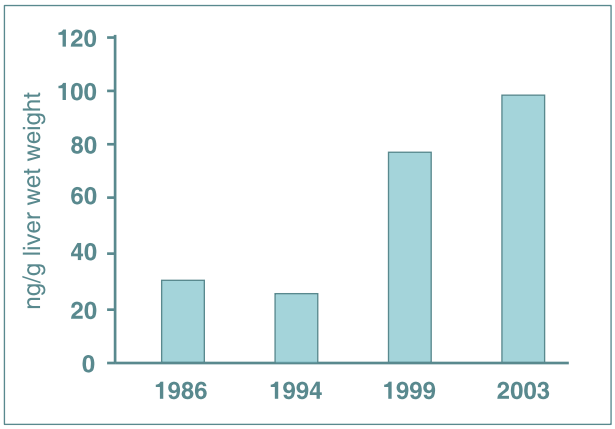

◄ **Figure 2**

Temporal trend of the PFOS concentrations (mean values) in livers of Greenland Ringed Seals (modified from Bossi et al., 2005).

▼ **Figure 3**

Distribution patterns of **PFOA (left)** and **PFBS (right)** concentrations in water samples of the German Bight in ng/L (data from Sebastian Felizeter).

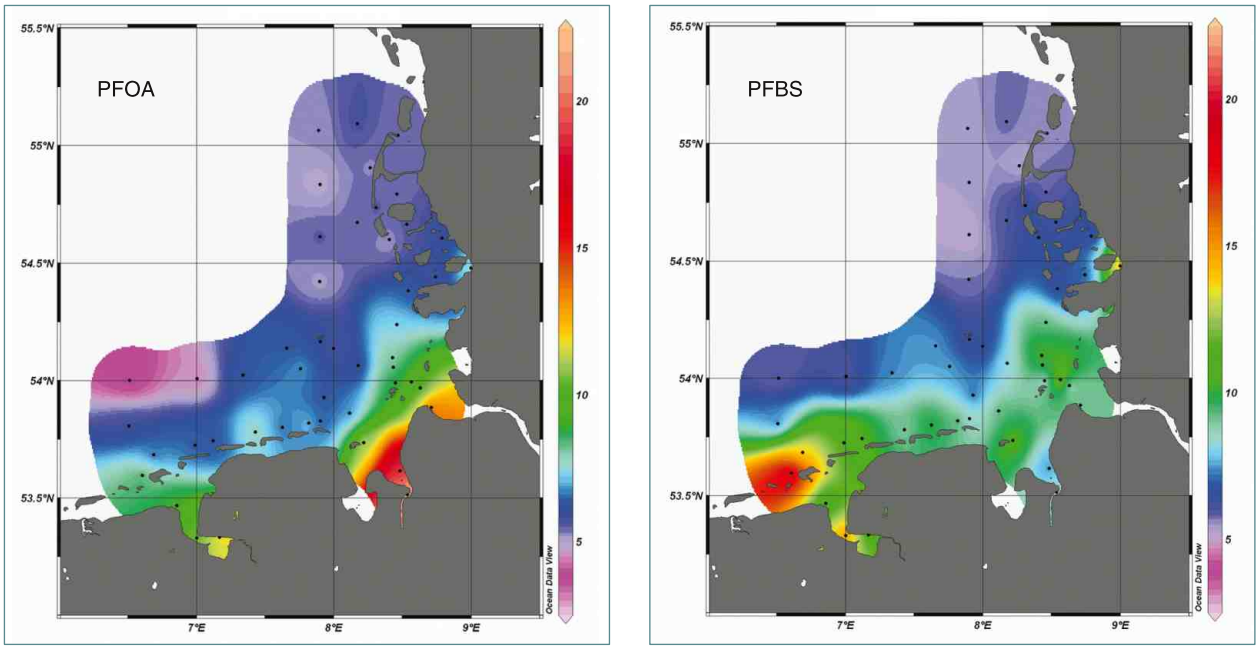

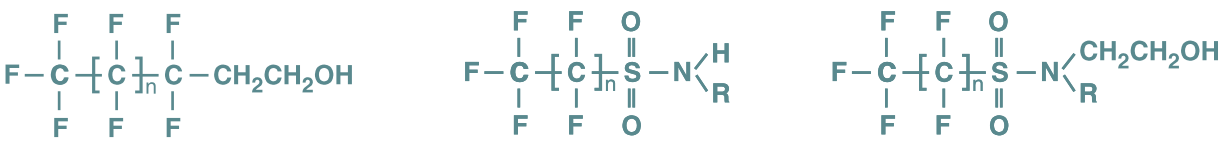

▲ **Figure 4**

Left: Fluorotelomer alcohols (FTOHs), **centre:** Fluorooctane sulfonamides (FOSAs), **right:** Fluorooctane sulfonamidoethanols (FOSEs).

Polyfluorinated compounds - a new class of global pollutants in the coastal environment

Methods & Results

Distribution of PFCs in the environment

PFOS found in marine mammals like seals and polar bears and even in the blood of the Inuits raise the question about the mechanisms of transportation: How did PFOS arrive at arctic or other pristine regions? Up to now, only limited information is available about the distribution and the long range environmental transport of PFCs.

Studies at the Institute for Coastal Research confirm the assumption of two pathways of distribution of the acids PFOS and PFOA. The first way is the direct transport by water currents. In the year 2007 numerous water samples (between 1 and 5 L) were taken along the River Elbe, in the German Bight and in the Atlantic Ocean. After solid phase extraction and subsequent elution with organic solvents the extracts were analysed using high performance liquid chromatography-electrospray ionisation-tandem mass spectrometry (HPLC-ESI-MS/MS). In these samples 18 different PFCs were found. The concentrations were up to 20 ng/L, whereas the concentrations of dissolved PFOA and other perfluorinated carboxylic acids were higher in the estuaries of the River Elbe and the River Weser than in regions of the North Sea far away from the coast. Thus, these rivers were identified to be one of the sources of single certain PFCs for the German Bight (Fig. 3). On the other hand significant inputs of dissolved PFOS from the rivers Elbe and Weser could not be detected. To the west of the River Ems high amounts of PFBS (perfluorobutane sulfonate) were detected. At the end of 2006 very high amounts of PFBS were determined in water of the River Rhine. The source of this contamination was located in the Aare catchment area in Switzerland. For a few years PFBS has been used as a replacement chemical instead of PFOS, because in Europe the use of PFOS will be restricted effective from June 2008. In contrast to PFOS, its substitute PFBS is considered to be neither bioaccumulative nor toxic. But because of its persistence and its ionic character this short-chain PFC is rather mobile in the groundwater. Trace amounts were determined also in drinking water. However, PFBS is an unwanted man-made trace contaminant in the aquatic environment.

The other pathway of global distribution is the transport via air. PFOS and PFOA are themselves non-volatile. But it might be possible that volatile precursor substances like fluorotelomer alcohols (FTOHs) (Fig. 4) can undergo long-range atmospheric transport. In the atmosphere these compounds physically degrade to PFOS and PFOA and subsequently are removed from the air to deposit on water or soil surfaces. This indirect transport results in a fast distribution of PFOS and PFOA over long distances. This hypothesis was the motivation for extensive investigations at the Institute for Coastal Research on the occurrence of polyfluorinated compounds in the atmosphere, their distribution patterns and the mechanisms of transport from their sources to pristine marine regions.

Over the last three years a substantial number of air samples were taken in the North Sea, the Atlantic Ocean and the Arctic (Fig. 5). Several volatile precursor substances like fluorotelomer alcohols (FTOHs), fluorooctane sulfonamides (FOSAs), and fluorooctane sulfonamidoethanols (FOSEs) (Fig. 4) were detected in the gaseous phase of the air in the pg/m^3 range of concentrations.

During the research cruises first concentration data sets of PFCs from the European atmosphere were generated. FTOHs were the dominating polyfluorinated compounds in all air samples. Highest concentrations of FTOHs (up to 200 pg/m^3) were found at the European, northwest African and Canadian coasts of the North Sea and the Atlantic Ocean, respectively. But this group of compounds could be detected in the atmosphere also in regions far away from production and consumption like the Arctic or the southwest African coast of the Atlantic Ocean (Fig. 6).

These results support the hypothesis of the long-range atmospheric transport of precursor substances. It is confirmed that transportation over long distances is theoretically possible (Ellis et al., 2003). The atmospheric lifetime of FTOHs determined by its reaction with atmospheric OH radicals is approximately 20 days. The final product of this atmospheric degradation is PFOA. In analogy to FTOHs FOSEs degrade to the persistent end-product PFOS. In 20 days FTOHs will be transported over long distances downwind from its point of emission. Taking into account that the global average wind speed is 4 ms^{-1} which corresponds to 13.8 km h^{-1} an air mass travelling at this speed covers 7000 km in 20 days.

PFOA and PFOS produced in the course of this atmospheric process are removed from the air by precipitation, are deposited onto the ocean or land surfaces, or are ingested by organisms and accumulated in the food chain.

Thus, both pathways are involved in the global occurrence and distribution of PFOS and PFOA.

Authors

Renate Sturm, Ralf Ebinghaus, Annekatrin Dreyer and Lutz Ahrens (GKSS)

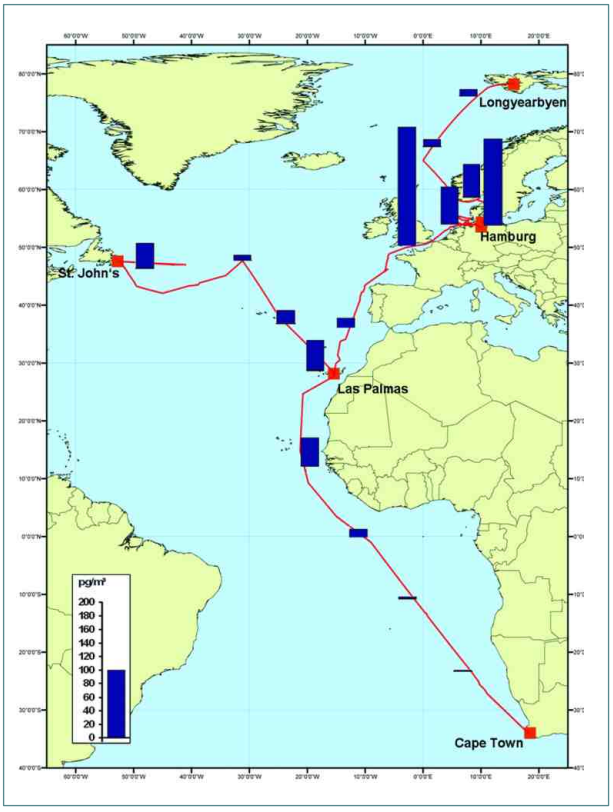

▲ Figure 6
Spatial distribution of 8:2 FTOH in air. Samples were taken during several expeditions in 2005 and 2007 (data from Annekatrin Dreyer and Annika Jahnke)

◀ Figure 5
Air sampling at the observation deck of the research vessel "Maria S. Merian".

Air sampling

Air samples were taken on board the German research vessel “Maria S. Merian” using high-volume air samplers located at the observation deck of the ship approximately 16 m above sea level. The air samplers were controlled by a computer connected to the ship’s meteorological system avoiding interference in the sampling by relative winds from aft.

In general, 350 m³ of air were sampled. Glassfibre filters (GFF) and cartridges filled with a sandwich of polyurethane foam (PUF) and Amberlite XAD-2 resin were used to collect particle-bound (GFF) and gaseous (PUF/XAD) polyfluorinated compounds. The cartridges were extracted with acetone:methyl tert-butyl ether 1:1 without heating. The solvent was allowed to soak for a few hours, afterwards evaporated with ethyl acetate as a keeper and finally reduced to a few microlitres under a gentle stream of nitrogen. Filters were extracted using fluidised bed extraction with acetone:MTBE 1:1 to elute the neutral volatile polyfluorinated compounds like FTOHs and with methanol to elute the ionic perfluorinated carboxylic and sulfonic acids, respectively.

During sampling and analyses, mass labeled compounds were used as internal and injection standards to correct for variations. Quantification of neutral compounds was performed by gas chromatography/mass spectrometry with positive chemical ionisation (PCI) using the selected ion monitoring (SIM) mode. Quantification of ionic compounds like PFOS and PFOA was made on an HPLC-ESI-MS/MS.

Monitoring the tidal flats

Tidal flats are unique habitats of soft bottom coasts. Worldwide the largest areas are found along the coast of the North Sea and the Korean coast of the Yellow Sea. They are feeding and nursery grounds for many organisms. Migrating birds coming from the Arctic region find here their main overwintering or feeding areas during migration.

The tidal flats also attract numerous tourists year by year. In Germany the whole Wadden Sea has become a national park.

To manage this unique but vulnerable ecosystem in a sustainable way frequent observations are required. Different techniques, which we present here, including visual observations from aircrafts and computer aided interpretation of satellite data, are already in use in operational monitoring programmes.

Content

Seagrass: An indicator goes astray

Methods & Techniques

Introduction

To measure ecological quality in the environment, powerful indicators are needed. In coastal waters seagrass has been suggested as a sensitive indicator for an overload of nutrient inputs from land use practices (Burkholder et al., 2007). Losses have occurred all over the world. Also in the Dutch and Lower Saxonian Wadden Sea seagrass beds had been in decline over several decades. A rough aerial survey in 2002 indicated the uneven distribution of seagrass between subregions within the Wadden Sea (Fig. 1). Seagrass was scarce in the south, while it was fairly common in the north. After measures to reduce nutrient emissions have lowered the discharge of nutrients into the coastal waters of the eastern North Sea, seagrass seems to be recovering (Reise et al., 2005).

The European Water Framework Directive requires a good ecological quality for all water bodies by 2015. For the North Sea coast, it is reasonable to use seagrass as an indicator to show when a good status has been reached. By using historical reference conditions from the Northfrisian Wadden Sea it has been estimated that good ecological quality comprises at least a 15 %-share of seagrass beds from the intertidal area. At present, seagrass beds cover about 90 km^2, which corresponds to 10 %.

An assessment of seagrass occurrence across such a wide area of difficult accessibility is only feasible from the air. However, green algae constitute a challenge for this method. On satellite images (Brockmann and Stelzer, 2008) and aerial photographs they are easily mistaken for seagrass. To distinguish between the two is essential, however, because contrary to the seagrass the opportunistic green algae respond to nutrient overloads with massive growth. This had happened twenty years ago when algal mats covered 15-20 % of intertidal flats in the Wadden Sea and smothered seagrass and the macrobenthic fauna underneath (Fig. 2; Reise and Siebert, 1994).

Methods

Each year, the Wadden Sea area is flown over at an altitude of 300 to 500 m in June, July and August during low tide exposure. In the course of summer, seagrass continuously grows denser while green algae appear to fluctuate. Both render the sediment surface darkish green. Only textural details indicate whether seagrass or green algae dominate. If a distinction cannot be made at first sight, questionable areas are flown over twice or more to reveal more structural features from different angles. If this does not help either, these problematic areas have to be visited by foot.

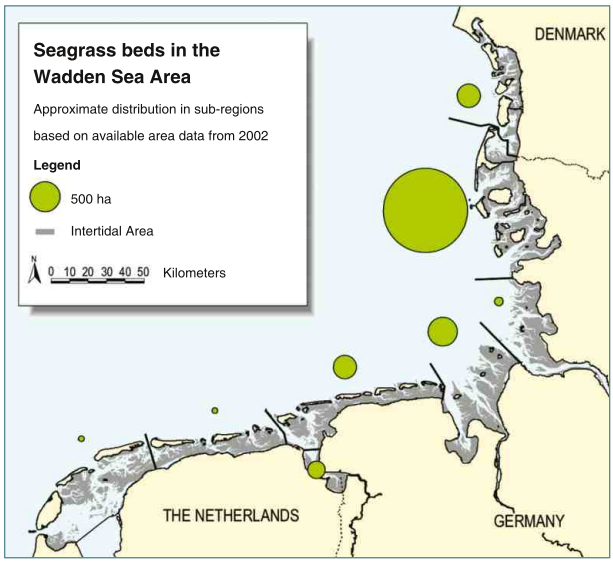

▲ Figure 1
Areal size (km^2) of seagrass beds (coverage of sediment >20%) in the intertidal of the Northfrisian Wadden Sea as estimated from aerial surveys in August or September between 1978 and 2007.

During flights notes are taken onto maps 1 : 100.000 made from satellite images to ease orientation over light (sandy) and dark (muddy) tidal flats dissected by branching creeks. Back on the ground, data are transferred to digital maps. Areal sizes covered by seagrass beds and green algal mats are calculated with a Geographical Information System (GIS).

Flying allows for rapid results but cannot replace ground observation entirely. Two species of seagrass occur in the region which differ in their indicatory value and can only be distinguished by experts (Fig. 2 a). Also, the species composition of green algal mats is variable, requires taxonomic expertise and provides information on the causes as well as the effects of massive green algal mats. Therefore, in the month of August, the entire region is surveyed area by area with trained personnel. This is very time consuming and the aim is to visit each area at least once within a period of six years.

The ecological quality will be evaluated over such six year intervals. This can level out fluctuations in seagrass bed area caused by unusual weather conditions or rough seas, and avoid mistaking inherent variability for environmental quality.

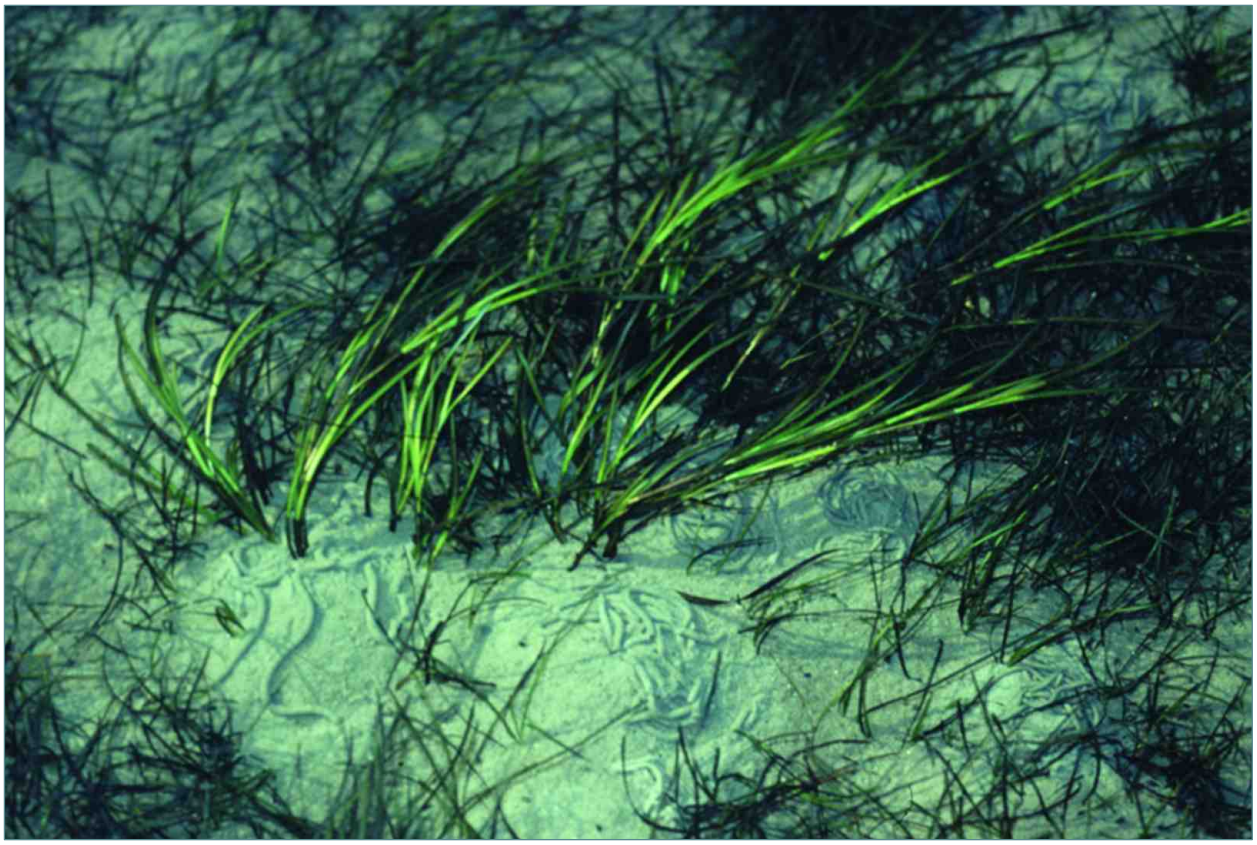

Figure a

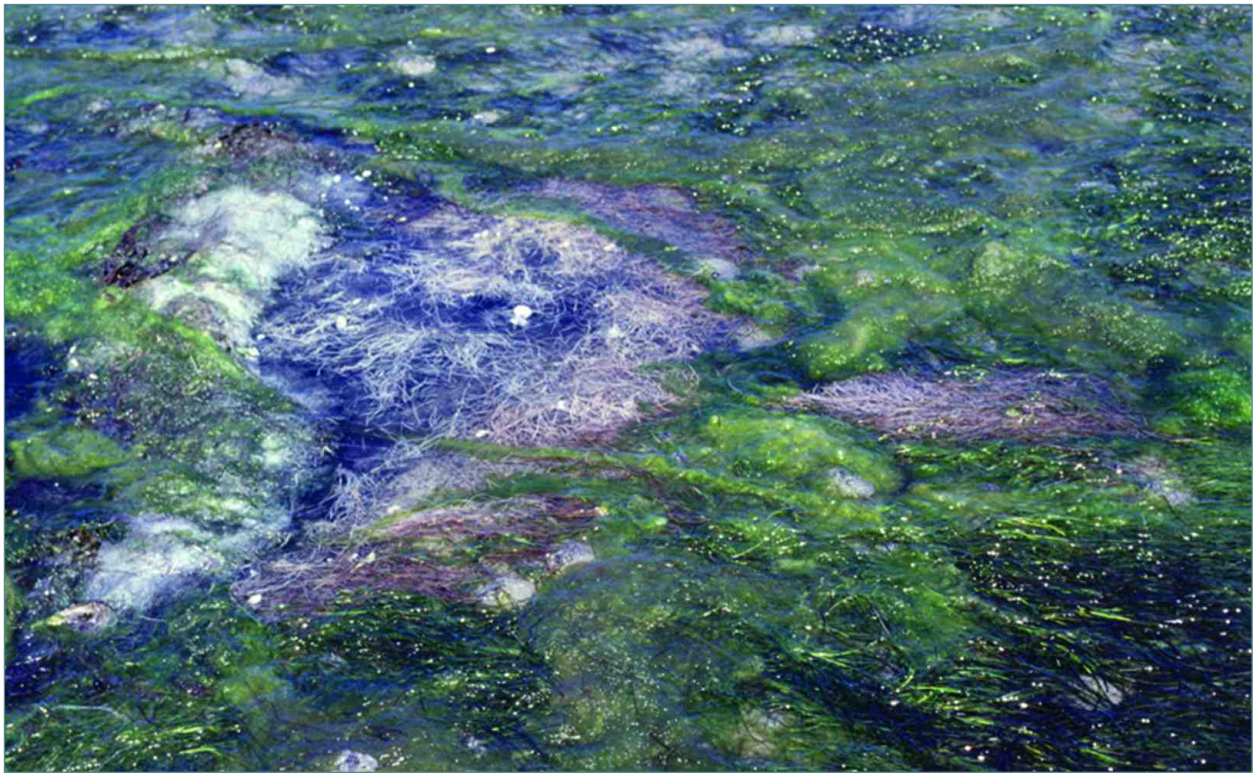

Figure b

▲ Figure 2 a-b

a) Seagrass (narrow leaves: *Zostera noltii,* wider leaves: *Z. marina*) and **b)** green algal mat with whitish patches from sulphur bacteria smothering seagrass.

Seagrass: An indicator goes astray

Implementation & Results

Results and outlook

Areal sizes of seagrass beds assessed from the air have increased gradually in the intertidal of the Northfrisian Wadden Sea, particularly since this millennium has commenced (Fig. 3). This may be correlated with declining nutrient inputs. If these could be reduced further and seagrass increases accordingly, the requirement of the EU for a good ecological quality of coastal waters could be fulfilled in the coming years, based among other things on the status of intertidal seagrass beds.

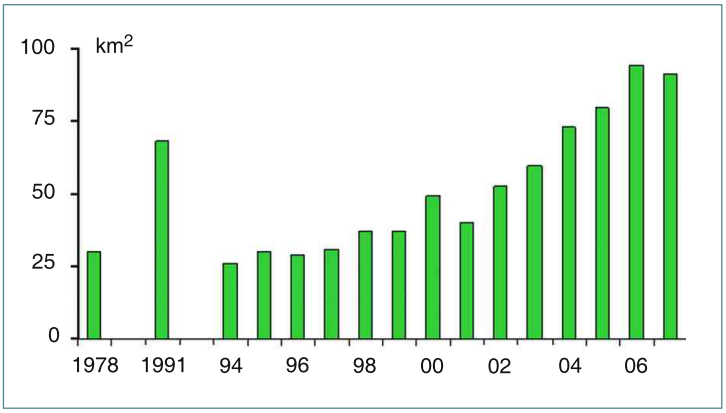

▲ **Figure 3**
Areal size (km^2) of seagrass beds (coverage of sediment > 20 %) in the intertidal of the Northfrisian Wadden Sea as estimated from aerial surveys in August or September between 1978 and 2007.

However, in contrast to the south, in the northern region of the Wadden Sea there is no evidence from earlier decades for a retreat in seagrass in response to a nutrient over-supply. May the apparent recovery of seagrass have causes other than the reduction of nutrient input?

According to Weisse and Plüß (2006) storm frequency in winter has increased since the 1960s and since the mid 1990s has decreased again. This is related to climatic oscillations in the Northern Atlantic. High water levels caused by storm surges in summer have declined slightly over the entire period. From field experiments it is known that seagrass is highly susceptible to sediment turnover as this may happen during storm surges (Cabaço und Santos, 2007).

Looking at the spatial pattern of intertidal seagrass (Fig. 4), it is apparent that seagrass predominantly occurs at sites sheltered against the prevailing surf from the south western direction in the Northfrisian region (Reise and Kohlus, 2008). In addition, field investigations have shown that the largest seagrass beds at the Halligen and the island of Pellworm are underlain by solid peat and clay in which seagrass roots get a fair hold. These observations support the assumption that sediment stability may serve as a key factor explaining why there is more seagrass in the Northfrisian region than in all the other regions of the Wadden Sea taken together (Fig. 1).

The pattern in Fig. 3 may also reflect an inverse relationship to storm frequency, which has declined since the mid 1990s. If this interpretation of seagrass occurrences is correct, than its future would be less a function of nutrient supply than of storm activity, and if the latter will increase again, and the last two winters do support just that, then seagrass will not achieve an areal share of 15 % as required for a good ecological quality status by the European Water Framework Directive.

A potential for further expansion of seagrass would be possible along the mainland coast if land reclamation works are phased out. These destroy seagrass beds in two ways. Between the brushwood fences traditionally set up in rectangular fields to calm down wave action, green algae tend to accumulate and then smother seagrass. Secondly, the digging of ditches in a grid-like pattern with the excacated material piled up between parallel ditches is detrimental to seagrass, either directly or by enhanced sedimentation within reclamation fields. These negative effects of land reclamation works on seagrass constitute a dilemma. The works are deemed beneficial for coastal protection if they are successful in building up a foreland to absorb wave energy in front of seawalls. In many cases, however, this aim is not achieved because of an insufficient sediment supply to the area. The net effect is merely an exclusion of seagrass beds and disturbance of other nearshore biota.

In the long run, it appears questionable whether seagrass beds could maintain their spatial share if sea level rise accelerates and storm activity will increase in the wake of global warming. Such a climatic effect is not yet considered in the Water Framework Directive but should better be taken into account.

Authors

Karsten Reise (AWI) and Jörn Kohlus (Regional Office of the Schleswig-Holstein Wadden Sea National Park)

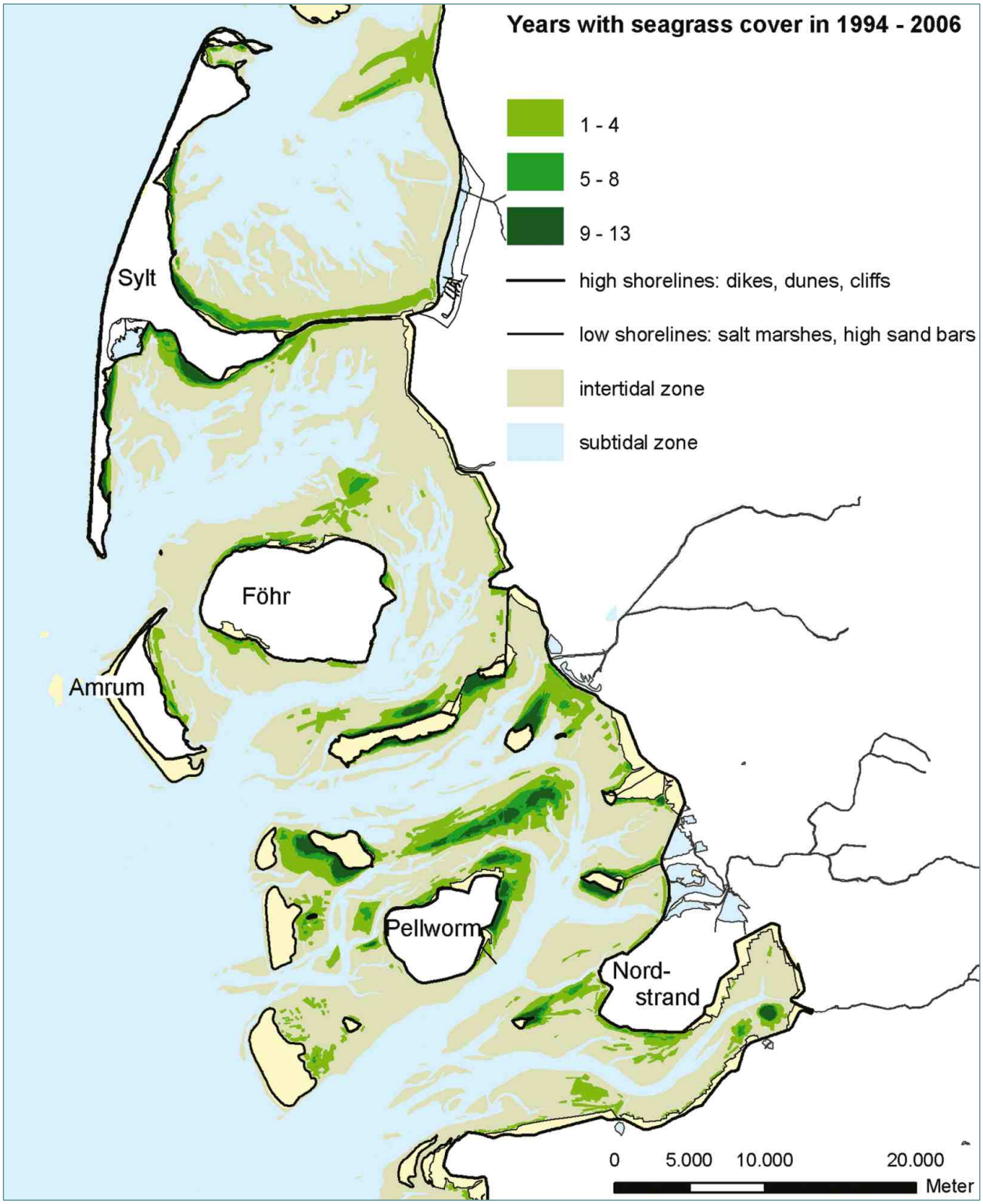

▲ **Figure 4**

Occurrence of seagrass (*Zostera noltii* and *Z. marina*) in the intertidal zone of the Northfrisian Wadden Sea in August/September 1994-2006. Intensity of green shading refers to the number of years seagrass has been observed. Beds with <20 % coverage are not included (from Reise and Kohlus, 2008).

Tidal flats from space

Introduction

Introduction

The objective of our research was to classify the different surface types of the tidal flat areas with satellite data in combination with ground truth measurements.

Remote sensing has many advantages such as large coverage and the recording of multi-temporal data. Both are useful for monitoring conditions in near real time as well as detecting changes of the environment when analysing historical data.

Tidal flats are unique ecosystems because of the water cover, which changes permanently with the tidal phase. They play an important role as a cleansing site for North Sea water, as a nursery for young fish and as a feeding ground for many bird species. They form a transitional zone between land and ocean.

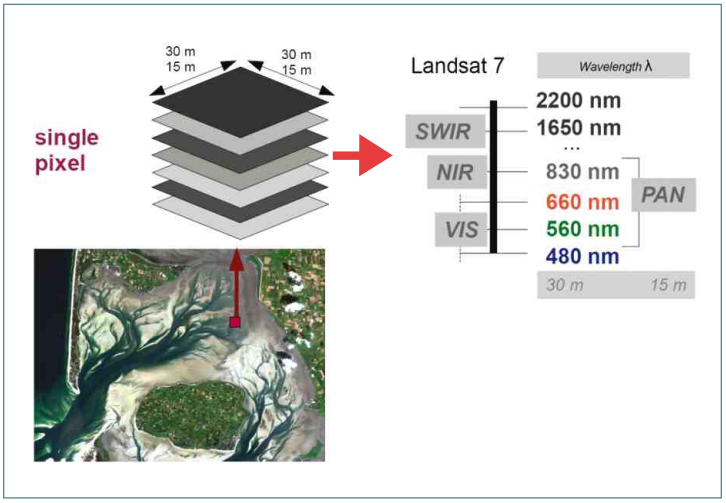

▲ **Figure 2**
Structure of satellite data: Each pixel has a specific spectral information.

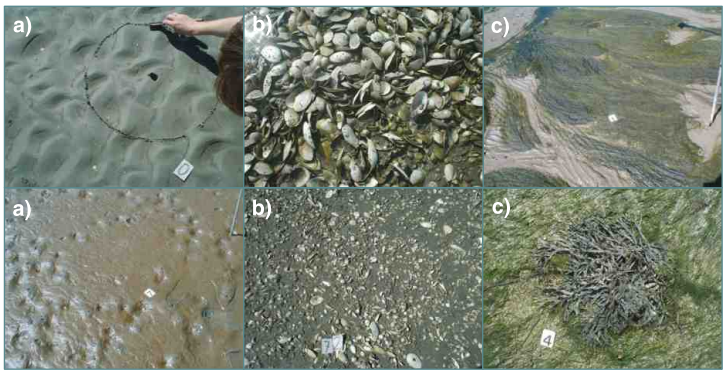

▲ **Figure 3 a-c**
Different surface types of the tidal flat **a)** bar sand **b)** mussels/mussel and sand **c)** *Zostera spec.* and *Z. spec.* with *Fucus spec.*

Traditional monitoring techniques of larger areas are limited by the factor time. This means that they are time-dependent and time-consuming. Due to the expanse of the tidal flat of nearly 10,000 km^2, the variability of water cover and the variability of the sediment, remote sensing has become an indispensable technique. The whole German Wadden Sea can be detected under the same environmental conditions with only two scenes of the Landsat satellite, which has been an operational satellite system since 1972.

Remote sensing data support mapping and monitoring programmes. They support the identification of proxi-parameters and indicators and fill the temporal gap between in-situ data and field measurements.

Fundamentals

The reflectance data, which we capture from the satellite, form a two-dimensional spatial grid, i.e. the satellite image (see Fig. 1). Each grid cell, the pixel (picture element), is represented in different spectral bands, the number of which depends on the sensor type. The context is depicted in Fig. 2.

Passive remote sensing technique measures reflected solar radiation or radiation emitted from the ground, atmosphere or clouds. The reflected solar spectrum covers the wavelength range from 400-3000 nm (VIS, NIR, SWIR).

The main information comes from the spectral signature of the surface materials. Different types of materials can be distinguished on the basis of differences in their spectral reflectivity. Fig. 3 shows different surface types of tidal flats. The corresponding spectral reflectances are illustrated in Fig. 4. Due to the variation of the reflectances the diverse surface types of the tidal flat can be distinguished and classified.

At present we are using satellite data from the Landsat series (Landsat 5 and 7) and ASTER. The coverage of both systems is shown in Fig. 1.

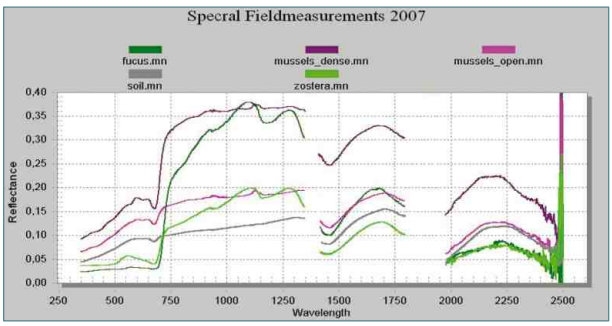

▲ **Figure 4**
Spectral reflectances sampled during field measurements with a hand held spectrometer (ASD Fieldspec).

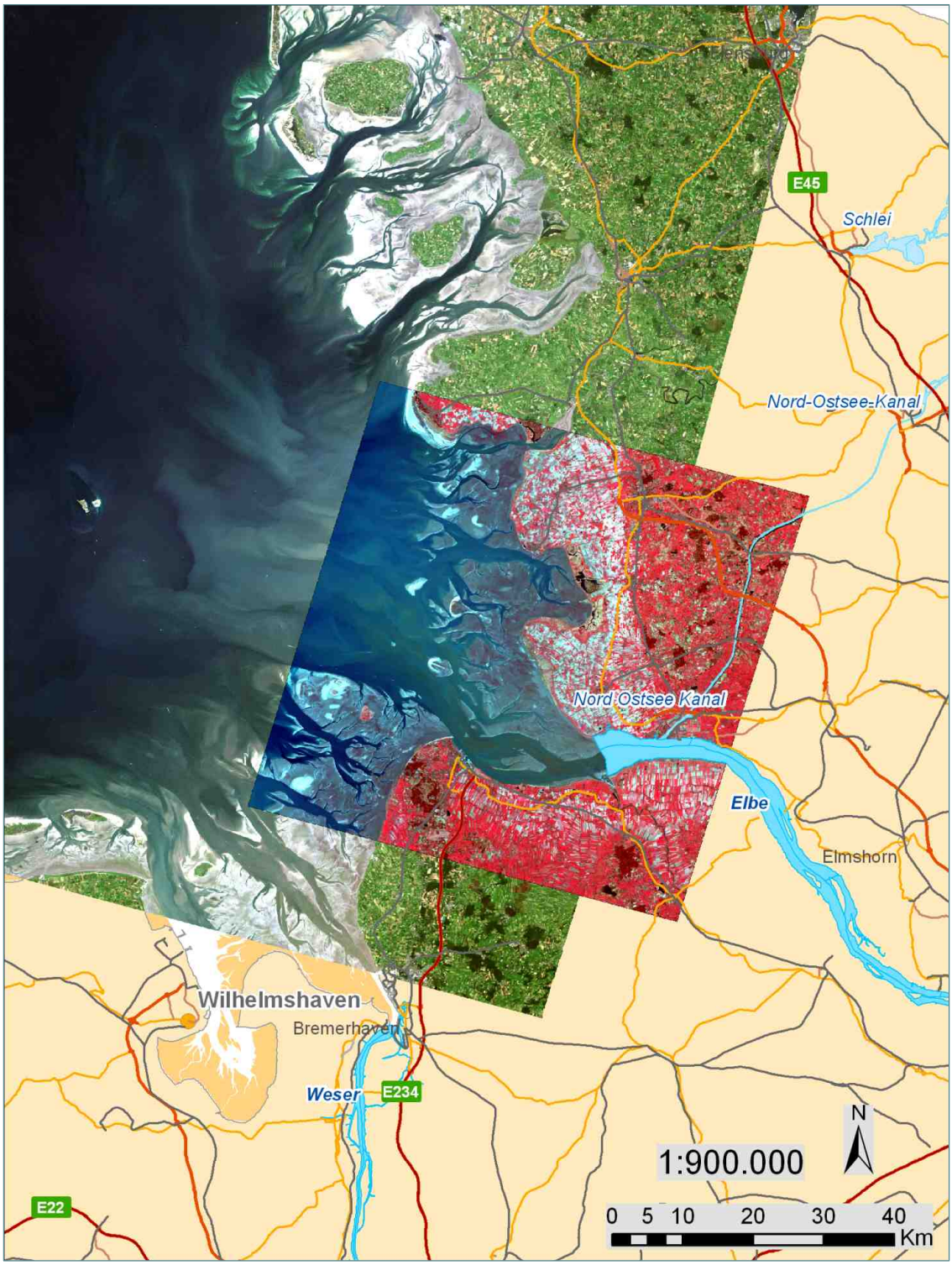

▲ Figure 1
True color image of Landsat 7 (July 15th 2002 - scene size 185 x 185 km) with overlayed false color image of ASTER (April 2nd 2005, scene size 60 x 60 km).

Tidal flats from space

Methods & Techniques I

Remote sensing data

The first multispectral satellites for land remote sensing, the Landsat series, were launched during the 1970s and have delivered data up to the present. The Landsat Programme is the longest running mission for the collection of multispectral digital data of the earth's surface from space. Current and historical data are very useful for research in the field of change detection and monitoring. Presently, the data from Landsat 5 (launched in March 1984) and Landsat 7 (launched in April 1999) are used for worldwide data analysis (Table 1). The ASTER sensor is part of NASA's Terra spacecraft, which was launched in December 1999 (Table 2).

Methods and techniques

The use of different methods and techniques depends on the information the user is interested in. If the analyst is interested in the documentation of morphological changes of the tidal flat, simple classification methods can be used for analysing multitemporal data sets. If the focus is on vegetation (seagrass, macroalgae) common vegetation indices can be used. For a more detailed analysis of the different surface types, and, in particular, of the sediment properties, additional data like spectral reflectance measurements on ground and in-situ samples are necessary. A general overview about methods and data is shown Fig. 5.

Pre-processing

At the beginning, some general pre-processing steps are necessary, like atmospheric correction (Fig. 6) and separation of the tidal flat areas from other surface types such as water and meadows (Fig. 7).

▲ **Figure 6**

Atmospheric Correction

The atmospheric correction is very important, because scattering and absorption processes in the atmosphere modify the spectral signature. The figure shows a Landsat/ASTER scene before **(left)** and after **(right)** atmospheric correction.

When working with scenes of different acquisition dates we need comparable values for each pixel. The product of the atmospheric correction are surface reflectances at the bottom of the atmosphere (BOA) for each pixel. The corrected data are the input for extracting the tidal flat areas, because the main processing will be based only on these pixels; the data from land and water will be ignored.

▼ **Figure 5**

Data and Methods for analysing surface structures in the tidal flats.

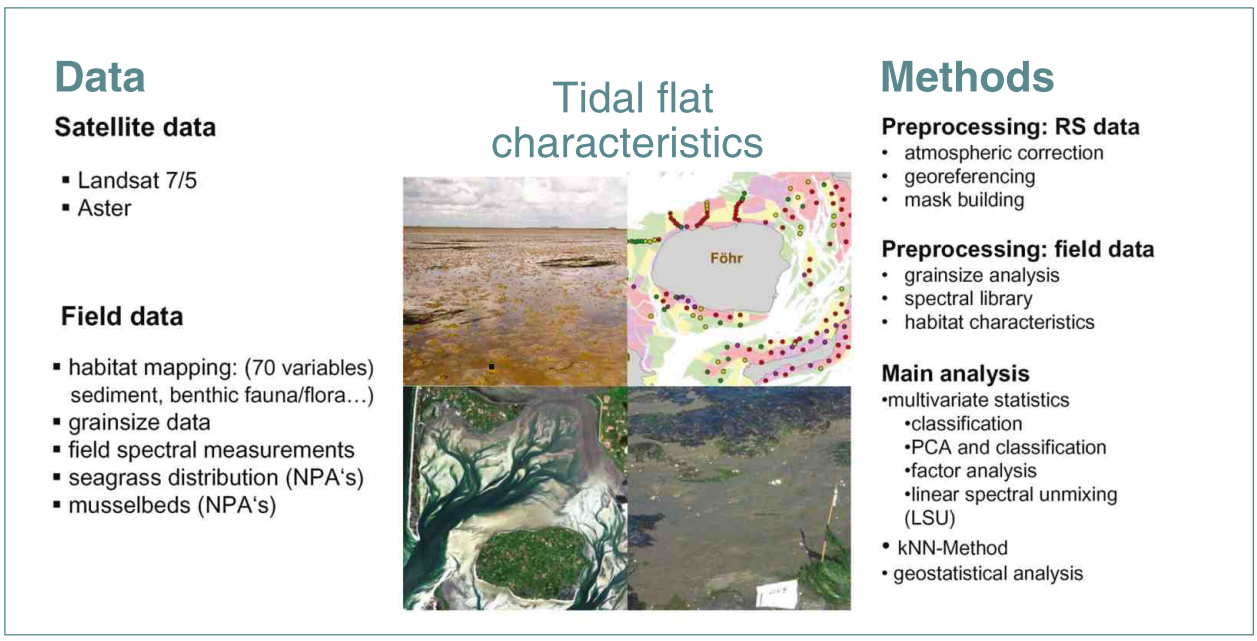

Spectral characteristic Landsat 7/5			Spatial Resolution [m]
Channel		Wavelength [µm]	
1	blue	0.450 - 0.515	30
2	green	0.525 - 0.605	30
3	red	0.630 - 0.690	30
4	NIR	0.750 - 0.900	30
5	SWIR	1.550 - 1.750	30
7	SWIR	2.090 - 2.350	30
6	TIR	10.40 - 12.50	60
8	Panchromatic	0.520 - 0.900 *	15

* band only on Landsat 7

- altitude 705 km
- repeat cycle of 16 days
- equatorial crossing between 9:30 and 9:45am local time.

◄ Table 1

Landsat 5 and 7 have very similar characteristics with respect to spatial and spectral resolution. This means that data of camparable quality are available for 20 years. The expected launch date for the next generation Landsat series satellite, Landsat 8, is in July 2011.

Spectral characteristic ASTER			Spatial Resolution [m]
Channel		Wavelength [µm]	
1	green	0.52 - 0.60	15
2	red	0.630 - 0.690	15
3N	NIR	0.78 - 0.80	15
3B	NIR	0.78 - 0.86	15
4	SWIR	1.6 - 1.7	30
5	SWIR	2.145 - 2.185	30
6	SWIR	2.185 - 2.225	30
7	SWIR	2.235 - 2.285	30
8	SWIR	2.295 - 2.365	30
9	SWIR	2.36 - 2.43	30
10	TIR	8.125 - 8.475	90
11	TIR	8.475 - 8.825	90
12	TIR	8.925 - 9.275	90
13	TIR	10.25 - 10.95	90
14	TIR	10.95 - 11.65	90

- altitude 705 km
- repeat cycle of 16 days
- equatorial crossing between 10:30 am

◄ Table 2

Compared to Landsat the ASTER sensor has a better spatial resolution in the visible range but no band in the blue spectral range. Instead, it has two bands in the NIR range (3N - Nadir and 3B backward) for stereoscopic observations. In the SWIR range it has very fine bands, specially defined for the analysis of soil and rocks.

▼ Figure 7

Tidal flat extraction

The following three figures show the input/result of the tidal flat extraction: **a)** input, **b)** supervised classification result (Maximum-Likelihood, with band 3,4,5) and **c)** the mask image derived from the classification. The calculation and analysis where done with the image processing software ENVI 4.3 from ITT. White pixels represent tidal flat pixels.

Tidal flats from space

Methods & Techniques II

Main analysis

After pre-processing, different methods can be used to analyse the spectral information of the tidal flats.

General aspects

All analysis methods are based on the spectral diversity of the single pixels, which form a multidimensional spectral space, the dimension of which is defined by the available bands of the sensor system.

The spatial resolution of the data plays an important role for the interpretation of the results and also for the selection of a method. We have to keep in mind that the reflectance value of a single pixel of a defined resolution (30 m Landsat and 15 m ASTER) might represent a mixture of different surface types. This depends on the homogeneity of the surface. The tidal flat can be characterised by regions of very inhomogeneous and homogenous areas; therefore some pixels represent a mixture of objects with different spectral reflectivity while other pixels include only one type of surface material. Tidal flat sediments have no sharp boundaries like those on land, in most cases they are distributed along a continuum between mud and sand (Fig. 8). The short term temporal variability of the tidal flat surface is shown in Fig. 9. This is also documented by the changing reflectance spectra.

Classification methods

The principle of image classification is to group pixels with similar patterns of brightness values in the available spectral bands. Two general approaches exist:

a) Unsupervised (common is the K-means algorithm): This method uses statistical parameters of the input data. The analyst has no control over the nature of the resulting classes, but he can define the number of resulting classes. This method is useful for exploring different surface types.

b) Supervised (common is the Maximum-Likelihood algorithm): This is a knowledge based algorithm, because the analyst has to define training areas at the beginning of the calculation. On the basis of these training areas the statistical information is calculated. All pixels are then compared to the spectral signatures of each predefined class and assigned to the class for which the pixel has the highest degree of similarity.

Linear spectral unmixing (LSU)

As mentioned above, the reflectance at each pixel is assumed to be a linear combination of the reflectivity of all surface types which are present within that pixel. The LSU method analyses the sub-pixel percentage (portion) of surface types within each pixel, based on the spectral reflectance of each surface type (endmember spectra). That means that this technique models an image pixel as a linear mixture of a specified number of materials with known spectral reflectances but unknown abundance fractions. The results are maps for each endmember with pixel values between 0 and 1, where for example 0.7 means that 70% of the pixel is covered by the endmember of that map (Richards & Xiuping, 2005).

PCA and unsupervised classification

The Principle Component Analysis (PCA) is a powerful method of analysing correlated multidimensional data. The PCA is known as compression and transformation technique and can be used if correlations between the spectral bands exist.

Principal component analysis determines the eigenvectors of a variance-covariance or a correlation matrix. The analysis consists of a linear transformation of n original variables to n new variables, where each new variable is a linear combination of the original.

The first PC band contains the largest percentage of data variance and the second PC band contains the second largest data variance, and so on. Depending on the spectral properties of the image and the frequency distribution of different pixel types, some of the last PC bands may contain only noise (Richards & Xiuping, 2005).

In a following step an unsupervised classification is performed, based on the calculated PC bands, in our case with the K-means algorithm.

Factor analysis

Factor analysis is another multivariate statistical analysis method, which extends the PCA to find factors which can be better interpreted in terms of - in our case - geophysical variables. The resulting factor scores calculated for each single pixel describe the relationship between the original data (reflectances) and the resulting factors, which can be the water content of the sediment or the coverage by diatoms.

The pixel values can then be correlated with the in-situ data, like grainsize parameters. However, the result of this method also depends on the frequency distribution of pixels with different properties.

kNN-Method

The k-nearest-neighbor-mehthod (kNN), a nonparametric method, can be used to estimate unkown values by means of similarity to reference units with known values. It requires a large amount of in-situ data to attain acceptable results.

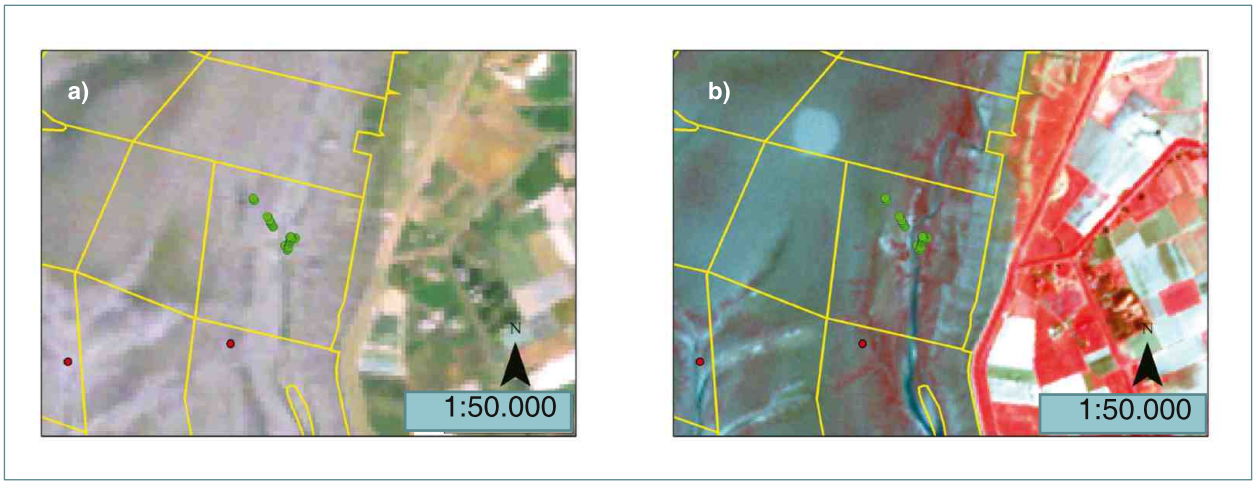

▲ Figure 8

Tidal flat in combination with field data and with different spatial and spectral resolution **a)** Landsat 30 m (R,G,B) **b)** ASTER 15 m (NIR,R,G).

▼ Figure 9

The true color images (RGB, Landsat-ETM) show the variability of seagrass growth within two weeks. **June 9th 2001:** spectral characteristics of sediment **June 26th 2001:** spectral characteristic of vegetation with mainly seagrass beds. The diagrams show the spectral reflectance at the yellow points **a)** spectral characteristics of sediment **b)** spectral characteristic of vegetation with mainly seagrass beds.

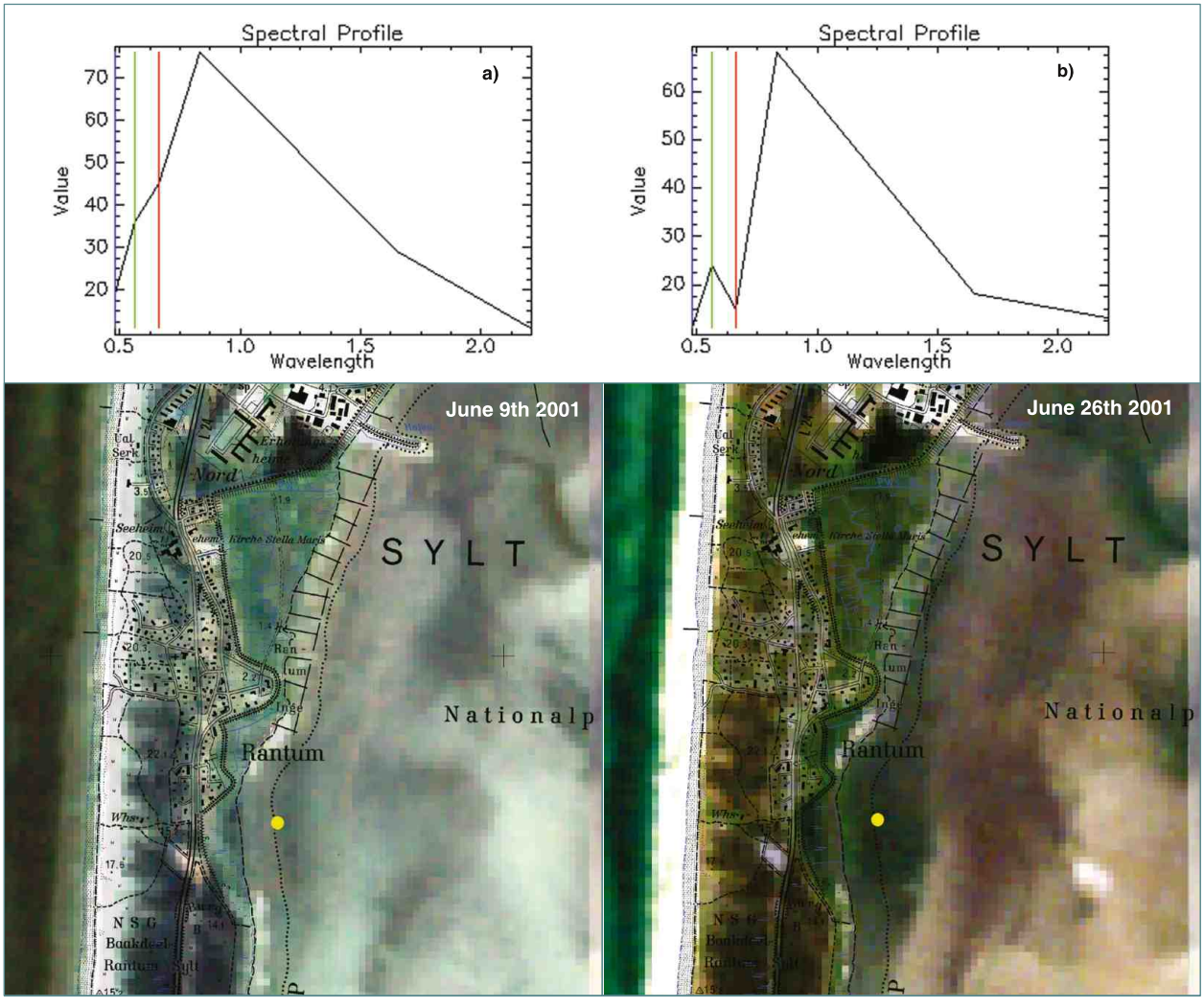

Tidal flats from space

Implementation & Results

Extraction of seagrass and macroalgae (vegetation analysis)

One result of multispectral analysis is the detection of the spatial distribution of vegetation on the tidal flat. This distribution is changing over the year and is sometimes very different from year to year, depending on the seasonal weather development.

Since a low level in 1996, the seagrass beds are growing epecially in the North Frisian Wadden Sea (Essink et al., 2005). Using satellite data, maps of the present distribution can be generated and changes can be documented.

The result of an unsupervised classification, which is based on the transformed channels (PCA- bands), is illustrated in Fig. 10. In this case the date of acquisition is July 15th 2002. In this month a great expansion of seagrass could be detected. The results correspond with data evaluated by the National Park Authorities, Tönning (Schanz and Reise, 2005).

Sediment classification

Fig. 11 depicts the workflow for sediment classification based on satellite and ground truth data. The resulting sediment map is shown in Fig. 12.

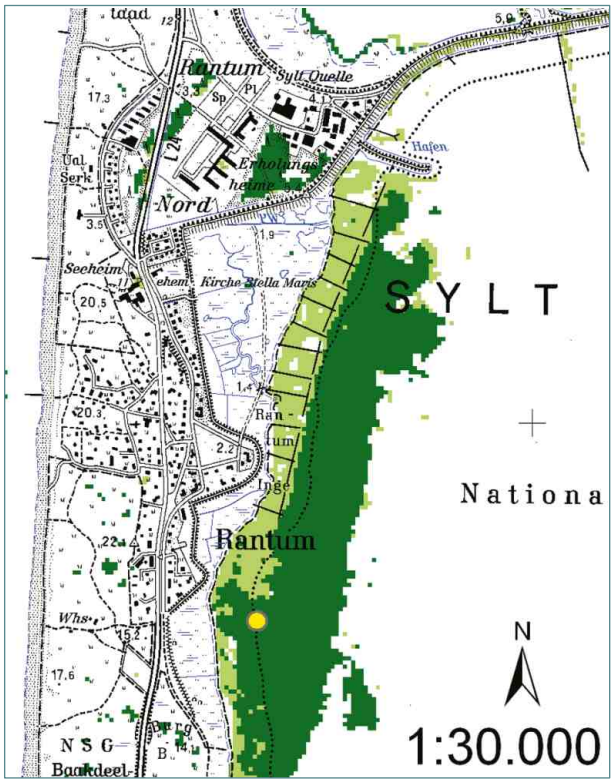

▲ **Figure 10**
Classification result using Landsat data 2002.

Authors

Ulrike Kleeberg and Karl-Heinz van Bernem (GKSS)

▼ **Figure 11**
Workflow with data and methods for sediment classification.

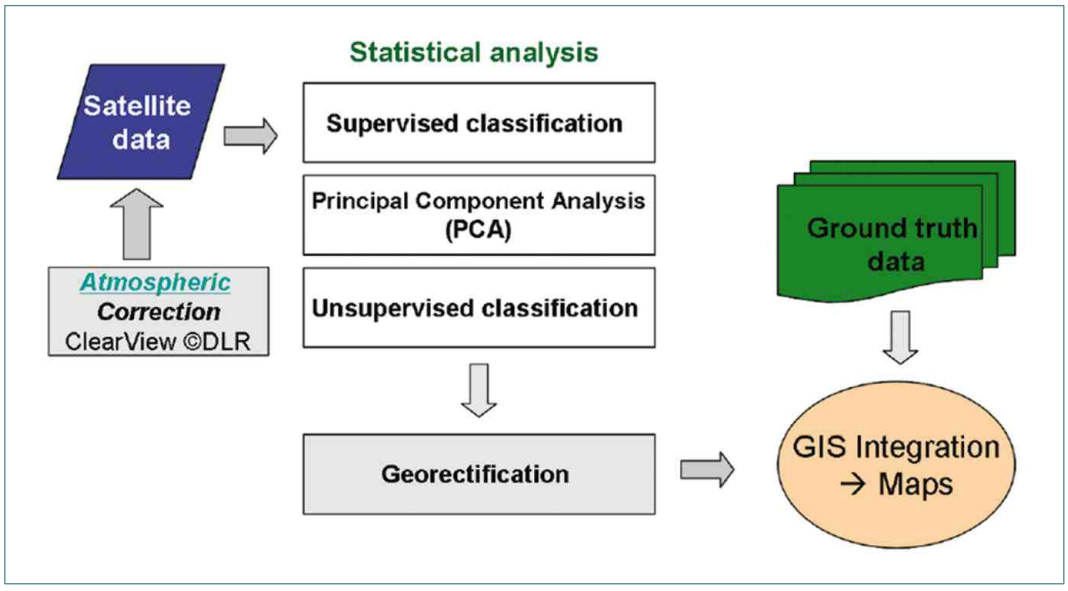

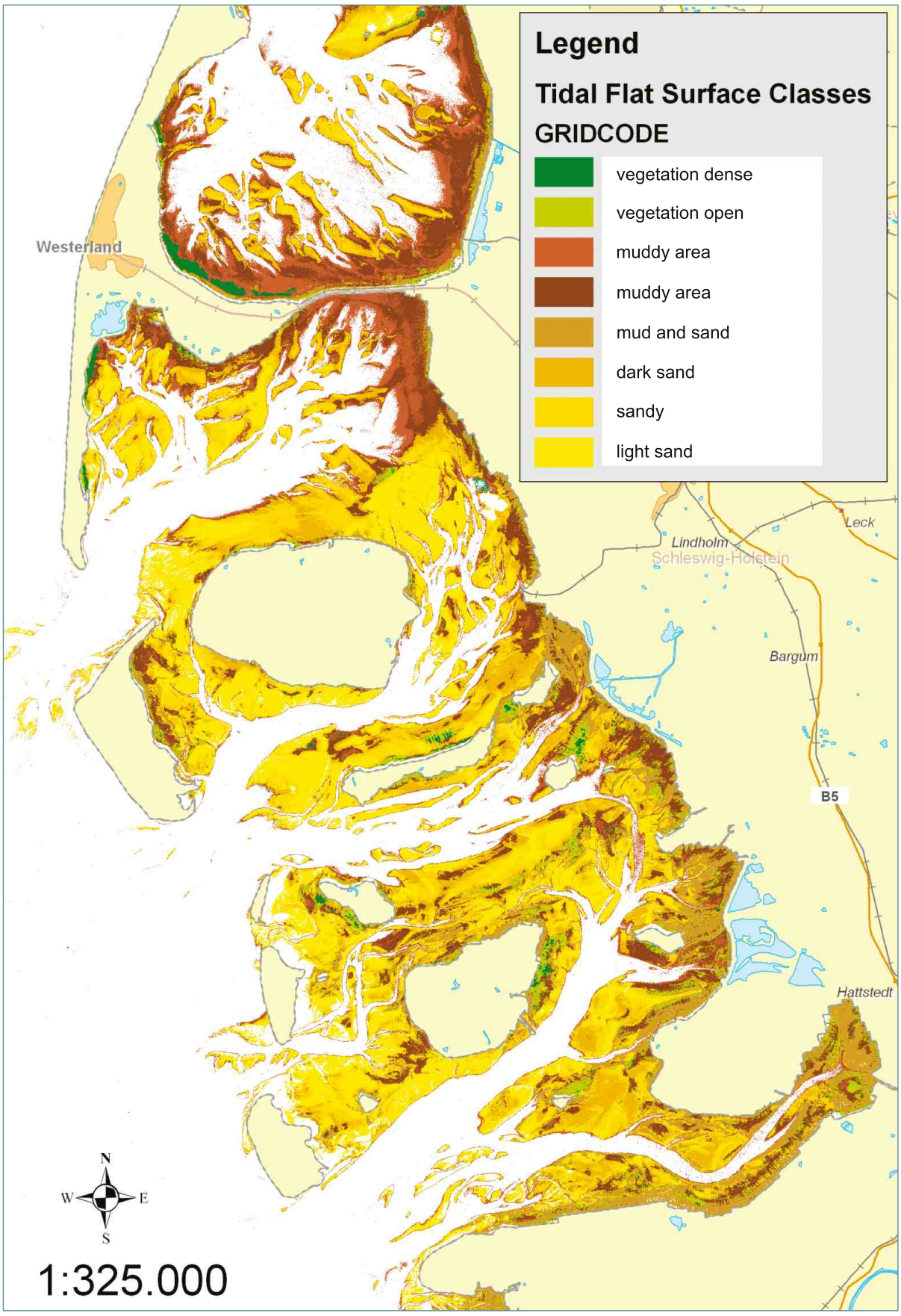

Figure 12
Sediment map of the North Frisian Wadden Sea based on Landsat ETM from July 15th 2002.

Large scale mapping of intertidal areas

Methods & Techniques

Introduction

The diversity and the changes in habitats over larger temporal and spatial scales is of great interest for regional stakeholders in the German Wadden Sea because of the high political priority of protecting natural developments within the national park areas. For ascertaining the influences of climate change as well as short term disturbances like large scale coastal constructions and accidents, the documentation of changes in habitat diversity can provide essential information on stability properties of the systems and subsystems involved. In addition, the quality assessments in the framework of TMAP (Trilaterial Monitoring and Assessment Plan) of the Netherlands, Germany and Denmark need a sound data basis to document changes in natural resources. Similar conditions hold for the quality assessment and development of monitoring strategies with respect to the EU-Water Framework Directive.

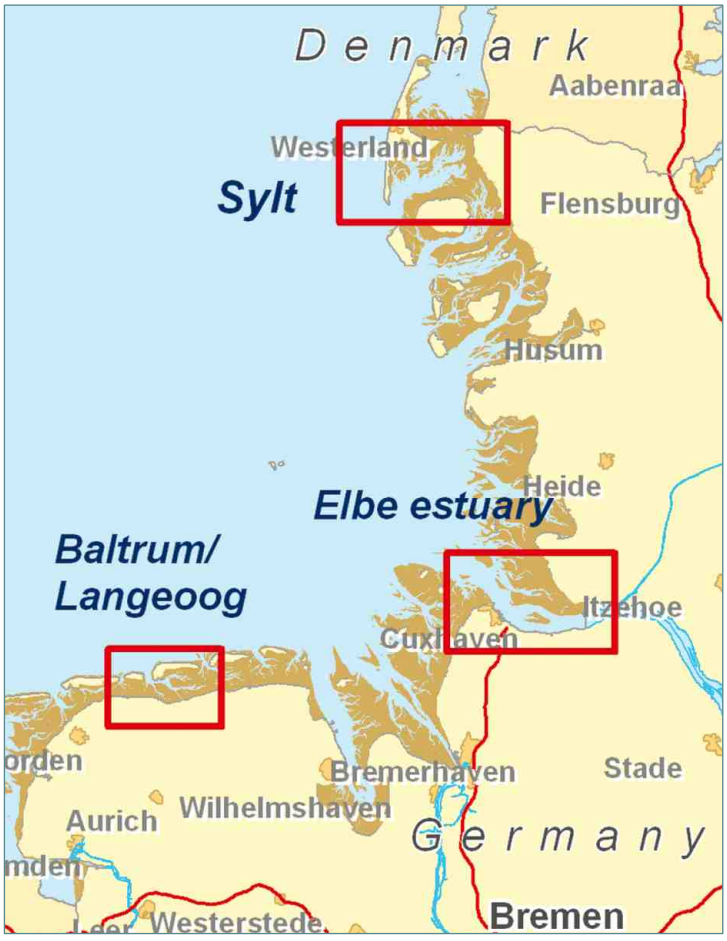

▲ **Figure 1**
Location of the 3 diagnostic sites in the German Wadden Sea.

Methodology

The field surveys for large scale mapping were conducted during June and August at three diagnostic sites in the German Wadden Sea: Hörnum Tief (2002), Elbe estuary (2003) and Baltrum/Langeoog (2004) (see Fig. 1, field work see Fig. 3). The sites are situated in areas of clearly different environmental conditions:
The East-Frisian tidal basin is comparatively small (about 5 km distance from the mainland to the islands) and highly sheltered by the barrier islands Baltrum and Langeoog. A moderate influence of freshwater (rich in nutrients) exists via two sluices. The Elbe estuary is wide open to north-west winds and characterised by a strongly changing salinity, depending on the tide. The "Hörnum-Tief" basin in the North-Frisian area is sheltered by the islands Sylt, Amrum and Föhr but open to south-west winds. The distance from the mainland to the seaward border of the tidal inlet is about 20 km.

The selection of methods to conduct the in situ mappings of intertidal habitats within the selected sites (overall covering an area of about 200 km^2 of tidal flats) was determined by two basic requirements: to achieve a maximum of information and to keep the effort as small as possible. To fulfill these prerequisites, a combination of estimated and measured values was selected to document the characteristics of habitats along a grid of locations (fixed by GPS and depicted by digital photography) with 1 km between. The estimated values, including biotic and abiotic parameters, were summarised on a standardised protocol (transect protocol) and at each location as well as at the habitat noted borders on the way between the locations (see Fig. 2).

The measured values were restricted to sediment cores (grain size and water content of sediments, macrofauna species) and shear strength.

About 80 parameters were recorded by the protocol, concerning the Elevation/Height (tidal level), the Slope or Inclination, the Surface Structure (form of ripples, etc.), Colour (light sand to dark mud), Sediment (sand, mud etc.), Depth of Layers (clay, gravel, shell particles, etc.), Water Cover (in %), Redox Condition (thickness of the oxidised zone), Macroalgae (*Ulva*, *Fucus*, etc., presence and coverage in %), Macrophytes (*Zostera*, *Spartina*, presence and coverage in %), Macrofauna (epibenthic species and endobenthic species forming visible life tracks; presence and estimated abundance), and others.

Conclusions on change and stability of habitats within the sites were made by comparing these results to those of a mapping campaign from 1987 until 1992, which covered the entire German Wadden Sea area.

Transect Protokol

Elevation/Height
1.1 1 close MTLW
2 middle
3 close MTHW
1.2 1 close to land (0)

Slope/Inclination
2.1 1 flat (0)
2.2 1 < 30° (0)
2.3 1 > 30° (0)
2.4 1 tidal channel edge (0)
2.5 1 gully edge (0)
2.6 1 surf zone (0)

Surface Structure
3.1 1 smooth (0)
3.2 ripple hight (cm)
3.3 ripple lenght (cm)
3.4 1 symmetrical (0)
3.5 1 asymmetrical (0)
3.6 strongly eroded (0)
3.7 1 large/mega ripples (0)
3.8 1 Arenicola hump (0)
3.9 1stones (0)
3.1 1 pebbles/gravel (0)
3.11 1 peat/turf (0)

Colour
4.1 1 light
2 dark

Sediment
5.1 1 sand (0)
5.2 1 muddy sand (0)
5.3 1 condition (0)
5.4 1 sand on mud (0)
5.5 1 shell bank (0)
5.6 1 mud (0)
5.7 penetration/sinking depth (cm)
5.8 0 no shell coverage
1 light, 2 strong

Depth of Layers
6.1 0 no shells
1 light, 2 strong
6.2 depth (cm)
6.3 1 turf/peat layer (0)
6.4 1 clay layer (0)
6.5 depth (cm)

Water Cover
7.1 water cover (%)
7.2 1 film of water (0)
7.3 1 filled troughs (0)
7.4 1 dry (0)

Redox Condition
8.1 ox-depth (cm)
8.2 1 sharp, 2 diffuse
8.3 1 black spots (0)
8.4 cover/m2

Microalgae
9.1 Diatom cov. (%)
9.2 1 patches, 2 homogeneous
9.3 0 no tubular diatoms
1 Amphipleura, 2 dense
3 Melosira, 4 dense, 5 both, 6 dense
9.4 1 Merismopedia, 2 dense (0)

Macroalgae
10.1 Enteromorpha (%)
10.2 1 isolated, 0 none
10.3 1 Ulva, 2 dense
10.4 1 Fucus, 2 dense (0)
10.5 1 Porphyra, 2 dense (0)
10.6 1 Chaetomorpha, 2 dense (0)
10.7 1 humps, 2 dense, 3 (0)

Macrophytes
11.1 Zostera marina (%)
11.2 1 isolated, (0)
11.3 Zostera noltii (%)
11.4 1 isolated, (0)
11.5 1 Spartina, 2 dense, (0)
11.6 1 Salicornia, 2 dense, (0)

Macrofauna
12.1 1 Arenicola < 1/m2
2 (1-10), 3 (-50), 4 (> 50),
5 (>> 50), 6 juv., 7 adult
12.2 1 Lanice, 2 dense
3 very dense, (0)
12.3 Lanice (Ind/Area, 10 SS)
12.4 (") on humps
12.5 (") beside humps
12.6 1 Heteromastus, 2 dense,
3 very dense (0)
12.7 1 Mya, (0)
2 juv. dense, 3 adults dense
4 both dense
12.8 1 Cerastoderma, (0)
2 juv. dense, 3 adults dense
4 both dense
12.9 1 Mytilus, (0)
12.1 1 isolated clumps, (0)
12.11 1 small isolated banks
2 small dense banks, (0)
12.12 1 connected banks, (0)
12.13 1 young, 2 old, 3 50/50
12.14 proportion of dead individuals (%)
12.15 1 Corophium, 2 dense, 3 v. dense, (0)

Description of Sample Area
13.1 1 samples from water covered areas,
2 samples from dry sediment
13.2 depth of cover (cm)
14.1 Location
14.2 Coordinates (D-GPS)
15.1 Remarks

▲ Figure 2
Transect protocol

▼ Figure 3
Field work for collecting habitat data.

Large scale mapping of intertidal areas

Implementation & Results

An overview of the mapping results of the three test sites is given in the following, with emphasis on the “Hörnum-Tief” tidal basin.

Backbarrier tidal flats of the islands Baltrum and Langeoog

Compared to the conditions during the field surveys in 1987/1992, the distribution of sediment properties (among others: grain size, water content and shear strength) showed no significant change during 2004. The same holds for the presence (or abundance) and distribution of key organisms/habitats like banks of the blue mussel (*Mytilus edulis*), meadows of the sand mason (*Lanice conchilega*) and cockles (*Cerastoderma edule*), shell mounds and muddy areas. A clear decrease in seagrass distribution, detectable during 1987/1992, continued. In 2004 only a small remainder of these habitat-forming macrophytes existed in a southern nearshore area (Fig. 4).

The protected location of this basin obviously prevented significant changes of morphology and habitat diversity after more than 10 years. Although some strong ice winters during this period eliminated nearly the entire intertidal stocks of the temperature sensitive organisms *Lanice conchilega* and *Cerastoderma edule*, their spatial distribution and density in 2004 corresponded to the conditions found during 1987/1992. Only with regard to the seagrass (*Z. noltii*) there was no resilience: its decrease, documented for the entire tidal flats of Lower Saxony, continued.

Tidal flats of the Elbe estuary

With respect to key species and habitats (for example: *Marenzelleria viridis* (invader from the USA, during the 1970s by ship ballast water), and the mud crab *Corophium volutator* (present over wide areas in high abundance: more than 150,000 Ind/m^2)) the change in habitats from 1987/1992 until 2003 was negligible. These organisms, settling in silty, stable areas beyond mid tide level, showed no significant change of presence (with regard to abundance) and distribution. On the other hand, severe erosion eliminated about 5 km^2 of tidal flats, mainly populated by another key species of this area, the soft shell clam (*Mya arenaria*). This mussel, living in a depth of 20-40 cm of mainly fine to middle sand occurred in this areas with an average biomass of 60g/m^2 ash free dry weight (afdw) during 1987/1992. If we assume a filtration rate of 2 l/h/Individuum, a loss of 300 t afdw and of 300 hl/h filtration capacity results (Fig. 5).

Hörnum-Tief catchment area

During 2002 extended muddy areas were found only in the north-east part of the Hörnum-Tief catchment area. Most tidal flats were characterised by light to dark sands (for sampling locations see Fig. 6). Compared to the conditions found during 1987/92, the amount of sandy habitats especially in the north-east part increased significantly. These findings, affirmed by grain size analyses of the sediment, coincide with further habitat conditions documented by the standardised protocol: presence and form of ripples as well as the abundance and distribution of the lugworm (*Arenicola marina*), well known as a "sand follower" (see Fig. 7).

The spatial distribution of seagrass is more extensive in 2002 compared to 1987/92, but the dominance-structure changed: during 1987/92 *Zostera marina* dominated, in 2002 *Zostera noltii*, which probably shows a lower sensitivity to current velocity and disturbances by wave energy (Fig. 8). The areas of presence of *Zostera* species remained widely stable. Thus, in a comprehensive observation, it can be assumed that a higher amount of hydrodynamic energy was transported into this tidal basin causing the shift of habitats with regard to the selected examples.

Conclusion

In situ monitoring of habitats provides a high number of results which can be used to assess the state of tidal basin systems. The different results can also be used to examine the consistency and plausibility of hypotheses of change. An evaluation of the vulnerability of habitats to natural or man-made disturbances is a valuable support in decision finding processes like for example the estimation of the resilience of habitat diversity following coastal constructions, the development of response strategies against oil pollution as well as the classification of reference areas (diagnostic sites).

Although the field investigations and analyses are very simple, the total application of the presented large scale mapping methods requires a sound knowledge of the operators with respect to tidal flat ecology. Remote sensing results of sediment structure and other identifiable properties of habitats form a suitable instrument to fulfill the temporal gaps between in situ assessments and help to define the spatial borders of habitat conditions recorded at fixed localities. On the other hand, the results of the field surveys help to find proxy parameters for remote sensing techniques and to classify remote sensing data.

Authors

Karl-Heinz van Bernem and Ulrike Kleeberg (GKSS)

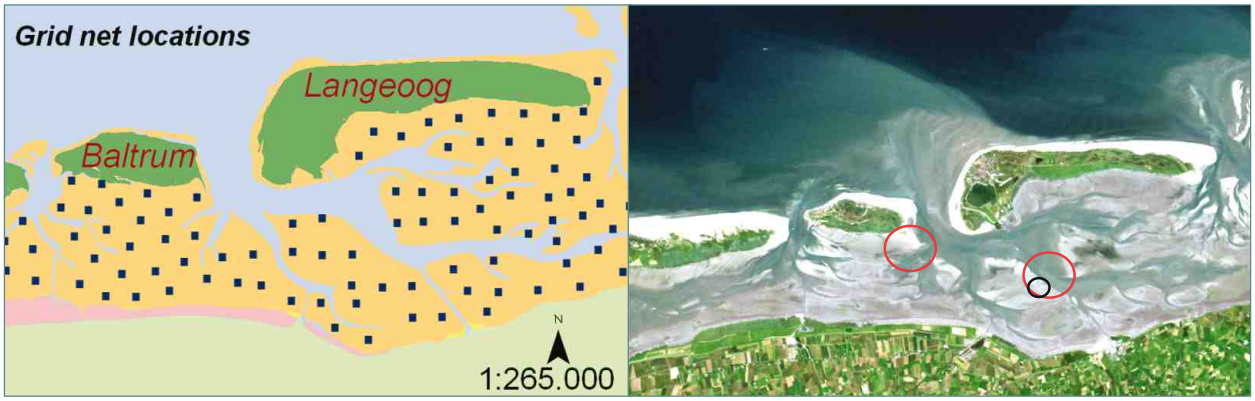

▲ **Figure 4**
Left: Locations on the backbarrier tidal flats of Baltrum/Langeoog. **Right:** The presence of *Zostera spp.* during 1987/92 is marked with red circles; for 2004 with a black circle.

▲ **Figure 5**
Locations on tidal flats of the Elbe estuary. The smoothed habitat borders (red) of 1987/1992 are shown as polygones to point up the high morphological change compared to the spatial conditions depicted by the TM image.

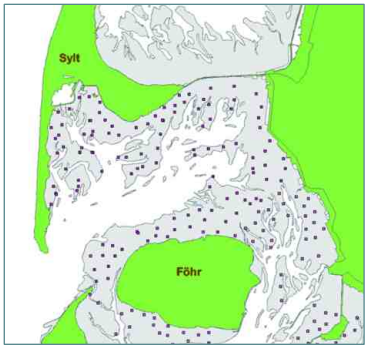

▲ **Figure 6**
Locations on the Hörnum-Tief tidal flats.

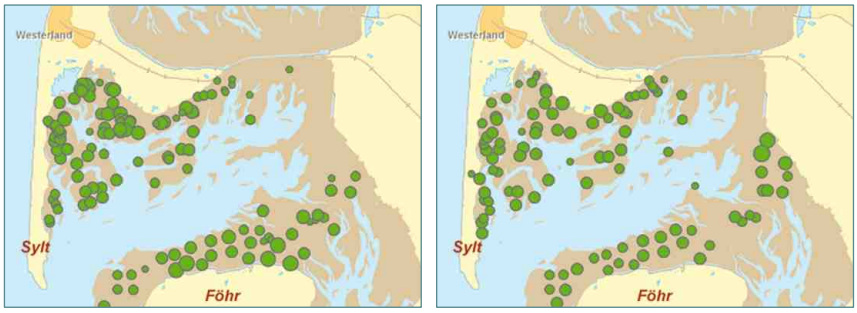

◄ **Figure 7**
Distribution and dominance of *Arenicola marina*, **left**: in 1987/92 and **right:** in 2002.

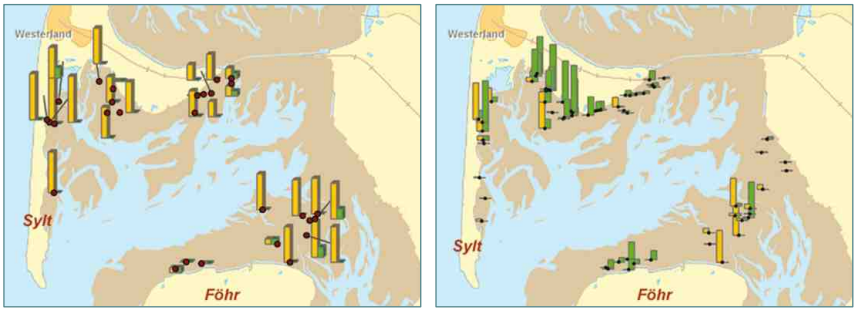

► **Figure 8**
Distribution and dominance of *Z. marina* (yellow) and *Z. noltii* (green), **left:** in 1987/92 and **right:** in 2002.

Mapping of tidal flat habitats with digital cameras

Methods & Techniques

Introduction

One of the most unique ecosystems in Europe are the tidal flats along the North Sea coast stretching from the Netherlands to Denmark. The vast extension and the changing coverage by water within the tidal cycle make it difficult to observe this area either by foot or by boat and to monitor the distribution of habitats, such as sea grass meadows and mussel beds. Remote Sensing is one possibility to solve this problem. Satellite data have the advantage of covering the whole area at once. But the spatial resolution of 10-30 m is too coarse for some applications. Furthermore, the coincidence of time of overpass, low tide and cloud free weather is rare. Survey aircraft with multispectral scanners or imaging spectrometers can fly at the right time and provide a high spatial and spectral resolution. However, their operation is expensive and flights have to be booked long time in advance with the risk of inappropriate weather during the scheduled period.

A further, very flexible and cheap option is to use digital cameras from a light aircraft. The data are available right after the flight and can be used to guide the ground work. Within this chapter we will report on our experiences with operating a consumer digital camera and a multispectral digital camera system on a Cessna 172 light aircraft. This test was part of the ORFEW project, which was supported by the environmental authorities of the states of Schleswig-Holstein and Niedersachsen (Lower-Saxony).

Method

The equipment consists of 2 independent camera systems: an Olympus 8080 RGB camera with a 0.7X wide angle lens converter and a system of 4 digital black & white cameras (MUVI, multispectral video imager), each of which is equipped with an interference filter. The wavelength bands of these filters were selected according to the results of spectral reflectance measurements on the ground. Both cameras were mounted in a rack with a vertical viewing direction (Fig. 1).

The Olympus RGB camera is fully controlled from a notebook computer via a USB connection. Images are transferred to the notebook right after capture so that a quality check is possible in nearly real-time. Furthermore, a continuous videostream from the camera is shown on a video display for the fine navigation of the aircraft over small targets. The notebook computer also records the navigational data with an interval of 1 s from a GPS-mouse. The precise GPS time is synchronised with the computer and the camera. The MUVI system includes a laser-gyro, an electronic compass and a GPS for recording position and altitude at the time of image capture. Since the four cameras are not perfectly aligned, the pixel co-registration of the 4 bands has to be performed during the later data processing. Basis for the co-registration is the wider image of the Olympus camera.

▲ **Figure 1**
Camera system:
Olympus 8080 3264 x 2448 pixel at 1000 m altitude, **swath:** 1569 m, **spatial resolution:** 48 cm.
MUVI IIIc 1280 x 960 pixel, **swath:** 733 m, **spatial resolution:** 57 cm, **spectral bands**: 568, 620, 855 nm, **bandwith:** 10 nm.

To cover larger areas, mosaics of the images are computed by using the Autopano software, which does an automatic determination of corresponding points in the overlapping areas of the image series. The thematic interpretation is performed by visual inspection and by using the supervised maximum-likelihood classification method. It requires to identify pixels on the ground with known surface types, such as mud flat, sea grass etc. which can be used as training areas. After classification a is computed as well as the area which is covered by an object such as sea grass. Together with ground samples also the biomass e.g. of seagrass, macro- and micro-algae can be estimated much more accurately than without the aerial survey.

Authors

Roland Doerffer, Wolfgang Cordes and Ulrike Kleeberg (GKSS)

◄ **Figure 2**
Image of Olympus and MUVI camera.

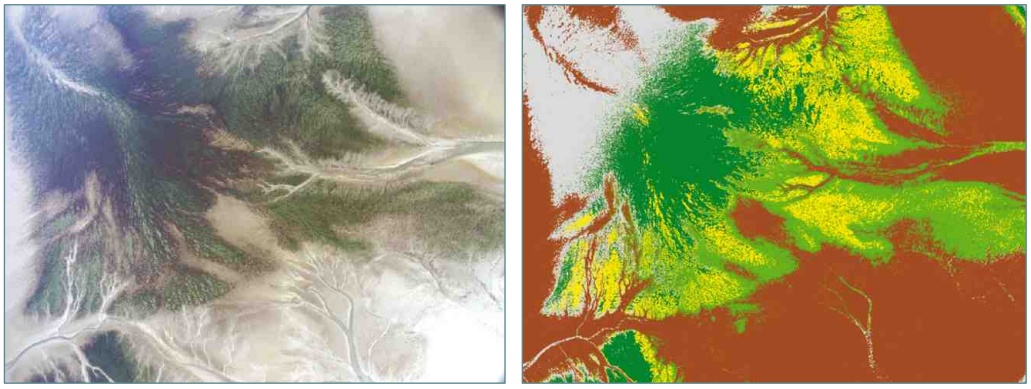

◄ **Figure 3**
Left: RGB image of a macro algae field. **Right:** Classification of the vegetation density.

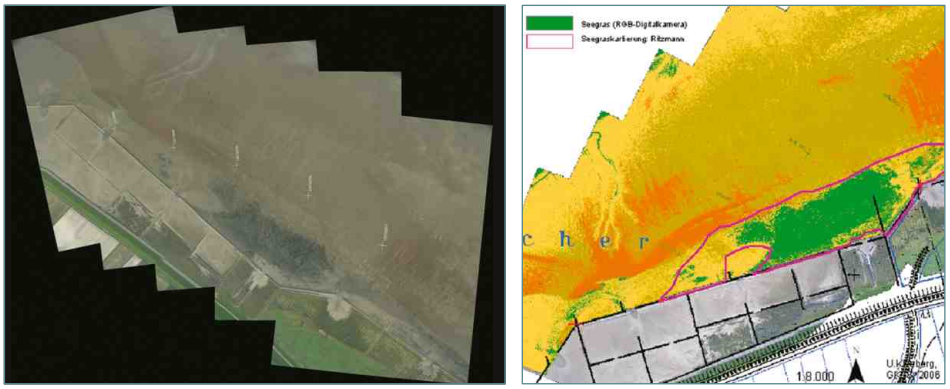

◄ **Figure 4**
Left: Mosaic of five images. **Right**: Seagrass mapping using maximum likelihood classification.

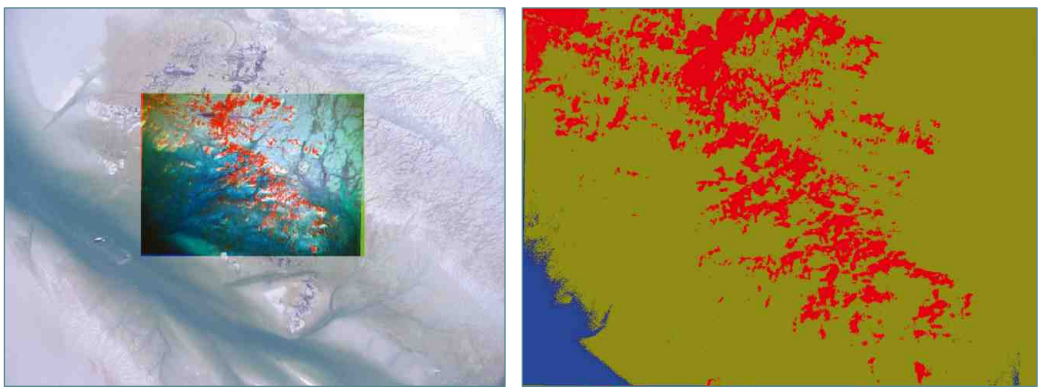

◄ **Figure 5**
Left: RGB and MUVI IR, false colour image of mussels. **Right**: Mussel classification.

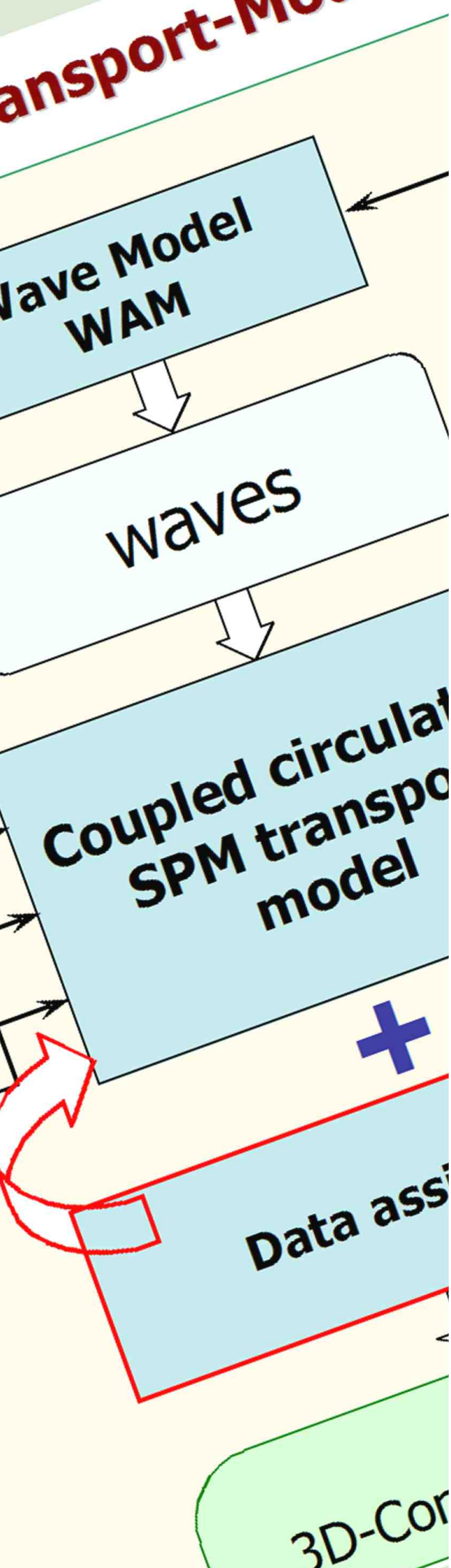

Using the synergy of methods

The coastal sea is a complex environment, where many processes happen on different spatial and temporal scales.

To understand the development of a habitat or the population of a species, it is necessary to observe all relevant variables and processes. For an understanding of this network of interacting elements also models are necessary to quantify the many feed-back mechanisms. For a monitoring programme this is the most challenging part. It requires a close teamwork between all experts as well as tools to integrate the many data of different nature, different spatial and temporal resolution and with different error bars.

Here we present examples, where observation and sophisticated data interpretation and modelling techniques have been combined to enable the extraction of information from observations and improve our knowledge about the coastal sea.

Content

FerryBox - Continuous and automatic water quality observations along transects

Methods & Techniques

Introduction

The lack of reliable monitoring systems that provide continuous observations of the marine environment in the coastal areas and shelf seas of Europe with an adequate data quality is a serious hindrance to an understanding of marine systems. Currently, operational monitoring is mainly carried out by manual sampling and analysis during ship cruises. Autonomous measuring systems on buoys allow measurement of standard oceanographic parameters (temperature, salinity, currents) and, in some cases, other parameters, e.g. turbidity, oxygen and chlorophyll fluorescence. However, existing observations mostly lack the spatial coverage and temporal resolution required to determine the state of the marine environment and changes within it. Furthermore, the automatic systems on buoys etc. are affected by biofouling and the operational costs are high due to ship costs for servicing.

To overcome these problems, the use of “ships-of-opportunity” (SoO) has been promoted by EuroGOOS (European Global Ocean Observing System). As a measuring platform, ferries on regular routes offer a cost-effective and reliable possibility to obtain regular observations on near surface water parameters. Applying such a FerryBox system on ferry boats or ships-of-opportunity has several advantages: (1) the system is protected against harsh environment, e.g. waves and currents, (2) bio-fouling can be more easily prevented (inline sensors), (3) no energy restrictions (in contrast to buoys), (4) easier maintenance when the ferry comes back "to your doorstep", (5) lower running costs, since the operation costs of the ship do not need to be calculated, (6) transects yield much more information, than point measurements (buoys) (Petersen et al., 2003).

▲ **Figure 1**
Small version of the FerryBox together with nutrient analysers onboard of the research vessel “Polarstern”.

Technology:

The principles of the FerryBox flow-through system are schematically shown in Fig. 2. For an unattended operation the system is controlled via position (by GPS) and an internal computer. The system is connected to a station on shore, via GSM (cell phone) for remote control and data transfer. The data transfer is in near real time after completion of a cruise at all times the ship is in a harbour. All data are archived in a data base system at GKSS and can be accessed by external users via a web interface (http://ferrydata.gkss.de).

The water intake is at a fixed depth of about 5 metres. A debubbling unit removes air bubbles, which may enter the system during heavy seas. Coupled to the debubbler is an internal water loop in which the water is circulated passing the different sensors. The basic sensors used are temperature & salinity, turbidity and chlorophyll-a fluorescence. In addition, an oxygen sensor (Clark electrode or oxygen optode) and a pH sensor were applied as well. The basic setup was extended to further sensors such as an optical nitrate sensor and an algal group detector as well as chemical analysers (after filtration by a hollow-fibre cross-flow filter) for nutrients (NH_4, NO_3/NO_2, o-PO_4, SiO_4). An automatic refrigerated water sampler can collect seawater at predefined positions for subsequent laboratory analysis (for quality control and further parameters).

Study area

The first FerryBox system was installed on a ferry between Cuxhaven (GE) and Harwich (GB) from 2002 until 2005. After the operation of this ferry line was terminated the equipment was reinstalled on a Roll-on/roll-off vessel (“TorDania”) between Cuxhaven and Immingham (GB) in September 2006 (Fig. 4). A second system was installed on a cargo ship (“LysBris”) cruising between Germany, England and Norway in 2007. The ferry transects are depicted in Fig. 3. In the GKSS-coordinated EU project "FerryBox", running from 2002 to 2005, different measuring systems - including the GKSS FerryBox - were compared and tested on nine different European ferry routes (Petersen et al., 2005). The results showed the good quality of the data and the applicability of this technology for operational monitoring purposes (see also http://www.ferrybox.org) (Petersen et al., 2007).

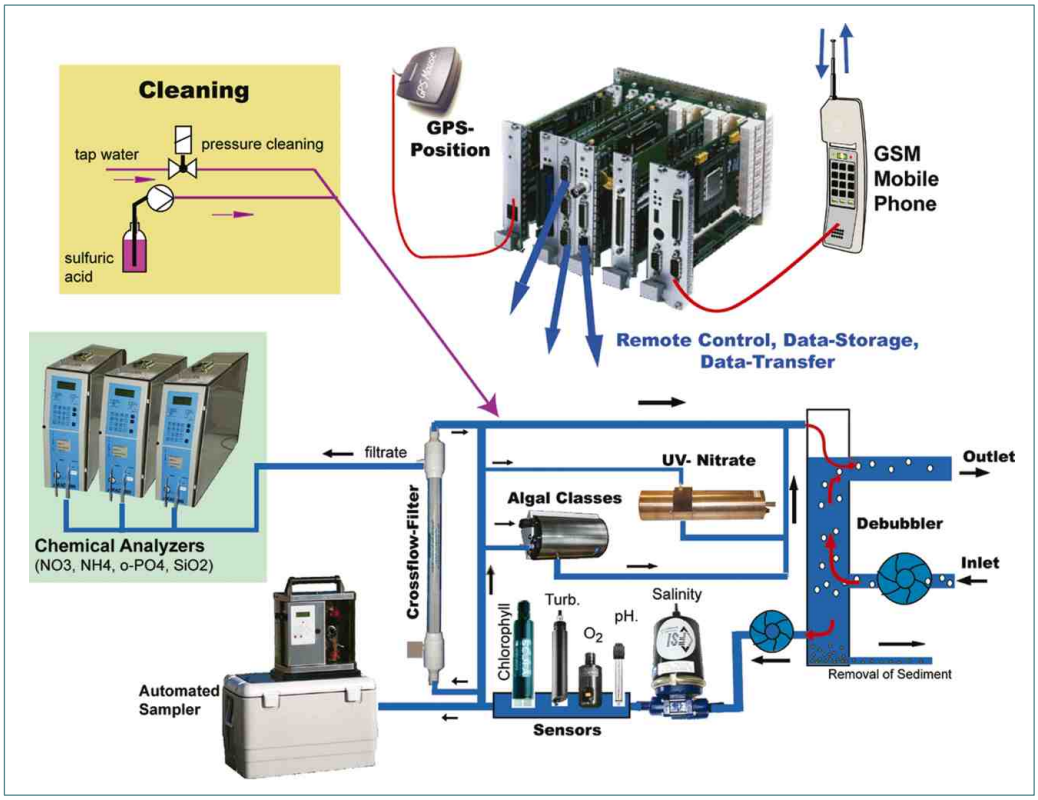

▲ Figure 2
Schematic design of the FerryBox flow-through and data system with special features for unattended operation (automatic cleaning system).

▼ Figure 3
Current FerryBox transects in the southern North Sea operated by GKSS:
Route Cuxhaven - Immingham: RoRo-ship TorDania,
Route Gemany - England - Norway: cargo ship LysBris.

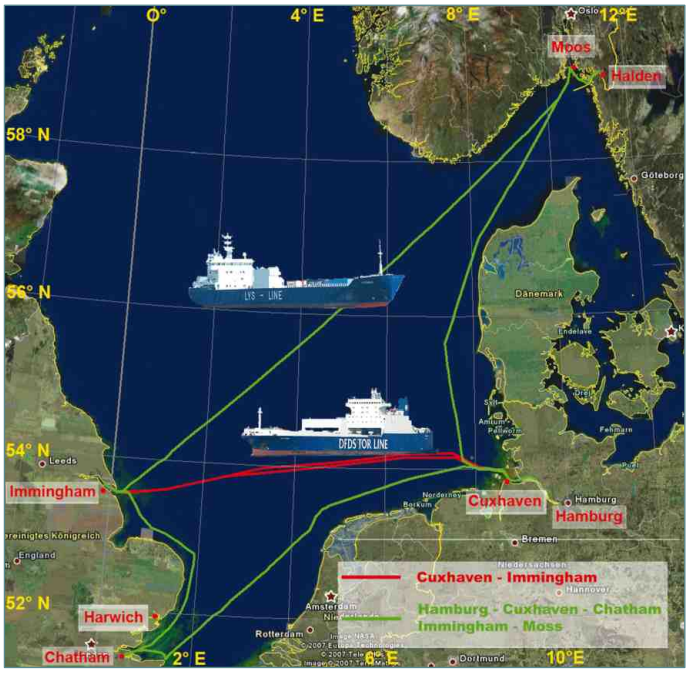

▼ Figure 4
FerryBox System onboard the vessel “TorDania” on the route Cuxhaven - Immingham.
Measured parameters: salinity, temperature, turbidity, chlorophyll-a, oxygten, pH, nitrate (UV-detection).

FerryBox - Continuous and automatic water quality observations along transects

Implementation & Results

FerryBox data on a single transect

One transect between Cuxhaven and Harwich from March 27th 2004 is shown in Fig. 6. The following parameters were measured:

Salinity

Low salinities near Cuxhaven indicate the freshwater outflow of the river Elbe, whereas the decrease near Harwich is only marginal. It is also evident that lower salinities are observed along the Dutch coast compared to the English Channel due to fresh water influence of the Ijsselmeer and the river Rhine.

Turbidity

Near Harwich high turbidities are measured which is characteristic of the coastal areas at the English coast, presumably due to erosion processes. Higher turbidities are also detected in the Elbe estuary (turbidity zone).

Chlorophyll-a

The total chlorophyll concentration shows a broad maximum along the Dutch coast between km 200 and 400 (distance from Harwich). Here, the groups of green algae and flagellates and the group of diatoms and flagellates are both prevailing. This early spring bloom is probably dominated by flagellates, which, unfortunately, contribute to both groups and therefore cannot be clearly separated.

Oxygen saturation and pH

These parameters show a maximum in the areas with high chlorophyll concentrations. This is expected since this reflects the processes during primary production (CO_2-uptake which increases the pH, and O_2-production).

Nutrients

Ammonium (NH_4) and nitrate (NO_3) show elevated values near the Elbe estuary since the Elbe is a source for these substances. Near the English coast, elevated ammonium concentrations are found as well.

Seasonal results from FerryBox measurements

The observations of single transects with the FerryBox can be pooled in a scatter plot to give an overview of the temporal and spatial variability of a parameter. In Fig. 7 time series of salinity, chlorophyll, oxygen and pH are shown from January to November 2005

Salinity

The higher salinities in waters which originate from the English Channel prevail over the whole year. Near the Elbe estuary several freshwater intrusions into the German Bight, which lower the salinities, can be seen. This may originate from rainwater and Elbe runoff.

Chlorophyll

Fig. 7 shows that plankton blooms started in early April in the waters west of the Dutch coast. The main reasons for this are presumably a low turbidity and stratification of these waters in springtime, which supports algal growth. From this area the bloom spreads along the Dutch coast northwards. In July the main nutrients are consumed and only small chlorophyll concentrations remain. During spring and early summer algae blooms occur in front of the Elbe estuary. Here, the high nutrient concentrations which are released from the Elbe (nitrate) and which are produced in the sediments of the wadden sea tidal flats (NH_4, PO_4) support the bloom.

Oxygen saturation

In general, the oxygen saturation values over 100 % follow the chlorophyll pattern due to primary production. In addition, oxygen deficiencies can be seen in decaying algal blooms due to bacterial mineralisation processes.

The new FerryBox system on the cargo ship "LysBris"

Since 2007, a second FerryBox system has been operating on a cargo ship which cruises between Germany, England and Norway on a weekly basis. Some preliminary results for salinity are shown in Fig. 5. The lower salinities in front of the Elbe estuary and in the Skagerrak (surface waters from the Baltic) can be seen clearly. In addition, it is evident that lower salinities are measured along the English coast than in the open North Sea and in the waters adjacent to the English Channel.

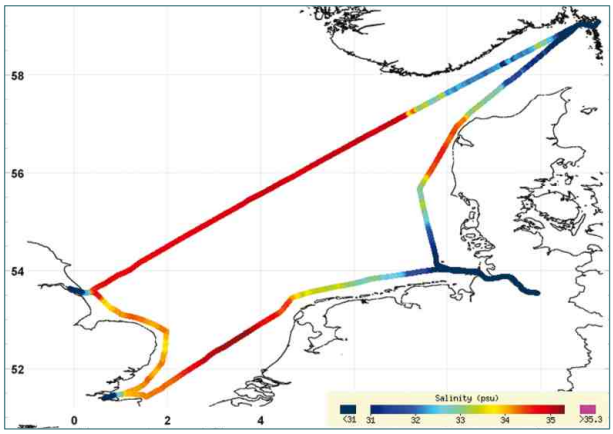

▲ Figure 5

Salinity data from a new FerryBox system on the cargo ship "LysBris" in December 2007. (Route: Hamburg (DE) → Cuxhaven (DE) → Chatham (GB) → Immingham (GB) → Moss (NO)).

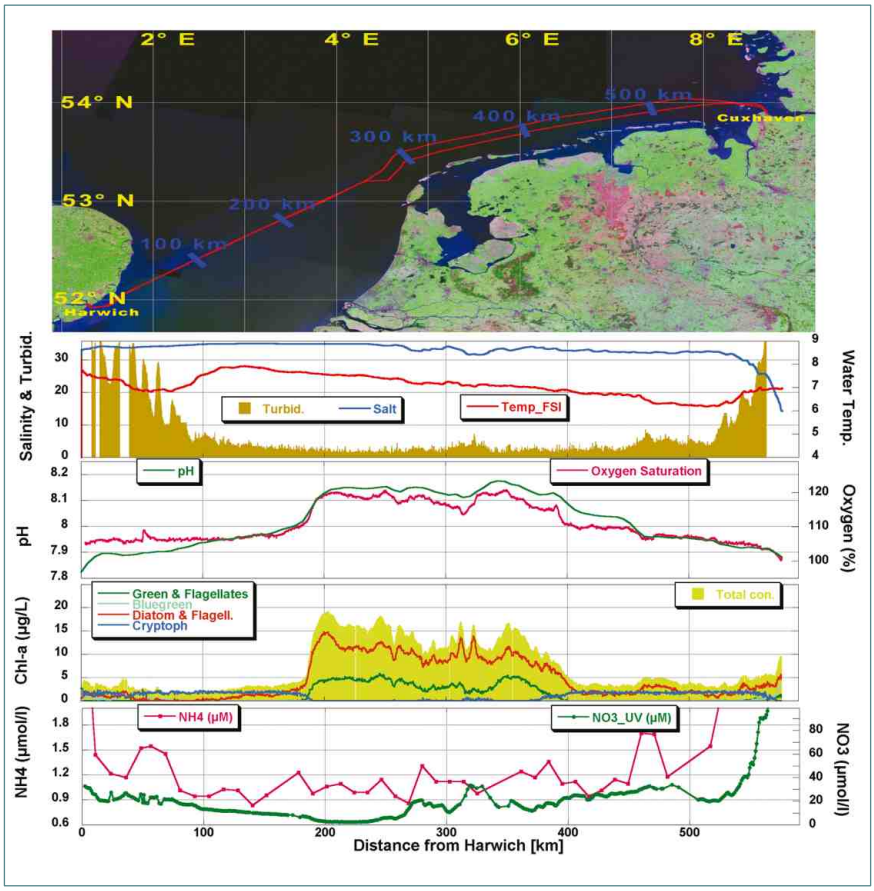

◄ **Figure 6**
Route of the ferry and data observed on a single transect between Cuxhaven and Harwich on March 27th 2004.

▼ **Figure 7**
Scatter plot of the parameters salinity, chlorophyll-a, oxygen saturation index and pH on the route Cuxhaven-Harwich in the year 2005.

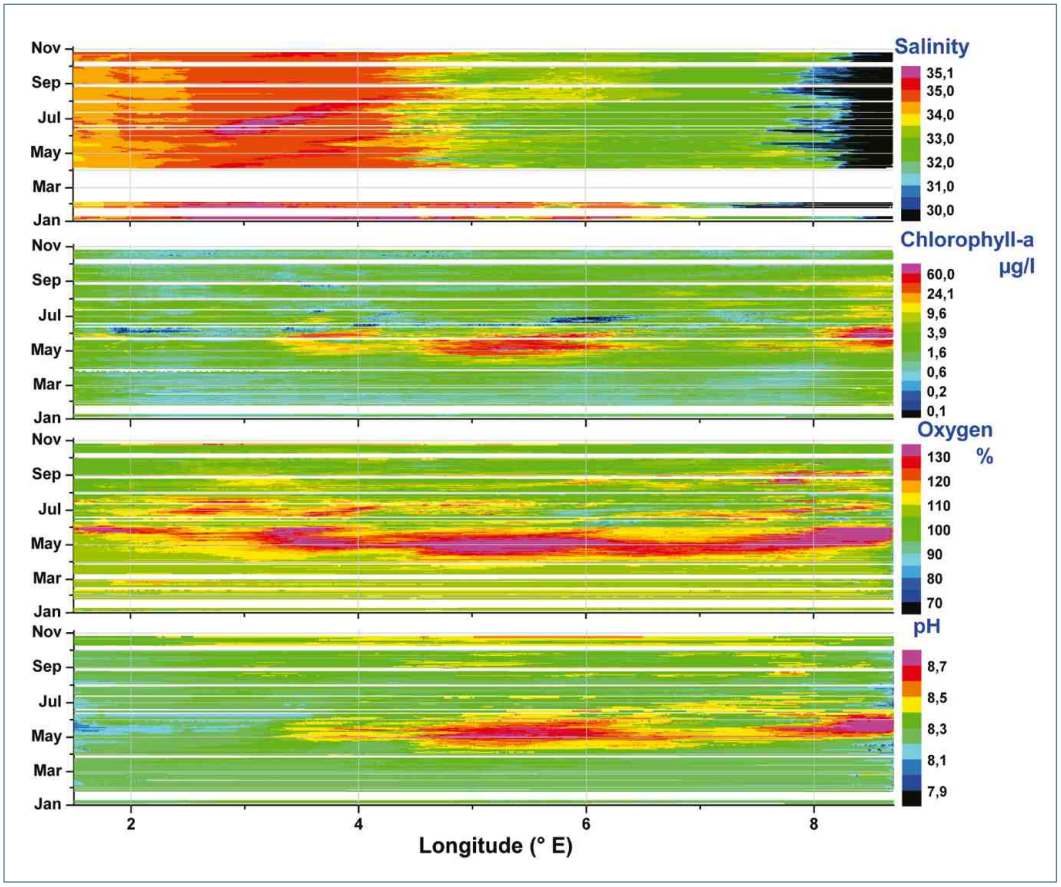

FerryBox - Continuous and automatic water quality observations along transects

Implementation & Results

Algal dynamics in 2004 and 2005

A more detailed picture of the spring bloom in the years 2004 and 2005 is shown in the two contour plots in Fig. 8. In general, the chlorophyll variations are similar to those in Fig. 7: The bloom starts west of the Dutch coast and subsequently spreads northwards. However, the start of the bloom in 2005 occurs later in the year (early April) than in 2004 (end of March), the bloom does not spread so far in 2005, and the intensity of the bloom is higher in 2005.

In addition, in 2005, a much more intensive bloom was observed in the German Bight off the Elbe estuary, starting in May and disappearing in mid June 2005. This bloom was characterised by considerably higher chlorophyll concentrations (factor 1.5) than in 2004.

The reasons for these differences are not yet clear and are the topic of further investigations, in which not only oceanographic parameters (temperature, turbidity, stratification) and nutrient availability have to be considered but which require numerical transport and ecological models for interpretation.

Comparison of remote sensing data with FerryBox measurements

In order to extrapolate from the two-dimensional FerryBox transects to larger areas satellites measuring optically active substances such as chlorophyll-a, yellow substance and suspended matter can be used. Especially the MERIS spectrometer on the satellite ENVISAT provides high spatial resolution data. As the data are measured by different physical principles - absorption of sunlight (MERIS) and fluorescence (FerryBox) - it is necessary at first to make a comparison before combining the two methods.

In Fig. 9, a chlorophyll image of processed MERIS/ENVISAT data of the North Sea is presented. In the bottom graph of Fig. 9, data from the satellite along the FerryBox track were extracted (orange) and compared with measured FerryBox data (green). The areas with large chlorophyll concentrations off the Dutch coast and outside the Elbe estuary are well reflected by the FerryBox measurements. However, the large peak at 5.5° E is underestimated by the satellite. The differences may be caused by (1) uncertainties in the satellite data due to shallow waters and high concentrations of suspended matter; (2) uncertainties of the in-situ method as the fluorescence of algae varies among different algal species and is highly influenced by their physiological status.

Taking these problems into consideration, the agreement between the two methods is not too bad and a combination can be used for interpretation purposes. This may be important, e.g. when data from consecutive FerryBox cruises imply a breakdown of an algae bloom (Petersen et al., 2008). With satellite images it can be determined whether such a breakdown occurred or if an algae field was just drifting out of the ship track. The main disadvantage of remote sensing in the North Sea is the frequent cloud coverage, which often prevents the use of satellite data.

Conclusions and outlook

In conclusion, it turns out that a FerryBox system is a cost-effective monitoring tool to get a high yield of reliable high frequency water quality data along a transect and improving on conventional monitoring strategies. The yield of reliable data is high due to low-maintenance inline sensors and easy access for servicing at the home port. The high resolution of FerryBox systems in space and time provides deeper insight into marine processes which can be used for better assessing the ecosystem and the underlying biogeochemical processes in the marine environment. Special events like strong short-term algae blooms, which will be detected only occasionally by standard monitoring methods, can be studied in detail and related to variations in influencing factors such as temperature, wind and nutrient load.

However, due to its limitations (surface measurements, certain ship tracks only) only a combination of research ship cruises, buoy measurements at strategic locations, remote sensing and numerical modelling will give the deep insight needed for an understanding of the ecosystem as a prerequisite for future management options.

Authors

Wilhelm Petersen and Friedhelm Schroeder (GKSS)

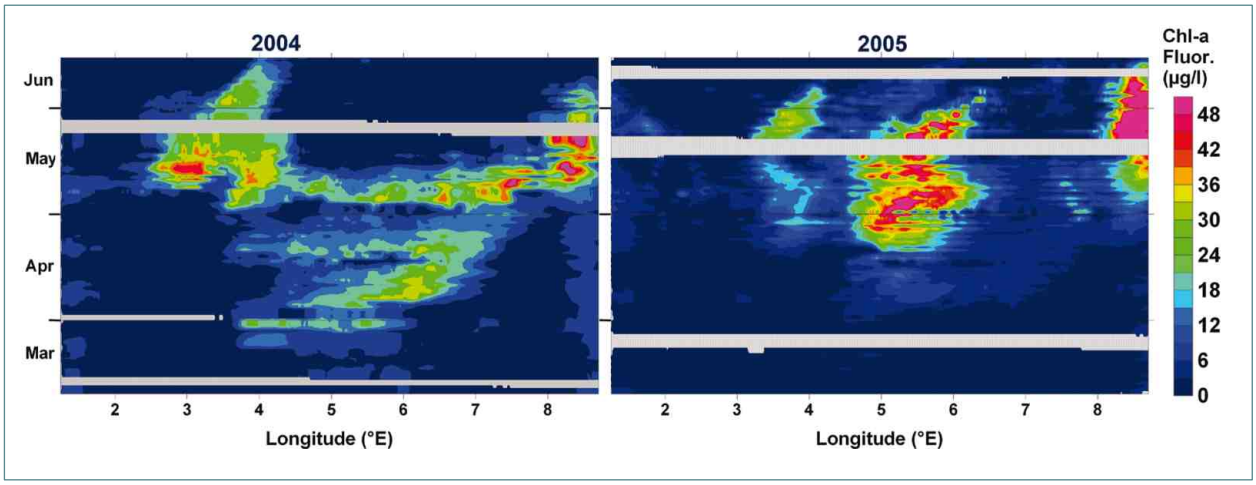

▲ Figure 8
Chlorophyll concentrations (measured by fluorescence) recorded between March and June in 2004 (left) and 2005 (right) on the FerryBox route Cuxhaven - Harwich.

▼ Figure 9
Comparison of processed satellite data (MERIS spectrometer on ENVISAT) with FerryBox data.
Top: Satelite image with calculated chlorophyll concentrations.
Bottom: Data extracted from the satellite data (orange) and measured FerryBox data (green).

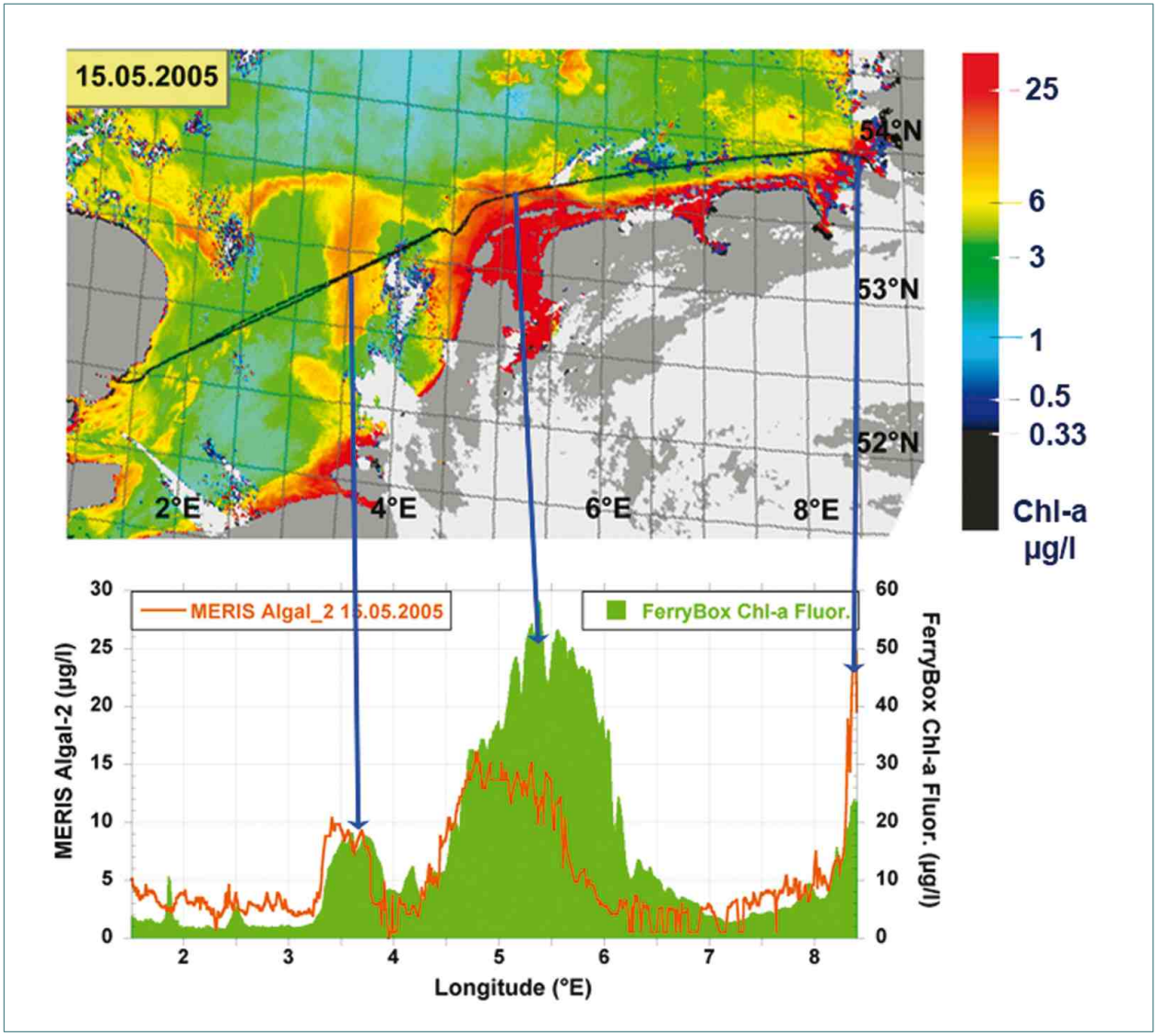

Using model simulations to support monitoring

Methods & Techniques

Introduction

Numerical models offer reliable information about the marine circulation, the atmospheric state (radiation, temperature and wind, for instance) and other sea parameters like wave action, even for places and variables for which measurements do not exist. Such information is very useful for supporting monitoring activities. Benefits of combining observations and simulations of the physical environment arise in two respects. Firstly, high resolution model simulations allow for the interpretation of continuously observed data in a more regional context. Secondly, long term model simulations of the physical environment are needed for a proper interpretation of long term observations in the presence of natural variability. We will give examples for these two types of application.

Data from coastDat

For the applications presented below we used data from coastDat that originated from the EU funded project HIPOCAS (Hindcast of Dynamic Processes of the Ocean and the Coastal Areas). The data consistently combine atmospheric simulations with simulations of currents, sea levels and waves. Fig. 1 outlines how these data are related to each other. Current and sea level fields were produced by running the finite element model TELEMAC (Hervouet and van Haren, 1996). For a more detailed discussion of the model setup the reader is referred to Plüß (2004).

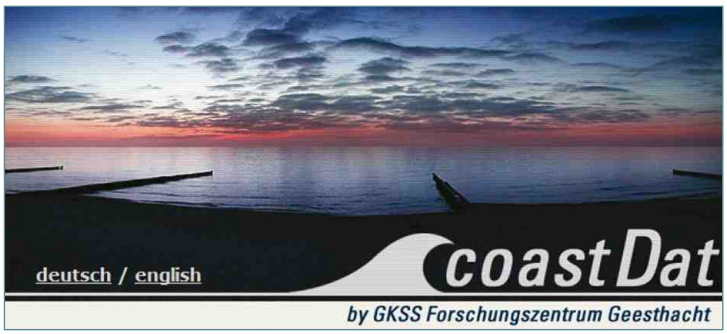

The data base coastDat

The idea of the portal coastDat (www.coastdat.de) is to provide a unique platform which hosts, describes and promotes consistently high resolution longterm data sets (Feser et al., 2001) and their key applications (Weisse and Plüß, 2006). Coastal scenarios provided for the near-future complement the numerical analyses of past conditions. Long and high-resolution reconstructions of recent offshore and coastal conditions have been produced using state-of-the-art model systems. It has been taken care that reliability of model results is as homogeneous as possible.

In the applications summarised below the data from coastDat were employed in different ways. The first approach is to aggregate detailed information on the North Sea flow regime in terms of characteristic flow patterns. The second is to link a tool for Lagrangian transport simulations to the fields from coastDat.

Flow patterns in the German Bight

To be in line with the concept of mass balance, we chose water flow (product of velocity and total water depth) as the relevant physical variable to be related to biological observations. Fourier analysis was applied to remove all variations in the model data that are related to astronomically prescribed frequencies with time scales up to one year. The filtered residual data contain neither tidal nor long term seasonal cycles.

Hourly fields of residual water flow were then subjected to Empirical Orthogonal Function (EOF) analysis (von Storch and Zwiers, 1999), a standard statistical technique also known as Principal Component Analysis (PCA). Two leading spatial patterns of water transport variability in the inner German Bight were identified (Fig. 2). They explain 70 % and 17 %, respectively, of total variance. Changing amplitudes of these patterns are represented by the time series of principal components (PCs, Fig. 3).

Lagrangian trajectories (PELETS-2d)

PELETS-2d (Programme for the Evaluation of Lagrangian Ensemble Transport Simulations) is a toolbox for Lagrangian drift modelling based on fields from coastDat. Particle trajectories calculated from the marine circulation fields may or may not take into account wind drift as an additional forcing factor. The latter is needed when dealing with oil slicks or drifting material, for instance. PELETS-2d has been designed in a way that it can easily be linked to the outputs of different hydrodynamic models, including models that are based on irregular grids.

The important feature of PELETS-2d is that it allows for an efficient production of ensemble simulations. A toolbox for the evaluation of such simulations is provided. Source and target regions may be defined in order to balance transport rates and travel times, for instance, between different subregions of an area of interest. Results of ensemble simulations may be studied in terms of composites for various original or derived variables. Patterns of variations can easily be analysed by the application of EOF analysis.

Authors

Ulrich Callies, Karina Stockmann and Ralf Weisse (GKSS)

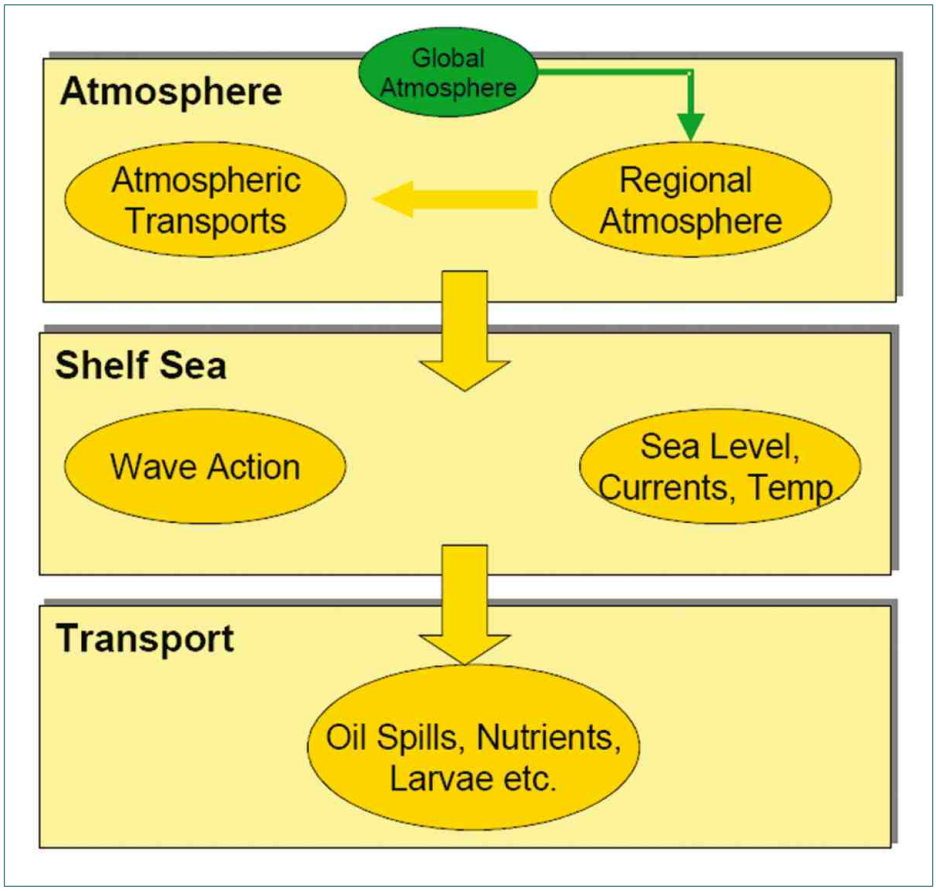

▲ Figure 1

Outline of the generation of consistent data sets stored in coastDat: Numerical models for the atmosphere, currents or waves are coupled to or nested within each other to provide necessary boundary conditions. Lagrangian trajectory calculations (transports) including estimates of travel times, for instance, may be based on shelf sea currents either with or without extra wind drift effects. Model results are stored for several decades with an hourly resolution. Time series used in our case studies start in 1958.

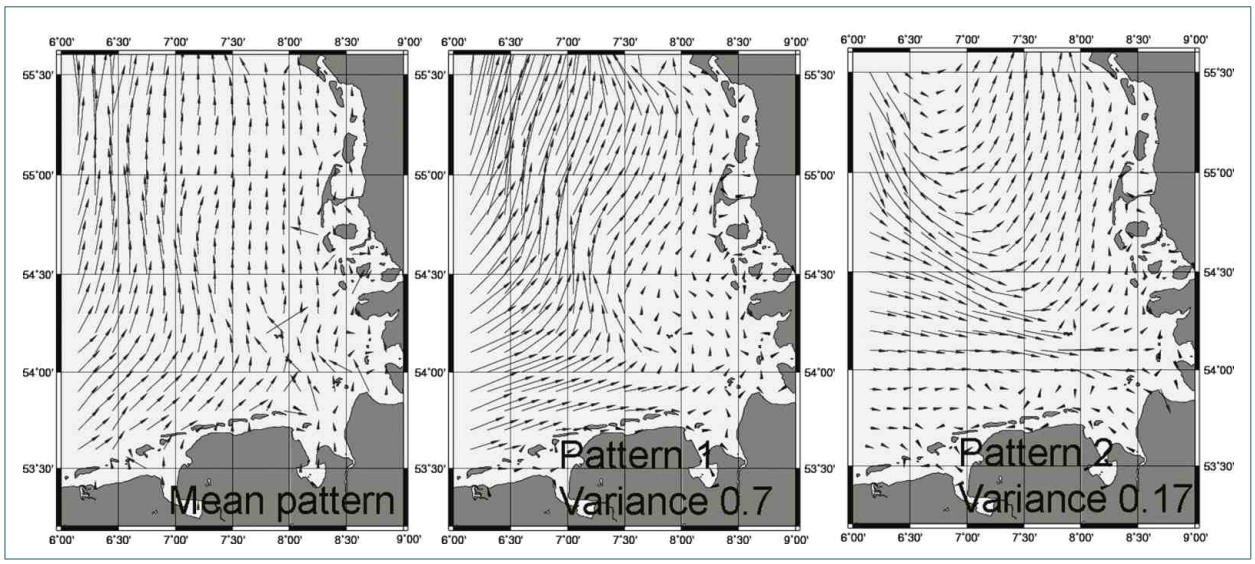

▲ Figure 2

Mean distribution and two patterns of variation of residual water flows as obtained from EOF analysis. The two anomaly patterns explain 70 % and 17 %, respectively, of total variance.

Using model simulations to support monitoring

Implementation & Results

Introduction

The examples discussed below summarise the use of model simulations in the context of different monitoring programmes. Only one example, the interpretation of FerryBox observations, does not explicitly emphasise the long term aspect of monitoring. Instead it takes advantage of the fact that model simulations stored in coastDat provide detailed reconstructions of environmental conditions rather than just statistics of natural variability. The same kind of detailed information is exploited in the project on survey data of oil contaminated beached birds. In the latter case, however, the analysis is performed on another level of temporal aggregation being set by the schedule of the fortnightly observations. In the analysis of freshwater signals observed at Helgoland the relevant time scale is somewhat in between.

Fresh water signals at Helgoland

In 1962 a long-term pelagic monitoring programme, including plankton species composition, was startet at the island of Helgoland (Helgoland Roads, 54°11.3'N, 7°54.0'E) in the North Sea by the Biologische Anstalt Helgoland on a workdaily basis (Franke et al., 2004). An important aspect for the interpretation of the long term data is the distinction between substantial changes within the biological network and changes that reflect variations or trends of the hydrodynamic regime. The coastDat data starting at 1958 covers the whole period of the Helgoland Roads observations and thus allows to demonstrate the added value which can be gained from combining long term biological observations with model based hindcasts of physical environmental conditions. Hydrodynamic changes on various time scales must be taken into account for a meaningful interpretation of biological time series.

Fig. 3 demonstrates the general idea by a simple example dealing with the interpretation of changes in the frequency of freshwater signals that have been observed at Helgoland Roads during the last decades. According to Fig. 3 these changes are consistent with a simulated changing variability of the dominant flow patterns in the German Bight.

Oil contaminated beached birds

Chronic oil pollution in the German Bight resulting from illegal oil dumping by ships is a severe problem that harms the marine environment. It is difficult to quantify, although model based estimates are possible (Fig. 4). The number of oil-contaminated beached birds is often used as an indicator for trends in the level of chronic oil pollution. It turns out, however, that data from such surveys may easily be misinterpreted if the variability of wind conditions is not properly taken into account. Fig. 5 shows that within a period of 13 years, for which reliable observations exist, changing atmospheric winter conditions might lead us to believe in a decreasing trend of oil pollution. The example clearly shows that a careful analysis of environmental conditions is indispensable for a sound and reliable interpretation of the results of the beached birds monitoring programme.

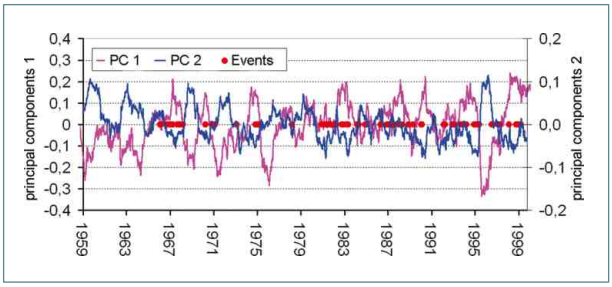

▲ **Figure 3**

Annually averaged time series of amplitudes (principal components, PCs) of the two anomaly patterns shown in Fig. 2. Red dots indicate observations of fresh water signals (low salinity in combination with high nutrient concentrations). The figure suggests that between about 1978 and 1995 the flow patterns in the German Bight behave differently from the rest of the period shown. It should also be noted that a precondition for freshwater inflow events is that the blue amplitude has a negative value. According to the data shown a changing frequency of freshwater inflow events being observed at Helgoland can be explained by changes in the prevailing flow patterns.

FerryBox and station Gabbard

Modelling of marine circulation offers several options for taking maximum advantage of observations that are made on moving platforms. Hydrodynamic drift modelling can be used to establish a link with observations from any other station. It can also be used for the construction of synoptic spatial distributions from non-synoptic observations along a given transect.

The example given here deals with the comparison of FerryBox salinity observations and corresponding observations at Gabbard station. Even though the ferry route passes close to Gabbard station (Fig. 6), a direct comparison of the respective observations is not successful due to small scale variability in the area of interest. According to Fig. 7, however, using the drift model as a link, the comparison can be much improved. A more detailed analysis of the method's performance reveals problems in those cases when FerryBox observations are taken close to the English coast. The reason for this failure may be either small scale patchiness of salinity or insufficient model resolution inshore.

Authors

Ulrich Callies, Alena Chrastansky, Markus Kreus, Karina Stockmann, Wilhelm Petersen (GKSS) and Karen Wiltshire (AWI)

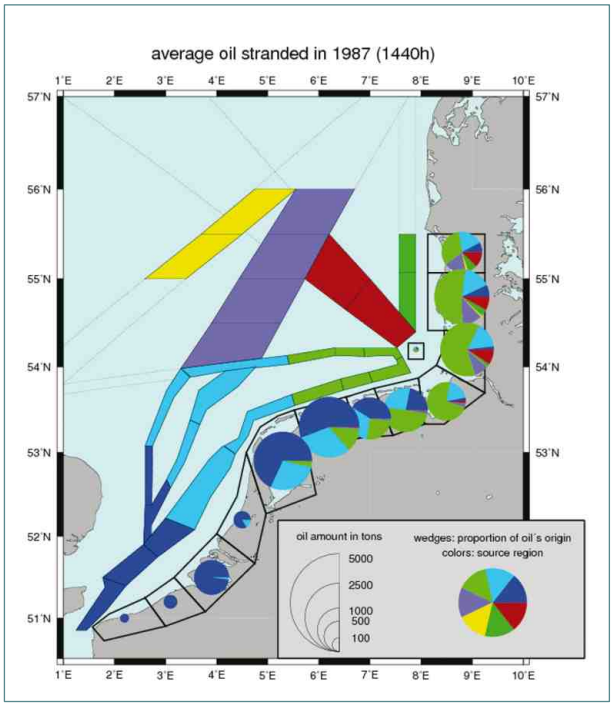

▲ **Figure 4**
Simulated oil slicks that originate from different (colour coded) sectors of the major shipping routes and hit the Dutch or German coast. For different target regions circle sizes indicate the total amount of stranded oil. Colour coded wedges indicate relative contributions from different source regions.

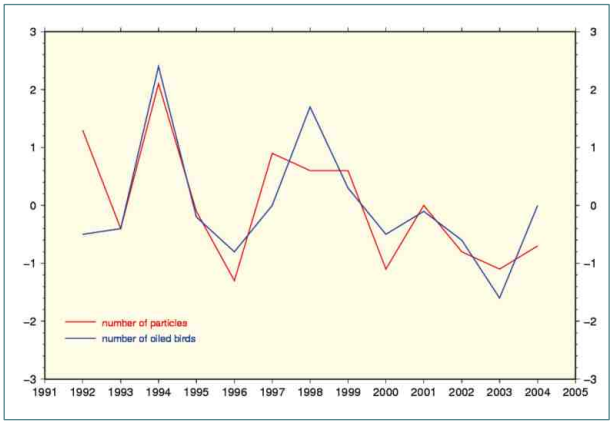

▲ **Figure 5**
Annual numbers of oil-contaminated sea bird corpses collected 1992-2004 along the German coast (blue line); numbers of drifting tracer particles that hit the German coast according to model simulations based on reconstructed past weather conditions (red line). All data are presented in standardised form. The changing strength of tracer particle advection reflects a major influence of prevailing weather conditions. From the similarity of the two curves one may conclude that impacts of changing weather conditions may easily be mistaken for a decreasing level of oil pollution.

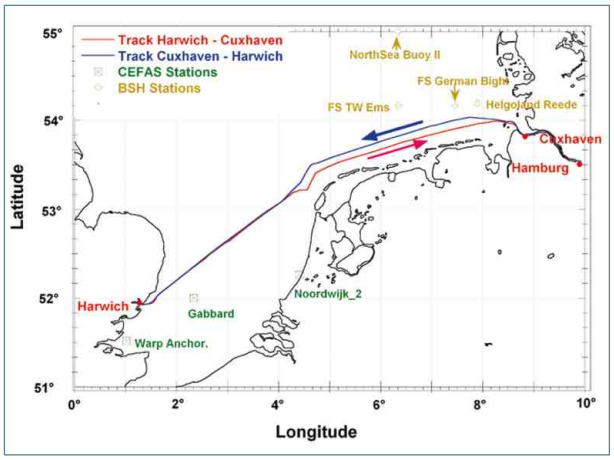

▲ **Figure 6**
Track of the ferry on which in 2002-2005 a FerryBox system was mounted. Drift simulations were used to establish a link between observations on the ferry and at station Gabbard, respectively (Fig 7).

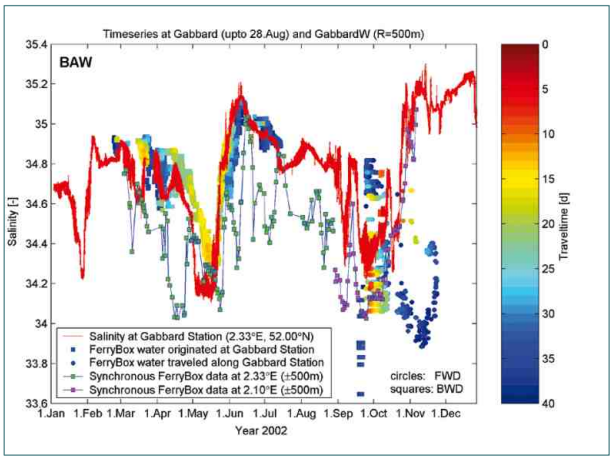

▲ **Figure 7**
Salinity observed at station Gabbard (red line). Corresponding FerryBox observations that were taken when the ferry passed by to the north of Gabbard (Fig. 6) are represented by small squares connected by a thin line. A numerical drift model was used to identify water parcels that were seen by both of the two systems and to estimate the water parcels' travel times between the two measurements. Coloured dots represent observations of the FerryBox after a proper time shift obtained from the drift model was applied. Travel times are colour coded according to the scale on the right. They may range up to about one month, still giving good results in spring. Unsatisfactory results in autumn occur in situations where observations by the ferry were taken close to the English coast.

Dynamics and structure of the water and matter exchange between the Wadden Sea and the German Bight

Methods & Techniques

Introduction

The coupling between the German Bight and the Wadden Sea is of high importance for the cycles of matter in this area and significantly affects the state and ecosystem key processes within the Wadden Sea: Sediments in the Wadden Sea are imported from the adjacent areas of the German Bight and overturned and decomposed there, and dissolved nutrients are exported from the Wadden Sea, depending on the nature and the time scale of internal and exchange processes.

The German Bight and the Wadden Sea are highly dynamic natural environments characterised by strongly varying physical impact from tidal currents and waves and significant changes in water temperature, salinity, and suspended matter concentration, to name a few parameters. This temporal and spatial variability requires long-term observations to understand the exact nature of exchange processes and to determine the direction of fluxes and the relevant time scales on which they occur. It is, for example, still unknown whether the Wadden Sea seafloor will grow, by accumulating suspended matter and sand, with sea level rise, or not.

The ideal observational tool would be a continuous monitoring of the exchanged water bodies including the dissolved and suspended matter and the bedload transport of the sand over a full cross-section of a tidal inlet connecting the Wadden Sea with the open North Sea. This was partly achieved in the Dutch Wadden Sea, implementing an acoustic doppler current profiler (ADCP) and a conductivity temperature depth sensor (CTD) onboard the ferry connecting Den Helder and Texel. For the German Wadden Sea, a comparable infrastructure is not yet available. As an alternative, GKSS is using fixed piles as permanent multiparameter measuring platforms, complemented by ship cruises checking the representativity of the pile positions.

Methodology

The method comprises three elements: continuous automated measurements at pile stations, ship surveys to assess the representativity of the pile location and repeated sampling at the piles and during ship surveys.

Since 1996, GKSS has operated pile stations at several locations in the German Wadden Sea (Fig. 1 and 2). For practical operation, the position of the piles has to be selected according to the following criteria: limited exposure to waves, allow regular maintenance work, water depth at low water of about 3 m, an optimum between pile stability and water coverage of the sensors at extreme low water. The piles are assembled out of several iron tubes with an outer diameter of 40 cm. A cage is mounted on top which carries solar panels for energy supply, data logger, telemetry units and standard meteorological sensors (Table 1). The overall length of the system amounts to some 15 metres, depending on the tidal range of the particular area. To assure stable fixing the tubes are flushed into the ground by seven metres. An underwater sensor unit (Table 1) is mounted on an elevator bar to raise it regularly for cleaning and to lower it into the operational position. Water level and 1D-wave spectra are measured by means of a floater attached to a readout-rod. All parameters are transmitted by mobile phone to the research centre as 10 min averages (Fig. 4), some parameters (e.g. water level to derive wave spectra) in parallel as five-minute long 2-Hz-time series (parameters in italics in Table 1). For long-term storage they are saved in a data base and published automatically within half an hour on the website of the institute. The piles are operated fully automatically with remote control. Personnel are required on the piles for maintenance work and to collect water samples for calibration. In order to protect the measurement equipment against ice forcing in winter, the observation period usually starts in early spring and ends in late autumn.

"Calibration/representativity campaigns" with a cruising research vessel (Fig. 3) are occasionally conducted close to the time series stations in order to convert the point-measurements of water properties to volume fluxes in the tidal channel. These campaigns with the GKSS-owned research vessels “Ludwig Prandtl” and “Storch” are carried out every year in order to extrapolate the point observations taken at the piles to the full channel cross-section at the pile location or even to a larger part of the tidal basin.

Continuous time series of suspended particulate matter concentration (SPMC) and chlorophyll fluorescence are derived by combination of indirect optical and acoustical detection methods with repeated sampling. SPMC of water samples is determined by gravimetric methods. To use chlorophyll fluorescence as a proxy to follow the development of phytoplankton biomass over time, concomitant measurements of PAR (photosynthetic active radiation) irradiance (400-700 nm) allow correcting for photochemical quenching. Fluorescence records are then converted into chlorophyll concentrations on the basis of regular water sample analysis for phytoplankton pigments by High-Performance Liquid Chromatography (HPLC).

Meteorological parameters	Oceanographic parameters
• wind speed	• *water level*
• wind direction	• 1D wave spectra
• air temperature	• *water pressure*
• air pressure	• *current speed*
• precipitation	• *current direction*
• global radiation	• water temperature
	• salinity
	• *turbidity*
	• chl. fluorescence
	• underwater PAR

▲ Table 1
Meteorological and oceanographic parameters measured at the pile stations.

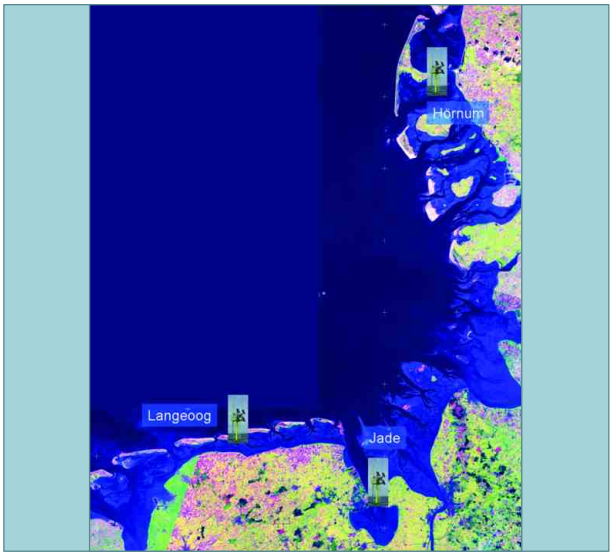

▲ Figure 1
Location of the pile stations in the German Wadden Sea.

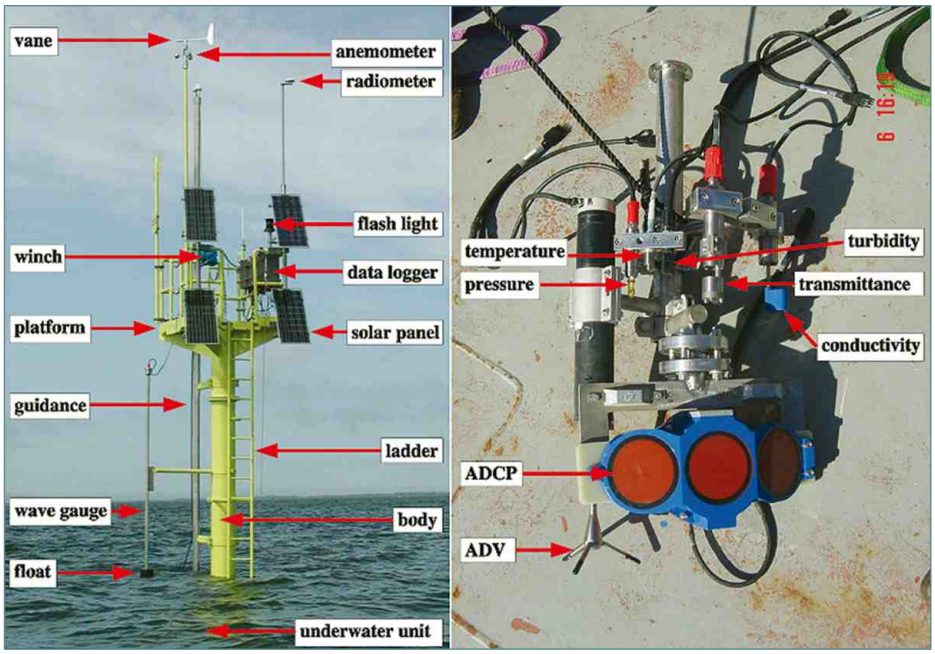

◄ Figure 2
Pile station as it is operated at three locations in the German Wadden Sea. On the left, the "above-water-unit" is shown, on the right the underwater unit. The meteorological and oceanographic instruments are indicated.

◄ Figure 3
Research vessel "Ludwig Prandtl", equipped among many other instruments with a downward-looking ADCP for the measurement of water flow and a multibeam echosounder for the observation of the seafloor.

Dynamics and structure of the water and matter exchange between the Wadden Sea and the German Bight

Implementation & Results

Problems

A problem common to all automated instruments in seawater is biofouling. Organisms of various sizes settle on the instruments and modify the measuring values. Regular maintenance is therefore of utmost importance to clean the instruments, in particular the optical surfaces (window for light transmission) and the cables where barnacles eat away the cable protection. The maintenance frequency depends on the seasons: in early spring and late autumn, a cleaning once in two weeks is sufficient, in late spring and summer this interval has to be reduced to 4-5 days.

Floc- and grain-size of the suspended matter changes with tidal phase and season, as does the relationship between sample SPMC and the optical and acoustical detection signals. This creates additional uncertainty in the SPMC-time-series, as sampling can occur only at widely scattered times.

In wintertime, when suspended sediment dynamics is expected to be highest, the stations must be removed because on the one hand ice may damage the pole, and on the other hand the energy supply of the solar panels may not be sufficient to operate the instruments.

Applications

1. Calculation of water exchange in the Langeoog-Baltrum bight using gauge level and hypsographic data

From the water level measured at the pole station we calculate for every time step the total water content of the backbarrier area (for this purpose, the system's topography must be known). Taking two subsequent volumes, a water flux in the respective time span can be calculated. In order to correlate this point measurement to a flux representative for the entire area, ship-based ADCP measurements of the water fluxes in the tidal inlet must be performed. This has been done, e.g., in the bight between the East Frisian Islands Langeoog and Baltrum, on four occasions in May and August 2000.

The flux values are compared to the values obtained from the ADCP measurements during the ship cruises (Fig. 5). The correlation is satisfactory; thus water fluxes through the tidal inlet can be calculated from the pole gauge data for the entire operation time of the station (Fig. 6).

These reconstructed water fluxes can be compared to the fluxes derived from the CoastDat database which contains results from a current and sea state model (Fig. 6) and thus serve as valuable boundary information in the highly dynamic Wadden Sea zone. The combination of these pieces of information will eventually lead to a better understanding of the suspended matter transport, settling and resuspension, processes that are very sensitive to water flow velocity.

2. Estimation of residence times from salinity signal decay

Exchange times of the Wadden Sea water bodies are an important factor determining water quality. In enclosed and semi-enclosed water bodies like the Baltic Sea, oxygen depletion is much more common than in well-mixed waters like the North Sea. Thus, a large exchange time decouples the Wadden Sea water from the German Bight whereas a smaller exchange time reduces the danger of oxygen depletion phenomena. The exchange times are estimated from hydrodynamic models but not measured.

A large part of the water in the tidal prism leaving the Wadden Sea comes back during the next tide. This means that a small part (5-20 %) of the water body is replaced by "fresh" North Sea water. As a consequence, any sudden influence on the water quality inside the Wadden Sea will decay with a characteristic decay time. We consider precipitation as such a signal: rainfall has a much larger influence on Wadden Sea salinity than that of the North Sea, simply due to the low average water depth. For an average water depth of 2 m, a precipitation event of 20 mm changes salinity by 1%, whereas the same event would influence the Southern North Sea water (average depth 20 m) only by 0.1 %.

If a stronger precipitation event in the Wadden Sea is followed by some days without rain, the signal (lower salinity) created by the freshwater input should decay with the characteristic "Wadden Sea time scale" that can be derived from the measurements (Fig. 7). This measured exchange time is altered by wind (high wind speed enhances exchange processes) and the spring/neap tidal cycle (at spring tide, flow velocities are twice as fast as during neap tide).

It is planned to compare the time scales derived from this method to numerical tracer experiments and thus to extend the determination of characteristic residence time scales at the location of the piles to the entire Wadden Sea.

Authors

Götz Flöser, Clivia Häse, Jan-Moritz Müller, Reiner Onken and Rolf Riethmüller (GKSS)

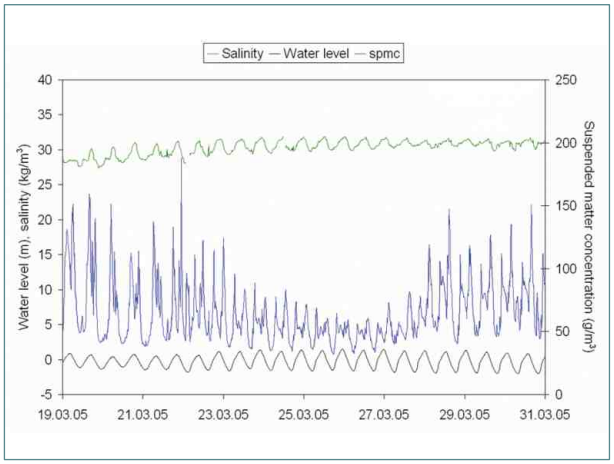

▲ Figure 4

Typical time series for salinity, water level and suspended matter concentration, measured at the pile station close to the East Frisian Island Langeoog. Salinity oscillates with the water level because the Wadden Sea water is usually fresher than the North Sea water. The reason is not the (small) freshwater inflow from the mainland but rainwater that has a larger influence here than in the deeper North Sea. The suspended matter concentration depends on flow velocity: during the periods with high current speed (half tide), the suspended matter concentration is also elevated, and at slack water the concentration is comparatively low.

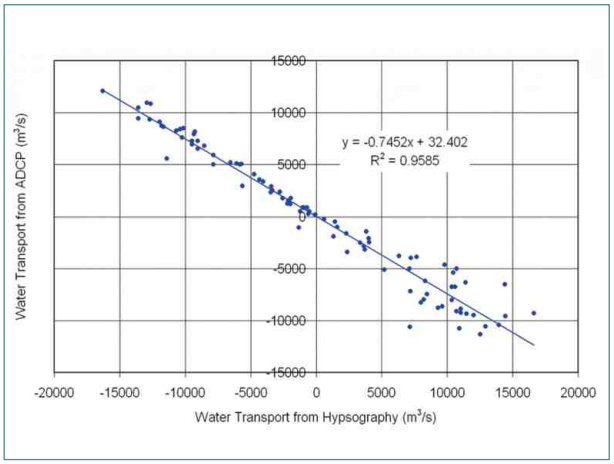

▲ Figure 5

Correlation of the water flow measured from shipboard using ADCP to the flow determined by using the gauge level and calculating the difference of corresponding water volumes. The dots contain all four experiments in the year 2000; thus the connection of the two data types may be considered typical – at least for the year 2000 and for the pile station's position.

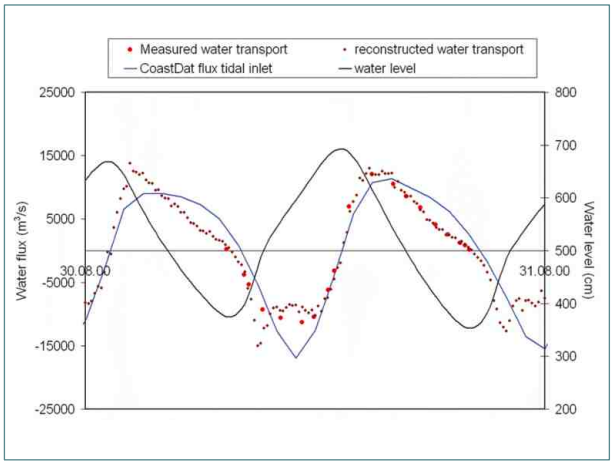

▲ Figure 6

Time series from August 2000 with ADCP measurements of water flow (red dots), water level (black curve), reconstructed water flow derived from water level and topography (brown dots), and the inflow through the tidal inlet as calculated from the CoastDat database. Considering the poor resolution of the model from which the CoastDat values were derived and the temporal resolution of one hour, the consistence between the reconstructed flow and the CoastDat curve is acceptable.

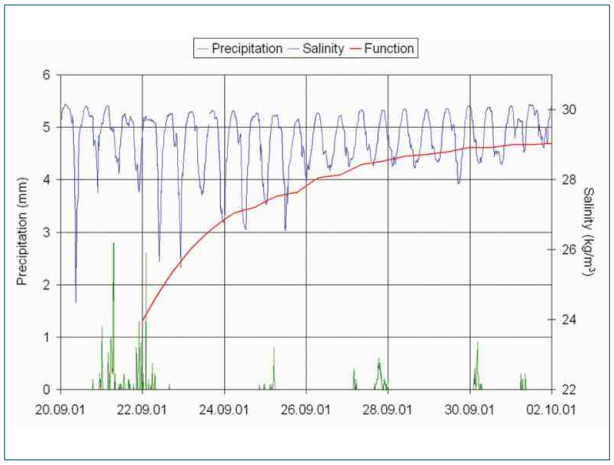

▲ Figure 7

Salinity, precipitation (10 min values) and a fitted curve for the decay of the salinity signal. In the 2001 case, the decay time is 2.5 days, for the 2003 values it is 1.5 days. Changing wind conditions and the spring and neap cycle modify the decay time.

The heat budget of tidal flats

Methods & Results

Introduction

A major objective of the research programme is to develop methods to monitor and quantify exchange processes between the Wadden Sea and the North Sea. The generic approach is to acquire high-frequency time series of basic physical quantities at choke points, i.e. in tidal inlets or tidal channels, to evaluate the present horizontal fluxes of heat, freshwater or suspended particulate matter (SPM), and then to integrate the fluxes between two consecutive low tides. This yields the tidal budget of the corresponding quantity for the upstream area. An intrinsic problem of this method is to interprete the measurements at the choke points in terms of volume fluxes being representative for the entire inlet or channel, respectively. Here, the whole method is exemplified for heat fluxes (Fig. 2).

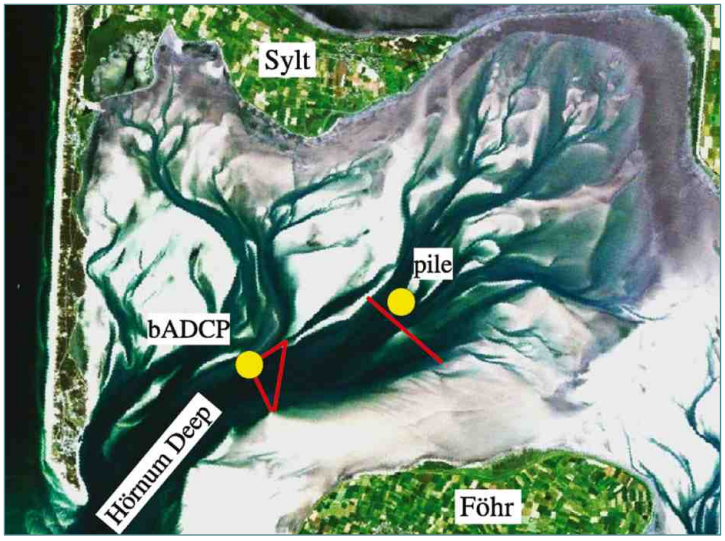

▲ **Figure 1**
In the Hörnum tidal basin, time series are available from a bottom mounted acoustic current profiler (bADCP) and a measuring pile. Ship's tracks of the volume flux calibrations are indicated by red lines.

Methods and Techniques

Time series are available from measuring piles located in the East Frisian Wadden Sea and in the Hörnum tidal basin (see previous chapter). The observations of the latter pile are complemented by time series from a bottom-mounted acoustic doppler current profiler (bADCP) located about 4 km southwest of the pile in the same tidal channel (Fig. 1); therefore, the above methods have been applied to the Hörnum basin.

Occasionally, 'representativity campaigns' with a research vessel were conducted close to the time series stations in order to convert the point-measurements of water velocities to volume fluxes in the tidal channel: the vessel is equipped with a downward looking Acoustic Doppler Current Profiler (ADCP), and by back and forth crossing of the channel the volume flux of water is measured directly. The volume flux is then related to the simultaneous velocity records at the bADCP or the pile, respectively (Fig. 3), and the relationship is applied to the entire point velocity time series.

The present heat flux in the channel is proportional to the product of the volume flux and the temperature. Integration of the flux between two successive low tides yields the tidal heat budget. As can be seen from Fig. 4, the tidal budget exhibits oscillations with a doubletidal period, which is related to the diurnal cycle of heating and cooling of the tidal flats. The diurnal cycle, together with the fortnightly inequality, are filtered out by averaging the budget with a running mean over one month.

The heat budget in the open ocean is solely controlled by advection and the net heat flux between the ocean and the atmosphere. In comparison, the heat budget in tidal flats is additionally impacted by the bottom heat flux between the sea bed and the overlying water column. An analytical model was developed, which in conjunction with a numerical transport model for the determination of the respective catchment area yields estimates of the bottom heat flux in dependency of the tidal heat budgets at the two time series stations. Both for the bADCP and the pile, the heat budget of the respective catchment area was evaluated for the year 2004 between the middle of March and late October, and the bottom heat flux was determined for the same period.

Results and Outlook

Fig. 5 shows that the budget at the bADCP is negative from April through the middle of August, hence relative to this choke point the upstream tidal flat area is exporting heat. From August the budget becomes positive which means import of heat. At the pile, the situation is reversed: the budget is positive from March through late August (import), and switches to an export situation in autumn. This is because during night time a fraction of the incoming water is releasing heat to the colder tidal flats. The relative contribution of that fraction being in contact with the flats is higher at the pile than at the bADCP. This is illustrated in Fig. 6. Corresponding evaluations of the mean heat budget for the years 2005 and 2006 show that the budgets exhibit interannual variations but the gross behaviour is similar among those years.

Presently, work is in progress to validate the results achieved so far by direct measurements of the sediment temperature of the tidal flats. Further on, the described method is being applied to determine the budgets of freshwater and SPM.

Authors

Reiner Onken, Ulrich Callies, Bernd Vaessen and Rolf Riethmüller (GKSS)

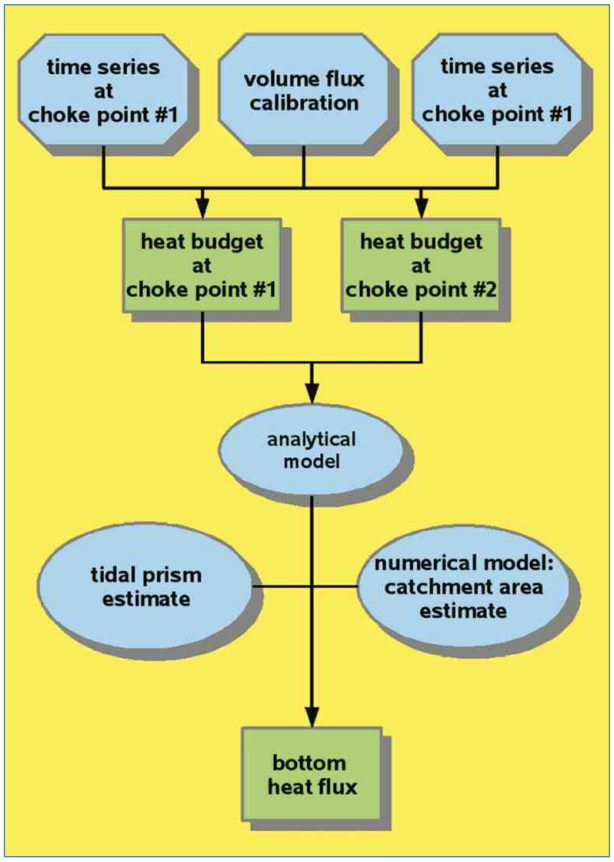

▲ **Figure 2**
The heat budget and the bottom heat flux are determined by melding observations with models.

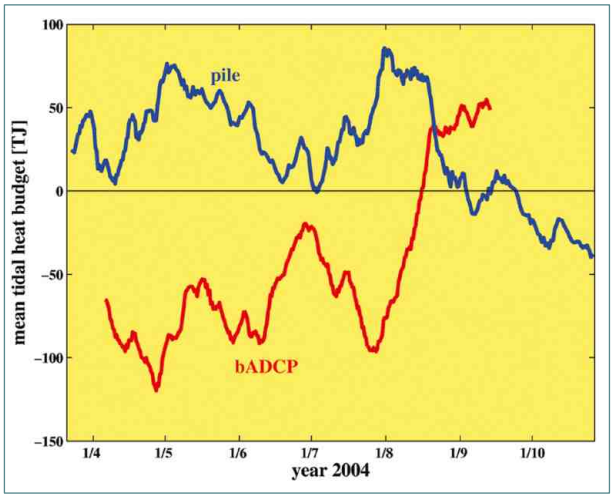

▲ **Figure 5**
The mean tidal heat budget for the catchment areas of the bADCP and the pile in the Hörnum tidal basin in 2004.

► **Figure 6**
The tidal heat budget of the catchment areas of the bADCP (top panel) and the pile (bottom) as a function of the daynumber and the time of high tide. Red indicates export, blue import of heat.

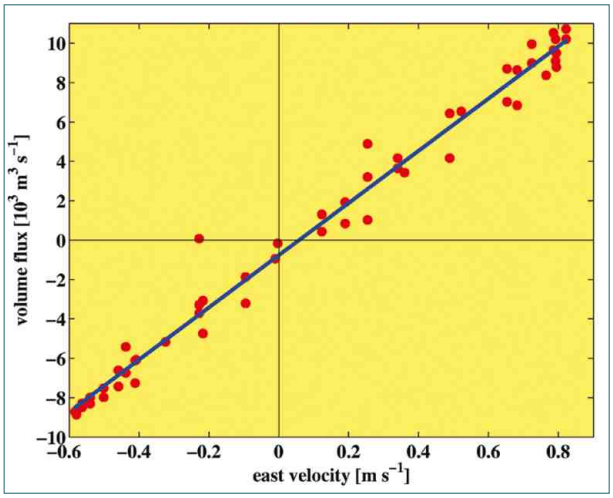

▲ **Figure 3**
Volume flux in the Hörnum Deep vs. the east component of water velocity recorded by a bADCP (red dots). The linear regression is indicated by the blue straight line.

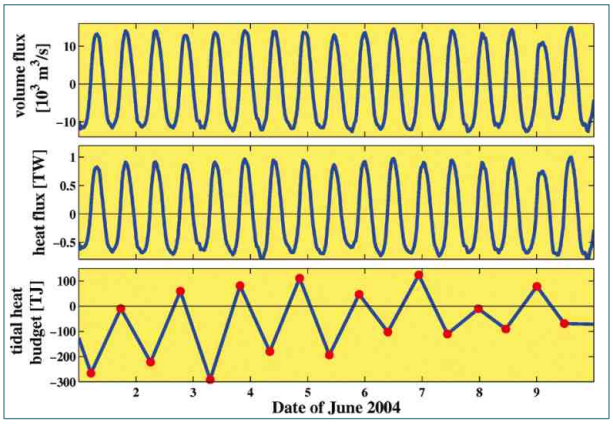

▲ **Figure 4**
Volume flux, heat flux, and tidal heat budget in the Hörnum Deep, evaluated at the bADCP time series station for early June 2004. The tidal heat budget was integrated between two successive low tides indicated by red dots.

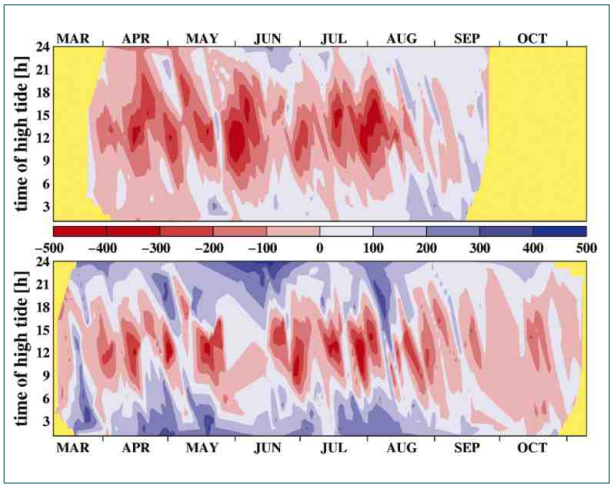

Small scale morphodynamics

Methods & Techniques

Introduction

Significant changes in bathymetry are the result of waves, tidal currents and storm events. In the area of the 'Lister Tief' the bathymetry is highly variable.

Here, we introduce a system called 'Radar Doppler Current Profiler' (RDCP) that, combined with Acoustic Doppler Current Profiler (ADCP) measurements and bathymetric data, can be used to assess areas with high potential of erosion or accumulation with a presentation of the results in a high resolution map.

Radar Doppler Current Profiler

The method to scan the surface current field horizontally has been developed in the Radar Hydrography group. It uses two coherent radar devices to produce high resolution current vector maps. In analogy to ADCP, this method is named Radar Doppler Current Profiler (RDCP). It consists of two radar systems, where the one antenna is permanently looking 45° ahead and the other 45° backward (Fig. 1).

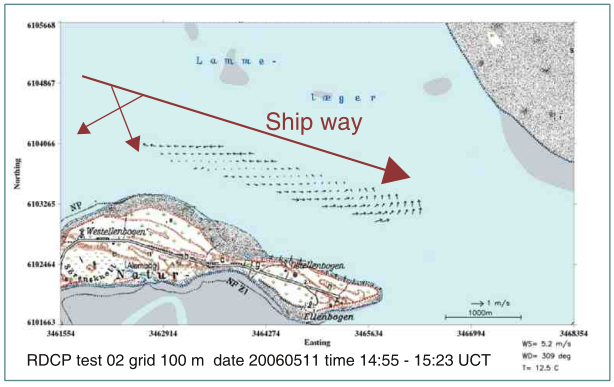

▲ Figure 1

Current vector field measured by RDCP. Grid resolution 100 m. Base map used from TOP50 Schleswig-Holstein and Hamburg.

While no long waves are acting, the radial Doppler speeds are the sum of the wind friction and the surface current. By the Doppler relation we calculate the radial velocities from the backscattered signal for each range bin (length ~7.5 m). Integrating the radar observations over one second, the radial speed results in an accuracy of 1.5 cm/s. The ship's movements are compensated with a precise differential GPS. The local impact of the actual wind friction is compensated by additional measurements from the stopped ship with the antenna looking in all wind directions with 10° steps. An automatic quality control rejects routinely faulty data. The post processing procedure is to compose the full surface current vector by merging the two components into a geo-coded grid with the grid distance up to 10 m. Fig. 1 shows an example of a geo-coded RDCP current map with a grid resolution of 100 m during ebb tide. An eddy with a diameter of about one nautical mile shows the outflow directed westward on the northern side of the gully and a counter current directed eastward on the south side. Comparison of the ADCP currents (Fig. 2), which were acquired during the same ship track, and the RDCP calculated vectors close by the ship demonstrates that this new scanning method fits. Fig. 3 a and b show the speed and direction of the surface current field within the tidal gully 'Lister Tief'. This is overlaid by a current modulation due to the change in the cross section over submerged sand dunes, which interact with the ebb current in a way that we observe acceleration over the crest of the dunes and slowing down where the cross section is widening. The ADCP profile in Fig. 2 confirms these features in a vertical cross section map. The mentioned areas with acceleration and deceleration over the sand dunes are visible horizontally as well as in the vertical (upper and lower slide) speed components.

Bottom shear stress

A model to estimate the bottom shear stress (BSS) was developed to assess the impact of the current field on the sand regime. As input this model needs the surface current, the bathymetry and the grain size of the sediment. Under the condition of a homogeneous water column, rough sea floor and no swell the impact of the tidal currents on the sea bottom is obtained. The homogeneous water column was verified by repeated CTD measurements in the area.

The base of the model is the Taylor Law which shows that we can calculate the current velocity at any depth of the water column if the velocity at another certain depth is known. By the knowledge of the surface current vector field the velocity within the water layer down to the bottom can be deduced. The RDCP provides the surface water speed in a broad stripe parallel to the ship course. The ADCP provides a vertical section to show the rotation of the current vector with increasing depth. The bathymetry data provides the local water depth and the terrain slope. The slope is important for the form drag component of the shear stress equation, which dominates the resulting stress. The rough sea floor condition is necessary for the calculation of the near bottom current. Over a smooth bed the change of the current velocity would be linear instead of logarithmic. Two options to display the bottom shear stress have been chosen: the absolute value of the resulting shear stress and the difference between this value and the critical bottom shear stress. The second option is helpful in localising areas where bed motion is initialised with high probability. Up to now we can show the initiation but no suggestion can be made about the transposition of the material. By this procedure, areas with potential erosion or deposition can be detected (further reading: Senet et al., 2001, Ziemer et al., 2006, Braun et al., 2008).

Authors

Marius Cysewski, Stephan Sedlacek and Friedwart Ziemer (GKSS)

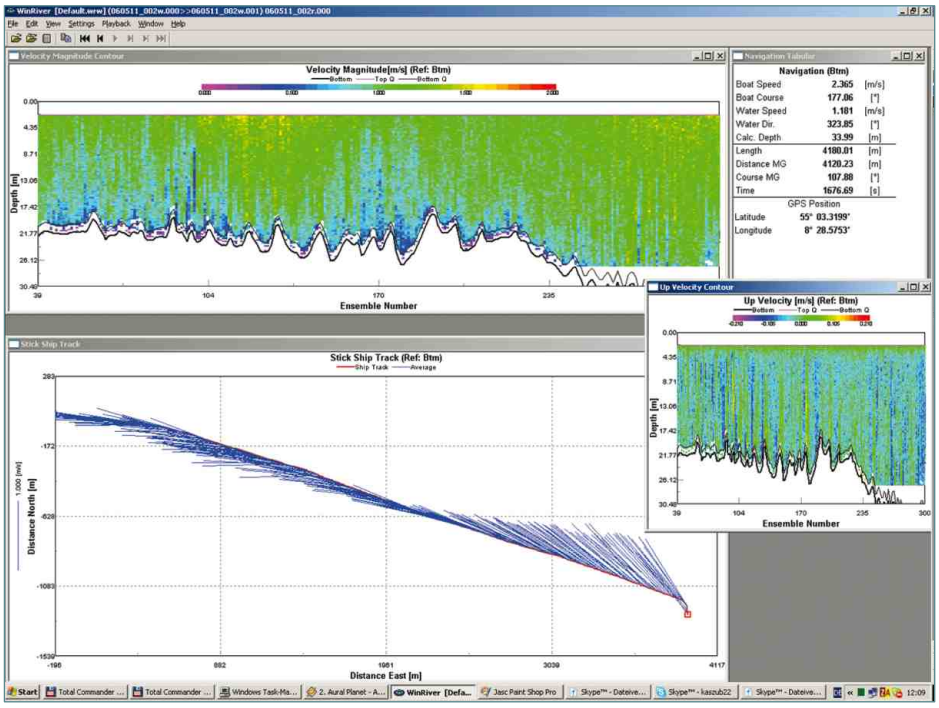

◄ Figure 2

ADCP data acquired during the same ship track as in Fig. 1. Left lower window shows the same current vectors as the RDCP measurement. The sand dunes on the sea bottom cause vertical disturbance. Zones of acceleration and deceleration result and are visible in the horizontal as well as in the vertical components.

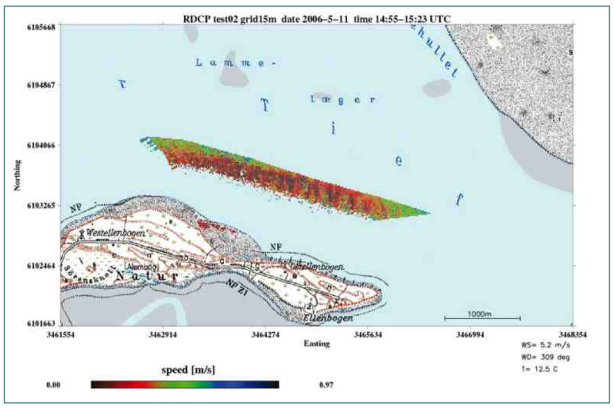

▲ Figure 3 a

Magnitude of RDCP currents gridded by 15m. Zones of acceleration (green) and deceleration (red brown) are visible. Base map used from TOP50 Schleswig-Holstein and Hamburg.

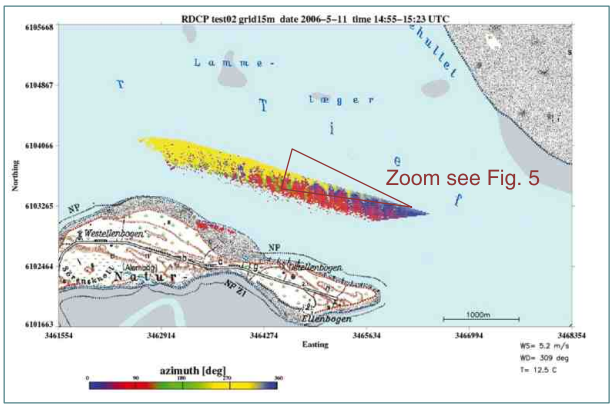

▲ Figure 3 b

Direction of RDCP currents gridded by 15 m. Outgoing water flow changes direction from north to west. Base map used from TOP50 Schleswig-Holstein and Hamburg.

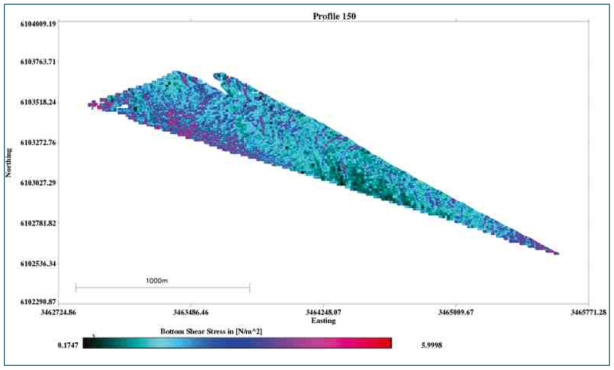

▲ Figure 4

Value of bottom shear stress in the Lister Tief during ebb tide on May 20th 2006.

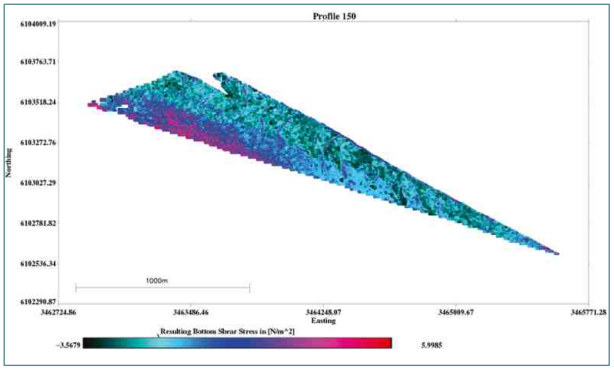

▲ Figure 5

Bottom shear stress deducted by the critical shear stress to make the areas of seafloor movement visible.

Suspended particulate matter distribution in the North Sea

Methods & Techniques

Introduction

Knowledge about the distribution of suspended particulate matter (SPM) is an important prerequisite for the description and prediction of the ecological conditions of the North Sea. The SPM concentration in the water column regulates the penetration depth of light and, therefore, it is an important parameter influencing the primary production of plankton.

Suspended particulate matter in the coastal zones

Plumes of turbid water are a quite frequent phenomenon in coastal waters, in particular in shallow soft bottom coasts and at the mouths of rivers and estuaries. Turbidity is caused by all kinds of small particles in the water, some of mineralic composition, such as clay minerals, and others of organic origin. They are summarised under the term suspended particulate matter (SPM).

The organic part, the detritus, is composed of decaying fragments of organisms or fecal material. The different particles form flakes of complex and undefined structure. These flakes are substrate for many microorganisms, which colonise the surface and holes in the flakes and which live from decomposing and mineralising the organic material. Due to the organic content, including their microbes, detritus is an important food for many benthic organisms. Furthermore, a number of different organic and inorganic trace substances, which are then transported by suspended matter, are adsorbed to the complex large surface of the flakes. Finally, SPM absorbs and backscatters light and thus reduces the available solar radiance for photosynthesis of phytoplankton and benthic algae and sea grass.

At GKSS a SPM module was developed which describes the exchange processes in the water column, in the sediment, and between the two compartments. These processes are controlled by currents, waves, and bioturbation and by the incorporation via filter and deposit feeders (Pleskachevsky et al., 2002, Gayer et al., 2006).

By implementing this module in (operational) hydrodynamical models (e.g. the transport model of the Federal Maritime and Hydrographic Agency (Bundesanstalt für Seeschifffahrt und Hydrographie, BSH), the circulation model of the Danish Meteorological Institute (DMI), and the circulation model HAMSOM of ZMAW, Hamburg), and additionally providing sea state data, the transport and distribution of SPM can be calculated.

The success of such a model depends on an adequate parameterisation of physical processes (partly derived in synergy with satellite data), as well as a careful preparation of maps of fine-grained sediment in the bottom and other sources of SPM (e.g. fluvial input and cliff erosion). Although much care was taken to accomplish this, simulations may result in (locally) incorrect SPM distributions, especially during long-term applications. Substantial progress could be made by assimilating surface SPM data derived from satellite.

Methodology & technique

The calculation of SPM concentrations is performed for three representative particle fractions differing in their sinking velocities as well as in their initial distribution in the water column and in the bottom sediment.

In addition to horizontal advection, the model takes into account vertical exchange processes due to currents and waves, the latter being an important new aspect. Data derived from satellite images during calm and stormy weather conditions enabled adequate model descriptions of these mixing processes during different conditions. Thresholds of the bottom shear stress velocity determine the beginning of the erosion (fine sediment is removed completely from the bottom sediment down to a certain erosion depth and brought into suspension instantaneously), re-suspension (erosion of the sedimentation layer), and sedimentation (particles sink to the sea floor and build a thin layer) processes (Fig. 1).

With the help of SPM surface concentrations, which have been derived from the Modular Optoelectronic Scanner (MOS) satellite, a constant could be adjusted which determines the erosion depth. Processes of uptake and bioturbation in the upper part of the bottom are simulated as well.

A distribution map initialises the content of fine sediment in the bottom (Fig. 2). SPM is prescribed at the English Channel boundary because a large amount of the SPM enters the southern North Sea via the Dover Strait.

Sea-state dependent cliff erosion is simulated at the English cliffs of Suffolk, Norfolk, and Holderness. SPM contributions of major rivers add to the budget of SPM in the modeled area. To improve the model performance, “surface” SPM concentrations derived from satellite images (e.g. MERIS) can be assimilated during model execution by using an optimum interpolation method. Due to the additionally provided information of the satellite’s “measurement depth”, for the first time it is possible to redistribute the measured SPM concentrations over a certain water depth.

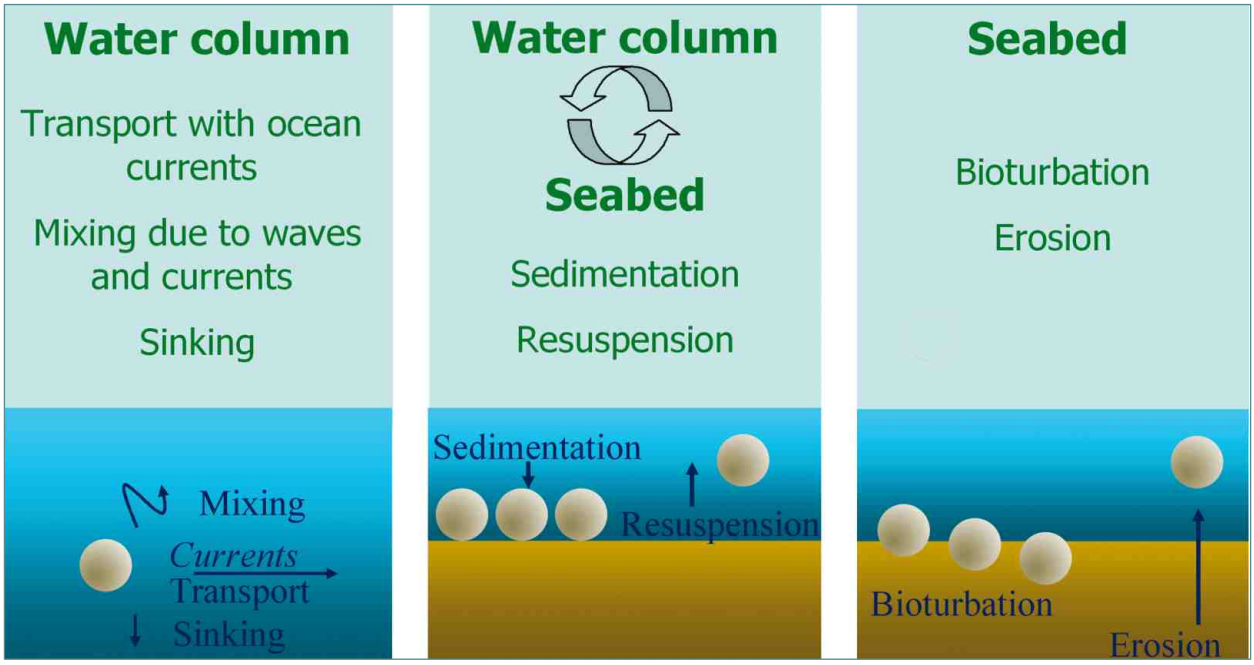

▲ Figure 1

Schematic description of processes: SPM particles, advected by ocean currents will gradually sink to the sea floor. This may be counteracted or amplified by shear currents and wave motion. On top of the sea bed, a thin sedimentation layer is formed, which may be destroyed gradually by consumption (e.g. by mussels) or bioturbation (e.g. by worms), or instantaneously by combined wave and current forces (shear stresses), bringing the SPM particles into suspension again. At even stronger stresses, fine sediment is eroded from the bottom sediment.

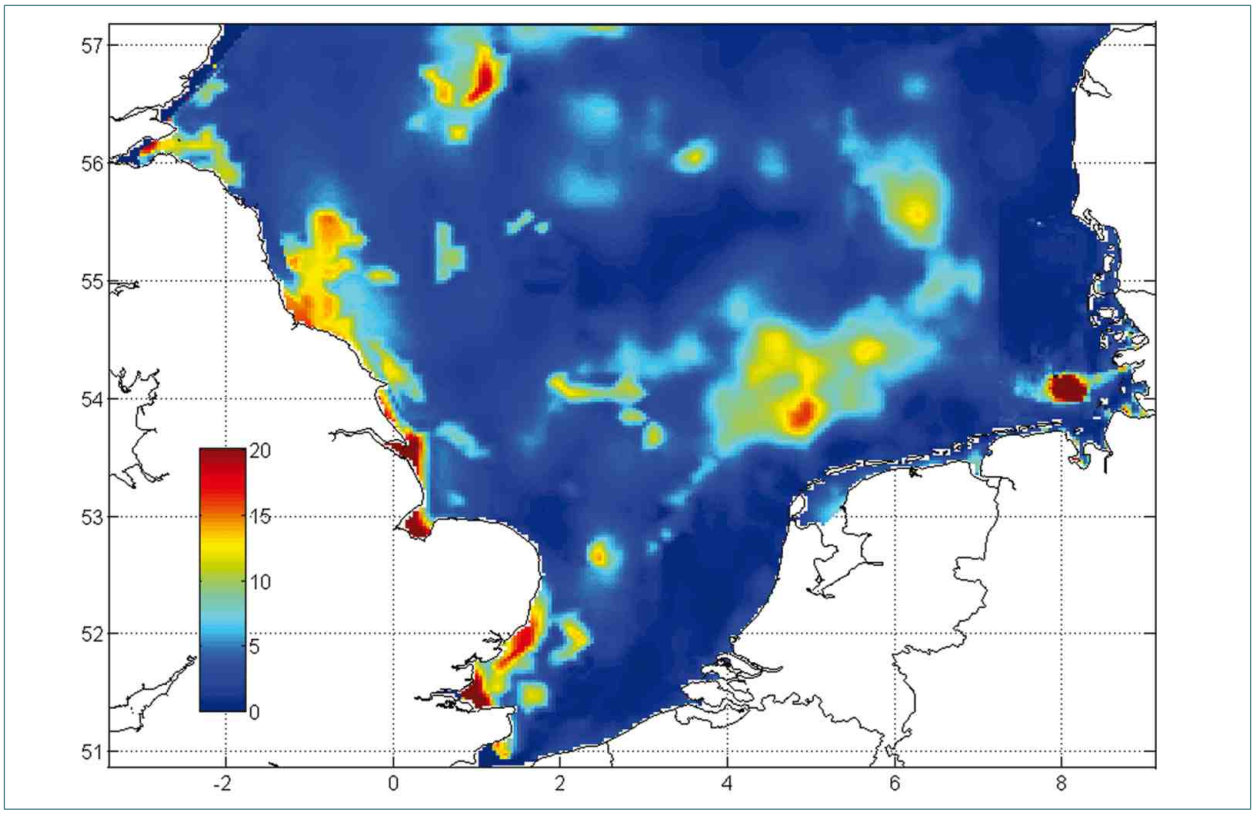

▲ Figure 2

Distribution map of percentage of fine sediment (grain sizes less than 20 µm) in the upper 20 cm of the bottom. This map was generated from measured grain-size data and partially improved by data derived from satellite images during storms. In this case, SPM is well mixed throughout the entire water column. The mass of the fine sediment can be concluded from the surface concentration.

Suspended particulate matter distribution in the North Sea

Implementation & Results

Data Assimilation

Especially for long-term calculations it may become necessary to update the model with the help of measurements, as is done for example during weather forecasts. Although the information retrieved from the optical sensors of satellites may not cover the whole North Sea due to cloud coverage, it is nevertheless regularly available. Actually, missing information can be filled by experience from what the numerical model would have predicted.

The problem of how to determine the thickness of the surface layer, over which the “measured” SPM has to be assimilated into the model, can be solved with the additional information of the penetration depth of the satellite signal (how deep did the sensor measure). The higher the SPM concentrations are (which is equivalent to higher turbidity), the lower is the signal penetration depth (Fig. 3).

A good example (only a small part of the area is obscured by clouds) is shown in Fig. 4. Clearly visible are coastal areas with high concentrations of about 30 mg/l. Accordingly, the signal depth is about 2 m (right panel).

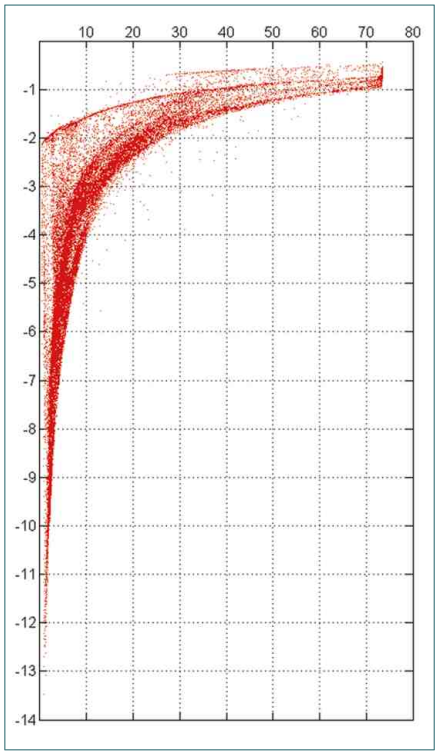

► **Figure 3**
SPM surface concentrations in mg/l versus signal penetration depth in m, as derived from a MERIS satellite scene (same as in Fig. 4). The higher the concentrations are (which is equivalent to higher turbidity), the lower the signal penetration depth is. One problem is also obvious: the algorithm to convert the optical information into SPM concentrations does not allow values greater than ~ 75 mg/l, which, of course is not correct, as is known from other measurements and model simulations.

In Fig. 5 it is shown how such satellite data is assimilated into the numerical transport model. The upper left panel shows the model result at a certain time (March 22 nd 2003, 10:00), the upper right panel shows the improved model result 20 minutes later, after the satellite data (lower left panel) was assimilated into the model. The satellite data, even if available, is not accepted everywhere, depending on quality flags (e.g. see white spots near the English coast). Especially near clouds, the measurements are erroneous.

When the new SPM concentration data is assimilated, the modeled profile keeps its shape over the total water depth but is adjusted to the new surface value. To keep the overall balance, a gain or loss of SPM in the water column is compensated by a loss or gain of fine sediment at the bottom. The differences between the model results before and after the data assimilation are shown in the lower right panel Fig. 5.

Several simulations have been performed to find out the temporal and spatial impact of the assimilated data. If the additional mass of SPM, introduced into the model by assimilation, is not compensated by a loss of fine sediment at the bottom, the total budget is increased by a certain percentage. Observing the total mass of SPM (integrated over the whole model domain) over time, it can be shown that it takes more than a week to reach the old value (from just before the assimilation).

Other model runs have shown that assimilation may lead locally to the generation of new patterns of surface SPM. Continuing the simulation, these patterns change their shape and location due to tidal currents. Sinking of particles and mixing processes (due to waves and shear currents) will change the intensities (SPM concentrations). Most likely, these patterns will still exist one week later (in the model as well as in nature), and thus when comparing the model results with the data of an actual satellite scene, this leads to a much better agreement than would have been the case without data assimilation.

Outlook

Two simulations will be performed over a two-year period, one without data assimilation at all, the other with assimilation of all available satellite data. Although the number of scenes with lesser cloud coverage is limited, this will have a major impact on the quality of model simulations.

Authors

Gerhard Gayer and Mikhail Dobrynin (GKSS)

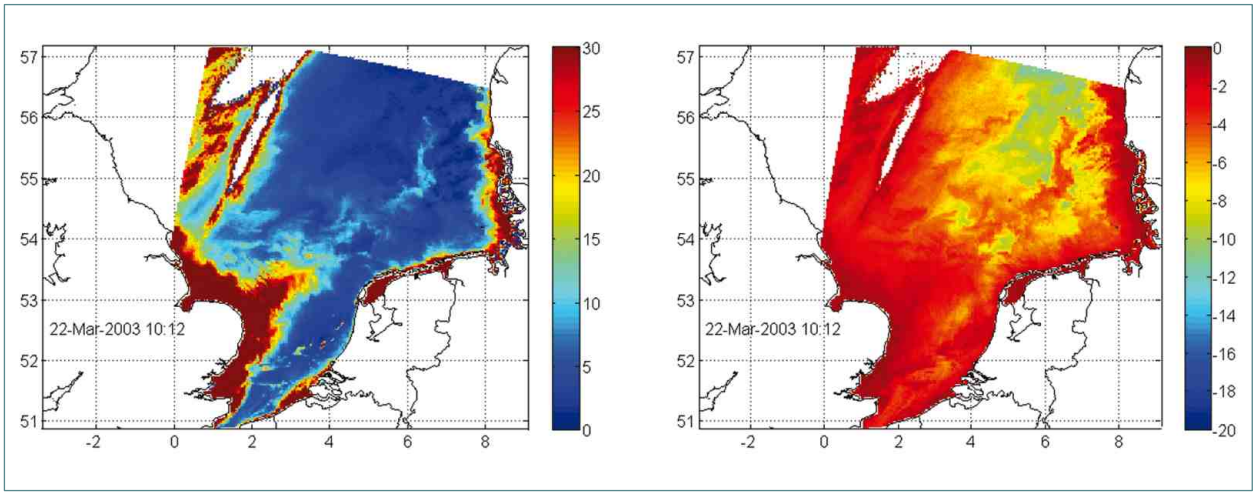

▲ Figure 4

SPM surface concentrations in mg/l (left panel) and signal penetration depth in m (right panel), as derived from a MERIS satellite scene. Such data is assimilated during model simulations to improve the performance. With the additional information of the signal penetration depth, it is now possible to redistribute the SPM over a known water depth.

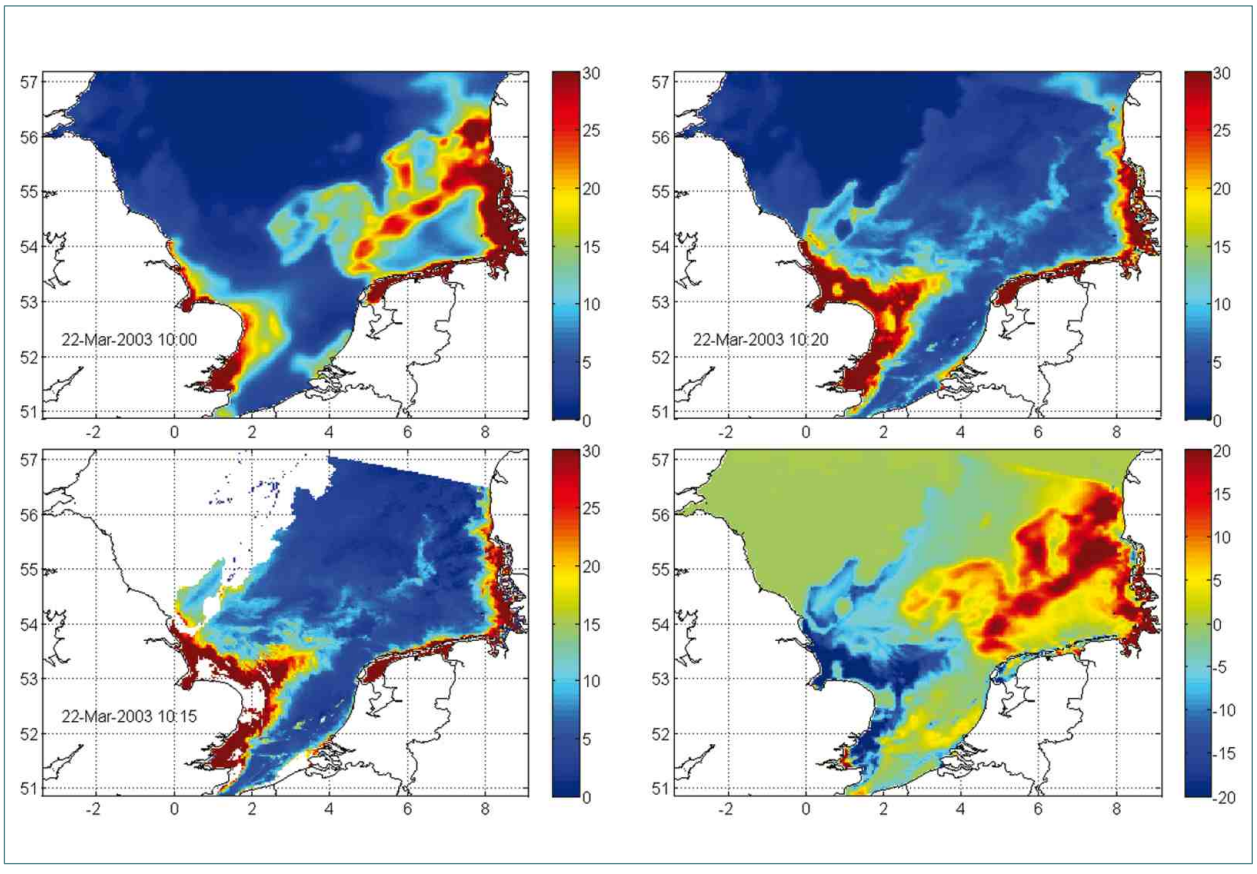

▲ Figure 5

Data assimilation by the Optimum Interpolation Method. Shown are SPM surface concentrations in mg/l as calculated by the model (upper left panel) on March 22nd 2003 at 10:00, and as derived from a MERIS satellite scene (lower left panel) 15 minutes later. The model result after the assimilation of the measured data is shown in the upper right panel for March 22nd 2003 at 10:20. The picture in the lower right panel shows the differences of model results before and after the assimilation.

Using satellite data for global wave forecasts

Methods & Techniques

Introduction

Ocean surface waves are the greatest environmental danger for all offshore operations. In particular the ships and offshore platforms are exposed to the severe wave forces (Fig.1). Therefore accurate prediction of the sea-state for the next 7 to 10 days, which is the typical travel period for ships to cross the oceans, is absolutely necessary to minimise the risk at sea. The Deutscher Wetter Dienst (DWD) responsible for this forecast service in Germany therefore has combined its wave prediction system with an assimilation system using wave data measured by satellites. The system was set up and introduced into the operational DWD model by the GKSS Research Centre.

▲ Figure 1
Picture of extremely high waves attacking an offshore oil platform during a severe storm. Wave forecasts are required here in sufficient time to down tools or to evacuate the platform if the predicted wave heights exceed a certain limit.

The wave model

The wave forecasting system is based on the third generation WAM Model (WAMDI, 1988; Komen et al., 1994). This community model was developed by the international WAM group and is maintained and distributed worldwide by GKSS.

Wind fields predicted by the atmosphere model of the DWD force the wave model. It accounts for wave propagation on a spherical grid and modifies the waves due to refraction and shoaling. Wave dissipation is done by white capping and bottom friction. The non-linear wave-wave interaction is implemented by the DIA approximation. Sea ice fields provided by the Bundesamt für Seeschifffahrt und Hydrographie (BSH) are used in the operational set-up to dissipate the wave energy in the ice covered areas.

The present model system consists of a global model (GSM) with a spatial resolution of 0.75° x 0.75° which provides boundary values for the local model (LSM) for the North Sea and Baltic Sea with a resolution of 0.1° x 0.167° and a model for the Mediterranean Sea (MSL) with a 0.25° x 0.25° resolution. Fig. 2 shows the three model areas with the results of the predicted significant wave height for September 3rd 2007 at 0 UTC. The forecast range is 7 days for the global and 3 days for the local area models. In addition the global model provides boundary forcing for a local area model of the Omani and Abu Dhabi meteorological services, which run operational wave models for the Persian Gulf and the Arabian Sea.

The wave data

Wave measurements provided in near real time through the Global Telecommunication System (GTS) of the World Meteorological Organisation (WMO) are used for verification and data assimilation.

Data from the radar altimeters on board the ERS-2, ENVISAT, and JASON satellites are assimilated into the model by first guess fields 8 times per day to improve the analysis of the global sea state and the initial fields for the forecasts.

Measurements from about 138 wave buoys are gathered but not assimilated. They are used as an independent data set for an automatic validation of the model forecast and analysis performance. Monthly statistics are evaluated.

The assimilation method

To assimilate the satellite data, a sequential optimum interpolation scheme is applied (Lionello et al., 1992). Significant wave heights and wind speeds measured about every 5 km along the satellite paths are merged with the model first guess fields. In a second step these analysed fields are used to update the wave spectra, which are the prognostic variables of the model.

An integral part of the assimilation system is an advanced quality control (QC) scheme for the altimeter data. This is based on statistical methods for checking absolute values and variances of the data along the satellite track and within individual model grid boxes.

Figure a

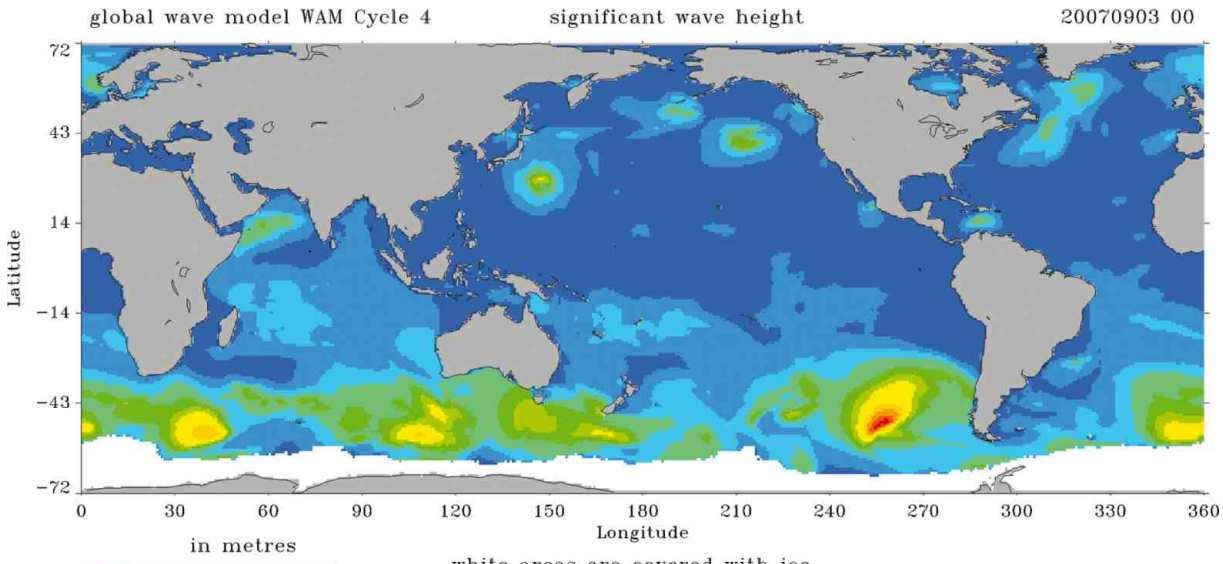

Figure b

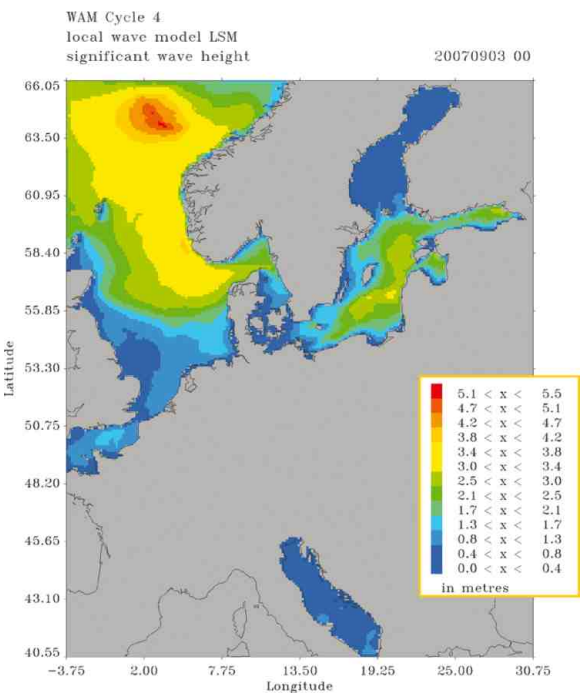

Figure 2 a-c

Distribution of significant wave height on September 3rd 2007 at 0 UTC in the three model areas of the numerical DWD wave forecast system

Figure c

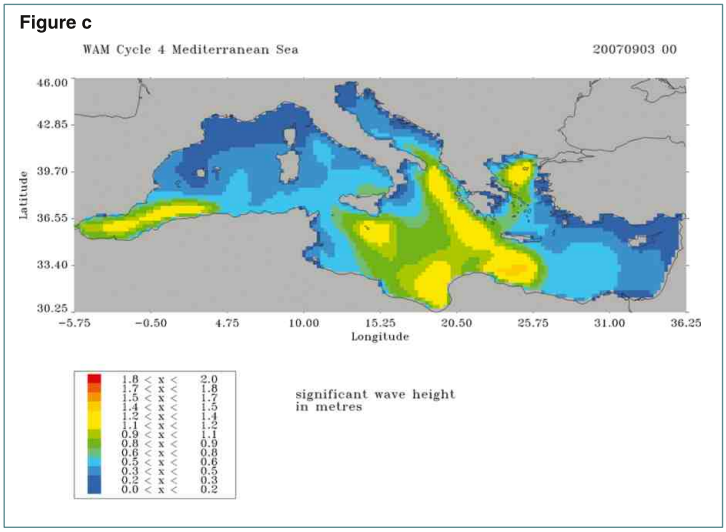

Using satellite data for global wave forecasts

Implementation & Results

Summary

In order to improve the start fields for the global wave forecasts in the numerical routine of the DWD, a 12-hour hindcast has been added that runs prior to the usual 7-day forecast. All satellite radar altimeter data that are available for this time period will be assimilated into the fields of the GSM. Fig. 3 shows pictures of the 3 satellites that continuously provide significant wave heights and wind speeds as a fast delivery product. A second advantage is the possibility to use the analysed wind fields of the global atmospherical model during the 12-hour hindcast period as the driving force for the wave model. Therefore it can be expected that the improved start fields for the usual 7-day forecast will also induce improved forecast results, especially during the first simulation day. The first example given below addresses a comparison of the results obtained by the wave forecast system including data assimilation and those computed without data assimilation. In both cases exactly the same wind fields have been used to drive the GSM. A second example discusses a regional application of the DWD wave forecast system and, although the regional model LSM does not include the data assimilation itself, it definitely takes advantage of the improved boundary values that are provided by the GSM.

▲ Figure 3
Pictures of the three satellites that provide radar altimeter data for the data assimilation into the fields of the global wave model GSM.

Global impact of the assimilation

The impact of the data assimilation on the fields of the global model GSM has been determined by comparing the results of two runs for the time period September 1st to September 30th 2007. The only difference in these runs was the data assimilation in one of the two. Fig. 4 shows the distribution of the difference of the significant wave heights obtained with data assimilation and without for September 3rd 2007 at 0 UTC. It is obvious that the general trend of the assimilation effect is an enhancement of the wave heights, especially in the southern hemisphere. Maximum differences occur on that day southwest of Australia (up to 4 m), south of Africa and east of Japan. A statistical analysis of the results of both runs in comparison with measurements at the 138 buoy locations shows an improvement due to the assimilation in 60.2 % of all cases for September 2007. The impact of the assimilation on the statistics is shown at three selected buoy locations in Table 1, two in the Atlantic and one in the Pacific. These comparisons are representative for all of the 138 buoys. The trend of the increased wave heights is confirmed by the bias (measurements - model results). The negative bias decreases for the two Atlantic locations and therefor all the statistical checks. .

A severe storm in the Baltic Sea

A spectacular application of the regional model for North Sea and Baltic is the investigation of the severe storm Gudrun, an extra-tropical cyclone that crossed over northern Europe in January 2005 and left behind extreme destruction in Scandinavia and the Baltic countries. Besides a storm surge at the coasts of the Baltic countries, the operational numerical regional wave forecast of the DWD predicted unusually high waves for the Baltic Proper and the Gulf of Finland. Fig. 5 shows the distribution of the significant wave height and the corresponding wind speed and direction in the LSM model area during the storm peak. The maximum wave height of about 11 m near the coast of Lithuania is emanated from a forecast released on January 8th 2005 at 12 UTC. A hindcast for the same time period, driven by the analysed wind fields of the local atmospherical model of the DWD provided a maximum wave height of about 10 m, which seems to be more realistic. Measurements were available during that period at 3 locations, one in the open Baltic Proper and two in the Gulf of Finland. Fig. 6 includes a time series plot for the measured and computed significant wave heights at the buoy location FIMRB (59°15' N, 21°00' E) in the Baltic Proper. Besides the results of the DWD model, the measurements have also been compared with the results of the forecast models of the Danish Meteorological Institute (DMI) and the Finnish Institute of Marine Research (FIMR). The maximum measured significant wave height is about 7 m at the storm peak at 3 UTC on January 9th 2005 and is well predicted by the forecast models.

This example shows how important high quality wave forecasts are. To know about such dangerous wave conditions already two days in advance can save lives and prevent economical damages.

Authors

Arno Behrens and Heinz Günther (GKSS)

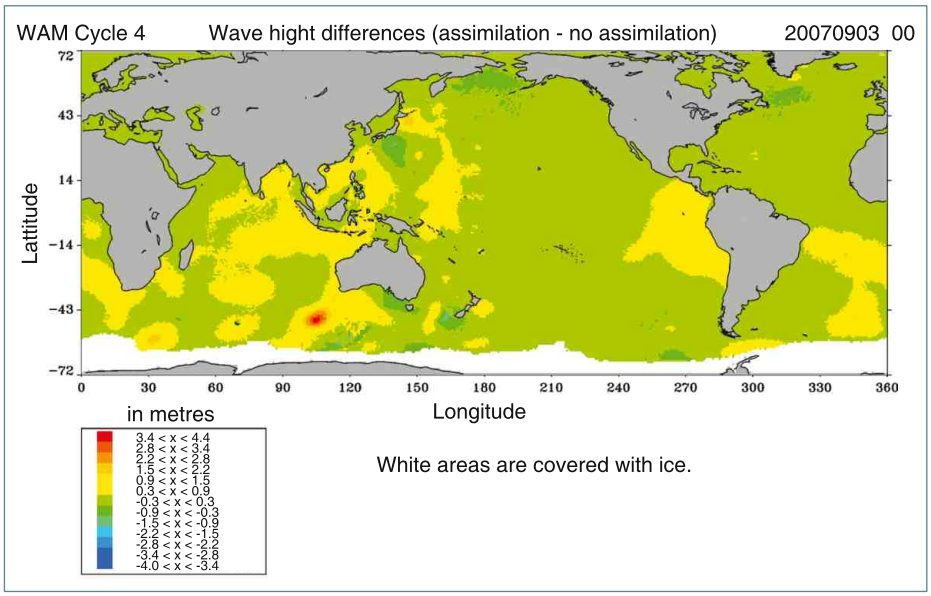

◄ Figure 4
Distribution of the difference between the significant wave heights obtained with and without data assimilation for September 3rd 2007 at 0 UTC.

buoy	number	mean	bias	Rmse	Regr.	Skill	Scatter
62108	239	2.90	-.39	60	1.37	.76	16
62108	239	2.90	-.18	40	1.17	.91	12
64045	233	3.34	-.33	.53	1.23	.78	12
64045	233	3.34	-.09	.38	1.07	.89	11
51001	239	1.89	.05	.37	.92	.53	19
51001	239	1.89	.23	.46	.78	.23	21

◄ Table 1
Statistics at 3 selected locations that are representative for the comparisons between the results of the runs without (**black**) and with data assimilation (**red and blue**). The buoys 62108 and 64045 are located in the Atlantic, west of the British Isles. Buoy 51001 is located in the Pacific near Hawaii.

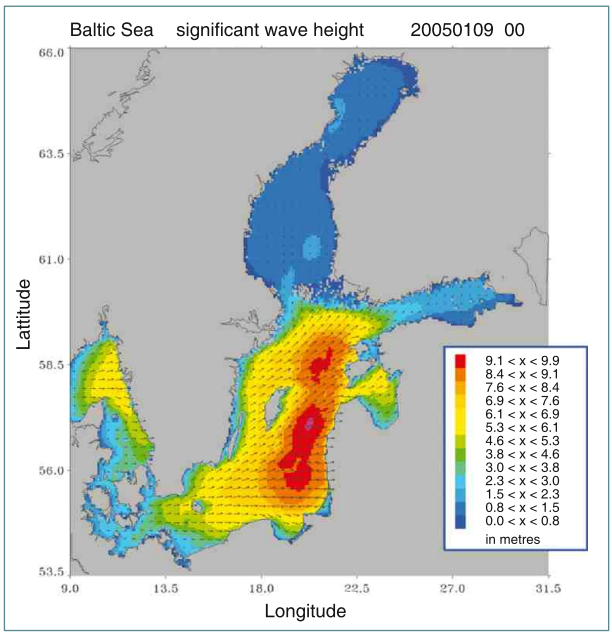

▲ Figure 5
Distribution of the significant wave height during the storm peak of Gudrun in the regional model LSM on January 9th 2005 at 0 UTC.

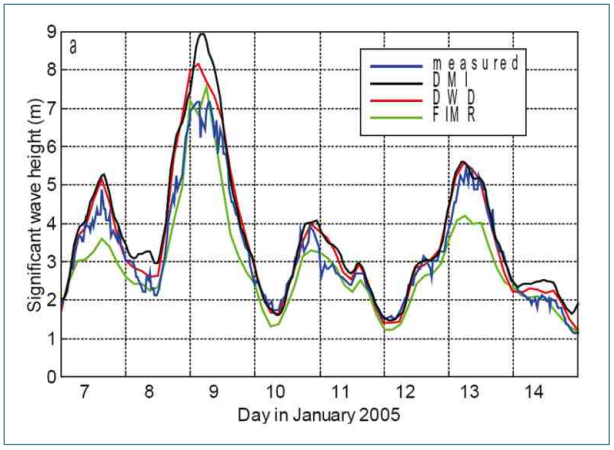

▲ Figure 6
Time series of measured and computed significant wave heights at the buoy location FIMRB in the Baltic Proper.

Which resource limits coastal phytoplankton growth/ abundance: underwater light or nutrients?

Introduction

Marine life is based on single-celled algae drifting in the water column and visible only under a microscope. In 1887 Victor Hensen termed them phytoplankton. Marine phytoplankton is the food basis for e.g. small crustaceans like zooplankton as well as for filter feeders such as mussels and oysters, which are then eaten by larger animals like fish or wading birds.

Phytoplankton requires light, carbon dioxide, and nutrients for its growth. Large rivers (e.g. IJssel, Rhine, Elbe) provide high amounts of nutrients to the North Sea. Riverine nutrient loads have increased up to eight-fold from 1950 till the late 1970s (van Beusekom, 2005) due to usage of artificial fertilizers in agriculture, phosphorus in washing powder and increased urban population size. After their peak in the mid 1980s riverine nutrient loads significantly decreased due to revised environmental laws, including international agreements and improved treatment plants (e.g. Colijn and Garthe, 2005) and have reached levels of the late fifties for phosphate. However, nitrogen loads did not decrease that much due to diffuse sources, especially from agriculture. Nutrient enrichment can stimulate algal production and biomass accumulation, leading to anoxia and large-scale mortality of fish and shellfish (Rosenberg and Loo, 1988), and alter phytoplankton species composition so that the whole coastal food web could be impacted (Lancelot et al., 1987; Reise and Siebert, 1994). An example of such a change in species composition was the strong increase in the bloom density of *Phaeocystis* in the Dutch coastal waters, which due to decreasing nutrient concentrations are returning to pre-eutrophication levels (Kuipers et al., submitted). However, coastal areas differ in their response to nutrient enrichment, since especially in highly turbid waters underwater irradiance will limit phytoplankton growth strongly. This coupling complicates the development of management strategies for coastal areas, since reduced riverine nutrient discharges might reduce the food supply, for example for mussels, fish, wading birds and mammals, and therefore may lead to contradictory positions for those who want to exploit coastal systems. To analyse the current state of the phytoplankton a simple method is presented which enables an estimate of the limiting factors.

Methodology

A useful index to indicate ecosystem sensitivity to eutrophication effects

Cloern (1999) presented a simple index that indicates the sensitivity of coastal ecosystems to eutrophication effects by assessing whether phytoplankton growth is light or nutrient limited. This index was developed from empirical data. Its application only requires the following parameters: water depth, global irradiance, water column irradiance (calculated from Secchi-depth or suspended matter content) and nutrient concentrations (N, P, and Si). Most parameters have already been included in monitoring programmes along the European North Sea coast for many years. The index provides a useful tool to estimate phytoplankton responses to changed anthropogenic nutrient supply.

Applying the index of Cloern to European Monitoring Data

The index of Cloern (1999) was used to estimate resource limitation at several coastal areas along the European continental coastal zone between 1985 and 2005 (Loebl et al., 2007 & submitted). Light limitation was tested against limitation of the dissolved nutrients nitrogen, phosphorus or silicate on a monthly basis.

Outcome

Resource limitation along the European continental North Sea coast

Applying Cloern's method to European coastal monitoring data showed that each investigated area exhibits its own limitation pattern, whereby light limitation during winter was a common feature of all sites (Fig. 1, 2). The List Tidal Basin (Island of Sylt) showed the longest period of nutrient limitation during summer, whereas phytoplankton growth at Büsum (Meldorfer Bucht) was limited by light during the whole year (Fig. 2). A significant increase of nutrient limitation in spring/summer within the past 15-20 years was observed at Sylt and Helgoland (Fig. 1 and 2), at Sylt presumably due to reduced riverine nutrient inputs. At Helgoland also altered hydrographical forcings might have changed nutrient levels. However, a future reduction of riverine nutrient loads could affect sites like Sylt more than turbid sites like the Meldorfer Bucht. In the Dutch coastal zone, strongly influenced by high nutrient loads from the River Rhine, a clear increase in nutrient limitation was observed, as was also the case in the Marsdiep area.

Cloern's index provides a useful tool to get a first answer to the question which resource might limit phytoplankton growth and how changing nutrient loads might influence coastal food webs.

Authors

Franciscus Colijn (GKSS), Martina Loebl, Justus van Beusekom and Karen Wiltshire (AWI)

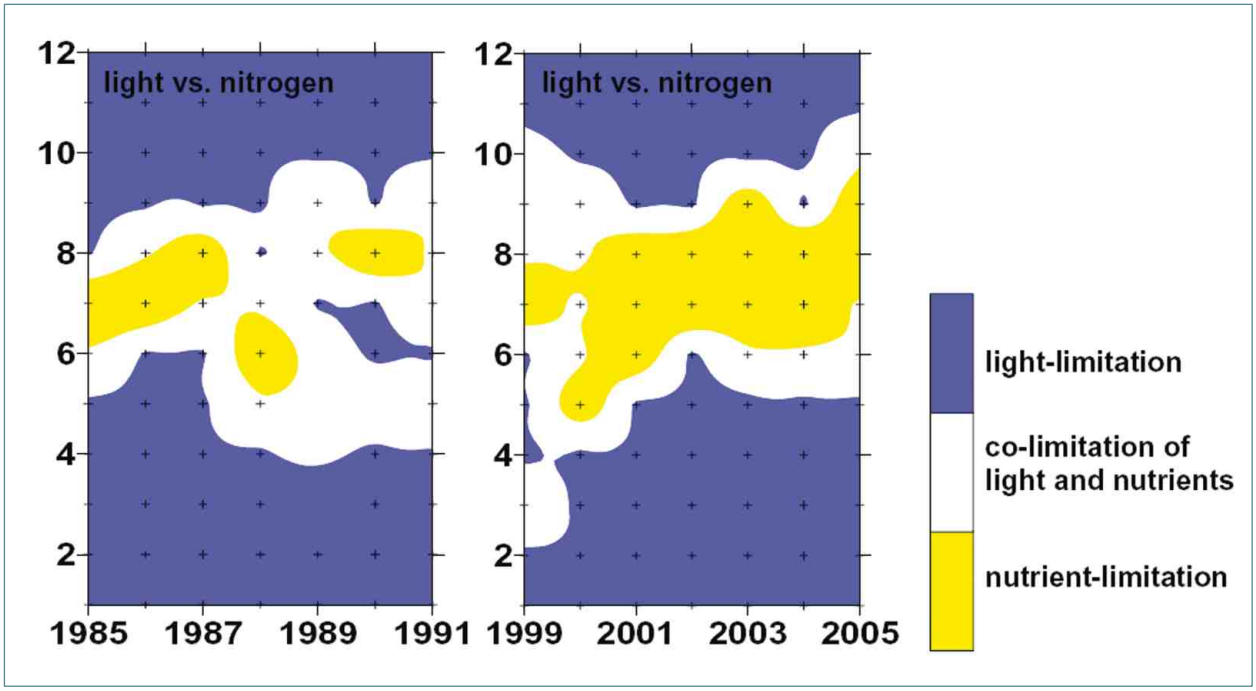

▲ Figure 1

Contour plot of resource limitation at the Island of Sylt (List Tidal Basin) calculated following the index of Cloern (1999). Blue fields indicate light limitation, yellow fields show nutrient (nitrogen) limitation, white fields indicate co-limitation of both resources. Crosses indicate data points. Missing data were interpolated by kriging. Comparing the 1985-1991 period with the 1999-2005 period shows that nitrogen limitation during summer has significantly increased (Loebl et al., 2007).

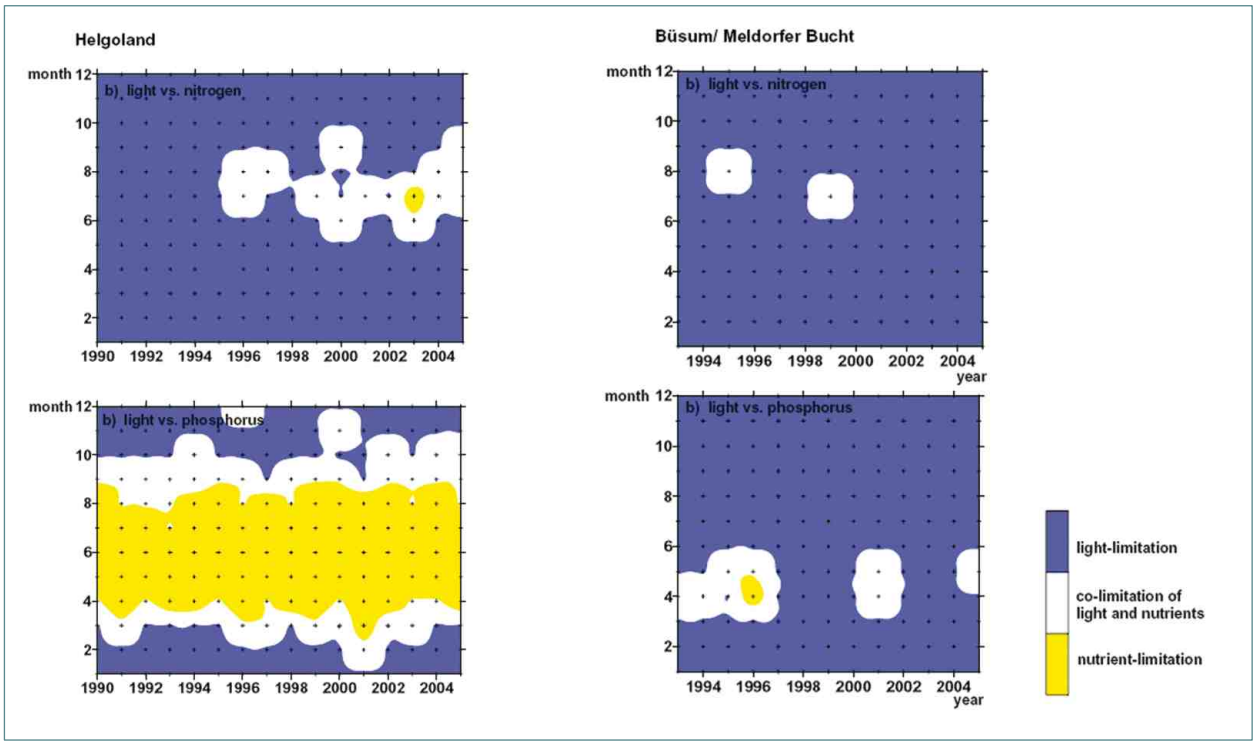

▲ Figure 2

Contour plot of resource limitation of phytoplankton growth at the Island of Helgoland and at Büsum/Meldorfer Bucht calculated following the index of Cloern (1999). Blue fields indicate light limitation, yellow fields show nutrient (plot a: nitrogen, plot b: phophorus) limitation, white fields indicate co-limitation of both light and nutrients. Crosses indicate data points. Missing data were interpolated by kriging. At Helgoland nutrient limitation of nitrogen and phophorus during summer increased significanttly between 1990 and 2005 (Loebl et al., 2007).

The HIMOM and OFEW approaches to monitoring intertidal flats

Methods & Techniques

Introduction

The proper management of coastal environments requires appropriate policy directives and tools that support fulfillment of the requirements of these directives. The European research project HIMOM (Hierarchical Monitoring Methods for Tidal Flats) provided a system of Hierarchical Monitoring Methods (HMM) consisting of different tools and methods to determine system change expressed by biological and physical variation within tidal flat areas (Brockmann et al., 2004). It includes 34 protocols for ground sampling, primary production, remote sensing and data management. The HMM includes also categorized cost estimates so that end users can estimate the investment and running costs of implementing monitoring strategies of differing complexities.

Remote sensing methods have been introduced as part of the HMM in HIMOM. In the subsequent national project OFEW (Operationalisierung von Fernerkundungsmethoden für das Wattenmeer Monitoring) these have been further developed towards an operationalisation and integration into the national marine monitoring programme. This project has been funded by the environmental agencies of Schleswig-Holstein and Lower Saxony.

▲ **Figure 1**
The HMM Toolbox - a Hierarchy of Monitoring Methods
Hierarchy of methods in terms of complexity, information content, applicability, resolution, costs (after: Consalvey, HMM CD)

The Hierarchy of HIMOM

A system of Hierarchical Monitoring Methods (HMM) has been the basic concept of the HIMOM project (HIMOM, 2005). In the first year of the project, the HMM elements were defined and protocols for taking measurements, analysing the samples and the management of data were developed. Thirty-four individual protocols are now defined on a detailed level. They include techniques for sediment sampling, grainsize analysis, pigment extraction and analysis, primary production or remote sensing (Fig.1).

The protocols have been compiled to a practical handbook for carrying out monitoring in intertidal areas. A hierarchy of methods exists in terms of costs, applicability, accuracy, information content, scale and detail. This means that several alternatives for measuring one parameter are included, and the HMM points out the alternatives, including their respective advantages and disadvantages. Therefore, it is possible for coastal managers to choose the best fitting methods for their monitoring concept and budget. An HMM-CD has been produced containing the book of protocols, demonstration material, an atlas of estuary maps and a case study for each member country. This gives the users all instructions and some practical hints for choosing and performing the different techniques. The HIMOM CD "HIMOM (2005): HMM-CD - Hierarchical Monitoring Methods for Intertidal Flats" can be obtained from Brockmann Consult or GKSS.

The Remote Sensing Approach in OFEW

While Remote Sensing was one of the monitoring methods amongst others within the HIMOM-HMM, this methodology has been further investigated and developed towards an operational application within the OFEW project. Here, the classification of intertidal flats on the basis of multispectral satellite data has been standardised and tools have been developed in order to enable the responsible agencies to perform their own analyses. For the classification of satellite images, a processing chain has been developed including steps such as atmospheric correction and georectification and, finally, a classification of intertidal surface types (Fig. 2) (Stelzer & Brockmann, 2006; Brockmann & Stelzer, 2008).

In a similar way as in HIMOM, OFEW also works along a hierarchal approach - remote sensing data of different spatial and spectral resolution have been tested and adopted. The data material ranged from low cost aerial digital photos to hyperspectral scanner images and also includes satellite images of different resolutions.

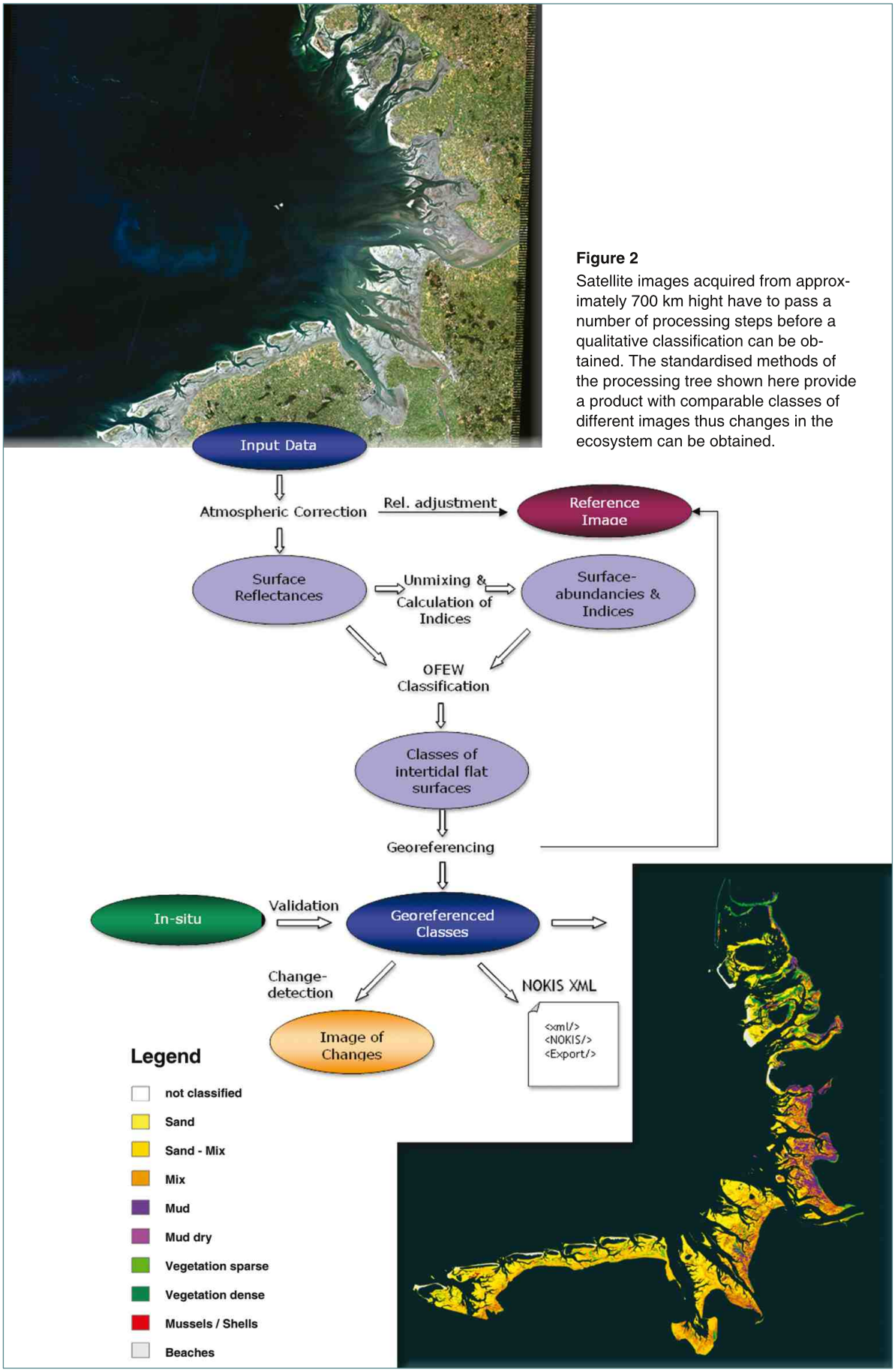

Figure 2
Satellite images acquired from approximately 700 km hight have to pass a number of processing steps before a qualitative classification can be obtained. The standardised methods of the processing tree shown here provide a product with comparable classes of different images thus changes in the ecosystem can be obtained.

The HIMOM and OFEW approaches to monitoring intertidal flats

Implementation & Results

Implementation

The protocols within HIMOM have been developed and successfully applied to tidal flats in Germany (Wadden Sea), The Netherlands (Westerschelde), Scotland (Eden estuary), Ireland (Barrow estuary) and Portugal (Tagus).

An atlas of classification results has been produced by HIMOM as well as by OFEW. In HIMOM, the Atlas of European Estuaries shows the classifications and maps of the 5 European Estuaries investigated during the project phase. Extending the atlas, case studies presenting examples of application of the HMM for different thematic questions have been developed for the HIMOM CD. For each of the studied estuaries one case study demonstrates how questions on the state of the environment can be answered by applying HMM methods. The OFEW Atlas shows a time series of Landsat images from 13 different dates that have been classified with the standardised OFEW classification method. The earliest images were acquired in 1987, the third year of the long-living Landsat 5 TM sensor. Meanwhile, the sensor has been over 20 years in orbit and is still sending high quality data and images of our environment. The latest data in the atlas are from 2006, enabling change analysis and statistical studies over a period of almost 20 years of a uniformly processed dataset. Fig. 4 shows some examples of the maps.

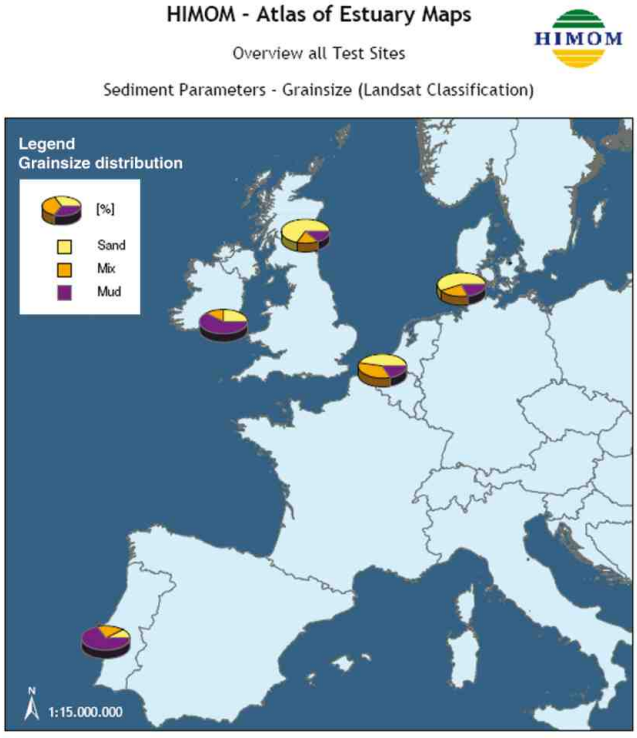

Grainsize Landsat Classification

Test Site	Sand [km2]	Mix [km²]	Mud [km²]	Vege-tation [km²]	Sand [%]	Mix [%]	Mud [%]	Vege-tation [%]
German Wadden Sea	1256.2	549.2	420.5	47.7	55.2	24.2	18.5	2.1
Eden Estuary	4.1	1.4	1.0	0.8	56.7	19.3	13.5	10.6
Barrow	1.7	1.0	4.0	1.1	21.5	13.1	51.3	13.1
Westerschelde	30.4	23.0	11.6	11.7	39.7	29.9	15.2	15.2
Tagus Estuary	7.7	18.2	53.0	22.2	7.7	17.9	52.4	22.0

▲ Figure 3
Comparison of average grain size distribution in European Estuaries (HIMOM project) derived from satellite classifications.

Results

The HIMOM book of protocols, case studies and demonstration material is all available on the HMM-CD for practical use.

The application of the methods in 5 different European Estuaries enabled a good comparison of methods and estuary characteristics (Fig. 3). Time series of intertidal flat classes can show changes in morphology and changes in sediment types over several years. Further, seasonal changes can be detected concerning the growth and extension of micro- and macrophytes (Fig. 5), assuming the availability of several images within one year.

The availability of data is one of the constraints when using remote sensing methods for the interpretation of inter- tidal flats because, besides cloud coverage, also the tidal situation limits the number of images per year.

Outlook

In future projects remote sensing methods shall be further developed by the combination of optical data with other information sources such as surface roughness derived from radar data and background information. The background information will bring in expert knowledge about the ecosystem into the classification system. The responsible agencies for the operational monitoring will furthermore be involved in these activities and follow the outcomes. Discussions will continue on how those techniques and products can be integrated into the monitoring programmes.

Authors

Kerstin Stelzer and Carsten Brockmann (Brockmann Consult)

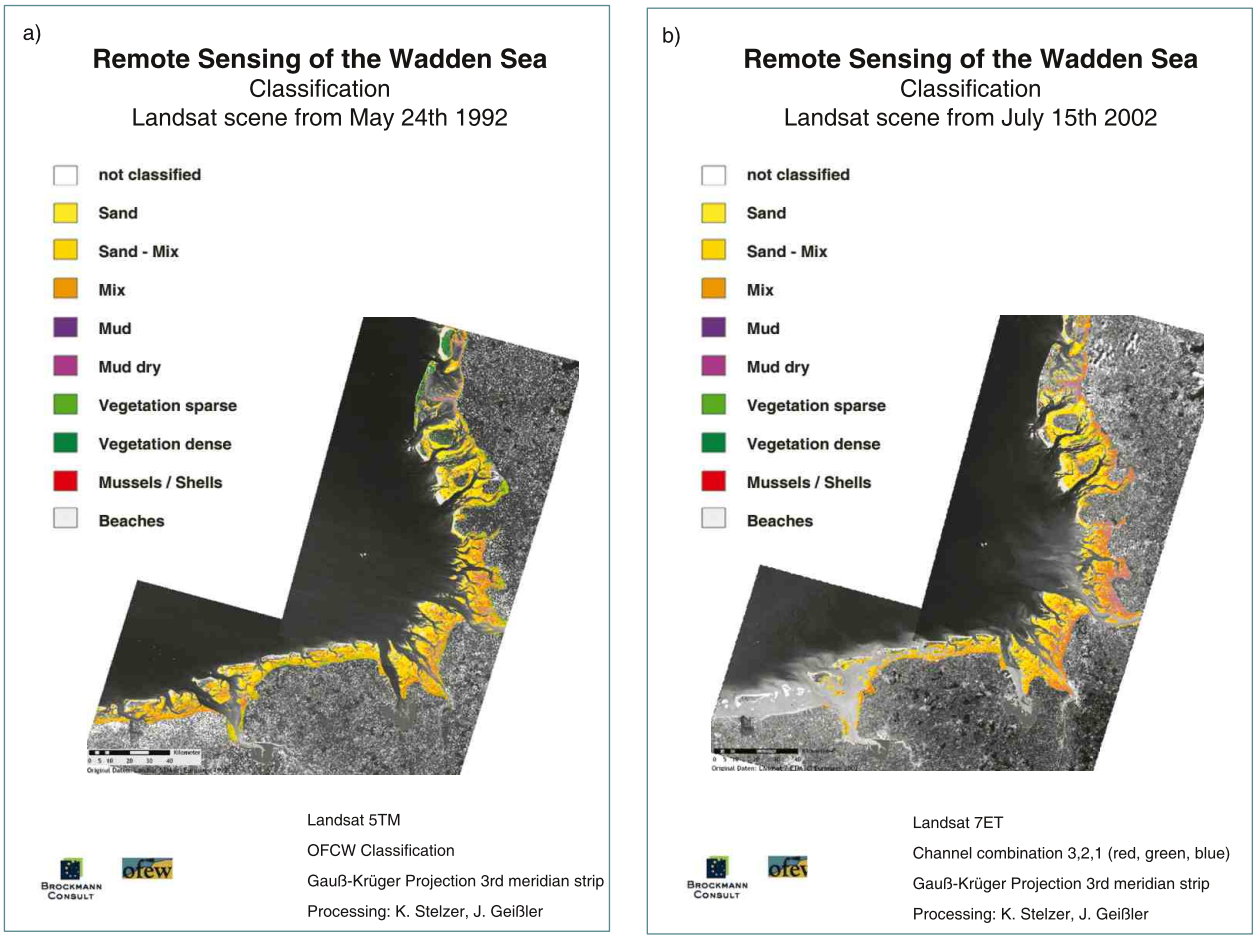

▲ Figure 4 a & b

Maps from the OFEW Atlas: Results of classification of different Landsat images; the maps show the classifications of the whole German Wadden Sea overlaying a grayscale image of the original satellite image. Original data: Landsat 5&7 (E)TM © Eurimage 1992 & 2002.

▼ Figure 5

Detecting changes on the basis of classifications derived from various satellite images. These subsets show the mouth of river Elbe.

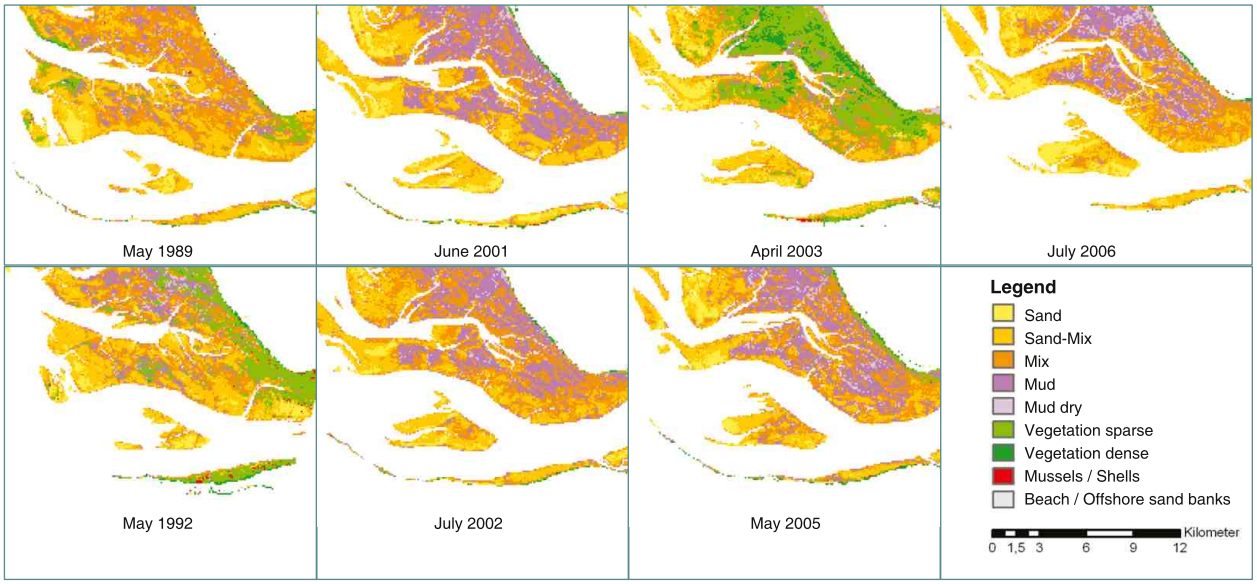

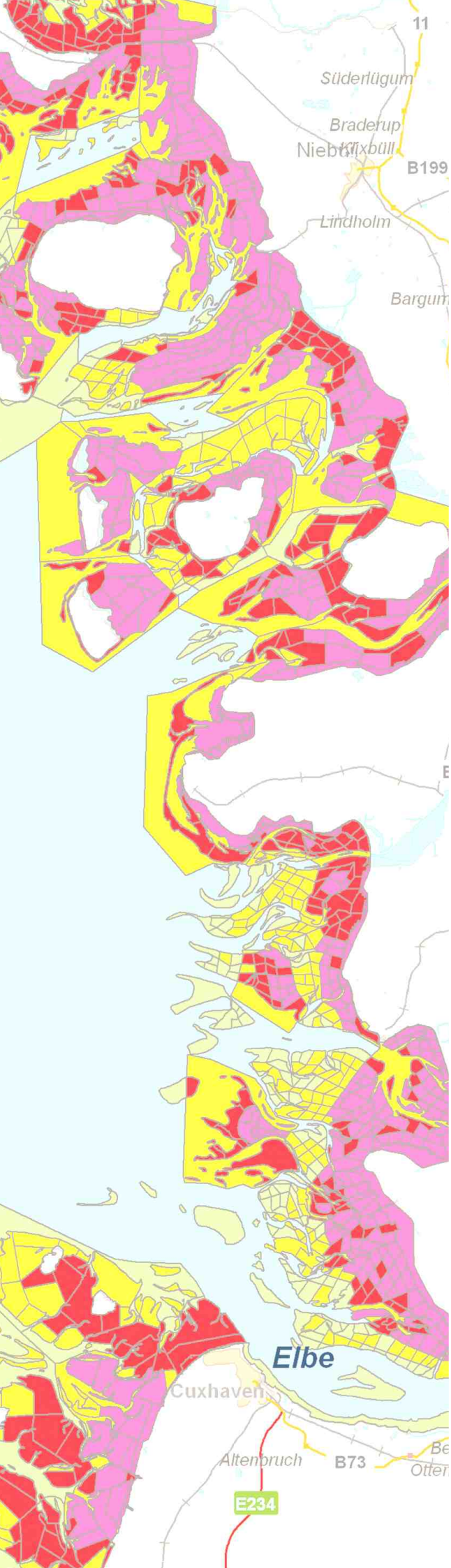

Integration into monitoring programmes

Finally, when new observational and data evaluation methods have demonstrated their maturity for a regular deployment by or for monitoring agencies they have to be integrated into monitoring services and programmes. These programmes are in most cases legally based on national laws or international agreements and conventions and have to follow accepted or prescribed standards.

Examples are the HELCOM convention and the European Water Framework Directive or the Ramsar Wetland Convention for protecting migrating birds. Some of the new methods are still in a testing phase by the authorities.

We present here three examples, where recently developed methods are already integrated into monitoring services or are in use by governmental authorities.

Content

Water quality services GMES - MarCoast

Methods & Results

Introduction

Monitoring of the marine environment in German waters of the North Sea and the Baltic Sea has been performed since 1976 in the framework of the so called “Bund-Länder Messprogramm” BLMP (common measurement programme of the federation and the federal states). In the past, this programme has been focussed on physical and chemical parameters as required by the HELCOM (Baltic Sea) and OSPAR (North Sea) conventions. The EC Water Framework Directive and the Natura 2000 set of directives require complementary measurements of biological and morphological parameters in order to assess the water quality from an ecological point of view. The BLMP is currently being extended in this respect, and parameters derived from space-borne remote sensing are beginning to become an integral part of the programme. The European GMES programme will be a major contributor in this respect.

In 1998 the Europe Commission decided to set-up the programme "Global Monitoring for Environment and Safety (GMES)". The aim is to provide services for users combining data from in-situ measurements, space observation and models. The services provide information and support policy decisions in terms of environment and security.

GMES is a shared activity carried out by the European Commission in its research and development programme, and the European Space Agency (ESA) through its GMES Service Element (GSE) (Commission of the European Communities, 2003).

GMES is currently in its implementation phase. As a long-term contribution to GMES, ESA is currently developing the Sentinel series of satellites, which deliver routinely- amongst others - information about the ocean state (surface height, waves, wind, temperature and ocean colour) over the next 20 years (Drinkwater et al., 2005).

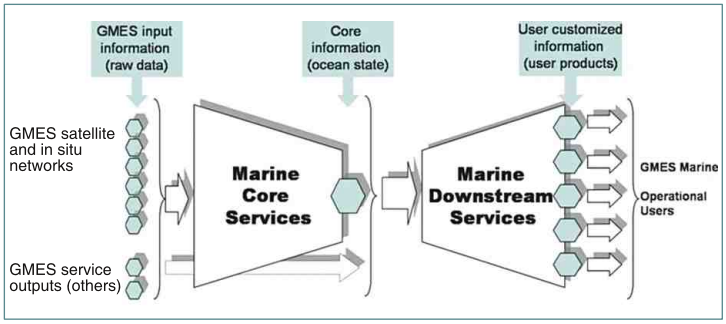

▲ **Figure 1**
Marine Core Service (from Ryder, 2007).

As part of GMES the EU will start the Marine Core Service (Fig. 1) in 2008, a large scale European effort to convert operationally raw data from satellites, in-situ observations and numerical models into ocean state and forecasting baseline information. This information will be taken up by so called Downstream Services, which add value to the data and deliver customised end user products. The Downstream Services will start in 2010 (Ryder, 2007). Currently, the ESA-GSE project MarCoast delivers satellite-based pre-operational services and is considered as a prototype for such a marine Downstream Service.

Methodology

MarCoast has the objective of delivering services to European users concerned with monitoring of the marine environment. The MarCoast Service Portfolio is composed of 2 service chains (Oil spill and Water Quality) containing 6 services:

- oil spill alert and polluter identification
- oil spill drift forecast
- water quality monitoring
- algae bloom detection and alert
- large scale water quality indicators
- MetOcean data

The Water Quality related services include products such as chlorophyll concentration, suspended matter concentration, turbidity, algal bloom indicators and sea surface temperature. In Germany, the DLR and Brockmann Consult are acting as regional MarCoast Service Providers, delivering products to the Federal Maritime and Hydrographic Agency (BSH), the Environmental Ministry of Schleswig-Holstein (LANU) and other monitoring agencies in Germany. The products are tailored to the needs of the agencies in the context of the BLMP. The products are operationally generated and published Europe wide through the MarCoast Services Portal and on the national scale via portals such as the Water Quality Service System (WAQSS, Fig. 2).

The WAQSS generates thematic maps by integrating the satellite data with in-situ measurements and delivers the results via electronic media. The validation of the services is an important component of MarCoast. The Validation Protocol requires intense user involvement in this process. Users contribute data, provide feedback and assess the quality of products and services (www.gmes-marcoast.com).

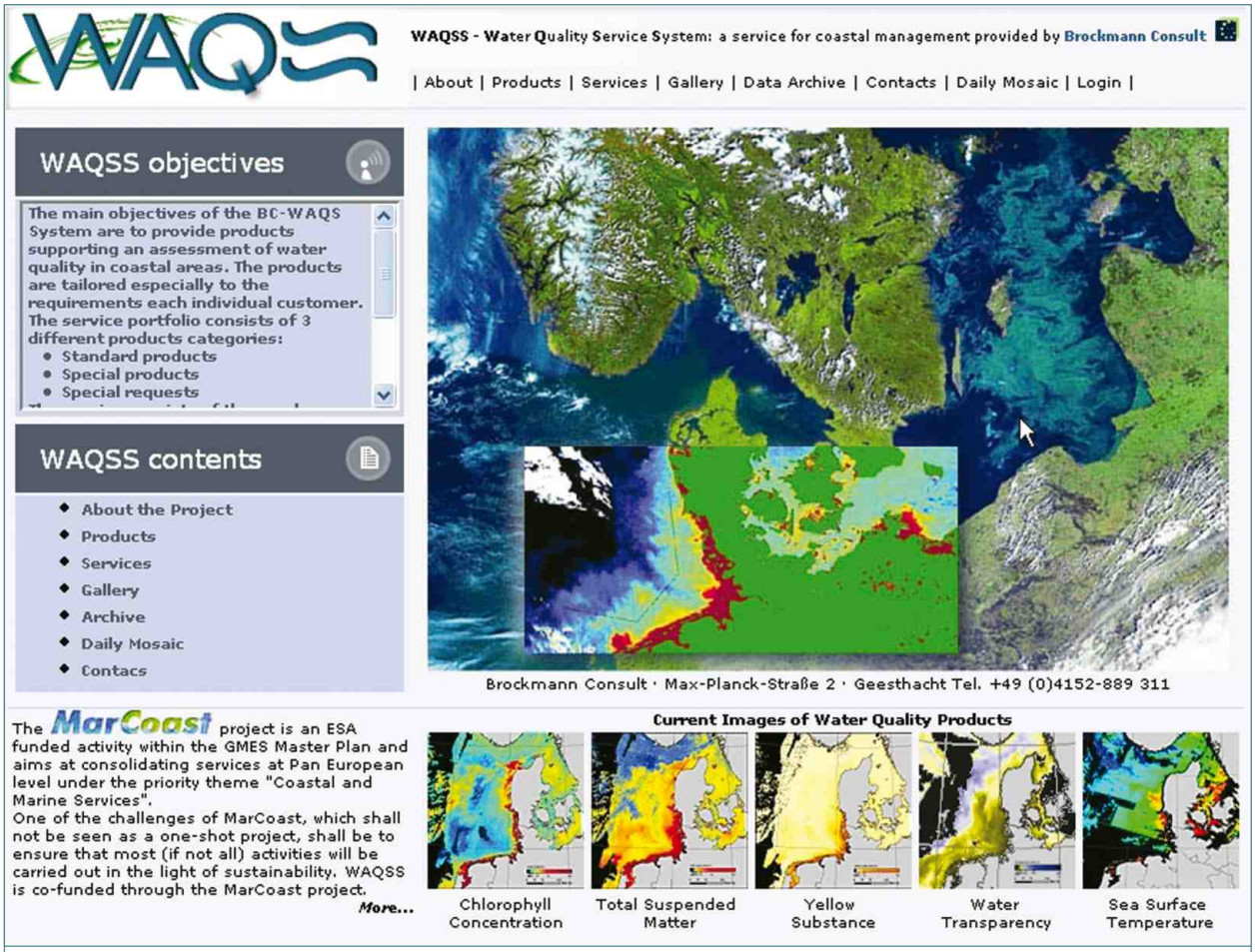

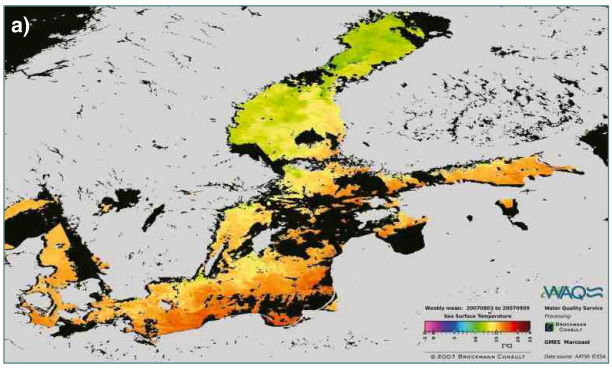

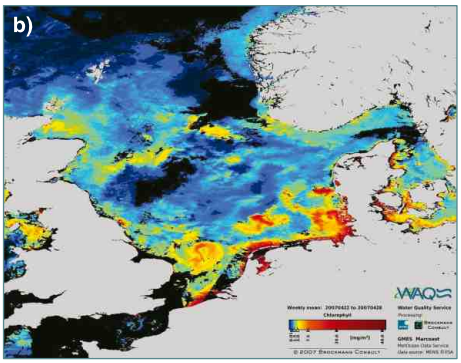

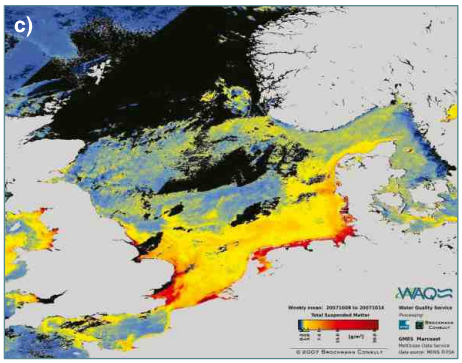

Figure 2
The Figure illustrates the marine services provided by Brockmann Consult through the Water Qualitiy Service System, WAQSS. Products of derived satellite data are provided to assess water quality in coastal areas. Examples of maps of **a)** suspended matter concentration, **b)** weekly average values of chlorophyll concentration and **c)** sea surface temperature are displayed (see www.waqss.de).

Water quality services GMES - MarCoast

Implementation & Results

Application

The MarCoast Services offered by Brockmann Consult are structured into standard and special products, and products generated on request. The standard products are basic datasets and thematic maps of the North Sea and the Baltic Sea, defined by Brockmann Consult and offered to every user. The special products and requests are designed to fit the needs of the different users. The requirements of the users are identified by the users and the WAQSS team and are fixed in so called Service Level Agreements (SLAs).

The WAQSS production chain (Fig. 3) is taking MERIS Reduced Resolution products (1.2 km spatial resolution) and AATSR SST products (1 km spatial resolution) as input. An extension of the production chain using MERIS Full Resolution products is currently under construction. The processing of the raw data into thematic maps of algal bloom indicators, chlorophyll-a and total suspended matter concentration, yellow substance absorption and sea surface temperature is fully automated (WAQSS). An archive is maintained where all products are stored. Standard products are published on the WAQSS website, however, more important is the direct delivery of requested products to users and the feedback-loop, which is part of this direct communication line. The products are used to assess the quality of the seas and as decision support to guide in-situ sampling.

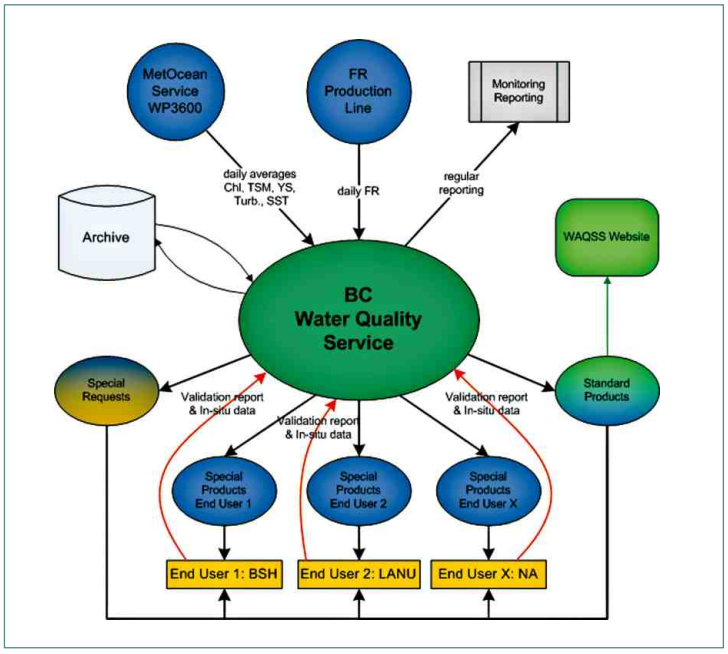

▲ **Figure 3**
Structure of the BC-Water Quality Service System (source: www.waqss.de).

Validation

Validation of the MarCoast products is essential for their acceptance by the users. The validation protocol requires a close involvement of the users. In-situ measurements are statistically compared with the satellite derived products. For example, the BSH conducted a ship cruise in the North Sea in August 2006. Measurements of different parameters were performed along transects at defined locations. These data have been compared with MarCoast Water Quality products. Fig. 4 shows a correlation between in-situ and remote sensing methods. Another example is the validation of respective Water Quality products with in-situ data from the North Sea and the Baltic Sea taken by helicopter and from a ship by the LANU. Chlorophyll values derived from MERIS products were compared with in-situ measurements. In Fig. 5 data from one station are exemplarily plotted as a time series. A good agreement between the two data sources was found.

A second aspect is the comparison of different algorithms, which are used to process the satellite data, to identify the best performing one for each area. This is particularly important for the optically complex waters of the North Sea and the Baltic Sea. In a case study the comparison included four algorithms: the standard MERIS Level 2 product, the standard MarCoast product, and a special method developed by the Freie Universität Berlin (FUB Case2 algorithm). The latter gave best results. Currently a dedicated Case 2 method is under development by GKSS which will be introduced in the MarCoast processing in 2008.

Perspectives

The preparatory phase of GMES is close to completion and after 2008 the system is going to enter into its operational phase. The European Space agency will be responsible for the space segment (Sentinel satellites) and the data portfolio, while the European Union is providing the service component. National supporting components are completing the system. The marine part of GMES is ensured by the Sentinels 1 and 3, complemented by the German TerraSAR-X and Rapid Eye satellites (Drinkwater et al., 2005), and the Marine Core Service and Downstream Services of the EU, which are nationally accompanied by the DeMarine project. The operational/ commercial market of service providers and users completes the scenario which will evolve and grow over the next 20 years.

Authors

Carsten Brockmann, Jasmin Geißler and Kerstin Stelzer (Brockmann Consult)

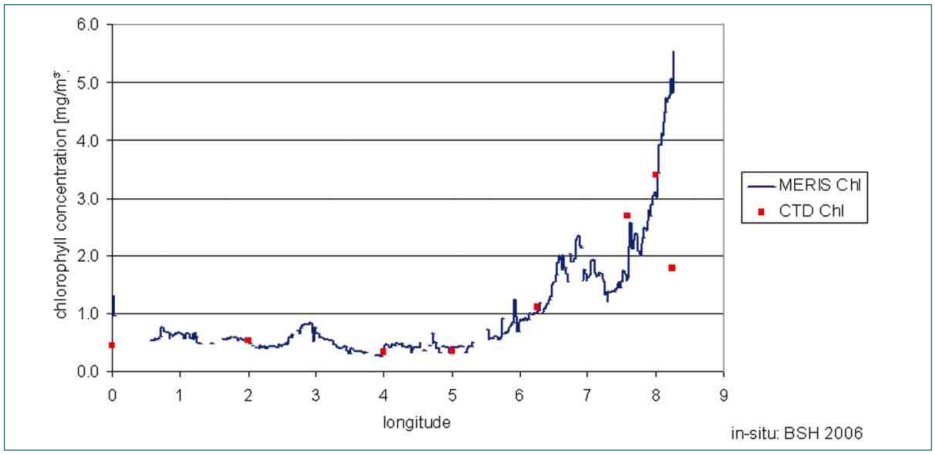

◄ **Figure 4**

The graph shows values of chlorophyll measurements at different stations (red dots), collected by BSH, plotted with MERIS values along the sampling transect connecting the sampling stations (blue line). Data source in-situ: Bundesamt für Seeschifffahrt und Hydrographie.

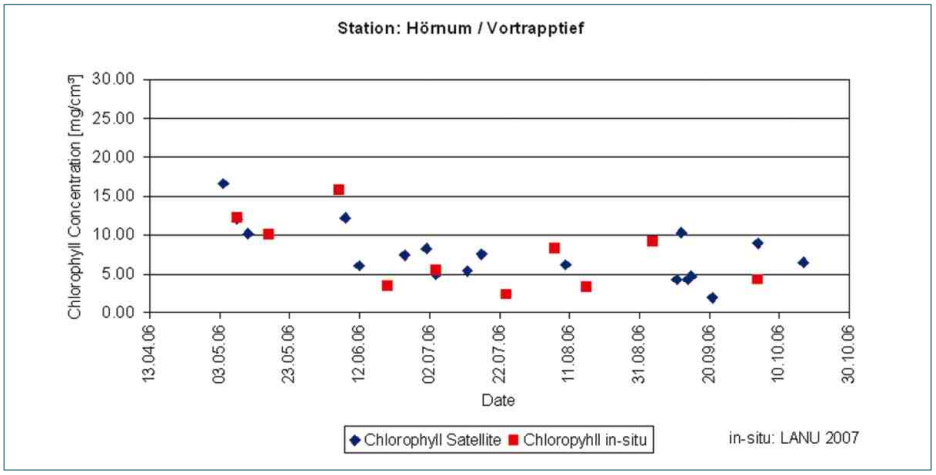

► **Figure 5**

Time Series of chlorophyll concentration derived from in-situ measurements (red dots) and satellite data (blue dots) at a certain station. Data source in-situ: Landesamt für Natur und Umwelt des Landes Schleswig-Holstein.

▼ **Figure 6**

In 2007, the evolution of the Spring Bloom in the Baltic Sea could be very well monitored with MERIS data because of clear weather conditions. The first image recognising an exceptional high chlorophyll concentration has been acquired on March 12th 2007. The following days show an increase of chlorophyll concentration towards a maximum around March 2th. The algal bloom was confirmed by the end users, namely LANU. The bloom almost disappeared at the end of March/April 1st but recovered again until April 3rd. The image of April 7th shows again decreasing chlorophyll concentrations.

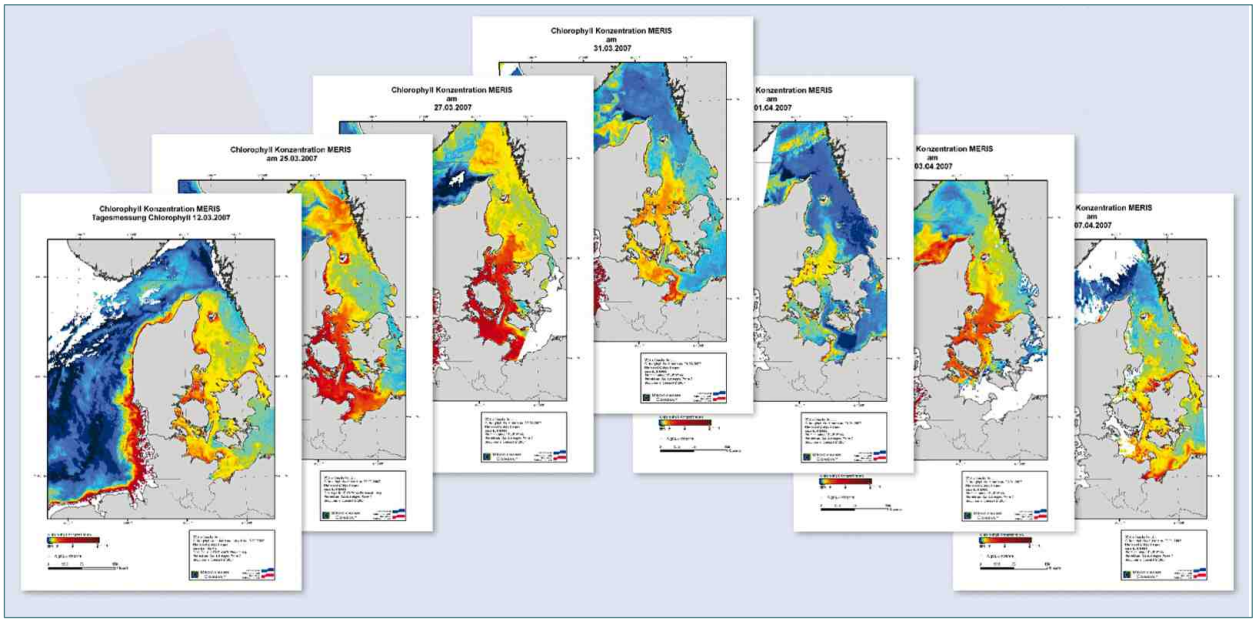

Marine geo-information system for the North Sea seafloor

Methods & Techniques

Introduction

Geo-Information Systems (GIS) are designed for the management, visualisation and analysis of geodata. Geodata refers to all measurements and information which are intrinsically tied to their location (latitude, longitude, depth) of observation. It includes data obtained during scientific marine and landside research as well as geodata compiled for economic and socioeconomic needs.

Data measured at distinct locations, thematic maps, georeferenced photographs, videos as well as other types of spatial information can be integrated and analysed by GIS. To facilitate such analysis, the geodata are structured in the form of information layers compiling one parameter set in one map (Fig. 1).

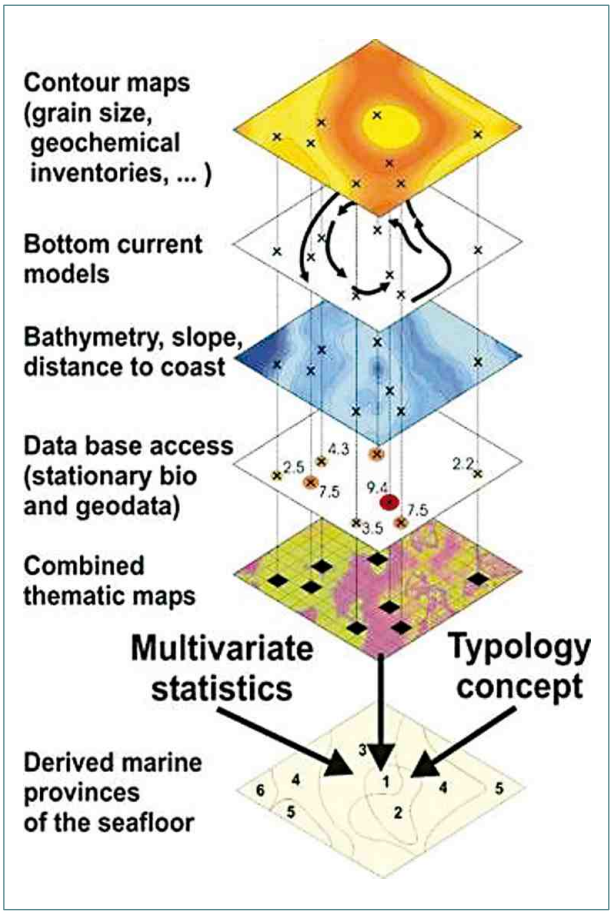

▲ **Figure 1**
Within a GIS, spatial information is organised in the form of information layers and archived in a geo database. This supports data mining, geostatistical analysis as well as specific GIS techniques supporting multicriteria decision analysis.

By overlaying information layers, including the attributes, frame, legend etc., the overall map is composed. This allows complex spatial analysis for research objectives such as identification of provinces of the seafloor (Jerosche et al., 2006) or calculation of geochemical budgets (Schlüter et al., 2000), as well as for applications like determination of location factors for the construction of e.g. offshore wind farms or areas suitable for sand and gravel recovery.

Motivation

Worldwide, the coastal zone has a dense population and coastal waters are often subject to different economic demands. Such activities as well as research objectives or issues like identification of natural conservation areas require detailed information and maps about the marine environment. Unfortunately, such maps are often unavailable, due to the lack or low accessibility of environmental data.

This is often a limiting factor, for example for identification of benthic habitats, e.g. according to the European Nature Information System (EUNIS) as well as for studies on submarine groundwater discharge, occurrence of methane in sediments or the release of nutrients from the seafloor. As a step towards the development of a digital information system we compiled an extensive dataset of bathymetric data, sediment maps, benthos biology, geochemical data, (e.g. concentrations of oxygen or nutrients in bottom waters and sediments), as well as about the use of the seafloor.

The data compilation and analysis was part of the EC Project METROL and the BMBF/DFG funded project MarGIS.

Application of a spatial database

For the compilation of a large data set covering a multitude of parameters for the purpose of comparing geo information the careful description of meta- information is essential (Fig. 2). Regarding maps, such meta-information includes the geographic projection, the geodetic datum (e.g. WGS84), the source or the publication date.

To cope with the large number of data sets, maps, and meta-information we developed a spatial database scheme. This scheme was implemented as a spatial database which is directly linked to the GIS and, in turn, supports the spatial analysis processes as well as visualisation of results. Combined with the Internet Map Server (IMS), it allows the interactive dissemination of geodata and maps to scientists and the general public.

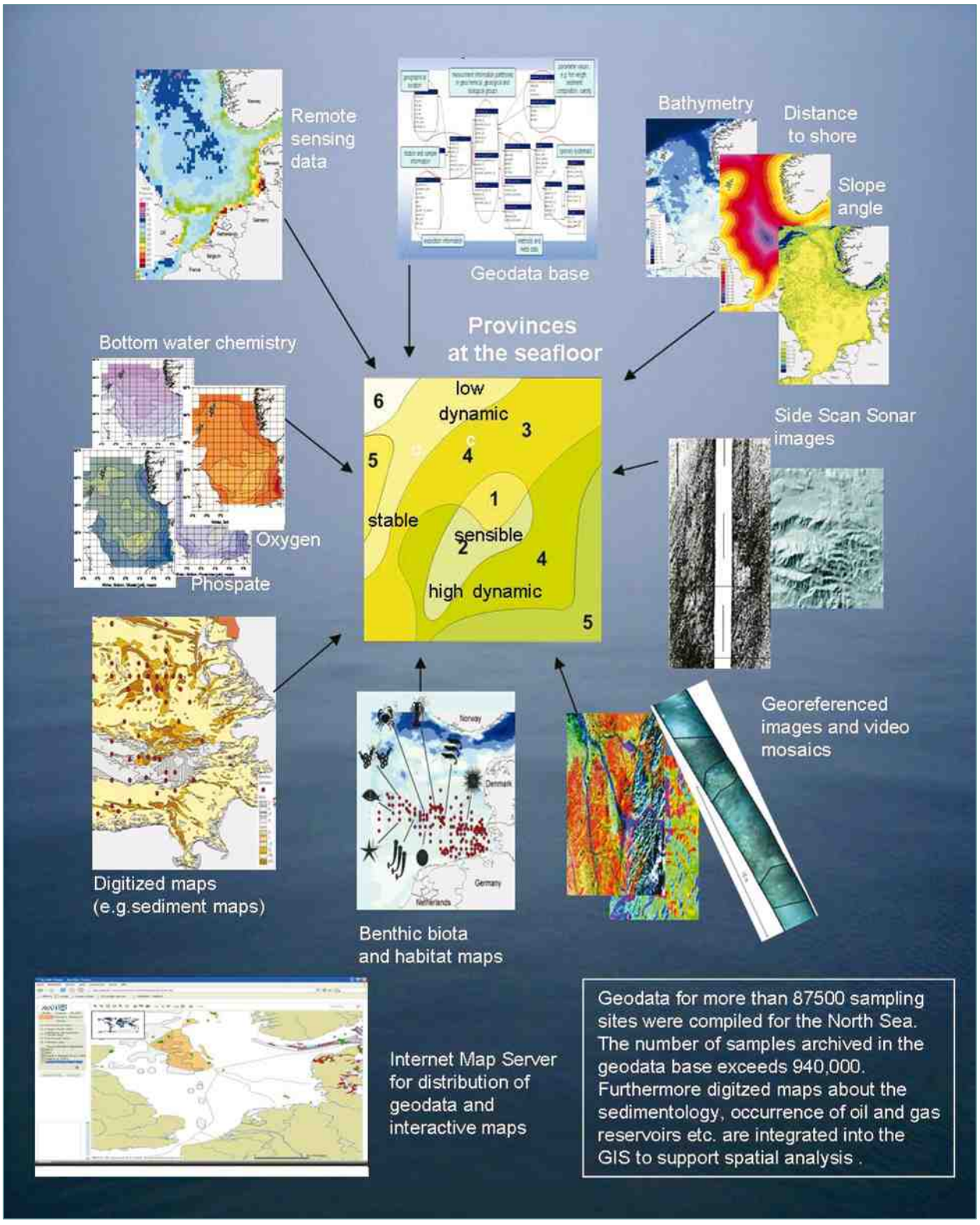

▲ Figure 2

The compilation of different types of measurements and thematic maps which describe the environmental conditions of the sediment-water-transition zone allows the identification of provinces at the seafloor. Depending on the specific scientific objective, natural conservation issues or economic interests, these provinces might be habitats according to the European Nature Information System (EUNIS), regions suitable for sand and gravel mining, or geochemical provinces characterised by e.g. methane concentrations and morphological features at the seafloor.

Marine geo-information system for the North Sea seafloor

Implementation & Results

Methane in sediments of the North Sea and Baltic Sea

Methane is an important energy resource and greenhouse gas. Due to its relevance we are interested in identifying regions at the seafloor which are characterised by high methane (CH_4) concentrations and locations where methane is transferred into the water column or atmosphere (Fig. 3).

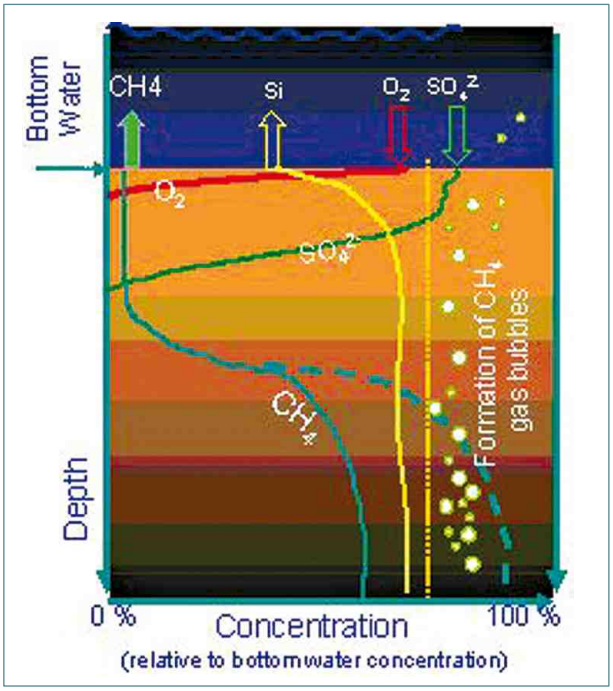

▲ **Figure 3**
This sketch visualises the formation of methane (CH_4) in surface sediments. Under anoxic conditions CH_4 is formed by the microbial turnover of organic matter. At sites where the methane concentration exceeds saturation, formation of gas bubbles occurs. These bubbles ascend to the sediment water interface and possibly into the water column.

For these objectives we compiled geodata about the occurrence of natural gas reservoirs in deeper geological strata, about fault structures which are possible conduits for the migration of fluids and gases, about the spatial distribution of gas-rich surface sediments as well as about morphological features at the seafloor. The later include so called pockmarks and seeps which are indicative of the occurrence of high concentrations of gas (Fig. 4).

For the data management, visualisation of geodata and spatial analysis we applied a geo-information system. This allows computation of the areas at the seafloor where high gas concentration in surface sediments is observed (Fig. 6, 7). Furthermore, GIS techniques allow to identify intersections of gas rich surface sediments with pockmark fields or fault zones. This provides information about pathways for fluids or gases.

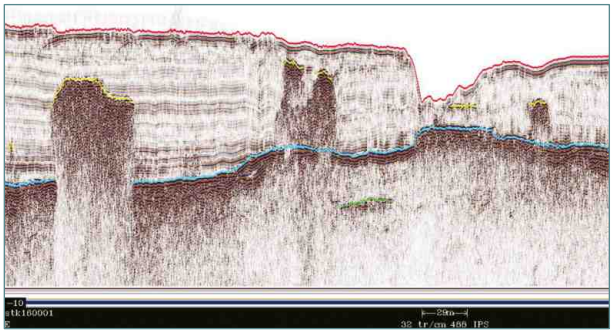

▲ **Figure 4**
This seismic transect shows the seafloor and sediment strata in the subsurface (to a depth of ~50 m below seafloor). In the right section of this transect a pockmark (a morphological depression at the seafloor) was detected. High concentrations of methane and the occurrence of gas bubbles (below the blue or yellow line) are indicated by the seismic records.

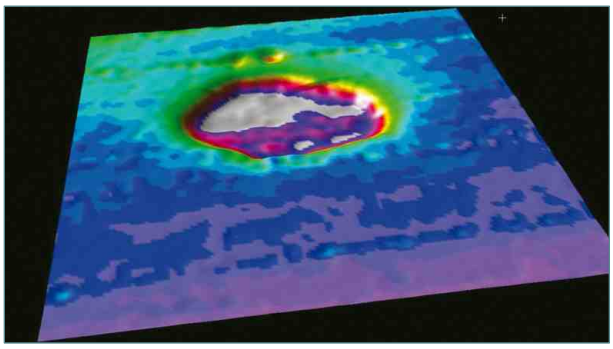

▲ **Figure 5**
High resolution mapping of a pockmark.

The spatial distribution, size and area of a pockmark field in the Eckernförde Bay were investigated by a survey with an Autonomous Underwater Vehicle (Schlüter et al., 2004). Integration of the survey data and previously measured geochemical data into the geo-information system enabled a characterisation of sediment types within pockmarks as well as the distribution of free gas in the subsurface.

Authors

Michael Schlüter and Kerstin Jerosch (AWI)

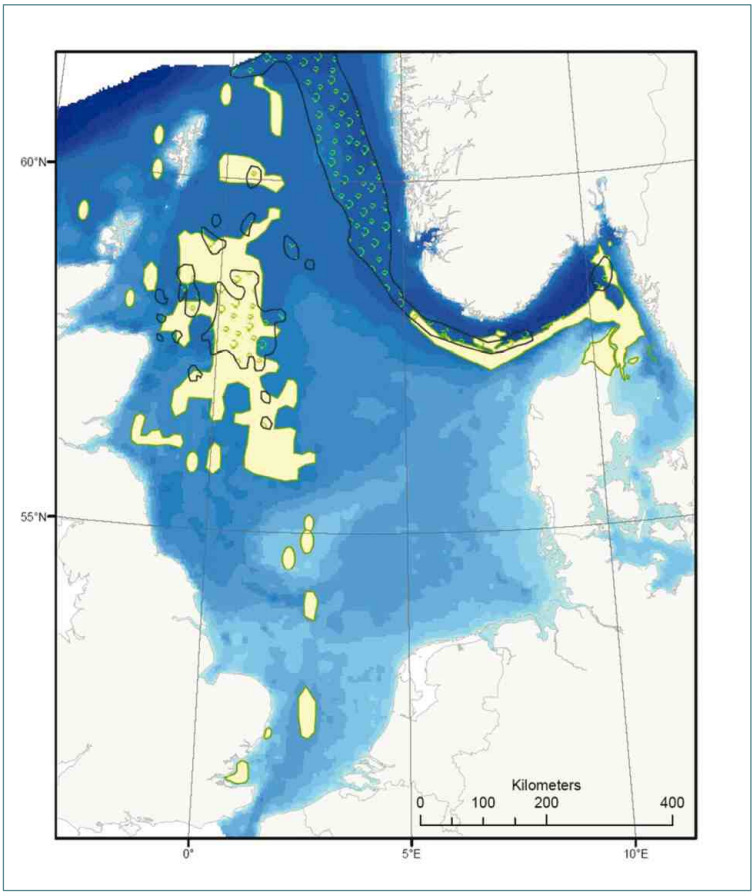

◀ Figure 6
Spatial distribution of major pockmark fields and occurrence of shallow gas in the North Sea and Skagerrak. The data were compiled from different sources, projected to a common basis and analysed within the geo-information system.

▼ Figure 7
High resolution bathymetric information, survey data about the location of pockmark fields, geochemical data, and geological profiles were combined and visualised in 3D. This allows a virtual flight over the seafloor. By this means the coincidence of structures can be identified. For example the alignment and orientation of pockmarks along the southern part of Norwegian Trench was studied.

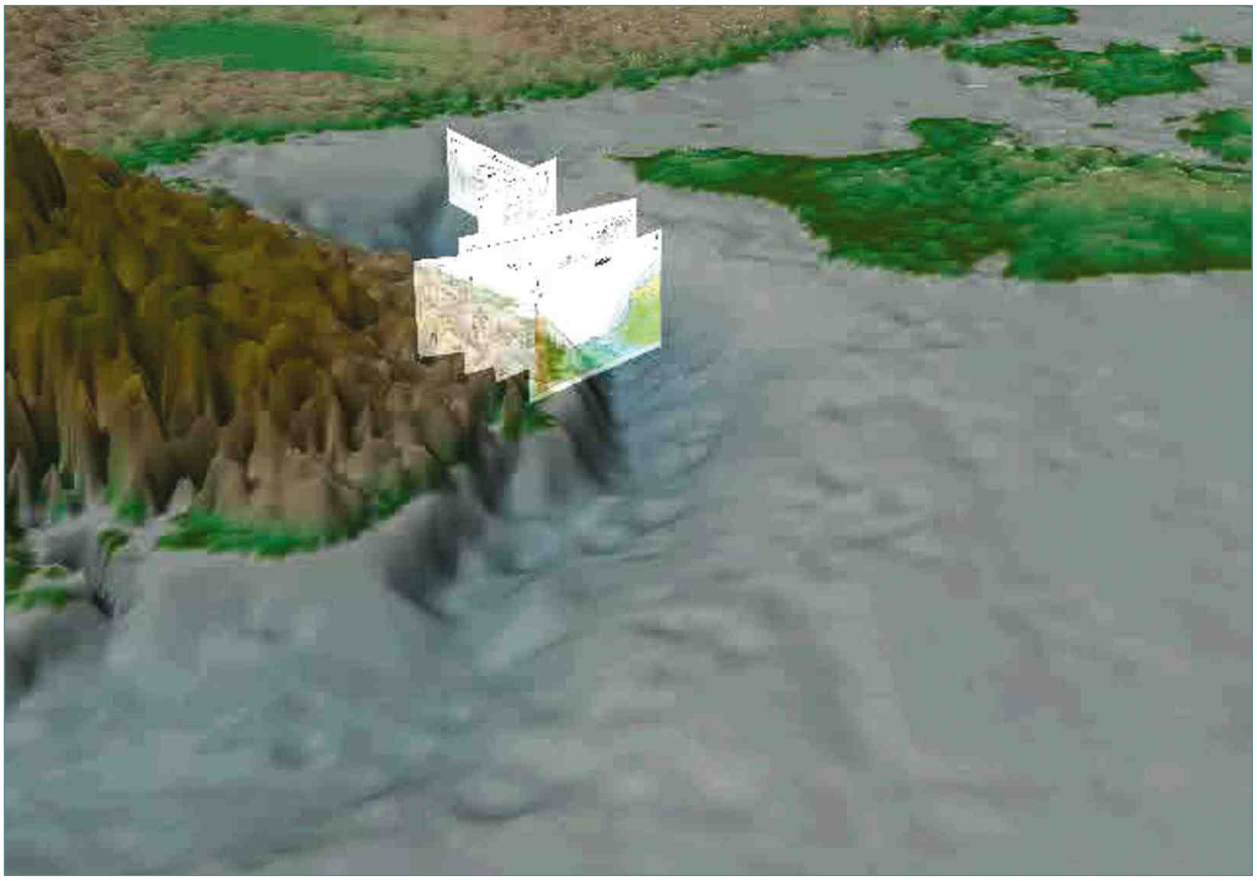

Oil sensitivity

Methods & Techniques

Introduction

The Wadden Sea, a region of tidal flats and salt marshes, is of enormous value as a cleansing site for North Sea water, as a nursery for young fish, as a feeding ground for many bird species and as a recreation area for thousands of tourists. It covers an area of nearly 10,000 km^2 along the North Sea coast of the Netherlands, Germany and Denmark. One major concern is that this nature reserve (a national park in Germany) could be damaged for many years by oil pollution in case of a ship accident. Although it is impossible to protect the whole coast in such a case, a contingency plan for oil spill response can help to minimise the effects for the most sensitive areas. For this purpose oil sensitivity maps have been developed, which consist of an automated expert model and digital maps (GIS) for different seasons.

The study comprises a large scale habitat-survey covering the entire intertidal of the German Wadden Sea, including a classification of their sensitivity with regard to distinct disturbances, especially oil pollution.

The project was financed by the Havariekommando (Central Command for Maritime Emergencies, Germany), which needs the results as a basis for strategic concepts.

Methods and Techniques

Four classes have been defined to scale the oil sensitivity from low (1) to high (4). The sensitivity of a particular area depends largely upon the physical characteristics of the habitat, the susceptibilities of individual benthic species and their roles within the community.

A central and intensive part of the study was the fieldwork for the habitat mapping, which was carried out during three years (2003 - 2006). For this part, the experience of the previous project “Sensitivity Mapping of Intertidal Flats” of GKSS (1987 until 1992) served as a very important basis. The data is devided into geographic and thematic data.

Geographic data

To get a digital map of the oil sensitivity, the thematic data must be linked to a reference map. To navigate the data of the habitat survey a recent map of the tidal flat topography and the borders of the analysis areas (areas with consistent habitat characteristics) are needed. This reference map is the base layer for the so called benthos sensitivity (Fig. 1). A second reference map is needed for the bird data. The map comprises the borders of bird censuses. Fig. 2 shows such “bird areas” in the East Frisian region. These areas are much larger compared to the benthos analysis areas. This map provides a base layer for the bird sensitivity.

Thematic data - Habitat mapping

During the years 2003 and 2006 a set of 70 different parameters were collected at nearly 1000 predefined locations (1 km grid). The parameter set consists of a combination of qualitative and quantitative values. The qualitative values were recorded on a standardised protocol (“record sheet”). They comprise for example information about the presence of different micro- and macroalgae, surface structure (i.e. ripple) and sediment properties. The quantitative values were restricted to sediment cores, like: grain size, water content of sediments and macrofauna species.

Thematic data - Bird census

The seasonal aspects of the sensitivity were calculated using monitoring data of breeding and migratory birds, which are compiled yearly by the national park authorities of Schleswig-Holstein, Hamburg and Lower Saxony. These tabular data have been entered into a database and preprocessed. The result is the sensitivity index for each bird counting area. An overview about all data and processing steps is given in Fig. 2.

▼ Figure 1

Reference map of the benthos and changes of tidal flat topography with a temporal distance of about 15 years.

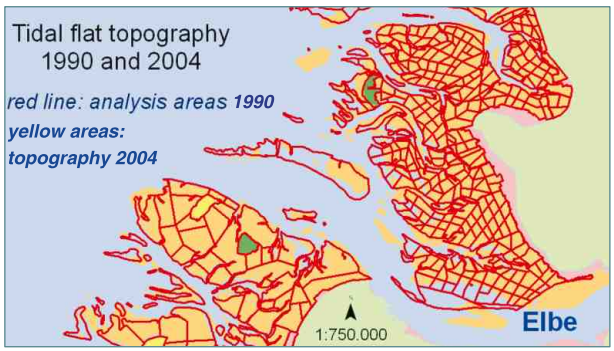

▼ Figure 2

Census areas for birds defined by GKSS.

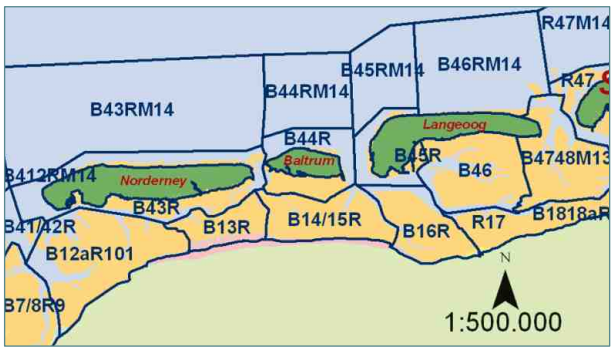

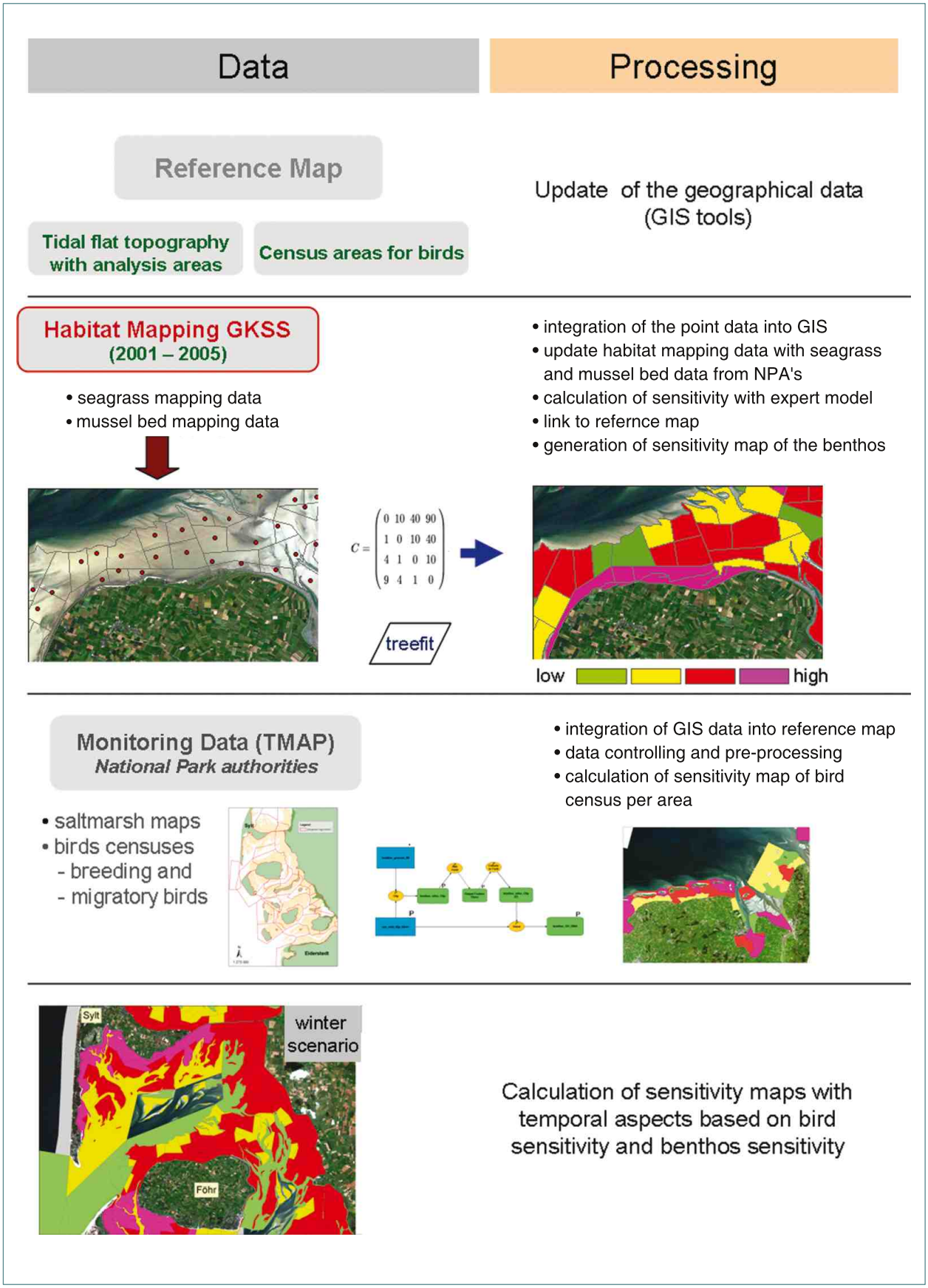

▲ **Figure 3**
Workflow of data, processing steps and results.

Oil sensitivity

Implementation & Results

Analysis

The complex and heterogeneous data from GKSS and National Park authorities were organised in form of a GIS and a database. All data were integrated into the reference maps for benthos areas and bird areas. For updating and formatting the geographic data the GIS editing tools were used also for the update and analysis of the thematic maps. This includes the information about the seagrass and mussel bed distribution and also the link between the bird statistics and the bird areas.

An intermediate step for the calculation of the final sensitivity map is the separate computation of the benthos and bird sensitivity maps.

Benthos – sensitivity (Index)

The sensitivity of each station was calculated on the basis of the collected and pre-processed data using an automated expert system developed by GKSS. This system is based on the artificial neural network technique and on advanced classification methods. The expert model makes it possible that other authorities, like the Havariekommando, can calculate the sensitivity of the benthos in most cases without an expert.

Bird – sensitivity (Index)

The bird censuses per area are split into two groups: breeding and migratory birds. The maximum number of a single bird species was calculated for a period of 5 years.

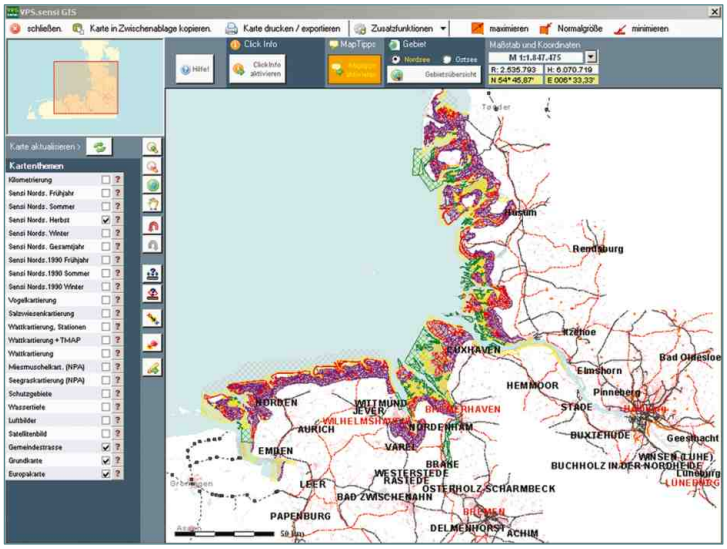

▲ **Figure 4**
Implementation of the digital sensitivity map into the VPS system of the Havariekommando

In the case of breeding birds the number of breeding pairs was counted. In a next step the resulting maximum number was weighted with a predefined value for each species. This weighting was defined by an expert with respect to the behaviour, ecological importance and rareness of the species (Red list of endangerd species). The resulting values were transformed to the four sensitivity classes. With GIS tools the highest possible sensitivity for a bird counting area was analysed and the sensitivity value was linked to the bird reference map.

Oil sensitivity of the Wadden Sea

The final value of the oil sensitivity was calculated by combining the sensitivities of benthos and bird areas based on their spatial and seasonal extension. For the benthos only one index value is determined while for the birds, the index value depends on the breeding and/or migration period. Tab. 1 shows the definition of the bird seasons. The final sensitivity map is shown in Fig. 5. The digital map in Fig. 4 is the input for the GIS system developed for the Havariekommando. More information on the sensitivity raster of the German North Sea is availablet in van Bernem et al., 2007.

	Season	Range	Index Data
1	Spring	February 16th until June 15th	• Benthos • Spring migration birds • Breeding birds
2	Summer	June 16th until September 31st	• Benthos • Autumn migration birds • Breeding birds
3	Autumn	October 1st until December 15th	• Benthos • Autumn migration birds
4	Winter	December 16th until February 15th	• Benthos • Winter migration birds

▲ **Table 1**
Seasonal aspects of bird data.

Authors

Ulrike Kleeberg, Karl-Heinz van Bernem and Hansjörg Krasemann (GKSS)

Figure 5
Part of the sensitivity map for benthos and birds – summer scenario.

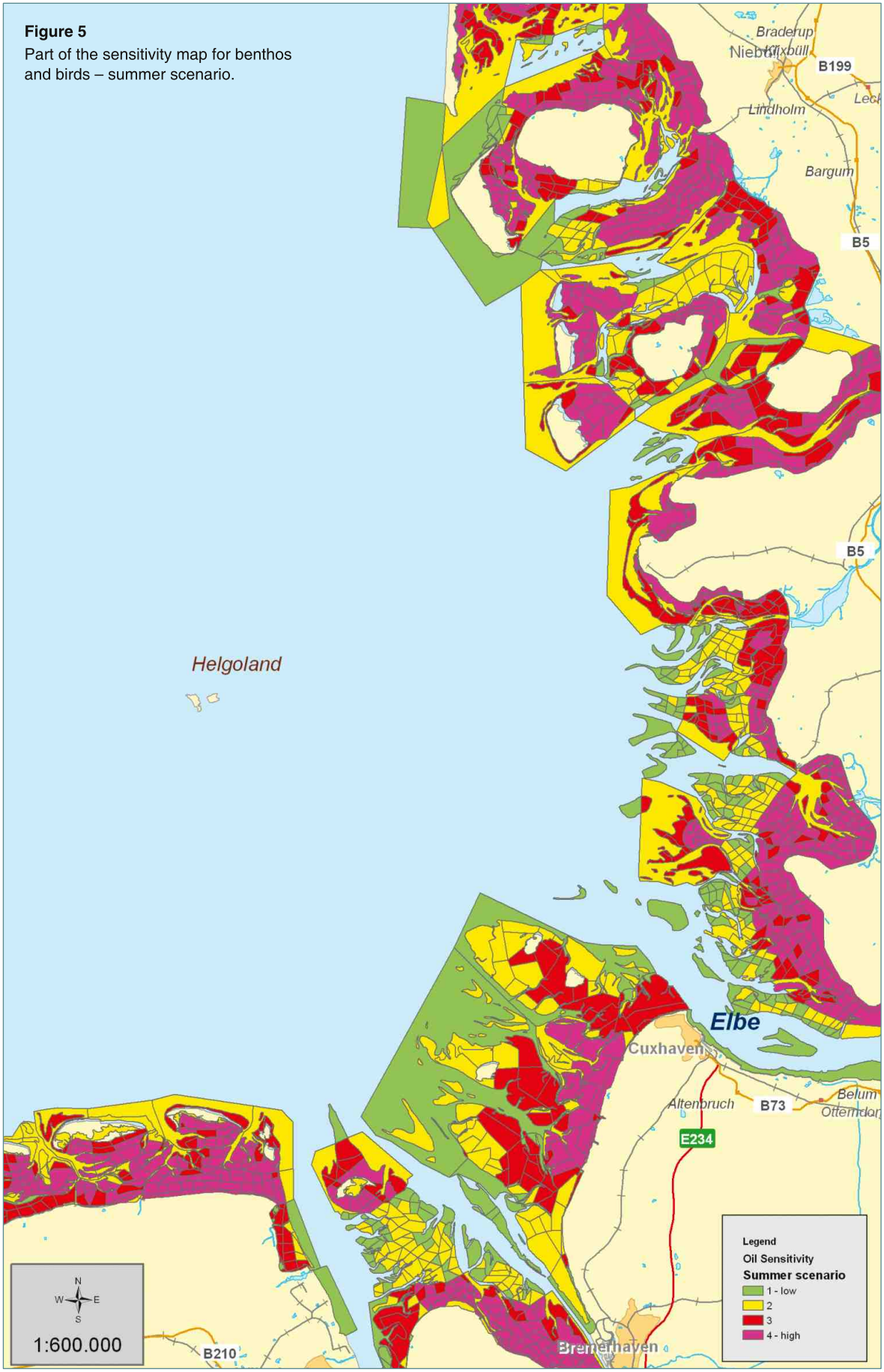

Glossary

Acoustic Doppler Current Profiler (ADCP)
An Acoustic Doppler Current Profiler (ADCP or ADP), is a type of sonar that produces a record of water current velocities over a range of depths. The current is determined by a Doppler shift in the backscatter echo from plankton, suspended sediment, and bubbles, all assumed to be moving with the mean speed of the water.

Algal blooms
Enhanced densities of algal cells, often causing a discoloration of the water. Causes of algal blooms are an exponential increase in phytoplankton cell densities under optimal growth conditions such as light and nutrients. Algal blooms are observed in coastal marine waters as well as freshwater environments, including lakes.

Anthropogenic
Caused by human activity.

Bathymetry
Study of water depth distribution, including topography. Typical instruments are sonar systems, using underwater sound waves with echolocation.

Benthos
All organisms living in or on the sea floor, either plants (phytobenthos) or animals (zoobenthos). Benthos is particularly important in the productive shallow (coastal) water where phytobenthic communities receive sufficient light to grow and to feed dense populations of benthic animals. Benthos is often well developed in intertidal and other littoral areas and high values of biomass are reached particularly in areas like coral reefs, tidal mud flats, mangrove forests and in restricted bottom areas with high sedimentation in shelf seas.

Coastal morphodynamics
Coastal morphodynamics is the study of processes which change the morphology and topography of coastal regions. Most prominently coastal morphodynamics are dynamic in regions with soft sediments, where waves and currents lead to erosion, sedimentation and transport of sediment, and to the evolution of large to small scale morphological patterns such as sand dunes, and ripples.

Community
A collection of species that live in close proximity to one another, share the same habitat, or live in the same region.

Conductivity temperature depth sensor (CTD)
A CTD is an instrument for determining conductivity, temperature and density of sea water in situ. It is used to determine vertical profiles or horizontal transects of these variables.

Current
An ocean current is a continuous, directed movement of ocean water. Ocean currents are rivers of warm or cold water within the ocean. Currents are generated from forces like planet rotation, wind, temperature and salinity differences and the gravitation of moon and sun.

Data
Data refers to the results of experience, observation, computations and simulations or experiments, or a set of premises. This may consist of numbers, words, or images, particularly as measurements or observations of a set of variables.

Doppler effect
Change in frequency of a wave (light, sound, etc.) due to the relative motion of source and receiver. While waves moving away from an object decrease in frequency, waves from an approaching object increase in frequency.

Environmental sensors
A measuring instrument that responds to physical stimuli (such as heat, light, sound, pressure, magnetism, motion) and produces an electronic signal.

Geographic Information System (GIS)
A system for archiving, retrieving, and manipulating data that has been stored and indexed according to the geographic coordinates of its elements. The system generally can utilize a variety of data types, such as imagery, maps, table, etc.

Gradient
The temporal or spatial rate of change of temperature, elevation, velocity, pressure, or other characteristics per unit time or distance.

Harmful algal blooms (HABs)
Harmful algal blooms are algal blooms which produce harmful effects such as fish kills or oxygen depletion. They occur when certain types of microscopic algae flourish. They mainly belong to the groups of e.g. *Dinoflagellates* and *Cyanobacteria*. HABs can occur in marine, estuarine and fresh waters.

High-Performance Liquid Chromatography (HPLC)

HPLC is a standard method used to separate substances in a mixture (by using liquid chromatography). The separated components can be identified and quantified.

In situ

Anything in its natural or original position or place is said to be in situ.

Littoral zone

The shore area or intertidal zone, where exposure and submersion by tides occur periodically.

(Artificial) Neural Network

A neural network consists of input neurons gathering information from an external environment, synapses which interlace the input neurons' information in complex but fairly predictable patterns, and output neurons which turn the patterns of the synapses into actions made on the external environment.
An artificial neural network is a mathematical construct which establishes the quantitative relationship between two sets of variables. It can be used to classify large and complex data sets by grouping cases together in a way similar to the human brain.

Numerical Model

A tool for simulating or predicting the behaviour of a dynamical system like the atmosphere or ecosystems. It is a mathematical representation of processes that can be used to determine the outcome of complex and non-linear interactions.

Plankton

Small, usually microscopic plants (phytoplankton) and animals (zooplankton) in aquatic systems, which generally have no locomotive organs and therefore are transported by currents or other water movements.

Radar

RAdio Detection And Ranging. A Radar is an electronic instrument that uses radio waves (microwaves) to find the distance and location of other objects. The time at which the echo is received indicates the distance from the antenna.

Radar Doppler Current Profiler (RDCP)

A radar scanning method which is used to achieve the full current vector of water surface. The radar doppler is a type of radar that calculates distance and shows direction of movement.

Radar X and C band

Radar systems work in a wide band of transmitted frequencies. The spectrum of the electromagnetic waves are subdivided into bands, which interact with the environment in different ways. The frequency bands are tagged with capitals. C band radars operate on a wavelength of 3.75 - 7.5 cm and a frequency of 4-8 GHz. X band radars operate on a wavelength of 2.5 - 3.75 cm and a frequency of 8-12 GHz.

Remote sensing

A Method to obtain information about an object from a distance. Here it predominantly refers to the process of detecting or monitoring features and objects on Earth from the air or from space by measuring reflected or emitted radiation with devices (e.g. sensors aboard satellites) sensitive to electromagnetic energy such as light, heat or radio waves. For underwater remote sensing acoustic waves are used.

Sensitivity

In an ecological/conservational context sensitivity means the intolerance of a species or habitat to influences from external factors and the time taken for its subsequent recovery.

Spectral band

An interval in the electromagnetic spectrum defined by two wavelengths, two frequencies, or two wave numbers.

Spectrometer

An optical instrument that separates radiation into energy bands (or, in a mass spectrometer, particles into mass groups) and indicates the relative intensities in each band or group. It is typically used to identify materials by their spectral absorption, scattering or emission properties.

(Inter)Tidal flats

Muddy (mud flat) or sandy (sand flat) areas have an elevation between the levels of mean high and mean low tide. Tidal flats are especially located along shallow soft bottom coasts, which are sheltered against waves. The environmental conditions of tidal flats are of a very specific nature, with alternating wet and dry periods during a tidal cycle of about 12 hours and corresponding strong current, temperature and salinity fluctuations. Thus, they are inhabited by a specialised fauna, which lives mostly buried in the sediment. Diversity in tidal flat ecosystems is low, but biomass and production can be very high, due to the input of organic matter from the sea.

Abbreviations

AWI
Alfred Wegener Institut für Polar und Meeresforschung / Alfred Wegener Institute for Polar and Marine Research

BMBF
Bundesministerium für Bildung und Forschung / Federal Ministry of Education and Research

BSH
Bundesanstalt für Seeschifffahrt und Hydrographie / Federal Maritime and Hydrographic Agency

DFG
Deutsche Forschungsgemeinschaft / German Research Foundation

DTM
Digital Terrain Model

DWD
Deutscher Wetterdienst / German National Meteorological Service

EEZ
Exclusive Economic Zone

FTZ
Forschungs- und Technologiezentrum Westküste der Universität Kiel / Research and Technology Centre Westcoast of the University of Kiel

GIS
Geographical Information System

GSM
Global Spectral Model (global wave model)

HIMOM
Hierarchical Monitoring Methods for Tidal Flats

LANU
Landesamt für Natur und Umwelt Schleswig-Holstein / Schleswig-Holstein State Agency for Nature and Environment

MERIS
Medium Resolution Imaging Spectrometer

PAR
Photosynthetically Active Radiation

SPM
Suspended Particulate Matter

TOA
Top of Atmosphere

UTC
Coordinated Universal Time

WAM
Wave Analysis Model

WMO
World Meteorological Organisation

WiRAR
Wind fields from RAR (Real Aperture Radar)

WiSAR
Wind fields from SAR (Synthetic Aperture Radars)

ZMAW
Zentrum für Marine und Atmosphärische Wissenschaften der Universität Hamburg / Centre for Marine and Atmospheric Sciences of the University of Hamburg

List of publications

Cited publications by the authors

Braun N., Ziemer, F., Bezuglov, A., Cysewski, M. & Schymura, G. (2008). Sea-Surface Current Features Observed by Doppler Radar. IEEE Transactions on Geoscience and Remote Sensing, 46 (4). 1125-1133. doi: 10.1109/TGRS.2007.910221.

Brockmann, C., Stelzer, K., Consalvey, M., Forster, R., Jesus, B., Carsey, D., van Leeuwe, M., van Bernem, C., MacGregor, C. & Liek, G. (2004). HIMOM: A System of Hierarchical Monitoring Methods for Assessing Changes in the Biological and Physical State of Intertidal Areas. In Green et al. (Eds.), Littoral 2004. Delivering sustainable coasts: Connecting science and policy (Proceedings Vol. 1, pp. 273-278). Aberdeen: Cambridge Publications.

Brockmann, C. & Stelzer, K. (2008). Optical remote sensing of intertidal flats. In V. Barale & M. Gade (Eds.) Remote sensing of the European Seas, pp. 117-128. Netherlands: Springer.

Colijn, F. & Garthe, S. (2005). EU Directives and their effects on the ecosystem of the Wadden Sea. Proceedings from the 11. Scientific Wadden Sea Symposium Esbjerg, Denmark, 4.-8. April 2005. Monitoring and Assessment in the Wadden Sea. NERI Technical Report 573, 13-20.

Dankert, H. & Horstmann, J. (2007). A Marine Radar Wind Sensor. Journal of Atmospheric and Oceanic Technology, 9 (9), 1629-1642.

Dankert, H., Horstmann, J. & Rosentha, W. (2003). Ocean Wind Fields Retrieved from Radar-Image Sequences. Journal of Geophysical Research,108 (C11), 3352. doi: 10.1029/2003JC002056, 2003.

Diercks, S., Metfies, K. & Medlin, L.K. (2008). Molecular probes for the detection of toxic algae for use in sandwich hybridization formats. Journal of Plankton Research, In press. doi: 10.1093/plankt/fbn009.

Doerffer, R. & Schiller, H. (2007). The MERIS Case 2 water algorithm. Int. Journal of Remote Sensing, 28 (3-4), 517-535.

Feser, F., Weisse, R. & von Storch, H. (2001). Multidecadal atmospheric modelling for Europe yields multi-purpose data. EOS Transactions, 82, 305-310.

Fonfara S., Siebert, U. Prange, A. & Colijn, F. (2007). The impact of stress on cytokine and Haptoglobin mRNA expression in blood samples from harbour porpoises (Phoconea phocoena). Journal of the Marine Biological Association of the United Kingdom, 87, 305-311.

Franke, H.-D., Buchholz, F. & Wiltshire, K.H. (2004). Ecological long-term research at Helgoland (German Bight, North Sea): retrospect and prospect – an introduction. Helgoland Marine Research, 58, 223-229.

Garthe, S., Sonntag, N., Schwemmer, P. & Dierschke, V. (2007). Estimation of seabird numbers in the German North Sea throughout the annual cycle and their biogeographic importance. Vogelwelt, 128, 163-178.

Garthe, S. (1997). Influence of hydrography, fishing activity and colony location on summer seabird distribution in the southeastern North Sea. ICES Journal of Marine Science, 54, 566-577.

Gayer, G., Dick, S., Pleskachevsky, A. & Rosenthal, W. (2006). Numerical modeling of suspended matter transport in the North Sea. Ocean Dynamics, 56 (1), 62–77.

Gehling, C. & Bartsch, I. (submitted). Changes in depth distribution and biomass of sublittoral seaweeds at Helgoland (North Sea) between 1970 and 2005. Submitted to Climate Research.

Griesel, S., Kakuschke, A., Siebert, U. & Prange, A. (2008). Trace element concentrations in blood of harbor seals (Phoca vitulina) from the Wadden Sea. Science of the Total Environment, 392 (2-3), 313-323.

Groben, R., John, U., Eller, G., Lange M. & Medlin L.K. (2004). Using fluorescently-labelled rRNA probes for hierarchical estimation of phytoplankton diversity – a mini-review. Nova Hedwigia, 79, 313-320.

Gurgel, K.-W., Antonischki, G., Essen, H.-H. & Schlick, T. (1999). Wellen Radar (WERA): a new ground-wave HF radar for ocean remote sensing. Coastal Engeneering, 37 (2-4), 219-234.

Gurgel, K.-W., Essen, H.-H. & Kingsley, S.P. (1999). High-frequency radars: physical limitations and recent developments. Coastal Engeneering, 37 (2-4), 201-218.

Horstmann J., Koch, W., Lehner, S. & Tonboe R. (2000). Wind Retrieval over the Ocean using Synthetic Aperture Radar with C-band HH Polarization. IEEE Transactions on Geoscience & Remote Sensing, 38 (5), 2122-2131.

Horstmann J., Schiller, H., Schulz-Stellenfleth, J. & Lehner, S. (2003). Global Wind Speed Retrieval from SAR. IEEE Transactions on Geoscience & Remote Sensing, 41 (10), 2277-2286.

Horstmann, J., & Koch, W. (2005). Comparison of SAR Wind Field Retrieval Algorithms to a Numerical Model utilizing ENVISAT ASAR Data. IEEE Journal of Oceanic Engineering, 30 (Iss.3), 508-515, doi 10.1109/JOE.2005.857514.

Horstmann, J., Koch, W., Lehner, S. & Tonboe, R. (2002). Ocean winds from RADARSAT-1 ScanSAR. Canadian Journal of Remote Sensing, 28 (3), 524-533.

Horstmann, J., Thompson, D.R., Monaldo, F., Graber, H.C. & Iris, S. (2005). Can Synthetic Aperture Radars be used to Estimate Hurricane Force Winds?. Geophysical Research Letters, 32, L22801. doi: 10.1029/2005GL023992.

Jerosch, K., Schlüter, M., Foucher, J.P., Allais, A.G., Klages, M. & Edy, C. (2007). Spatial distribution of benthic communities affecting the methane concentration at Håkon Mosby Mud Volcano. Marine Geology, 243, 1-17. doi:10.1016/j.margeo. 2007.03.010.

Kakuschke, A. (2006). Einfluss von Metallen auf das Immunsystem von Meeressäugern. Dissertation, Universität Hamburg.

Kakuschke, A., Valentine-Thon, E., Fonfara, S., Griesel, S., Siebert, U. & Prange, A. (2006). Metal sensitivity of marine mammals: a case study of a gray seal. Marine Mammal Science, 22 (4), 985-997.

Kakuschke, A., Valentine-Thon, E., Griesel, S., Fonfara, S., Siebert, U. & Prange, A. (2005). The immunological impact of metals in Harbor Seals (Phoca vitulina) of the North Sea. Environmental Science & Technology, 39 (19), 7568-7575.

Koch, W., (2004). Directional analysis of SAR images aiming at wind direction. IEEE Transactions on Geoscience & Remote Sensing, 42 (4), 702-710.

Leonhard, P., Pepelnik, R., Prange, A., Yamada, N. & Yamada, T. (2002). Analysis of diluted sea- water at the ng L-1 level using an ICP-MS with an octopole reaction cell. Journal of Analytical Atomic Spectrometry, 17, 189-196.

Lionello, P., Günther, H. & Janssen, P.A.E.M. (1992). Assimilation of Altimeter Data in a Global Third-Generation Wave Model. Journal of Geophysical Research, 97 (C9), 14453-14474.

Loebl, M., Colijn, F. & van Beusekom, J.E.E. (2008). Increasing nitrogen limitation during summer in the List tidal basin (northern Wadden Sea). Helgoland Marine Research, 62 (1), 59-65. doi: 10.1007/s10152-007-0089-0.

Loebl, M., Colijn, F., Beusekom, J. E. E. van, Baretta-Bekker, J. G., Lancelot, C., Philppart, C. J. M., Rousseau, V. & Wiltshire, K. H. (submitted). Recent changes in phytoplankton limitation patterns along the Northwest European continental coast - Consequences of nutrient reduction measures.

Metfies, K., Huljic, S., Lange, M. & Medlin, L.K. (2005). Electrochemical detection of the toxic dinoflagellate Alexandrium ostenfeldii with a DNA-biosensor. Biosens. Bioelectron, 20, 1349-1357.

Onken, R., Callies, U., Vaessen, B. & Riethmüller, R. (2007). Indirect determination of the heat budget of tidal flats. Continental Shelf Research, 27 (12), 1656-1676.

Petersen, W., Colijn, F., Hydes, D. & Schroeder, F. (2007). FerryBox: from online oceanographic observations to environmental information. EU Project FerryBox 2002–2005. EuroGOOS Publication series 25. Southampton: Southampton Oceanography Centre.

Petersen, W., Petschatnikov, M., Schroeder, F. & Colijn, F. (2003). Ferry-Box Systems for Monitoring Coastal Waters. In: H. Dahlin, N.C. Flemming, K. Nittis & S.E. Petersson (Eds.): Building the European Capacity in Operational Oceanography, Proc. 3rd Int. Conf. on EuroGOOS, EuroGOOS Publication series 19 (pp. 325-333). Amsterdam: Elsevier.

Petersen, W., Wehde, H., Krasemann, H., Colijn, F. & Schroeder, F. (2008). FerryBox and MERIS-Assessment of Coastal and Shelf sea Ecosystems by Combining In situ and Remote Sensed data. Estuarine Coastal and Shelf Science, 77 (2), 296 - 307. doi: 10.1016/j.ecss.2007.09.023.

Petersen, W., Colijn, F., Dunning, J., Hydes, D.J., Kaitala, S., Kontoyiannis, H., Lavin, A.M., Lips, I., Howarth, M.J., Ridderinkhof, H., Pfeiffer, K. & Sørensen, K. (2005). European FerryBox Project: From Online Oceanographic Measurements to Environmental Information. In: H. Dahlin, N.C. Flemming, M. Marchand, S.E. Petersson (Eds.): European Operational Oceanography: Present and Future. Proc. 4th Int. Conference on EuroGOOS, EuroGOOS Publication series 19 (pp. 551-560). Luxembourg: Office for Publications of the European Communities.

Pleskachevsky, A., Gayer, G., Horstmann, J. & Rosenthal, W. (2005). Synergy of satellite remote sensing and numerical modelling for monitoring of suspended particulate matter. Ocean Dynamics, 55 (1), 2–9.

Reise, K. & Kohlus, J. (2008). Seagrass recovery in the Northern Wadden Sea?. Helgoland Marine Research, 62 (1), 77-84. doi: 10.1007/s10152-007-0088-1.

Reise, K. & Siebert, I. (1994). Mass occurrence of green algae in the German Wadden Sea. Deutsche Hydrographische Zeitschrift, Supplement, 1, 171-180.

Reise, K., Jager, Z., de Jong, D., van Katwijk, M. & Schanz, A. (2005). Seagrass. In K. Essink, C. Dettmann, H. Farke, K. Laursen, G. Lüerßen, H. Marencic, W. Wiersinga (Eds.), Wadden Sea Quality Status Report 2004, Wadden Sea Ecosystem 19 (pp. 201-207). Wilhelmshaven: Common Wadden Sea Secretariat.

Röttgers, R., Häse, C. & Doerffer, R. (2007). Determination of the particulate absorption of microalgae using a point-source integrating-cavity absorption meter: verification with a photometric technique. Limnol. Oceanogr.: Methods 5, 1-12.

Schanz, A. & Reise, K. (2005). Seegras-Monitoring im Schleswig-Holsteinischen Wattenmeer - Forschungsbericht zur Bodenkartierung ausgewählter Seegraswiesen im Schleswig-Holsteinischen Wattenmeer 2003. Flintbek: Landesamt für Natur- und Umwelt des Landes Schleswig-Holstein.

Senet, C.M., Seemann, J. & Ziemer, F. (2001). The Near-Surface Current Velocity Determined from Image Sequences of the Sea Surface. IEEE Transactions on Geoscience and Remote Sensing, 39 (3), 492-505.

Schiller, H., Schönfeld, W., Krasemann, H. & Schiller, K. (2007). Novelty Detection - Recognition and Evaluation of Exceptional Water Reflectance Spectra. Environmental Monitoring Assessment, 132 (1-3), 339-350. doi: 10.1007/s10661-006-9538-5.

Schiller, H. & Doerffer, R. (2005). Improved Determination of Coastal Water Constitutent Concentrations from MERIS data. IEEE Transactions of Geoscience and Remote Sensing, 43, 1585-1591.

Schlüter, M., Sauter, E. J., Andersen, C. E., Dahlgaard, H. & Dando, P. (2004). Spatial Distribution and Budget for Submarine Groundwater Discharge in Eckernförde Bay (W-Baltic Sea). Limnology and Oceanography, 49 (1), 157-167.

Schlüter, M., Sauter, E. J., Schäfer, A. & Ritzau, W. (2000). Spatial budget of organic carbon flux to the seafloor of the northern North Atlantic (60°N - 80°N). Global Biogeochemical Cycles, 14 (1), 329- 340.

Schulz, J. (2007). Ring lamp for illuminating a restricted volume and the use thereof. Publication No. WO/2007/045200. International Application No.: PCT/DE2006/001657.

Schulz, J., Möllmann, C. & Hirche, H.J. (2007). Vertical zonation of the zooplankton community in the central Baltic Sea in relation to hydrographic stratification. Journal of Marine Systems, 67, 47-58.

Seeberg-Elverfeldt, J., Schlüter, M., Feseker, T. & Kölling, M. (2005). Rhizon sampling of pore waters near the sediment/water interface of aquatic systems. Limnology and oceanography: Methods, 3, 361-371.

Senet, C.M., Seemann, J. & Ziemer, F. (2001). The Near-Surface Current Velocity Determined from Image Sequences of the Sea Surface. IEEE Transactions on Geoscience and Remote Sensing, 39 (3), 492-505.

Siebert, U., Joiris, C., Holsbeek, L., Benke, H., Failing, K., Frese, K. & Petzinger, E. (1999). Potential relation between mercury concentrations and necropsy findings in cetaceans from German waters of the North and Baltic Seas. Marine Pollution Bulletin, 38 (4), 285-295.

Stelzer, K. & Brockmann, C. (2006). Optische Fernerkundung für die Küstenzone. In K.P. Traub & J. Kohlus (Eds.), GIS im Küstenzonen Management - Grundlagen und Anwendungen (pp. 56-65). Heidelberg: Hüthig GmbH & Co. KG.

Stockmann, K., Riethmüller, R., Heineke, M. & Gayer, G. (submitted). On the morphological long-term development of dumped material in a low-energetic environment close to the German Baltic coast. Submitted to the Journal of Marine Systems.

van Beusekom, J.E.E. (2005). A historic perspective on Wadden Sea eutrophication. Helgoland Marine Research, 59, 45-54.

von Bernem, K.-H., Doerffer, R., Grohnert, A., Heymann, K., Kleeberg, U., Krasemann, H., Reichert, J., Reichert, M. & Schiller, H. (2007). Sensitivitätsraster Deutsche Nordseeküste II - Aktualisierung und Erstellung eines operationellen Modells zur Vorsorgeplanung bei der Ölbekämpfung - Projektbericht im Auftrag des Havariekommandos. Geesthacht: GKSS Forschungs-zentrum Geesthacht GmbH.

Weisse, R. & Plüß, A. (2006). Storm-related sea level variations along the North Sea coast as simulated by a high-resolution model 1958-2002. Ocean Dynamics, 56 (1), 16-25. doi:10.1007/s10236-005-0037-y.

Ziemer, F. & Cysewski, M. (2006). High Resolution Sea Surface Current Maps produced by Scanning with Ground Based Doppler Radar. 2006 IEEE International Geoscience & Remote Sensing Symposium & 27 Canadian Symposium on Remote Sensing, 31 July – 04 August 2006, Proceedings (pp. 1864-1866), Denver, Colorado USA. doi: 10.1109/IGARSS.2006.481.

Other cited publications

Andersen, P., Enevoldsen, H. & Anderson, D.M. (2003). Harmful algal monitoring programme and action plan design. In G.M. Hallegraeff, D.M. Anderson & A.D. Cembella (Eds.), Manual on Harmful Marine Microalgae (pp. 627-647). United Nations Educational, Scientific and Cultural Organization.

Bennett, P. M., Jepson, P. D., Law, R. J., Jones, B. R., Kuiken, T., Baker, J. R., Rogan, E. & Kirkwood, J. K. (2001). Exposure to heavy metals and infectious disease mortality in harbour porpoises from England and Wales. Environmental Pollution, 112 (1), 33-40.

Borge, J.N., Reichert, K., & Dittmer, J. (1999). Use of nautical radar as a wave monitoring instrument. Coastal Engineering, 37 (3-4), 331-342.

Brown, C.J., Mitchell, A., Limpenny, D.S., Robertson, M.R., Service, M. & Golding, N. (2005). Mapping seabed habitats in the Firth of Lorn off the west coast of Scotland: evaluation and comparison of habitat maps produced using the acoustic ground-discrimination system, RoxAnn, and sidescan sonar. ICES Journal of Marine Science, 62, 790-802.

Buckland, S.T., Anderson, D.R., Burnham, K.P., Laake, J.L., Borchers, D.L. & Thomas, L. (2001). Introduction to distance sampling. Estimating abundance of biological populations. New York: Oxford University Press.

Burkholder, J.M., Tomasko, D.A. & Touchette, B.W. (2007). Seagrasses and eutrophication. Journal of Experimental Marine Biology and Ecology, 350, 46-72.

Cabaço, S. & Santos, R. (2007). Effects of burial and erosion on the seagrass *Zostera noltii*. Journal of Experimental Marine Biology and Ecology, 340, 204-212.

Chivers, R.C., Emerson, N. & Burns, D. (1990). New acoustic processing for underway surveying. Hydrographic Journal, 42, 8-17.

Cloern, J.E. (1999). The relative importance of light and nutrient limitation of phytoplankton growth: a simple index of coastal ecosystem sensitivity to nutrient enrichment. Aquatic Ecology, 33, 3-16.

Commission of the European Communities (Ed.) (2003). White Paper, Space: A new European frontier for an expanding Union - An action plan for implementing the European Space Policy [electronic version].

Cosson, J. (1999). Sur la disparition progressive de Laminaria digitata sur les côtes du Calvados (France). Cryptogamie Algol, 20, 35-42.

Daranas A. H., Norte M. & Fernandez, J. J. (2001). Toxic marine microalgae. Toxicon, 39, 1101-1132.

Drinkwater, M., Rebhan, H., LeTraon, P.Y., Phalippou, L., Cotton, D., Johannessen, J., Ruffini, G., Bahurel, P., Bell, M., Chapron, B., Pinardi, N., Robinson, I., Santoleri, L. & Stammer, D. (2005). The Roadmap for a GMES Operational Oceanography Mission [electronic version], ESA Bulletin, 124, 43-48.

Essink, K., Dettmann, C., Farke, H., Laursen, K., Lüerßen, G., Marencic, H. & Wiersinga, W. (Eds.) (2005). Wadden Sea Quality Status Report 2004. Wadden Sea Ecosystem No. 19. Trilateral Monitoring and Assessment Group. Wilhelmshaven (Germany): Common Wadden Sea Secretariat.

Hallegraeff G. M. (2003). Harmful algal blooms: a global overview. In G.M. Hallegraeff, D.M. Anderson & A.D. Cembella (Eds.), Manual on Harmful Marine Microalgae (pp. 25-49). United Nations Educational, Scientific and Cultural Organization.

Hamilton, L.J. (2001). Acoustic seabed classification systems. Victoria (Australia): Defence Science and Technology Organisation. Aeronautical and Maritime Research Lab.

Harff, J. et al. (2003). Projekt: DYNAS - Dynamik natürlicher und anthropogener Sedimentation. Vorhaben: Sedimentationsprozesse in der Deutschen Bucht (Final Report). Rostock: University of Rostock & Warnemünde: Leibniz Institute for Baltic Sea Research.

Harff, J. et al. (2005). Projekt: DYNAS - Dynamik natürlicher und anthropogener Sedimentation. Vorhaben: Sedimentationsprozesse in der Deutschen Bucht - Phase II (Final Report). Rostock: University of Rostock & Warnemünde: Leibniz Institute for Baltic Sea Research.

Hervouet, J. M. & van Haren, L. (1996). TELEMAC2D Version 3.0 Principle Note. Rapport EDF HE-4394052B, Electricité de France. Chatou Cedex: Département Laboratoire National d'Hydraulique.

Hiby, A.R. (1999). The objective identification of duplicate sightings in aerial survey for porpoise. In G.W. Garner, J.L. Amstrup, J.L. Laake, B.F.J. Manly, L.L. McDonald & D.G. Robertson (Eds.), Marine Mammal Survey and Assessment Methods (pp. 179-189). Rotterdam: Balkema.

Hiby, A.R. & Hammond, P.S. (1989). Survey techniques for estimating the abundance of cetaceans. Reports of the International Whaling Commission, Special Issue, 11, 47-80.

Hiby, A.R. & Lovell, P. (1998). Using aircraft in tandem formation to estimate abundance of harbour porpoises. Biometrics, 54 (4), 1280-1289.

Humborstad, O.B., Nøttestad, L., Løkkeborg, S. & Rapp, H.T. (2004). RoxAnn bottom classification system, sidescan sonar and video-sledge: spatial resolution and their use in assessing trawling impacts. ICES Journal of Marine Science, 61, 53-63.

Jepson, P. D., Bennett, P. M., Allchin, C. R., Law, R. J., Kuiken, T., Baker, J. R., Rogan, E. & Kirkwood, J. K. (1999). Investigating potential associations between chronic exposure to polychlorinated biphenyls and infectious disease mortality in harbour porpoises from England and Wales. Science of the Total Environment, 244, 339-348.

Kirihara, S., Nakamura, T., Kon, N., Fujita, D. & Notoya, M. (2006). Recent fluctuations in distribution and biomass of cold and warm temperate species of Laminarialean algae at Cape Ohma, northern Honshu, Japan. Journal of Applied Phycology., 18, 521-527.

Kirk, J. T. O. (1995). Modeling the performance of an integrating-cavity absorption meter: theory and calculations for a spherical cavity. Applied Optics, 34, 4397-4408.

Komen, G.J., Cavaleri, L., Donelan, M., Hasselmann, K., Hasselmann, S. & Janssen, P.A.E.M. (1996). Dynamics and modelling of ocean waves. Cambridge, UK: Cambridge University Press.

Laake, J.L., Calambokidis, J., Osmek, S.D. & Rugh, D.J. (1997). Probability of detecting harbor porpoises from aerial surveys: estimating g(0). The Journal of Wildlife Management, 61 (1), 63-75.

Lancelot, C., Billen, G., Sournia, A., Weisse, T., Colijin, F., Veldhuis, M.J.W., Davies, A. & Wassman, P. (1987). Phaeocystis blooms and nutrient enrichment in the continental coastal zones of the North Sea. Ambio, 16, 38-46.

Lüning, K. (1970). Tauchuntersuchungen zur Vertikalverteilung der sublitoralen Helgoländer Algenvegetation. Helgoländer wissenschaftliche Meeresuntersuchungen, 21, 271-291.

Markones, N. (2007). Habitat selection of seabirds in a highly dynamic coastal sea: temporal variation and influence of hydrographic features. Dissertation, University of Kiel.

Markou, M., & Singh, S. (2003). Novelty detection: A review – Part 1: Statistical approaches. Signal Processing, 83 (12), 2481–2497.

Marsh, H. & Sinclair, D.F. (1989). Correcting for visibility bias in strip transect surveys of aquatic fauna. The Journal of Wildlife Management, 53 (4), 1017-1024.

Millie, D.F., Schofield, O.M.E., Kirkpatrick, G.J., Johnsen, G. & Evens, T.J. (2002). Using absorbance and fluorescence spectra to discriminate microalgae. European Journal of Phycology, 37, 313-322.

Moestrup, O. (2004). IOC Taxonomic Reference list of Toxic Algae. In O. Moestrup (Ed.), IOC taxonomic reference list of toxic algae. Intergovernmental Oceanographic Commission of the UNESCO.

Morizur, Y. (2001). Changements climatiques ou surexploitation? Gros temps sur les algues brunes. Les nouvelles de l'Ifremer, 25, 1-1.

Moy, F., Aure, J., Dahl, E., Green, N., Johnsen, T.M., Lømsland, E.R., Magnusson, J., Omli, L., Olsgaard, F., Oug, E., Pedersen, A., Rygg, B. & Walday, M. (2003). Landtidsovervåking av miljøkvaliteten i kystområdene av Norge. Årsrapport for 2002, 1-69.

Plüß, A. (2004). Das Nordseemodell der BAW zur Simulation der Tide in der Deutschen Bucht. Die Küste 67, 83-127.

Richards, R. & Xiuping, J. (2005). Remote Sensing and Digital Image Analysis: An Introduction. New York: Springer-Verlag

Rosenberg, R. & Loo, L.O. (1988). Marine eutrophication induced oxygen deficiency: effects on soft bottom fauna, western Sweden. Ophelia, 29, 213–225.

Ryder, P. (2007). GMES Fast Track Marine Core Service. Strategic Implementation Plan, Final version 24.04.2007 [electronic version].

von Storch, H. & Zwiers, F. W. (1999). Statistical Analysis in Climate Research. Cambridge: Cambridge University Press.

WAMDI group (1988). The WAM model – a third generation ocean wave prediction model. Journal of Physical Oceanography, 21, 149-172.

Weisse, R. & Plüß, A. (2006). Storm-related sea level variations along the North Sea coast as simulated by a high-resolution model 1958-2002. Ocean Dynamics, 56 (1), 16-25.

Wiebe, P.H. & Benfield, M.C. (2003). From the Hensen net towards 4D-biological oceanography. Progress in Oceanography, 56, 7-136.

Zingone, A. & Enevoldsen, H.O. (2000). The diversity of harmful algal blooms: a challenge for science and management. Ocean & coastal management, 43, 725-748.

List of authors

Ahrens, Lutz	GKSS	lutz.ahrens@gkss.de
Bartsch, Inka	AWI	inka.bartsch@awi.de
Bartsch, Stefan	AWI	stefan.bartsch@awi.de
Barz, Kristina	AWI	kristina.barz@awi.de
Basilico, Adrian	AWI	adrian.basilico@awi.de
Behrens, Arno	GKSS	arno.behrens@gkss.de
Brockmann, Carsten	Brockmann Consult	carsten.brockmann@brockmann-consult.de
Callies, Ulrich	GKSS	ulrich.callies@gkss.de
Chrastansky, Alena	GKSS	alena.chrastansky@gkss.de
Colijn, Franciscus	GKSS	colijn@gkss.de
Cordes, Wolfgang	GKSS	wolfgang.cordes@gkss.de
Cysewski, Marius	GKSS	marius.cysewski@gkss.de
Dankert, Heiko	California Inst. of Technology	heiko@vision.caltech.edu
Diercks, Sonja	formerly GKSS	
Dobrynin, Mikhail	GKSS	arno.behrens@gkss.de
Doerffer, Roland	GKSS	roland.doerffer@gkss.de
Dreyer, Annekatrin	GKSS	annekatrin.dreyer@gkss.de
Ebinghaus, Ralf	GKSS	ralf.ebinghaus@gkss.de
Flampouris, Stylianos	GKSS	stylianos.flampouris@gkss.de
Flöser, Götz	GKSS	goetz.floeser@gkss.de
Fonfara, Sonja	FTZ	fonfara@ftz-west.uni-kiel.de
Garthe, Stefan	FTZ	garthe@ftz-west.uni-kiel.de
Gayer, Gerhard	GKSS	gerhard.gayer@gkss.de
Gehnke, Steffen	GKSS	steffen.gehnke@gkss.de
Geißler, Jasmin	Brockmann Consult	jasmin.geissler@brockmann-consult.de
Gentz, Torben	AWI	torben.gentz@awi.de
Gilles, Anita	FTZ	gilles@ftz-west.uni-kiel.de
Griesel, Simone	GKSS	simone.griesel@gkss.de
Günther, Heinz	GKSS	heinz.guenther@gkss.de
Gurgel, Klaus-Werner	ZMAW	gurgel@ifm.uni-hamburg.de
Häse, Clivia	GKSS	clivia.haese@gkss.de
Hass, Christian	AWI	christian.hass@awi.de
Heineke, Martina	GKSS	martina.heineke@gkss.de
Henrich, Milan	formerly AWI	
Heymann, Kerstin	GKSS	kerstin.heymann@gkss.de
Hirche, Hans-Jürgen	AWI	hans-juergen.hirche@awi.de
Horstmann, Jochen	GKSS	jochen.horstmann@gkss.de
Jerosch, Kerstin	AWI	kerstin.jerosch@awi.de
Kakuschke, Antje	GKSS	antje.kakuschke@gkss.de

Kleeberg, Ulrike	GKSS	ulrike.kleeberg@gkss.de
Koch, Wolfgang	GKSS	wolfgang.koch@gkss.de
Kohlus, Jörn	Nationalpark Schleswig-Holstein	joern.kohlus@nationalparkamt.de
Kramer, Katharina	GKSS	katharina.kramer@gkss.de
Krasemann, Hansjörg	GKSS	hansjoerg.krasemann@gkss.de
Kreus, Markus	GKSS	markus.kreus@gkss.de
Loebl, Martina	AWI	martina.loebl@awi.de
Medlin, Linda	AWI	linda.medlin@awi.de
Mengedoht, Dirk	AWI	dirk.mengedoht@awi.de
Metfies, Katja	GKSS	katja.metfies@awi.de
Müller, Dagmar	GKSS	dagmar.mueller@gkss.de
Müller, Jan-Moritz	GKSS	jan-moritz.mueller@gkss.de
Onken, Reiner	GKSS	reiner.onken@gkss.de
Pepelnik, Rudolf	GKSS	rudolf.pepelnik@gkss.de
Petersen, Wilhelm	GKSS	wilhelm.petersen@gkss.de
Pröfrock, Daniel	GKSS	daniel.proefrock@gkss.de
Reise, Karsten	AWI	karsten.reise@awi.de
Ricklefs, Klaus	FTZ	ricklefs@ftz-west.uni-kiel.de
Riethmüller, Rolf	GKSS	rolf.riethmueller@gkss.de
Röttgers. Rüdiger	GKSS	ruediger.roettgers@gkss.de
Schiller, Helmut	GKSS	helmut.schiller@gkss.de
Schlüter, Michael	AWI	michael.schlueter@awi.de
Schönfeld, Wolfgang	GKSS	wolfgang.schoenfeld@gkss.de
Schroeder, Friedhelm	GKSS	friedhelm.schroeder@gkss.de
Schulz, Jan	AWI	jan.schulz@awi.de
Sedlacek, Stephan	formerly GKSS	
Siebert, Ursula	FTZ	ursula.siebert@ftz-west.uni-kiel.de
Stelzer, Kerstin	Brockmann Consult	kerstin.stelzer@brockmann-consult.de
Stockmann, Karina	GKSS	karina.stockmann@gkss.de
Sturm, Renate	GKSS	renate.sturm@gkss.de
Vaessen, Bernd	GKSS	bernd.vaessen@gkss.de
van Bernem, Karl-Heinz	GKSS	carlo.bernem@gkss.de
van Beusekom, Justus	AWI	justus.van.Beusekom@awi.de
Vanselow, Klaus Heinrich	FTZ	vanselow@ftz-west.uni-kiel.de
Weisse, Ralf	GKSS	ralf.weisse@gkss.de
Wiltshire, Karen	AWI	karen.wiltshire@awi.de
Ziemer, Friedwart	GKSS	friedwart.ziemer@gkss.de

Photoindex

Photos other than by the authors

Page 15 Figure 3 Red Algae © www.nies.go.jp

Page 15 Figure 3 Green Algae © www.wwa-bayern.de

Page 15 Figure 3 Dinoflagellates © www.io-warnemuende.de

Page 18 Figure 1 © Miriam Godfrey

Page 19 Figure 2 *Dinophysis acuta* © www.imr.no

Page 19 Figure 2 *Dinophysis accuminata* © www.diatomloir.eu

Page 19 Figure 2 *Dinophysis norvegica* © www.itameriportaali.fi

Page 19 Figure 2 *Alexandrium minutum* & *Alexandrium ostenfeldii* © www.ifremer.fr

Page 19 Figure 2 *Alexandrium tamarense* © www.inape.gnb

Page 50 Figure 1 © Carsten Wanke

Page 54 © Reinhard Reshöft

Page 71 Figure 5 © Frank Riedel, Jan Bödewadt and Annekatrin Dreyer

All other Photos

© at the respective authors